GROWTH KINETICS OF *Bacillus thuringiensis*
BATCH, FED-BATCH AND CONTINUOUS BIOREACTOR CULTURES

by
DAVID RIVERA

Faculty of Engineering Science
Department of Chemical and Biochemical Engineering

Submitted in partial fulfillment
of the requirements for the degree of
DOCTOR OF PHILOSOPHY

Faculty of Graduate Studies
The University of Western Ontario
London, Ontario
December, 1998

National Library
of Canada

Acquisitions and
Bibliographic Services

395 Wellington Street
Ottawa ON K1A 0N4
Canada

Bibliothèque nationale
du Canada

Acquisitions et
services bibliographiques

395, rue Wellington
Ottawa ON K1A 0N4
Canada

Your file Votre référence

Our file Notre référence

0-612-40287-8

Canada

ABSTRACT

Cells of *Bacillus thuringiensis* during their late stationary growth phase produce both spores and the bioinsecticidal crystal protein delta-endotoxin. *B. thuringiensis* cells also evolve depending on the environmental conditions. Thus, it is necessary to adopt a broad approach to study the growth kinetics of *B. thuringiensis* considering not only the typical cell growth but also the metabolic changes occurring while spores and crystal protein are being produced.

This study presents the results of cell growth kinetics study of *Bacillus thuringiensis* subspecies *kurstaki*, strain HD-1 (ATCC 33679), grown under batch and fed-batch growth conditions. In addition, *B. thuringiensis* growth was investigated under continuous steady-state growth conditions in a single stage 2-L bioreactor system and a two-stage continuous bioreactor system which consisted of a 2-L followed by a 15-L bioreactor system.

Optical microscopy and transmission electron microscopy (T.E.M.) were used extensively in this study to assess the morphology and metabolic state of *B. thuringiensis* cells at different growth conditions during batch, fed-batch and continuous steady-state experiments. Significant morphological differences in *B. thuringiensis* cells, as a function of growth time for the batch experiments and as a function of dilution rates in the steady-state continuous experiments were observed.

The separation of crystal protein from the fermentation broth for analytical purposes presents serious problems. In this study a new method to isolate the crystal protein was developed which produced crystal protein with a purity up to 95%. ± 5% .Additionally, high performance liquid chromatography (HPLC) was employed to detect this protein.

Experimental results demonstrated the high dependence of the formation of spore and

crystal protein with the type of culture. In batch cultures, the formation of spore and crystal protein caused a decrease in biomass growth rate, reducing the final biomass concentration. Whereas in the continuous culture, a reduction in biomass concentration was observed at low dilution rates. Finally, in fed-batch growth, no spores neither crystal protein were produced even though the limiting substrate was completely depleted.

An in depth analysis of the experimental data showed that the classical growth kinetic model cannot predict accurately the biomass concentration for the complete time span of a batch and at all the dilution rates of a continuous culture of *B. thuringiensis*. Thus, a new growth kinetic with sporulation model, which involved a term representing the specific spore formation rate, was developed and tested successfully with both batch and continuous experimental data.

Experimental results were also employed to determine new and reliable cell growth kinetic parameters (μ_{max} and K_S), as well as the growth yield and respiration rate coefficients for batch and continuous cultures.

Keywords: *B. thuringiensis*, growth kinetics, cell morphology, batch reactor, fed-batch reactor, continuous stirred tank reactor.

ACKNOWLEDGMENTS

I wish to express my appreciation to my Ph.D. thesis Supervisor, Dr. A. Margaritis for his encouragement, enthusiastic support and guidance throughout the course of this project. Also I wish to thank Professor A. Margaritis for reviewing my thesis and the suggestions for changes and corrections, including discussions and advice regarding the development of the sporulation kinetic model.

Thanks go to Dr. A. Khan, for his invaluable assistance with the High Performance Liquid Chromatography tests, and to Mr. R. Smith and Mr. R. Davidson for their help with the Transmission and Scanning Electron Microscope. I would also like to thank Dr. M.A. Bergougnou and Dr. A. Bassi for their suggestions during the course of this work. I would like to express my sincere gratitude to Dr. de Lasa and Dr. G.E. Rowe for their invaluable advice during the development of the growth kinetic model. I truly appreciate their support, guidance and friendship.

I would like to thank the Instituto Tecnologico y de Estudios Superiores de Monterrey, Leon Campus for granting my leave to pursue my Ph.D. degree.

I wish to express my appreciation to the Consejo Nacional de Ciencia y Tecnologia (CONACYT) from Mexico for awarding me a generous four year scholarship to develop the present study.

This work was supported by the Natural Sciences and Engineering Research Council of Canada (NSERC) through Research Grant No. OGP4388, awarded to Dr. A. Margaritis.

TABLE OF CONTENTS

LIST OF TABLES

LIST OF FIGURES

LIST OF PLATES

LIST OF APPENDICES

List of Abbreviations, Symbols and Nomenclature.

Bt	*Bacillus thuringiensis*
CFU	Colony Forming Unit
CP	Crystal protein
Cry^-	Non-forming crystal protein bacillus strains
Cry^+	Forming crystal protein bacillus strains
cry	Gene from *B. thuringiensis* encoding a parasporal inclusion protein
*cry*I	Lepidoptera specific crystal protein gene
*cry*II	Lepidoptera and Diptera specific crystal protein gene
*cry*III	Coleoptera specific crystal protein gene
*cry*IV	Diptera specific crystal protein gene
HPLC	High Performance Liquid Chromatography
D	Dilution rate , h^{-1}
D*	Critical dilution rate, h^{-1}
F	Input volumetric flow rate, in continuous and fed-batch growth, L/h
K_S	Saturation constant, g/L
k_s	Kinetic constant in the new cell growth with sporulation kinetic model
NX_v	Number of vegetative cells (without a spore)
NX_s	Number of cells forming a spore.
qO_2X	Oxygen uptake rate, mg O_2/L-h
qO_2	Respiration rate coefficient, mg O_2/g cell -h
r_x	Cell growth rate, g/L-h
r_s	Substrate consumption rate, g/L-h
S	Substrate concentration, g/L

S_0	Initial substrate concentration in the batch growth, and the substrate concentration in the feed stream for continuous or fed-batch growth, g/L
S_i	Glucose concentration at the beginning of the transient state in continuous cultures
t	Time, h
t_w	Time at the beginning of the washout, h
V	Reaction volume at any time, L
V_0	Reaction volume at the beginning of the fed-batch growth, L
X	Cell concentration, g/L
X_0	Initial biomass concentration in the batch or Fed-batch growth, g/L
X_i	Biomass concentration at the beginning of the exponential stage in batch cultures, and at the beginning of the transient state in continuous cultures
X_v	Biomass concentration corresponding to vegetative cells
X_w	Biomass concentration at the begining of the washout, g/L
X_s	Biomass concentration corresponding to sporulated cells
$Y_{X/S}$	Growth yield, g cells/g substrate
α_0	Substrate uptake enzyme fraction of the biomass when $\mu = 0$
α_m	Substrate uptake enzyme fraction of the biomass when $\mu = \mu_{max}$
μ	Specific growth rate, h^{-1}
μ_{max}	Maximum specific growth rate, h^{-1}
ρ_0	Density of the liquid in the input, in continuous growth g/L
ρ	Density of the liquid in the reactor, g/L

CHAPTER 1

INTRODUCTION

Dispersion and migration of pesticides in the ecosystem to control agricultural pests pose a major environmental concern. Chemical insecticides are not only toxic to insects but also to humans and other living species, and remain and accumulate in the ecosystem for extended periods of time. Due to extensive use of chemical insecticides, more than 400 insect species have developed resistance to chemical insecticides (Stix, 1998). In any event and in spite of their well documented negative environmental impact, chemical insecticides are still used extensively worldwide.

Among possible alternatives, a promising one is the use of biological insecticides. Biological insecticides are bio-degradable and non toxic to mammals and humans. Among the biological pests control methods, *Bacillus thuringiensis* based insecticides is an excellent example. *Bacillus thuringiensis* is a Gram-positive spore-forming bacterium that produces a protein inclusion called crystal protein or delta-endotoxin together with the endospore. This protein is toxic to a high number of insect pests, is bio-degradable and non-toxic to other species, with only few insect species developing resistance. In addition, it has been reported an increased insecticidal effect when both spore and crystal protein are used as bioinsecticides (Dubois and Dean, 1995; Johnson and McGaughey, 1996). The bioinsecticide is sprayed on the leafs of plants which is then ingested by the larvae resulting in their death from damages to the endothelial cells of their intestine system (Avignone-Rossa andMignone, 1995).

The active agent, delta-endotoxin, is obtained through the fermentation (Rowe and Margaritis, 1987) of several subspecies of *B. thuringiensis*. This protein is commercially produced in a powder form, and used in sprays (Bryant, 1994). With only 0.5% of the global insecticide market, *Bacillus thuringiensis* (Bt) is nowadays the basis of most biopesticides.

While bioinsecticides still have a relative small share of the market, given the relative high production cost, it is expected that their manufacturing costs will be reduced significantly due to improvements in fermentation technology and the economies of scale in commercial production (Cannon, 1993).

Regarding *B. thuringiensis* toxins, another approach for crop protection is the development of genetically engineered plants which can produce the *B. thuringiensis* toxins by themselves (Estruch et. al., 1997). However, there are serious concerns about the possibility of increasing insect resistance to *B. thuringiensis* toxins because these genetically engineered plants provide exposure throughout the entire growing season, increasing in this way the selection pressure on the insects. (McGaughey et al., 1998; Holmes, 1997; Stix, 1998)

Another important advantage of *B. thuringiensis* spray application is that these insecticides degrade quickly making the insect resistance less likely to develop. However, its effectiveness is reduced given its short time of exposure. Thus, in order to have an effective pesticide action, a more frequent application of *B. thuringiensis* sprays is needed, and this translates on high utilization costs.

Production of *B. thuringiensis* based insecticides is currently performed in batch reactors whose volumetric productivity is low compared with the productivity that could eventually be obtained in continuous or semi-continuous reactors.

Because the bacterium *B. thuringiensis* produces the toxic protein simultaneously with the formation of the spores, it is important to culture the bacterium under nutrient limitation and slow or negative cell growth. However, under these conditions, the production of cells is extremely limited and the productivity is significantly reduced. Moreover, the delta-endotoxin production depends on the number of cells carrying the crystal protein produced in the reactor. Therefore, a process that increases the production of cells and at the same time

allows the formation of spores and crystal protein under starvation condition is highly desirable.

B. thuringiensis is a bacterium that has a very complex growth characteristics. During the batch growth, *B. thuringiensis* cells change from vegetative to sporulated cells, and during this process undergoing significant metabolic, physiological and kinetic changes. These complex changes preclude the use of a existing simple kinetic models which are used to describe the cell growth of non-sporulating microbial cell cultures.

The systematic survey of the literature on *B. thuringiensis* revealed that there is no kinetic growth model that accounts for vegetative and sporulated cells. Moreover, the basic growth kinetic constants for *B. thuringiensis* cells growth reported in the literature are scarce and inconsistent. A main problem with previous kinetic studies about *B. thuringiensis* growth is the lack of proper accounting of the effects of the metabolic changes on the cell growth, and of the connection between physiological, metabolic changes, and growth rate.

In this respect, lack of studies on the growth of the bacterium *B. thuringiensis* under different conditions has hindered the development of new processes with improved productivity and as a result reduced bioinsecticide price. Thus, studies of the growth kinetics incorporating metabolic changes, formation of spore and the crystal protein and the response of the *B. thuringiensis* in different reactor configurations will help considerably.

In summary, the following research objectives are set in order to provide new and valuable research results of potential importance on the commercialization of bioinsecticides production by *B. thuringiensis*.

1. To study the growth of *B. thuringiensis* in batch, continuous and fed-batch reactors in order to verify the metabolic changes occurring during its culture, and to relate this changes with measurable parameters such as pH, oxygen requirements, and growth rate.

2. To correlate the different growth phases with time in batch and with dilution rate in continuous CSTR cultures.

3. To establish reliable kinetic growth parameters for *B. thuringiensis* subspecies *kurstaki*, as well as respiration rate coefficient and growth yield by using continuous steady-state bioreactor systems.

4. To identify the morphological changes by using optical and transmission electron microscopy in order to correlate these changes with growth stages.

4. To establish a new growth kinetic model that includes both vegetative and spore forming cells to describe the *B. thuringiensis* cells growth.

5. To examine the feasibility of using a single and a two-stages continuous CSTR bioreactor system for the production of delta endotoxin bioinsecticide.

CHAPTER 2

LITERATURE REVIEW

2.1 *B. thuringiensis* classification and characteristics

Bacillus thuringiensis is a species of the Group I of the genus *Bacillus*. Species of this group are Gram positive spore-forming bacteria. The endospores in *Bacillus* species are round or oval structures that are highly refractile and contain dipicolinic acid. The spores are resistant to the lethal effects of heat, drying and many disinfectants, and thus they survive in nature in a dormant state for long periods. *B thuringiensis* is a rod shaped bacterium of 1.0 to 2.0 μm width and 3 to 5 μm length (Sneath, 1986).

B. thuringiensis is closely related to *B. cereus* and *B. anthracis* and is well known as an insect pathogen. (Dean, 1984). Of the five species of *Bacillus* that are insect pathogens *B. thuringiensis* is also by far the most important in the biological control of insects. The other four are *B. larvae*, *B. lentimorbus*, *B. propilliae* and *B. sphaericus* (Sneath, 1986).

The life cycle of the *Bacillus* species has two main stages: the vegetative stage and sporulation stage. The vegetative stage is characterized by an active cell growth, while the sporulation stage is characterized by cell growth cessation and spore formation. These stages involve changes in both the morphology and the biochemistry of the cells.

B. thuringiensis produces a proteinaceous body known as crystal protein or delta-endotoxin that possesses insecticidal properties. These insecticidal proteins are synthesized during the stationary phase and accumulate in the cell as a crystal inclusion which can account for up to 25% of the dry weight of the sporulated cells (Agaisse and Lereclus, 1995). Various forms of crystals have been observed using phase contrast microscope. The most common shape is a bypiramidal structure (Kumar et al, 1996).

There are more than 50 different varieties of *B. thuringiensis*, classified by De Barjac and Bonnefoi, and revised by De Barjac and Franchon (Kumar et al., 1996). The following table shows the classification of *B. thuringiensis*

Table 2.1 Classification of *Bacillus thuringiensis*.

Variety	Toxicity (a)
aizawai	L, D
alesti	L
amagiensis	
andalousiensis	
brasiliensis	
cameroun	
canadensis	L
colmeri	
coreanensis	
dakota	
darmstadiensis	L, D
entomocidus	
finitimus	
fukuokaensis	D
galleriae	L, C
guiyangiensis	
higo	
huazhongensis	
indiana	
israelensis	D
japonensis	C
jegathesan	D
jinghongensis	
kenyae	L, D
konkukian	
kumamotoensis	C
kurstaki	L, D
kyushuensis	L, D
leesis	
londrina	
malaysiensis	D
medellin	D
mexicanensis	L
monterrey	
morrisoni	L, D, C
neoleonensis	

Table 2.1 Classification of *Bacillus thuringiensis* (continued)

Variety	Toxicity (a)
nigeriensis	
novosibirsk	
ostriniae	L
oswaldocruzi	
oyamensis	
pakistani	
pondicheriensis	L
roskildiensis	
seoulensis	
shandongiensis	L
silo	
sooncheon	
sotto	L
sumiyoshiensis	
thompsoni	L, D
thuringiensis	L, D
tochigiensis	
toguchini	
tohokuensis	
tolworthi	L, D
toumanoffi	
yosoo	
yunnanensis	L

(a) L. lepidoptera active; D, diptera active; C, coleoptera active

From: Kumar., P.A., Sharma., R.P., and Malik, V.S., (1996), The insecticidal proteins of *Bacillus thuringiensis* In Advances in Applied Microbiology, Neidleman., S.L. and Laskin, A.I., (eds) Vol 42, Academic Press Inc., pp 1- 43.

It has to be mentioned that *B. thuringiensis* subspecies *kurstaki* of Table 2.1 is the one employed in the present study.

2.2 Metabolism and sporulation of *B. thuringiensis*

B. thuringiensis (Bt) is a Gram positive aerobic bacterium able to grow in simple media, including on nutrient agar (Sneath, 1986). There are in the technical literature a number of studies describing the nutrients needed for the growth of *B. thuringiensis*. Some

of these studies have been focused on the optimization of the production of delta-endotoxin, and others on the minimum nutrients required for the development of the cells, and others yet on the use of industrial and cheap sources of nutrients.

B. thuringiensis requires a source of carbon, amino acids and some salts to increase the growth and the crystal protein production. Moreover, it has also been shown that other factors such as the dissolved oxygen, pH and temperature are important for the growth of *B. thuringiensis*.

The minimal nutritional requirements for *B. thuringiensis* (Proom and Knight, 1955), include basal salts (KH_2PO_4, $(NH_4)_2HPO_4$, $MgSO_4$, $CaCl_2$, $MnSO_4$, $FeSO_4$ and ammonium molybdate), supplemented with seven aminoacids (L-aspargine, L-proline, L-leucine, DL-alanine, L-glutamic acid, DL-serine, DL-methionine).

Because *B. thuringiensis* is an aerobic bacterium, it needs oxygen to grow. Foda et al. (1985) conducted physiological studies on *Bacillus thuringiensis* var. *entomocidus* revealing the failure of the organism to survive or sporulate under low aeration levels, and this was specially true at high sugar concentrations. The size and specific toxicity of the parasporal inclusion is also affected by the oxygen supply (Scherrer et al., 1973), with the production of delta-endotoxin being increased with good air distribution throughout the growth medium (Sikdar et al., 1993).

The temperature as well as the level of aeration are important factors in the growth of *B. thuringiensis*. Ignatenko et al. (1983) studied the development of *Bacillus thuringiensis* var. *galleriae* using a semi-synthetic medium (yeast hydrolysate, glucose and salts) and the effect of temperature and level of aeration on the culture. The results of this study showed that the vegetative growth of the culture increased with an increase in aeration from 5 to 25 mg O_2/liter-min. On this basis, and to increase the yield of viable spores with high heat resistance, it is advisable to culture these microorganisms in variable temperature regimes, i.e.

keeping the medium at 30 °C, until the growth retardation stage is reached. Following this, increasing the temperature to 35 °C.

The carbon source is an important factor in *B. thuringiensis* growth. In this respect, a number of studies describe the effect of the glucose concentration on cell growth (Yudina et al., 1992; Scherrer et al, 1973; Arcas et al., 1987; Goldberg et al., 1980).

For example, Scherrer et al. (1973) used a yeast extract-glucose-salts medium to culture *B. thuringiensis* subspecies *thuringiensis* finding that an increase in glucose concentration led to bigger crystal inclusions with a higher content of protein and insecticidal activity. Arcas et al. (1987) studied in a batch culture the influence of increasing concentration of components of a glucose-yeast extract - mineral salts medium on the bacterial insecticide production using a strain of *Bacillus thuringiensis* var. *kurstaki*. These authors found that when the concentration of glucose was increased from 8 to 56 g/L, spore counts were increased from 1.08×10^{12} spores/mL to 7.36×10^{12} spores/mL and the toxin level augmented from 1.05 mg/mL to 6.85 mg/mL. A further increase (> 56 g/l glucose) appeared to be harmful to the microorganism, given the observed decrease in the cell population.

B. thuringiensis growth requires not only glucose as substrate but also a protein supplement. In this respect, Nickerson and Bulla (1974) used a basal medium consisting of salts and glucose to culture 18 strains of *B. thuringiensis*. None of these 18 strains grew on the unsupplemented basal medium. However, these strains grew, sporulated, and produced the parasporal crystal when the basal medium was supplemented with either aspartate or glutamate. Finally, most strains were capable of growing when glutamate or citrate were added to a glucose-free basal medium although in these cases, the absence of glucose generally resulted in a defective sporulation. In addition, as demonstrated by Arcas et al. (1984); Liu and Bajpai (1995) an effective medium for the cultivation of *B. thuringiensis* requires an adequate organic nitrogen source like yeast extract, peptone, or corn steep liquour

The salt content in the medium is also important for the growth of *B. thuringiensis*. The presence of magnesium, calcium, manganese, iron, zinc, cooper and potassium is highly recommended in the medium. Manganese is considered essential for growth and endospore formation (Arcas et al., 1984).

The possibility of attaining high yields of spore-crystal preparations during the growth of *B. thuringiensis* subsp. *kurstaki* and *entomocidus* using a cheap medium was studied by Salama et al. (1983). These authors studied a variety of agro-industrial products, including cotton seed meal, fish meal, beef blood and corn steep liquour as possible medium ingredients. These authors obtained a yield of 40 X 10^7 spores /mL using a medium with cotton seed meal without glucose and yeast extract. Arcas, et al., (1984) substituted corn steep liquour and malt extract for yeast extract in media composition while growing *B. thuringiensis* subspecies *kurstaki*. Pearson and Ward (1988) used molasses, corn steep, soya flour, and starch. Results presented in all these studies did not show enough information to select the best agro-industrial products to be used in growth media for the cultivation of *B. thuringiensis*. In fact, a comparison with defined media was absent in these studies. Therefore the selection of a cheap complex medium is still an open area of research.

In addition, Anderson (1990) studied the carbon/nitrogen ratio in a glucose-yeast extract-soya peptone-salts medium for the culture of *B. thuringiensis* subspecies *kurstaki*. Anderson (1990) found that a carbon/nitrogen ratio of 7.5/1 was optimum for the production of delta-endotoxin.

The metabolism of *B. thuringiensis* was studied by several researchers (Rowe, 1990; Aronson et al., 1975; Yousten and Rogoff, 1969; Nickerson and Bulla, 1975). Figure 2.1 shows the metabolism of *B. thuringiensis* as described by Aronson et al. (1975). *B. thuringiensis* catabolizes glucose during vegetative growth over the Embden-Meyerhof-Parnas (EMP) pathway and the pentose-phosphate (PP) pathway (Nickerson et al., 1974; Bulla et al., 1969). The EMP pathway serves primarily for the degradation of glucose to pyruvate and acetate. The accumulation of these organic acids is responsible for the drop in

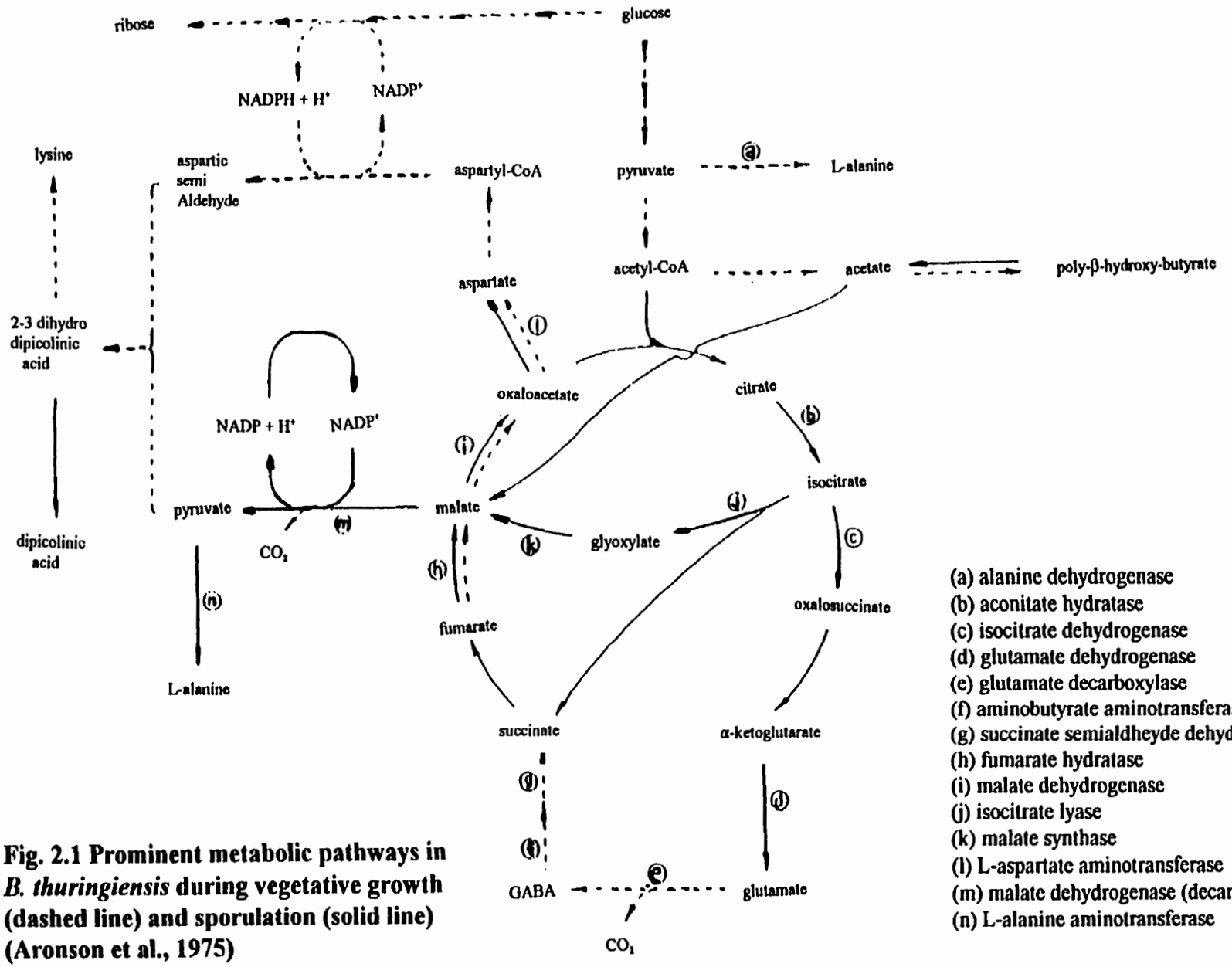

Fig. 2.1 Prominent metabolic pathways in *B. thuringiensis* during vegetative growth (dashed line) and sporulation (solid line) (Aronson et al., 1975)

(a) alanine dehydrogenase
(b) aconitate hydratase
(c) isocitrate dehydrogenase
(d) glutamate dehydrogenase
(e) glutamate decarboxylase
(f) aminobutyrate aminotransferase
(g) succinate semialdheyde dehydrogenase
(h) fumarate hydratase
(i) malate dehydrogenase
(j) isocitrate lyase
(k) malate synthase
(l) L-aspartate aminotransferase
(m) malate dehydrogenase (decarboxylating)
(n) L-alanine aminotransferase

pH of the culture medium during the vegetative growth (Luthy et al., 1982). Following this stage and during the transition from growth to sporulation, enzymes of the tricarboxylic acid (TCA) cycle are synthesized. As well, pyruvic and acetic acids that accumulated during vegetative growth are oxidized in the early stages of the sporulation process (Bulla et al., 1971).

B. thuringiensis uses a modified TCA cycle which catabolizes glutamate and α-ketoglutarate via the γ-aminobutyric acid (GABA) pathway (Aronson et al., 1975). The GABA pathway transforms glutamate to succinate by the action of the enzymes glutamate dehydrogenase, aminobutyrate aminotransferase and succinate semialdehyde dehydrogenase. Then succinate is transformed by two enzymes of the second part of the tricarboxylic acid cycle, fumarate hydratase and malate dehydrogenase (Luthy et al., 1982).

At the end of the vegetative growth, the exhaustion of the medium induces the initiation of the sporulation. The stationary state begins and the cells start a morphological transformation which leads to the formation of the spore. The TCA cycle is coordinated with the beginning of sporulation and supplies the cells with energy and carbon for aminoacids synthesis (Luthy et al., 1982). *B. thuringiensis* uses an incomplete TCA cycle through the action of two key enzymes, isocitrate lyase and malate synthase, which transform isocitrate to malate through the glyoxylic acid pathway (Luthy et al., 1982; Aronson et al., 1975).

A polymer of β-hydroxybutyric acid is a major component of bacterial lipid granules. The existence of this polymer, formed in the presence of glucose in the medium, has been related with the refractile fatty cytoplasmic granular material exhibited by *Bacillus* species. The depletion of this polymer in the later stages of growth suggests a storage function (Macrae and Wilkinson, 1958). Production of this polymer in *B. megaterium* was studied by Slepecky and Law (1961). These authors observed that this polymer was formed during the growth stage, reached a maximum at the time cells entered the stationary phase, and decreased with the formation of spores. Thus, there was indication that the polymer was

utilized by the cells during spore formation, suggesting that sporulation and polymer consumption were connected.

In order to elucidate spore formation, electron microscopy has been employed. The spore formation mechanism has been subdivided into seven stages (I-VII), (Luthy et al., 1982) (Fig. 2.2). During stage I an elongated axial filament is formed, and a forespore septum is initiated during stage II. The area of cytoplasm destined to be incorporated into the forespore is termed incipient forespore (Bulla et al., 1980).

Stage III includes the engulfment of the forespore. The septum forms an apex pointed towards the mother cell cytoplasm with the junction of the forespore septum and plasma membrane pointing towards one of the poles of the cell. Mesosomes are present at the junction of the septum and plasma membrane during engulfment (Bulla et al., 1980). Once the engulfment is completed the septum becomes detached from the plasma membrane isolating the incipient forespore from the mother cytoplasm. *B. thuringiensis* cells that have reached this stage are not able to reverse to the vegetative growth and therefore are fully committed to sporulation (Bechtel and Bulla, 1976).

The parasporal crystal of *B. thuringiensis* is observed during the engulfment (stage III) with already the characteristic crystal lattice fringes. Finally, the crystal is almost full sized at the time that the exosporium appears (stage IV) (Bechtel and Bulla, 1976).

Following the engulfment, numerous other processes occur, including primordial cell wall and cortex synthesis, exosporium formation, development of the spore coats, and transformation of the spore nucleoid. The primordial wall is the first part of the spore wall to form during the stage IV. During this stage, the lamellar spore coat is formed, the primordial wall thickens, and the exosporium engulfs the spore. Once the primordial wall has attained the maximum thickness, the cortex develops (stages IV to VI). The cortex is located between the primordial wall and the outer forespore membrane and the undercoat is located between the spore coat and the outer membrane. All these layers define the structure of the mature

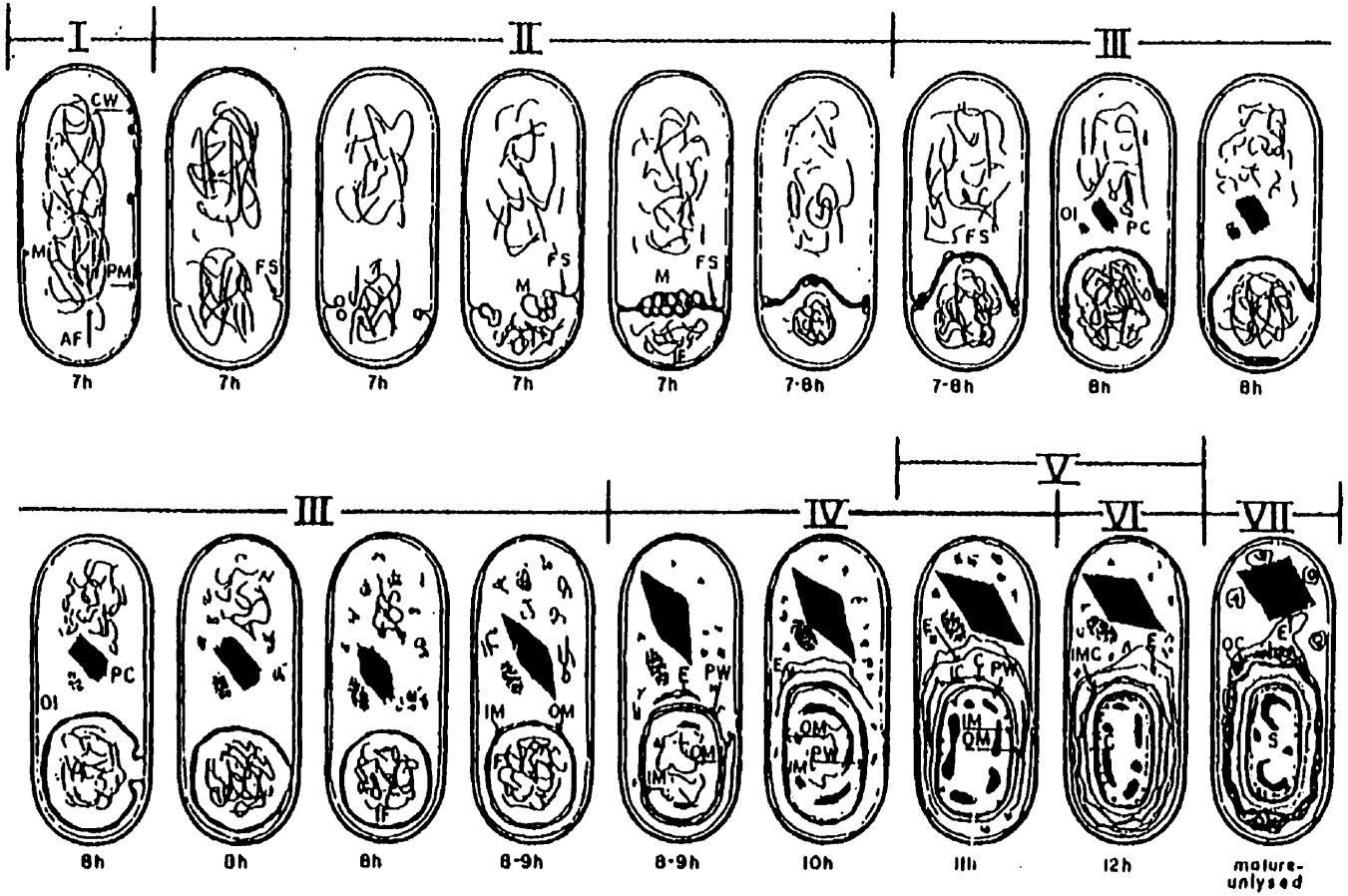

Fig. 2.2 Diagramatic scheme of sporulation in *B. thuringiensis*. Abbreviations: M, mesosome; CW, cell wall; PM, plasma membrane; AF, axial filament; FS, forespore septum; IF, incipient forespore; OI, ovoid inclusion; PC, parasporal crystal; F, forespore; IM, inner membrane; OM, outer membrane; PW, primordial cell wall; E, exosporium; LC, lamellar spore coat; OC, outer spore coat; C, Cortex; IMC, incorporated mother cell cytoplasm; S, mature spore in an unlysed sporangium. (Bulla, L.A., and Bechtel, D.B., 1976)

spore as illustrated in Fig. 2.2. Fig. 2.3 also shows a diagram of this structure providing additional details (Bulla et al., 1980). Beginning with the spore cytoplasm (S) the spore walls components are: inner membrane (IM), primordial cell wall (PW), cortex (C), undercoat (UC), lamellar spore coat (LC), outer fibrous spore coat (OC), and exosporium (E).

2.3 Crystal Protein: properties, composition, and production

During sporulation of *B. thuringiensis* the spore and the protein parasporal inclusion are formed within each cell. The crystal protein or delta-endotoxin is of a regular and bipyramidal shape. The crystals are composed of glycoprotein toxin units whose molecular weight is approximately 68,000 daltons (Bulla et al., 1979). These crystals contain no nucleic acids (Monro, 1961). The crystals are insoluble in water and they can be dissolved under alkaline conditions or in the presence of a denaturant reagent (Bulla et al., 1977). The parasporal crystal, when dissociated by mild alkali titration, is made up of many subunits whose molecular mass is approximately 138,000 daltons (Bulla et al., 1981).

In order to establish the molecular weight and aminoacid composition of crystal proteins, the toxin proteins have been studied in detail through polyacrylamide gel electrophoresis (Hofte and Whiteley, 1989). These studies have resulted in a complete description of the molecular weight and amino acid composition of crystal proteins.

In this respect, Debabov et al. (1984) concluded that all delta-endotoxins from *B. thuringiensis* variants are made up of similar but not identical proteins, and have the same crystal structure. These authors compared the molecular weight of proteins from crystals of different *B. thuringiensis* strains. Some different strains contained proteins with the same molecular mass. For example, the varieties *alesti* (III) strain 1225, *kenyal* strain 1228, *dendrolimus* strain 1277, *morrisoni* strain 1252, and *darmstadiensis* strain 1154 contained a 135,000 daltons protein.

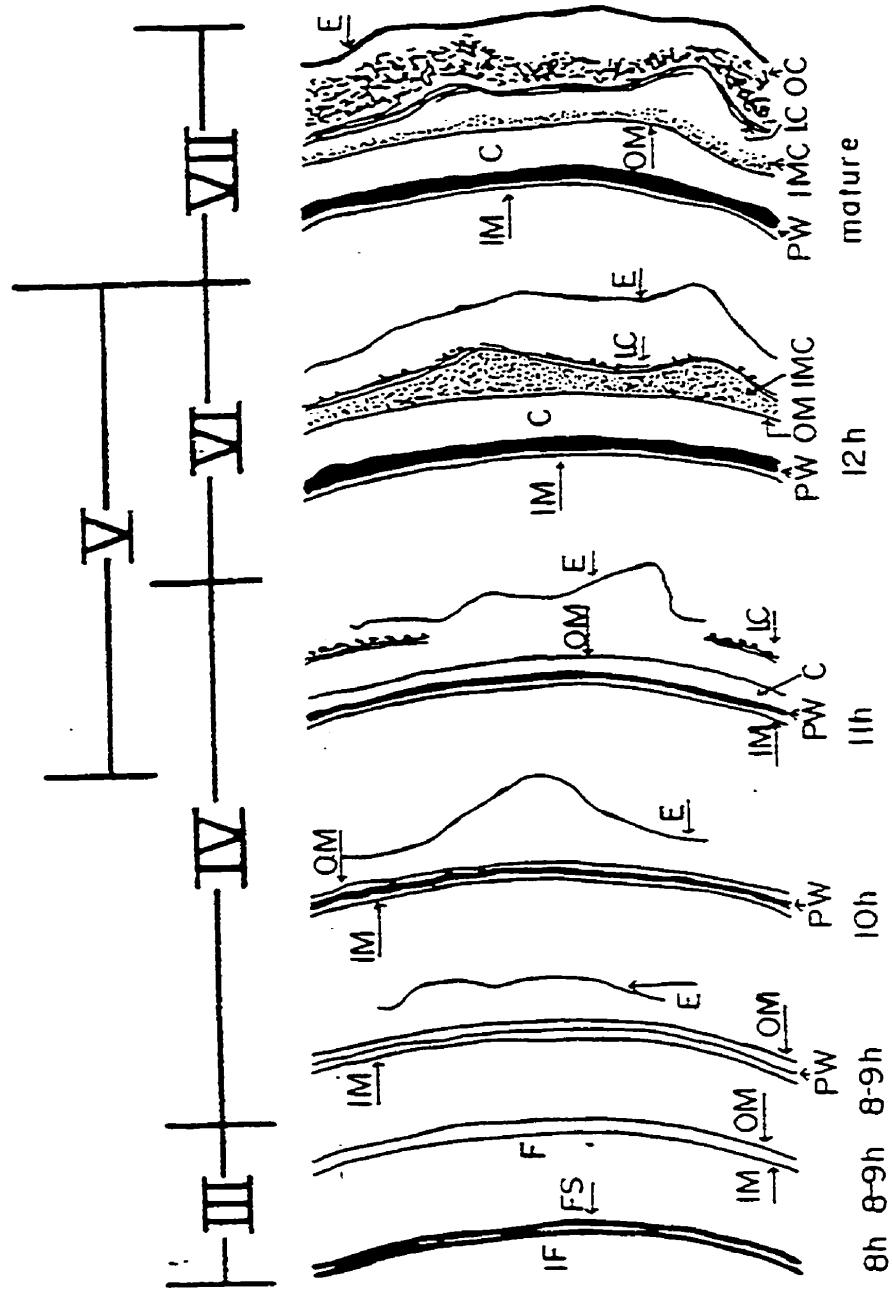

Fig. 2:3 Diagramatic scheme of spore wall elaboration in *B. thuringiensis*. Symbols same as Fig. 2.2 (Bulla, L.A., and Bechtel, D.B., 1976)

The amino acid content of the crystal protein has also been determined. For example, Debabov et al. (1984) determined the amino acid composition of crystal-forming protein of *B. thuringiensis* subsp. *alesti* while Tyrell et al. (1981) elucidated the amino acid composition of the crystal protein for *B. thuringiensis* subsp. *kurstaki, berliner, alesti, tolworthi*, and *israelensis.*

It can be concluded that many strains produce several crystal proteins simultaneously and that the same (or very similar) crystal proteins occur in *B. thuringiensis* strains in different subspecies (Hofte and Whiteley, 1989).

The structure of the crystal protein has been studied by Holmes and Monro (1965) using X Ray Diffraction, while Li et al. (1991) examined the structure of the delta-endotoxin from *B. thuringiensis* subspecies *tenebrionis* and reported a three dimensional diagram of the CryIIIA.

While the crystal protein is formed during sporulation, studies of mutants demonstrated that the synthesis of the crystal and sporulation are apparently not dependent on each other (Wong et al., 1983). The crystal protein is derived entirely from material present in vegetative cells, with at least 80% of the crystal protein synthesized from aminoacids arising through the breakdown of other proteins (Monro, 1961).

2.4 Plasmids and crystal protein production

The irreversible loss, in some *B. thuringiensis* strains, of the ability to produce the insecticidal crystal protein (ICP) has suggested that the ICP is encoded in plasmids. To clarify this point, several investigations on the timing of the ICP have shown that ICP is produced at the beginning of the stage II of sporulation (Fig. 2.2) with its synthesis continuing until late sporulation (stage V). For example, crystals are detected in most sporulation mutants blocked at stage II or later, but mutants blocked at stage 0 of sporulation fail to make the ICP.

Acrystalliferous mutants on the other hand, sporulate normally. This indicates that although ICP production is not a necessary condition for sporulation, at least some of the factors regulating sporulation are required for ICP synthesis (Schnepf and Whitley, 1985).

Several studies on *B. thuringiensis* plasmids have been made by Carlton and Gonzalez (1985a, 1985b, 1984, 1980), Gonzalez et al., (1981), and Lereclus et al. (1982). Each strain contains its own array of multiple extra-chromosomal DNA elements. The number of plasmid size classes per strain ranged from one to 12 and their molecular weight from 1.5 Md. to 150 Md.

Another important matter is the loss of crystal ICP production, which has been associated with the loss of plasmids. For example, Gonzalez et al. (1981) demonstrated that a 50 Md. plasmid of strain HD-73 was lost in the Cry^- mutants, while retaining a complex array of plasmid molecules. Then, in every strain, the loss of crystal production can be associated with the loss or modification of one specific plasmid molecule with the rest of the complex plasmid array being retained. Comparison of Cry^- and Cry^+ pairs of *B. thuringiensis* strains showed that each Cry^- variant lacks of one of the plasmids of its Cry^+ counterpart.

Hofte and Whiteley (1989) proposed a nomenclature and classification scheme for crystal proteins based on their structure as well as their host range. They classified 42 Bt crystal protein genes in 14 types, 4 major classes and several subclasses characterized by both the structural similarities and the insecticidal spectra of the encoded proteins. The four major classes were: Lepidoptera specific (*cry*I), Lepidoptera and Diptera specific (*cry*II), Coleoptera specific (*cry*III), and Diptera specific (*cry*IV) .

Each class can contain subclasses designated by capital letters (A, B, C and D) and secondary subclasses designated by lower case letters enclosed between parenthesis. Table 2.2 lists the insecticidal crystal protein genes of *B. thuringiensis* given by Hofte and Whiteley (1989).

Table 2.2 Insecticidal crystal protein genes of *B. thuringiensis* (a)

Gene type	Host range (b)	No. of amino acids	Predicted mol mass (kDa)
cryIA(a)	L	1,176	133.2
cryIA(b)	L	1,155	131.0
cryIA(c)	L	1,178	133.3
cryIB	L	1,207	138.0
cryIC	L	1,189	134.8
cryID	L	1,165	132.5
cryIIA	L/D	633	70.9
cryIIB	L	633	70.8
cryIIIA	C	644	73.1
cryIVA	D	1,180	134.4
cryIVB	D	1,136	127.8
cryIVC	D	675	77.8
cryIVD	D	643	72.4
cytA	D/cytol.	248	27.4

(a) From Hofte and Whiteley (1989)

(b) Specified host ranges: L, Lepidoptera; D, Diptera; C, Coleoptera; cytol, cytolitic and hemolytic

Many more insecticidal crystal protein genes of *B. thuringiensis* have been sequenced and analyzed. For example, Feitelson et al. (1992) added two new major classes *cryV* and *cryVI*. In this respect, the *B. thuringiensis cry* Gene Nomenclature Committee, a standing committee of the *Bacillus* Genetic Stock Center, defines *cry* as "a gene from *B. thuringiensis* encoding a parasporal inclusion protein that exhibits pesticide activity or is homologous to a known *cry* gene" (Kumar et al., 1996).

2.5 *B. thuringiensis* growth systems

2.5.1 Batch growth

Because the crystal protein is a secondary metabolite, the process most frequently used to produce delta-endotoxin from *B. thuringiensis* is the batch growth (Bryant, 1994; Avignone-Rossa and Mignone, 1995; Rowe and Margaritis, 1987).

A batch growth is a non-steady state process; that is, the content of the bio-reactor changes with time. The nutrients and the inoculum are added to the bio-reactor at the beginning of the batch operation and air is supplied continuously. After a short lag time, *B. thuringiensis* cells begin the exponential growth; the carbon source is oxidized and owing to organic acids accumulation, the pH drops dramatically. The biomass concentration and the cell count increases as the carbon source decreases. The oxygen demand increases during the exponential stage and there are no spores present in the bio-reactor (Avignone-Rossa and Mignone, 1995).

Batch growth of *B. thuringiensis* can be divided in two stages. In the first stage, the nutrients are consumed and the vegetative growth takes place. As nutrients are consumed, the second stage begins and sporulation is initiated. The mechanism of spore formation was reported in section 2.2. The process is completed with the rupture of the cellular wall and the spore-crystal complex is released into the medium.

Batch culture of *B. thuringiensis* has been the most commonly process used for studies of metabolism (e.g. Rowe, 1990) and the effect of medium composition on cell growth (e.g. Anderson, 1990).

As well, other researchers used the batch operation for comparison with other modes of growth as a reference. Liu et al. (1994) compared the results obtained in a batch growth with a fed-batch growth of *B. thuringiensis* subspecies *kurstaki*. The maximum biomass concentration obtained in batch growth was 5.9 g D.W./L whereas the maximum biomass concentration was 53.7 g D.W./L in fed-batch growth. Jong et al. (1995) used a batch growth of *B. thuringiensis* subsp. *darmstadiensis* to compare its results with a fed-batch growth in an airlift bioreactor.

Batch growth has been used mainly to study the nutrient requirements and the formation of spores. However, the kinetics of *B. thuringiensis* in batch growth has not been studied extensively. Sakharova et al. (1985) studied the kinetics of the growth of *B. thuringiensis* subsp. *galleriae*. The medium was composed of glucose, yeast extract, and

salts, air was supplied at 0.25 L/liter medium-min, and the temperature was kept constant at 30 °C. The cell titer, spore titer, crystal titer, residual glucose concentration, and pH was recorded with respect to time. On this basis, the specific growth rate and the specific rate of glucose consumption were calculated. The maximum specific growth rate was estimated in 1.4 h^{-1}. A kinetic model, however, was not established and the effect of changes in the metabolism of *B. thuringiensis* cells on the cell growth was not studied in detail.

Holmberg and Sievanen (1980) discussed the complexity of batch growth and of the estimation of kinetic constants. However, these authors used the largely inadequate classical growth kinetic and Monod models for describing a non homogeneous and an unbalanced bacterial growth. Given the importance of this topic, a suitable kinetic model is being developed in the present dissertation.

The maximum specific growth rate reported by other researchers ranges from 0.4 to 1.9 h^{-1} (Avignone-Rossa and Mignone, 1995; Rodriguez-Monroy and de la Torre, 1996). This wide variation in the values for the maximum specific growth rate demonstrates the lack of a systematic study of the growth kinetics of *B. thuringiensis*.

2.5.2 Fed-batch growth

Fed-batch growth is considered appropriate to obtain a high cell density of microbial cells. It has the advantage of actively controlling the extracellular environment and creating of nutrient deficiency to initiate sporulation (Liu et al., 1994).

B. thuringiensis varieties have been cultured in fed-batch bio-reactors in order to obtain a higher productivity compared with that obtained using a batch bio-reactor. (Kang et al., 1992; Avignone-Rossa and Mignone, 1993; Liu et al., 1994; Stradi, 1992).

A fed-batch bioreactor can be operated at constant or variable volumetric flow rate of the feed stream. Although the decision to use a constant or variable volumetric flow rate should in principle be based on the study of the growth kinetics, the fed-batch growth conditions for *B. thuringiensis* continued to be implemented using a quite empirical approach.

Given that he main purpose of fed-batch operation is to increase productivity, Stradi (1992) explored the effect of the changes in the feed stream glucose concentration on delta-endotoxin production. The productivity of delta-endotoxin was found to be four times higher in fed-batch than in a batch bioreactor. However, the volumetric flow rate of fresh medium in that study was intermittent and therefore, the possible extrapolation of these results remains unclear.

Kang et al. (1992) found that a constant feed flow rate in a fed-batch culture did not produce sporulated cells even after cells were subsequently kept in the reactor in batch operation. This result does not agree with the reports for other *B. thuringiensis* cultures indicating that sporulation occurred when the culture is in glucose limited conditions or during continuous culture at slow growth rates. It should be mentioned, however, that an intermittent addition of fresh glucose in the feed stream during the fed-batch growth gave better results, with a biomass concentration of 72.6 g/L and 1.25×10^{10} spores/mL being obtained. While these results are intriguing, the authors did not explain the reasons why the fed-batch bioreactor gave better results with an intermittent glucose supply.

Liu et al. (1994) studied the effect of several feeding strategies on vegetative cell growth, spore formation, crystal protein content, carbon dioxide production, and oxygen consumption in a fed-batch growth of *B. thuringiensis* subspecies *kurstaki*. The conditions for operation of the fed-batch bio-reactor were determined based on a desired biomass concentration to be achieved at the end of the process. The glucose feeding rate (g/min), was varied during the fed-batch run in order to meet the demand of cells growing at a constant specific growth rate. At the end of the fed-batch operation, the reactor was operated as a batch bio-reactor in order to allow the cells to sporulate. The spore count per milliliter of

broth increased proportionally with the cell density. In this case, it was not possible to have spore and crystals during the operation of the fed-batch bio-reactor.

Avignone-Rossa and Mignone (1993) studied the spore count and toxicity of batch and fed-batch cultures of *B. thuringiensis* subspecies *israelensis*. While the fed-batch growth produced a higher concentration of biomass and spores, compared with those obtained in the batch growth, the levels of toxicity found in fed-batch culture were lower than those attained in the batch culture.

In summary, even though it has been possible to obtain a high cell density of *B. thuringiensis* in fed-batch cultures, there still is no reliable procedure for the operation of these units under optimum conditions. The approach, as reported in the literature based on the determination of the limiting substrate concentration and/or the volumetric flow rate of the feed stream is not satisfactory. It is in this context that it is important to develop of a suitable kinetic model, as attempted in this study, to provide a deeper understanding of optimum conditions for *B. thuringiensis* cultures.

2.5.3 Continuous growth

The continuous culture of a sporogeneous microorganism presents special challenges given two opposing conditions that have to be maintained within the process: a) those facilitating accumulation of microbial biomass and b) those favouring conversion of this biomass into spores.

The continuous growth of *B. thuringiensis* has been studied with the aim of increasing the production of crystal protein. A continuous two-stage system was used to increase the cell mass production in the first stage and to encourage the sporulation of cells in the second stage (Freiman and Chupin, 1973; Khovrychev et al., 1985). The results of these studies are preliminary and inconclusive. Khovrychev et al. (1987) studied the continuous

culture of *B. thuringiensis* subspecies *galleriae* using two-stage continuous system. During the first stage, vegetative growth of the cells occurred, while during the second stage formation of spores and protein took place. In order to obtain sporulation in the second reactor, the authors suggested to use a ratio of the dilution rate in the first stage over the dilution rate in the second stage of four or higher. However, the authors did not report the relationship between the dilution rate and the metabolic state of *B. thuringiensis* cells or the required operational dilution rate to obtain sporulated cells. Freiman and Chupin (1973) used a similar approach. However, these authors could not obtain a high degree of sporulation in the second reactor, and also used the second reactor in the batch mode to obtain free spores and crystals.

Another interesting alternative in a continuous process is the use of a tubular or continuous plug flow reactor (CPFR) for producing delta-endotoxin from *B. thuringiensis*. Moser (1990) discusses the advantages of using a tubular bio-reactor instead of a batch reactor for this purpose. However, some practical problems may arise, such as the need of an effective air supply, the control of the flow regime and the possible migration of cells toward the section of the reactor that contains more nutrients.

One of the main problems of continuous culture is the emergence of non spore forming cells. These non-spore forming cells correspond to the spontaneous mutation of cells to either asporogeneous or acrystalliferous mutants (Boudreaux and Srinivasan, 1981). Sachidanandham and Jayaraman (1993) observed the formation of spontaneous asporogenic (Spo^-) and crystalliferous (Cry^+) variants of *B. thuringiensis* var. *galleriae* under continuous culture. The cessation of sporulation also affected the crystal assembly, producing a crystal protein with low toxicity. These authors suggested that the sporulation was interrupted given the lack of use of optimum medium components. This hypothesis was supported by Sachidanandham et al. (1997), who showed that the addition of a group of amino acids to the medium improved the stability of the culture and the volumetric productivity of biomass. Continuous cultures carried out using an amino acid supplemented medium showed no asporogeneous variants, and the formation of spores and larvicidal potency was increased.

Afkhami et al. (1993) found that the temperature had a marked effect on toxin synthesis in continuous cultures. Crystal production was the highest at 25 °C and the lowest at 42 °C. Also these authors reported the presence of two acrystalliferous mutants of *B. thuringiensis* 81, one of which was asporogeneous. Thus, the formation of spores with a lack of crystal protein in the culture indicated the inability to synthesize the crystal protein was not related with a sporulation defect in this strain.

The lack of formation of crystal protein during *B. thuringiensis* culture has been associated with the loss of plasmids. In this respect, Kamda and Jayaraman (1983) observed the spontaneous formation of an acrystalliferous strain when *B. thuringiensis* var. *israelensis* H-14 was cultured. The analysis of the acrystalliferous strains showed the loss of a high molecular weight plasmid.

Some studies demonstrated that *Cry* genes are carried on plasmids (Carlton and Gonzalez, 1985a, 1985b, 1984, 1980), Gonzalez et al. (1981)) where the absence of some or all of these plasmids causes an increase in acrystalliferous mutants. However, in some cases the formation of acrystalliferous mutants might be due to other factors. Roy et al. (1987) reported the formation of asporogeneous and acrystalliferous variants during a continuous phase culture of *B. thuringiensis* var. *kurstaki* (HD-1). The plasmid profile remained constant throughout 328 h of cultivation. These authors could not find any evidence for plasmid segregational instability during the continuous phased culture.

Selinger et al. (1988) investigated the growth, sporulation, insecticidal crystal protein production, and plasmids of *B. thuringiensis* var. *kurstaki* (HD-1) during batch and continuous phased cultivation. During the batch culture, 93% of the cells sporulated and produced insecticidal crystal protein within 10 h of commencement of stationary phase, whereas in continuous phase culture, the population shifted toward a predominant asporogenous and acrystalliferous state after 25 cycles. Examination of the plasmid profiles showed that segregational instability was not present. These authors suggested that the

asporogeneous variants arising during continuous culture were mutants blocked early in the sporulation.

The formation of asporogeneous cells also has been reported by Kang et al. (1993) in a culture of *B. thuringiensis* subspecies *kurstaki* grown in a two-stage continuous culture using an internal ceramic membrane filter system.

In summary, the exact mechanism leading to loss of the ability to produce the crystal protein by *B. thuringiensis* has still to be elucidated (Sachidanandham and Jayaraman 1993). The absence of crystal production in a *B. thuringiensis* culture might be due to a blockage in the formation of the spore in the early stages of sporulation, a loss in one or some plasmids (segregational instability), and/or an spontaneous mutation (structural instability).

While the formation of asporogenous and acrystalliferous mutants is not exclusive to cells cultivated in a continuous bio-reactor, this problem is more evident during a continuous growth. Having the complete set of plasmids or the ability to form spores causes in the cells a lower growth rate compared with that of cells without this metabolic burden. As a result, in a continuous culture the population with the highest growth rate has a competitive advantage over the cells with the ability to produce the spore-crystal complex. Therefore, it can be expected that eventually the continuous reactor operation may drift towards a condition where only cells with no ability to produce spores remain.

2.6 Conclusions of the literature review

This literature review shows that *B. thuringiensis* needs a carbon source, amno acids, and salts for its growth. On this basis, a medium containing glucose, bacto peptone and salts were chosen for use in this study.

Based on the information provided in the literature about the metabolic changes during cell growth and the process of spore formation, it can be stated that *B. thuringiensis* cells change their morphology depending on the metabolic state. For example, during the transition stage, granules of the polymer β-hydroxy butiric acid are expected to be present in the cell, while the pH of the medium should increase as a consequence of the consumption of pyruvic and acetic acids. This information will be helpful to relate the metabolic state with the cell growth rate during the culture of *B. thuringiensis* at different bioreactor operations.

This literature review also reveals the lack of a systematic kinetic study and the associated kinetic model for *B. thuringiensis* growth, whch has a negative impact on accurate predictions while developing this culture in various reactor configurations and different operating conditions. Thus, based on the available information, this work is aimed to determine the effect of the sporulation process on cell growth, and to establish a reliable kinetic model for *B. thuringiensis* growth.

According to the literature review, the different bioreactors used to culture *B. thuringiensis* have not presented optimum results. For example, fed-batch cultures have to be coupled to batch cultures to obtain the desired results. Moreover, as documented here, the continuous culture has in principle an associated higher productivity compared with that of a batch reactor. However, a continuous reactor is more difficult to operate, the spore and crystal formation by *B. thuringiensis* requires slow cell growth conditions, and in addition, there is the extra complication of potential formation of asporogeneous and acrystalliferous mutants.

CHAPTER 3

KINETICS OF CELL GROWTH.

3.1 Introduction

Modeling the cell growth process, assuming a homogeneous population and a balanced growth, requires an expression for the change in cell concentration with respect to time. The following equation represents the cell growth of unicellular microorganisms that reproduce by cell binary fission.

$$dX/dt = \mu X \tag{3.1}$$

where:

X	is the biomass concentration, g/L
t	is the time, h
μ	is a constant, h^{-1}

The specific growth rate, μ, is dependent on several factors, including, the growth medium composition, temperature, pH and dissolved oxygen, and is defined by equation 3.2.

$$\mu = (1/X)\, dX/dt \tag{3.2}$$

The specific growth rate depends on the limiting substrate concentration according to the Monod equation.

$$\mu = \mu_{max}\, S /(K_S + S) \tag{3.3}$$

Where :

μ	is the specific growth rate, h^{-1}
μ_{max}	is the maximum specific growth rate, h^{-1}
K_S	is the substrate saturation constant, g/L
S	is the limiting substrate concentration, g/L

Combining equations 3.1, and 3.3 gives the cell growth rate (dX/dt) illustrated in equation 3.4.

$$dX/dt = [\mu_{max} S /(K_S + S)] X \quad (3.4)$$

When the substrate concentration, S, is much higher than the saturation constant, K_S, the growth rate is a first order reaction rate and cell growth is described by the following equation:

$$dX/dt = \mu_{max} X \quad (3.5)$$

When the substrate concentration is very small compared with the saturation constant, the growth rate is a second order reaction rate and cell growth is described by equation 3.6.

$$dX/dt = (\mu_{max} / K_S) X S \quad (3.6)$$

In this case, the cell growth rate depends not only on the cell concentration, but also on the substrate concentration and a constant with two parameters (μ_{max} and K_S).

The substrate is consumed by the cells, and as a result the change in substrate concentration with respect to time is proportional to the biomass concentration and the yield coefficient.

$$dS/dt = - \mu X/Y_{X/S} \quad (3.7)$$

Where :

$Y_{X/S}$ is the cell growth yield, g cells produced/g substrate consumed

In a batch reactor, the growth rate changes as a consequence of the variation in substrate concentration and in metabolic state. These changes are represented by the four main phases of batch growth, namely, the lag phase, the exponential, transition, and stationary phases.

In a continuous reactor working at a given volumetric flow rate (or dilution rate), the substrate and cell concentrations, as well as all the environmental conditions in the reactor, are constant and thus, a constant growth rate is expected.

As previously illustrated the specific growth rate, μ, depends on the substrate concentration as described by the Monod model. The maximum specific growth rate, μ_{max}, is a constant defined as the specific growth rate when the substrate concentration approaches infinity or is at least very high compared with the saturation constant, K_s. Thus, the maximum specific growth rate is then a constant that determines the cell growth rate when there are no limitations for cell growth.

The saturation constant, K_s, is a measure of the affinity of the cell for the limiting substrate; the smaller the saturation constant, the higher the substrate affinity (Slater, 1990; Arbige et al., 1993). Unlike the maximum specific growth rate, which is a true constant, it has been suggested that the saturation constant may change with the specific growth rate, although in practice, this effect is negligible (Bazin et al., 1990).

3.2 Limitations of the cell growth model

The Monod model is a simplified and non structured model where the cell growth depends only on the substrate uptake rate (Arbige et al.,1993). This assumption implies that the cells are ready for the utilization of the substrate and that this state does not change during the cell growth. The cells however, may change their physiological state during their growth (Malek, 1968), and some studies have shown that the content of protein, DNA, RNA, and other chemicals in the cell, change with the specific growth rate (Stouthamer et al., 1990). Moreover, "the cell growth is determined by the intrinsic metabolic pathways rather than extrinsic factors" (Postgate and Calcott, 1990).

The Monod equation has been modified in order to account for the internal mechanisms of the cells during their growth. According to the substrate uptake enzyme (SUE) bottleneck theory (Pirt, 1990), the saturation constant from the Monod equation is related with the fraction α_m/α_0 where α_m and α_0 are the substrate concentration inside the cell reacting with enzymes of the cells when $\mu = \mu_{max}$ and $\mu = 0$ respectively. This bottleneck model gives meaning to the parameters of the Monod equation based on the kinetics of the enzymatic reaction. The specific growth rate, according to the bottleneck model, is given by the following equation:

$$\mu = \mu_{max}\, S/(\,(\,\alpha_m/\,\alpha_0)K_S + S) \qquad (3.8)$$

The usual cell growth kinetics model is based on an exponential cell growth (see equation 3.1) and on the Monod model. The exponential cell growth assumes that the culture is at balanced growth, that is, all cells have the same specific growth rate and also all cell components grow at the same rate. This condition can, strictly speaking, only be achieved when the cells are in a non-changing culture environment. In addition, the Monod model postulates a relationship between the specific growth rate and the limiting substrate concentration, and assumes that there are no other factors affecting the specific growth rate. While the Monod model is widely used, in some cases however, the hyperbolic function described by this model may not predict the specific growth rate with a change in substrate concentration. Thus, modifications have therefore been proposed (Arbige et al.,1993)

Cell growth is a complex process where cells do not form a homogeneous population. While the classical cell growth kinetic model does not accurately describe the process, the high number of cells present in a culture reduces the variability in the process and makes the typical cell growth kinetic model suitable for many cell growth cases. However, in the case of *B. thuringiensis*, the variability in the properties of the cells in a given population is increased when they change from vegetative to sporulated cells. Therefore, the classical growth kinetic model may in principle be challenged to describe *B. thuringiensis* cell growth kinetics. This matter is investigated in detail in the present study.

3.3 Modeling *B. thuringiensis* cell growth with sporulation

Optical microscopy and transmission electron microscopy observations in this study showed that *B. thuringiensis* cells change from vegetative to sporulated cells during batch growth. This change reduces the normal cell growth rate, and therefore, a simple growth model based on the existence of an homogeneous population and on a balanced growth cannot be used to describe this more complex process.

In this section a new growth model which accounts for the effect of the reduction in cell growth as a result of the evolution of the cells during their preparation to sporulate and their spore formation stage is proposed.

The classical cell growth kinetics model describes both changes in substrate and biomass with equations 3.1, 3.3 and 3.7. This model assumes that the cell growth is proportional to the total concentration of cells in the culture and that the specific growth rate follows the Monod model. However, during the batch growth of *B. thuringiensis* cells spores are formed. And as a result, the kinetic model has to be modified by introducing a factor that accounts for the reduction in the number of cells that are available for growth by binary fission.

The process can be summarized by stating that cells under study can either divide to form new vegetative cells or alternatively begin to form spores. These processes can be pictured as follows:

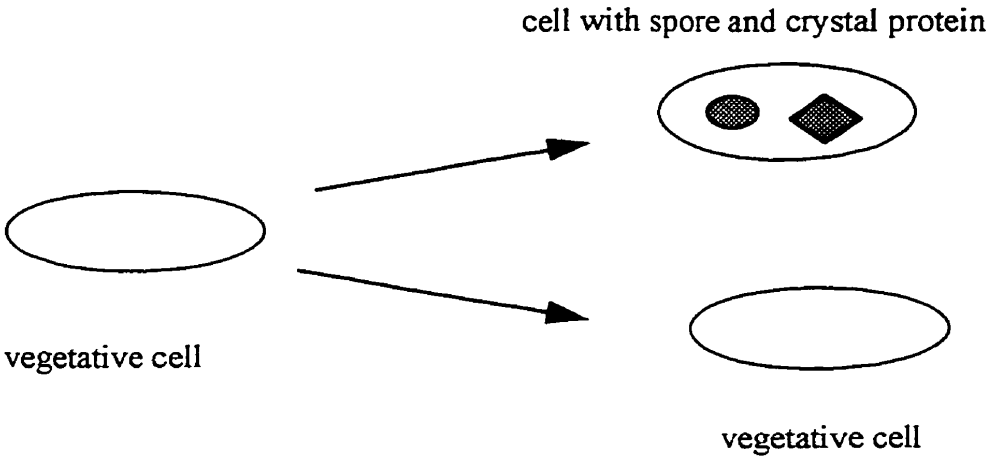

$$NX_v \xrightarrow{\mu} 2\,NX_v \qquad (3.9)$$

and

$$NX_v \xrightarrow{k_s} NX_s \qquad (3.10)$$

where:

- NX_v represents the number of vegetative cells (without a spore)
- NX_s represents the number of cells forming a spore.
- μ specific growth rate
- k_s rate constant for the formation of sporulating cells

As well, expressing the steps 1 and 2 in terms of mass concentration with the assumption that the mass/cell ratio is constant, the previous steps can be rewritten as:

$$X_v \xrightarrow{\mu} 2X_v \qquad (3.11)$$

and

$$X_v \xrightarrow{k_s} X_s \qquad (3.12)$$

where:

X_v represents the mass concentration of vegetative cells

X_s represents the mass concentration of spore forming cells

Thus, the change in the total cell mass is the sum of the rate of formation of the new vegetative cells and the rate of formation of the cells forming spore.

The new model was developed based on the accurate description of the cell growth of *B. thuringiensis* available in the literature. Studies on metabolism, spore and crystal protein formation, and batch cultures, provided valuable insights for the development of this new model. Also the optical and transmission electron microscopy observations made in this study were valuable to determine the growth stages. The most important considerations in the development of the model were the following:

a) There is a shift in the metabolism from vegetative to sporulating cells during a batch culture of *B. thuringiensis* (Luthy et al., 1982).

b) Spore and crystal protein formation begins as a consequence of the depletion of nutrients (Wong et al., 1983)

c) The formation of crystal proteins and spores involves a turnover of proteins. Thus, the spores and crystal proteins are formed with amino acids synthesized during the vegetative growth phase. (Monro, 1961)

d) There is a heterogeneous population during the batch culture and the spores and crystal proteins are formed mainly during the stationary growth phase. (Agaisse and Lereclus, 1995)

e) The relationship between vegetative cell growth and limiting substrate concentration is described by the Monod model. (Holmberg and Sievanen, 1980)

The main goal of the development of the new model was to find a kinetic growth model that could describe the batch growth accurately during all the growth phases. To do so, the classical model was modified by adding an extra term that considers the slowdown in the growth rate as a consequence of the spore formation process.

The new growth kinetic model incorporates the following assumptions:

1. There are two types of cells, those with the ability to divide and those that have lost this ability because they have begun to form a spore.

2. The cell growth is caused only by the division of those cells with no spore.

3. The cell growth is slowed down by the generation rate of spores forming cells.

4. The substrate depletion is mainly due to its consumption by the cells still active in the binary division process.

5. The cell mass is proportional to the number of cells, (i.e. the mass per cell is constant) and thus, the biomass concentration is used in the derivation of the equations of the model to represent the increase in the number of cells in the culture.

6. The death of vegetative cells is negligible and it was not considered in the model

Given the conservation of cellular mass, the total concentration of cells at any time in the process, X, is equal to the concentration of those cells with complete ability to divide, X_v plus the concentration of sporulating cells (which have lost the ability to divide) X_s.

$$X = X_v + X_s \tag{3.13}$$

Then, the change in total biomass concentration has to be the sum of the change in the vegetative cells and the change in spores-forming cells.

$$dX/dt = dX_v/dt + dX_s/dt \tag{3.14}$$

As a result, in the growth process of *B. thuringiensis* the change in substrate concentration is expected to be proportional to the vegetative cells concentration (X_v) and to the specific growth rate (μ).

$$dS/dt = - \mu (X-X_s)/Y_{X/S} \tag{3.15}$$

In this case, $\mu = \mu_{max} S/(K_s + S)$, according to the Monod model. Consequently, the substrate consumption rate can be given by equation 3.16

$$dS/dt = - [\mu_{max} S/(K_s + S)] (X-X_s)/Y_{X/S} \tag{3.16}$$

At the same time, in this system the net cell growth will be the result of the competitive contribution of the rate of cell growth, proportional to X_v, and the rate of cell sporulation, proportional as well to X_v.

The rate of formation of sporulating cells can be modeled as being proportional to the non-sporulating cells.

$$dX_s/dt = k_s X_v \quad (3.17)$$

The cell division rate is determined by the number of vegetative cells (NX_v) available to divide and according to the stoichiometry of the process (eqs. 3.9 and 3.10) for each cell converted to a spore-forming cell (NX_s), two new cells will not be formed. Therefore, the net rate of formation of cells without spore is given by the division rate of cells itself minus two times the rate of cells forming spores (equivalent to a rate of loss of division ability).

$$dX_v/dt = \mu X_v - 2(k_s X_v) \quad (3.18)$$

Then the change in the biomass concentration can be described by the following equations:

$$dX/dt = dX_v/dt + dX_s/dt = \mu X_v - 2(k_s X_v) + k_s X_v \quad (3.19)$$

$$dX/dt = \mu X_v - k_s X_v \quad (3.20)$$

or

$$dX/dt = \mu (X - X_s) - k_s (X - X_s) = (\mu - k_s)(X - X_s) \quad (3.21)$$

In summary, the proposed new model that includes cell sporulation is formed by a set of three differential equations for the substrate, the cells, and the sporulating cells respectively.

1. Substrate consumption.

$$dS/dt = - [\mu_{max} S/(K_s + S)] (X-X_s)/Y_{X/S} \quad (3.16)$$

2. Total cells

$$dX/dt = ([\mu_{max} S/(K_s + S)] - k_s) (X - X_s) \quad (3.22)$$

3. Sporulating cells

$$dX_s/dt = k_s (X - X_s) \quad (3.23)$$

Simultaneous numerical solution of these three equations provides the changes in substrate concentration (S), total cell concentration (X) and forming-spore cell concentration (X_s).

3.4 Batch growth

Batch growth takes place in a closed vessel where a constant liquid volume of nutrient medium is inoculated with the microorganism to be grown. The batch bioreactor can be considered to be a closed system because there is no input or output of material, although for aerobic microorganisms air must be supplied into the reactor. After inoculation, the microorganisms begin to grow according to equation 3.1, until a substrate component is exhausted or an inhibitor accumulates. In the beginning of a batch growth, the cells are in an environment rich in nutrients which are consumed with time, and eventually the cell growth stops when one of the essential nutrients is depleted.

Batch growth has three main phases: the lag, the exponential, and the stationary phases. The lag phase is characterized by the absence of change in the number of cells and it has been associated with a period of adaptation of the cells to the new environmental conditions. During the exponential phase, the cells divide actively, producing an exponential population growth. Finally in the stationary phase, growth stops due to a lack of nutrients.

Cell growth is determined by the presence of nutrients and usually one limiting nutrient or substrate affects the specific growth rate. The effect of the substrate concentration on the specific growth rate is given by the Monod relation (equation 3.3). As a result of the consumption of the substrate during batch growth the specific growth rate changes with time. Therefore, the cell concentration also changes with time depending on the specific growth rate and the cell concentration. The mass balance in a batch reactor gives the design equations for this reactor:

$$r_x = \mu X = dX/dt \qquad (3.24)$$

where:

r_x represents the cell growth rate

The substrate concentration varies during batch growth according to the following equation and is based on a substrate mass balance in the batch reactor as follows:

$$r_s = - \mu X/Y_{X/S} = dS/dt \qquad (3.25)$$

Where :

$Y_{X/S}$ is the growth yield, g cells/g substrate

r_s is the substrate consumption rate

The solution of the differential equations 3.24 and 3.25 gives the variation in biomass and substrate concentrations with growth time. Equation 3.26 is the solution of the equations 3.24 and 3.25 derived by Pirt (1975), with the assumption that $Y_{X/S}$, K_s and μ_{max} are constants during batch growth.

$$P \ln(X/X_0) - R \ln \{ (Y S_0 + X_0 - X)/Y_{X/S} S_0 \} = \mu_{max} t \qquad (3.26)$$

Where:

$$P = (K_S\ Y_{X/S} + S_0\ Y_{X/S} + X_0)/(Y_{X/S}\ S_0 + X_0)$$

$$R = (K_S\ Y_{X/S})/(Y_{X/S}\ S_0 + X_0)$$

S_0 is the initial substrate concentration in the batch bioreactor, g/L

X_0 is the initial biomass concentration in the batch bioreactor, g/L

When the substrate concentration is much higher than K_s, the specific growth rate is approximately equal to the maximum specific growth rate ($\mu = \mu_{max}$). Assuming that the specific growth rate is constant, equation 3.24 can be integrated to give the following equation, where X_i and t_i are the biomass concentration and the time when μ approaches μ_{max}.

$$\ln (X/X_i) = \mu_{max}\ (t-t_i) \qquad (3.27)$$

Equation 3.27 describes an exponential cell growth (i.e. the exponential growth phase). Theoretically, the maximum specific growth rate can be estimated with equation 3.27 during the exponential phase of the batch growth.

The estimation of the kinetic constants (μ_{max} and K_s) using batch culture experimental data has several limitations. The specific growth rate is equal to the maximum specific growth rate only when the substrate concentration is very high compared with the saturation constant. Achieving this condition is not always feasible. In addition, this condition lasts only for a short time making the determination of the maximum specific growth rate difficult with batch growth experimental data obtained under common laboratory conditions.

The absence of a balanced growth compounds this problem, making the use of equation 3.24 questionable. Moreover, environmental conditions change constantly and the cells can modify their growth rate depending on the state of their metabolic processes. The growth rate, therefore, is not only affected by the substrate concentration, but also by cell metabolic state.

It is a common practice to estimate the specific growth rate with experimental data obtained at the beginning of the exponential growth phase in batch cultures. This is reasonable

given the concentration of substrate is a maximum at this condition and the microorganisms are ready to use it. However, the substrate concentration at the beginning of the exponential growth stage is not necessarily very high compared with K_S.

Given these experimental problems and that batch cultures do not represent a balanced growth, the estimated specific growth rate may not be the true maximum specific growth rate (μ_{max}). Despite these limitations, the scientific literature tends to accept these estimates as true maximum specific growth rate values.

While equations 3.24, and 3.25 describe the change in biomass and substrate concentrations in a batch culture with a homogeneous population and a balanced growth, the spore formation in *B. thuringiensis* makes necessary the modification of these equations as in equations 3.16, 3.22 and 3.23. The numerical solution of this set of equations provides the change in biomass and substrate concentrations for cultures under spore formation condition.

3.5 Fed-batch growth.

A fed-batch culture is an intermittent process. A reactor with a small volume of medium is inoculated with a cell suspension and fresh medium is fed to the reactor, increasing the reaction volume. The cells remain in the reactor until they are harvested at the end of the run. Fig. 3.1 shows a diagram of a fed-batch reactor.

A fed-batch reactor can be operated at a constant or variable feed volumetric flow rate. The biomass concentration and the substrate concentration at the end of the run depend on the operation of the reactor.

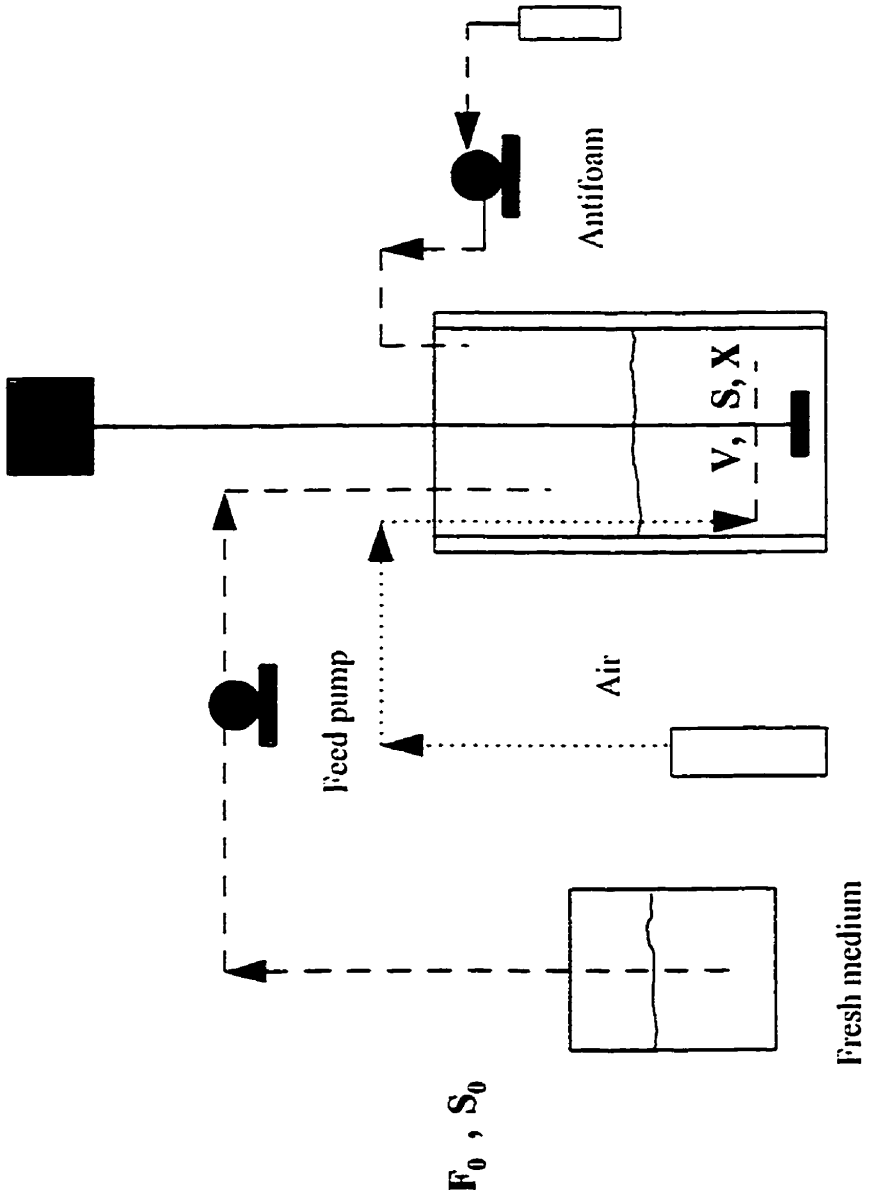

Fig. 3.1 Fed-batch bioreactor Diagram

The model for a fed-batch reactor is obtained from an overall cell and substrate mass balance and is described by the following equations:

$$V = V_0 + \int F\, dt \tag{3.28}$$

$$\mu = \mu_{max}\, S /(K_S + S) \tag{3.3}$$

$$D = F/V \tag{3.29}$$

$$dX/dt = \{ [\mu_{max}\, S/(K_S + S)] - D \}\, X \tag{3.30}$$

$$dS/dt = D\, (S_0 - S) - X\, (\mu /Y_{X/S}) \tag{3.31}$$

where:

D	is the dilution rate as defined by eq. 3.29, h^{-1}
V_0	is the working volume at the beginning of the fed-batch operation, L
F	is the feed volumetric flow rate, L/h
V	is the reaction volume at any time, L
t	is the time, h
X	is the biomass concentration in the bio-reactor at any time, g/L
μ	is the specific growth rate, h^{-1}
S_0	is the substrate concentration in the feed stream, g/L
S	is the substrate concentration in the reactor at any time, g/L
$Y_{X/S}$	is the growth yield, g cells/g substrate

From the above equations, the following observations can be made:

1. In the fed-batch bio-reactor, the reaction volume, V, is a function of time and depends on the volumetric flow rate, F, as indicated in equation 3.28
2. The volumetric flow rate, F, is an operational variable and therefore, can be kept constant or varied as a function of time.
3. The specific growth rate, μ, depends on the substrate concentration, S, according to the Monod equation (3.3).

4. The biomass concentration, X, and substrate concentration, S, in the reactor at any time, t, change with respect of time.

The solution of these equations gives the biomass and substrate concentrations at any time in the bioreactor.

According to the first term in equation 3.31, the substrate concentration in the bio-reactor is increased when the substrate concentration in the feed stream and the volumetric flow rate are increased (i.e., at a high dilution rate). In contrast, the substrate concentration in the reactor is reduced via cell consumption, as indicated by the second term of equation 3.31. As indicated by equation 3.26, biomass concentration is increased by the growth of cells and reduced when the dilution rate is increased.

The fed-batch bioreactor can be operated at low or high volumetric flow rates and at low or high substrate concentrations in the feed stream. Thus, it is also possible to control the biomass and substrate concentrations at the end of the fed-batch culture. Fed-batch growth has been used to obtain high concentration of biomass and can also be used for the determination of the kinetic constants (Esener et al., 1981, Webster, 1983). A method to estimate the maximum specific growth rate using fed-batch experimental data can be developed through the use of equation 3.30. When the fed-batch reactor is operated at a constant flow rate and with a high substrate concentration in the feed stream, the substrate concentration in the reactor will be high at all times during the fed-batch culture. Under these conditions, the specific growth rate will be constant and equal to the maximum specific growth rate. Assuming μ is constant, equation 3.30 can be integrated to give the following equation:

$$\ln(X/X_0) = \mu\,(t-t_0) - \ln(V/V_0) \qquad (3.32)$$

A graph of $\ln(X/X_0) + \ln(V/V_0)$ versus time should be a straight line with slope equal to the maximum specific growth rate.

The fed-batch reactor operation is a non-steady state process. In this reactor, the environmental conditions change continuously and the cells may not have the time to adapt to these conditions, and change their metabolism accordingly. Therefore, the behaviour of the culture may in principle be different from that expected in a continuous culture (Esener et al., 1981).

Similarly to the changes proposed to equations for batch growth model, the equations for fed-batch culture can be modified to consider the sporulation process in *B. thuringiensis*. The introduction of the proposed model into the fed-batch equations yield the following set of modified equations:

$$dX/dt = (\mu\text{-}D) - \mu X_s - k_s(X - X_s) \quad (3.33)$$

$$dS/dt = D(S_0 - S) - \mu(X - X_s)/Y_{X/S} \quad (3.34)$$

$$dX_s/dt = k_s (X - X_s) \quad (3.23)$$

These equations include the effect of the sporulation process on the fed-batch growth. The simultaneous solution of this set of equations, together with equations 3.3 and 3.28, describes the change in biomass, sporulated cells, and substrate concentrations in the fed-batch reactor under non steady-state and non homogeneous population.

3.6 Continuous Stirred Tank Reactor (CSTR) growth

Continuous growth is a steady state process. Firstly, a bioreactor is filled with medium and inoculated with a cell suspension. An input stream is then used to feed the reactor with fresh medium while an output stream is used to withdraw the cells and liquid medium simultaneously from the bioreactor. The reaction volume is kept constant, controlling the input and output volumetric flow rates. At steady state, the biomass and substrate

concentrations remain constant during the continuous run. Fig. 3.2 shows a schematic of a stirred tank continuous bioreactor.

The model for a stirred tank continuous bioreactor is obtained by making a cell and substrate mass balance in the bio-reactor. When the bioreactor begins its operation, a non-steady state condition takes place before it reaches the ideal steady-state operation of a continuous bioreactor. Therefore, the following two sets of equations describe a continuous stirred tank bioreactor at non-steady and at steady state operating conditions.

1. Non-steady state operation

$$dX/dt = \mu X - D X \tag{3.35}$$

$$dS/dt = D(S_0 - S) - \mu X / Y_{X/S} \tag{3.36}$$

$$\mu = \mu_{max} S /(K_S + S) \tag{3.3}$$

2. Steady-state operation

$$D X = \mu X \tag{3.37}$$

At steady state the dilution rate is equal to the specific growth rate.

$$D = \mu \tag{3.38}$$

$$(S_0 - S) = X / Y_{X/S} \tag{3.39}$$

$$D = \mu_{max} S/(K_S + S) \tag{3.40}$$

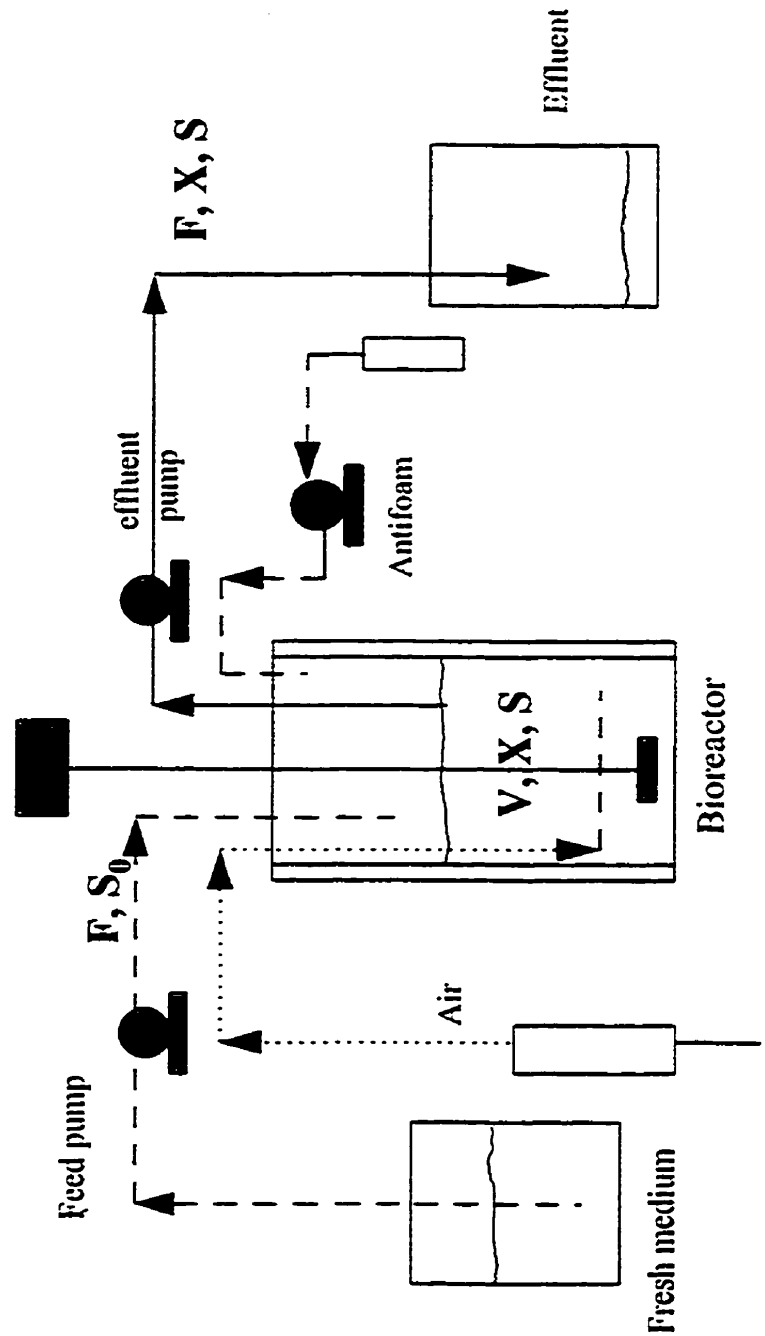

Fig. 3.2 Continuous Stirred Tank Reactor Diagram

Equations 3.38 to 3.40 describe the operation of a continuous stirred tank reactor (CSTR) for a non-sporulating culture at steady state. It is assumed that the dilution rate, D, and the kinetic constants, μ_{max} and K_S, are constant during the continuous growth. Also, it is postulated that at steady state, the conditions in the reactor do not change with time. Thus, the cells are kept in a controlled environment and should therefore, remain in a constant metabolic state. While there may be a number of conditions affecting the steady-state (e.g. reaction volume oscillations, non uniform concentration of nutrients and/or oxygen due to imperfect mixing, formation of foam producing zones with cells at a different metabolic states), this model is considered reasonably adequate. This is particularly true when experimental conditions are such that the bioreactor operation approaches the ideal CSTR reactor operation. This ideal operation was reasonably reached in the present study.

An important matter is given by the fact that the stirred tank bioreactor must be operated at a dilution rate lower than the maximum specific growth rate. Otherwise the cells will be withdrawn at a higher rate than they are produced, and this will cause a cell washout. It has to be mentioned that the washout is a non steady state operation and it is described by the following equation:

$$dX/dt = (\mu_{max} - D)\, X \tag{3.41}$$

When the dilution rate is higher than the maximum specific growth rate, the concentration of cells in the reactor drops exponentially. By integrating equation 3.41, the biomass concentration in the reactor may be given by the following equation:

$$X = X_w \exp [\, \mu_{max} - D] \, (t-t_w) \tag{3.42}$$

or

$$\ln (X/X_w) = (\mu_{max} - D)\, (t-t_w) \tag{3.43}$$

Where:

X_w is the biomass concentration at the beginning of the washout, g/L

t_w is the time at the beginning of the washout, h

The experimental data from a washout operation and equation 3.43 can be used to estimate the maximum specific growth rate. A graph of the logarithm of the biomass concentration vs. time will give a straight line with a slope of (μ_{max} - D). The constant μ_{max} can then be calculated from the slope.

In addition, the experimental data from the operation at steady state at different dilution rates and equation 3.40 can be used to estimate the saturation constant and the maximum specific growth rate. Given that the specific growth rate is a function of the substrate concentration, according to the Monod equation, at steady state, the dilution rate is equal to the specific growth rate (refer to eq. 3.40). A graph of D vs. S will show the typical shape for the Monod model. This curve can be fitted to the Monod model by nonlinear regression and the maximum specific growth rate, μ_{max}, and the saturation constant, K_S, can be estimated. To this end, equation 3.40 can be rearranged to give the linear equation:

$$1/D = (K_S/\mu_{max})\ (1/S) + 1/\mu_{max} \qquad (3.44)$$

A graph of 1/D vs. 1/S will produce a straight line with a slope equal to (K_S/μ_{max}) and an intercept equal to $1/\mu_{max}$

It has to be mentioned that the operation of a continuous reactor to estimate the kinetic constants has a limitation. It is not possible to operate the reactor at a dilution rate higher than the critical dilution rate, D*, which is defined by the following equation:

$$D^* = \mu_{max}\ S_0/(K_S + S_0) \qquad (3.45)$$

Where:

S_0 is the substrate concentration in the feed stream, g/L

Given that during the continuous run the maximum value for S is S_0, then the maximum operational specific growth rate is given by the critical dilution rate, D*. (refer to

equation 3.41). In summary, in a CSTR, the critical dilution rate is considered to be the maximum operational dilution rate and is equal to the maximum operational specific growth rate. When the reactor is operated at a dilution rate higher than the critical dilution rate, the operation cannot be at steady state given there is a washout of cells. This consideration is particularly important when K_S is comparable to S_0 because the critical dilution rate, D^*, decreases as K_S increases (refer to equation 3.45).

It has to be mentioned that in the context of the present study, the use of experimental data from a stirred continuous bioreactor for the estimation of the kinetic constants was limited to data obtained at steady state and at dilution rates lower than the critical dilution rate. Thus, there was no effect of cell washout on the validity of the experimental data.

In addition, the equations describing the unsteady state operation in a continuous culture can be modified to take into account the sporulation process of *B. thuringiensis* cells. To obtain the new model for a continuous reactor, equations 3.15 and 3.21 were introduced in the mass balance of biomass and substrate in a continuous reactor at non steady state. The following set of equations were obtained:

$$dX/dt = (\mu - k_s)(X - X_s) - D X \quad (3.46)$$

$$dS/dt = D(S_0 - S) - \mu (X - X_s)/Y_{X/S} \quad (3.47)$$

$$dX_s/dt = k_s (X - X_s) - D X_s \quad (3.48)$$

The simultaneous solution of this set of differential equations provide the biomass, substrate and spore-forming cells with time during a non steady state operation in a continuous reactor.

3.7 Conclusions.

A review of available kinetic models for cell growth showed the importance of developing a new kinetic model for *B. thuringiensis* growth accounting for the formation of spores. This new kinetic model, whose main characteristics were described in this section, is applied to batch, fed-batch and continuous (CSTR) reactor operations.

CHAPTER 4

EXPERIMENTAL METHODS

4.1 Analytical methods

4.1.1 Biomass concentration

The biomass concentration was determined in all the experiments by the dry weight method. Approximately 10 mL samples of fermentation broth were withdrawn from the culture throughout the experimental time and filtered on a previously dried 0.45 μm cellulose filter under vacuum. The filters were kept at 100 °C for 24 hours in an oven, and the dry weight, expressed as g/L, was calculated as the difference in weight of the filter before and after the filtration.

4.1.2 Viable cells and spore count

The plate count method was used to determine the number of viable cells during *B. thuringiensis* growth (Postgate, 1969). This method is based on the spreading of a diluted population of cells on nutrient agar, such that after incubation, each viable cell forms a colony. The number of colony forming units (CFU) per mL is estimated from the colony count and by knowing the dilution factor.

A one mL sample was taken from the fermentation broth and serial dilutions were prepared with distilled, sterile water. Then an agar plate with nutrient agar was inoculated with 0.1 mL of several dilutions in duplicate. The plates were incubated for 24 hours at 30 °C and the number of colonies were counted.

The spores were counted in the same way as the vegetative cells, but the population was first subjected to a treatment at 80 °C for 15 min. to kill vegetative cells. Decimal serial dilutions were prepared. A petri dish containing nutrient agar was inoculated with 0.1 mL of these dilutions and incubated for 24 hours at 30 °C. The number of colonies was counted and the spores number was estimated from the colony count.

4.1.3 Glucose analysis

The glucose concentration was determined by the glucose oxidase method using the Glucose Kit Catalog No. 510 from SIGMA Co., St. Louis Mo. The glucose concentration in the liquid medium in the reactor was determined after filtration of a 10-mL sample of fermentation broth through a 0.45 µm cellulose filter under vacuum. The filtrate, free of cells and other solids, was used to determine the glucose concentration in the sample, according to the instructions of the manufacturer.

4.1.4 Crystal protein analysis

A 20-mL sample of lysed cell suspension was taken from the reactor and centrifuged at 7000 rpm (111 g) for 15 min. to eliminate the fermentation broth. The supernatant was discarded and the pellet, containing a mixture of spores, crystal protein and cell debris, was washed at least three times with 10 mL of 0.14 M NaCl - 0.01% Triton X-100 solution. This washing helped in eliminating the soluble proteins and proteases that can affect the integrity of the crystal protein.

The crystal protein in the pellet was dissolved with 0.02 N NaOH (pH 12) for five hours with stirring. The suspension was centrifuged at 7000 rpm for 15 min. and the pellet, containing spores and cell debris was discarded. The supernatant, containing the crystal protein was kept for further analysis.

This procedure allowed the dissolution of crystal protein in alkaline conditions. The pellet contained mainly spores and some cell debris, while the solution contained the dissolved crystal protein. The effectiveness of the method was tested by observation under the optical microscope of the mixture spore-crystal protein before and after the dissolution. The purity of the protein dissolved with this procedure was tested also by the gel electrophoresis.

4.1.4.1 Spectrophotometric methods

After the dissolution of the crystal protein with 0.02 N NaOH, the supernatant containing the dissolved crystal protein was used for the determination of total protein by the biuret or Lowry assay. Bovine Serum Albumin (BSA) was used as a standard protein and the protein content in the sample was determined by measuring the absorbance at 750 nm or 540 nm for Lowry or biuret assays, respectively (Damm, et al 1966).

4.1.4.2 Flotation-settling method for isolation of delta-endotoxin

The purification of crystal protein for analytical purposes presents challenges because the physical properties of spores, cells debris and crystal protein are very similar. Several methods such as two phases separation (Angus, 1959), and density gradient separation (Faust, 1972; Sharpe et al., 1975; Mahillon and Delcour, 1984) have been used with varied results.

Thus, a new method of separation of the crystal protein (CP) from the mixture obtained from the fermentation broth, is proposed in this study. This method is based on the difference in densities of the spores and the protein inclusion. The formation of foam during the shaking of a suspension of the mixture spores-cell debris-crystal protein helps in the separation of the spores. The method consists of three stages: separation of the mixture spores-crystal protein-cell debris from the fermentation broth, separation of spores, and separation of cell debris. These different stages are discussed in more details below.

1) Separation of the mixture spores-crystal protein-cell debris from the fermentation broth

A batch culture of *Bacillus thuringiensis* var. *kurstaki* HD-1 ATCC 33679 was grown in a 1 L bioreactor. The temperature and the dissolved oxygen were maintained at 30 °C and above 20% saturation respectively. After 24 hours of operation the cells suffered lysis, and 600 mL of fermentation broth were taken from the reactor in order to harvest the crystal protein. The biomass concentration was 6 g/L dry weight at the end of the batch culture. The biomass was separated by centrifugation at 7000 rpm (111 g) at 4 °C for 20 min. The supernatant was discarded and the pellet was suspended in 40 mL of 0.14 N NaCl with 0.01 % Triton X-100, mixed vigorously and centrifuged again. This operation was repeated three times.

2) Separation of spores

The pellet was re-suspended in 40 mL of 0.14 N NaCl with 0.01 % Triton X-100 and put in a separation funnel to allow the solids settle overnight. The suspension showed two sections: the upper section was turbid and contained spores, cell debris and approximately 10% CP as evidenced by microscopy. The lower section was brown in colour, thick and contained a mixture of spores, cell debris and CP particles. The composition of particles in the phases was verified by observation at 1000X and 1500X magnification in a phase contrast microscope. The particles were stained with basic fuchsin before the observation with the microscope.

The upper section contained mainly the spores and cell debris and the lower section mainly CP. The lower section was separated and put in a separation funnel, stirred vigorously, and left for 5 hours to allow the solids to settle. When the bottom layer appeared to be too thick and the top layer was too small to be separated effectively, 10 to 20 mL of 0.14 M NaCl

with 0.01 % Triton -100 were added. After five separations, the CP purity in the lower section was approximately 80% to 90% with practically no spores.

3) Separation of cell debris

The suspension formed by CP and cell debris taken from the last settling operation had a volume of 10 mL approximately; it was centrifuged at 5000 rpm (57 g) at 4 °C for 15 min in a 13 x 100 mm tube and washed two times with 10 mL distilled water. The pellet showed two sections: the top layer was brown and the bottom layer was white. The top layer formed by cell debris was removed with a gentle addition of 5 mL distilled water and a slight shaking, to avoid the disturbance of the white portion of the pellet; then was decanted. The bottom layer was re-suspended in 10 mL of distilled water and observed under the microscope. This suspension contained more than 99% of the CP.

4.1.4.3 Gel electrophoresis

A sodium dodecyl sulphate - polyacrylamide gel electrophoresis was performed in a Bio-Rad Electrophoresis cell (Bio-Rad Micro cell), as recommended by Bateman (1995). Three different types of samples were examined by gel electrophoresis: delta-endotoxin HD-1 S, 16,000 IU/mL, a purified crystal protein obtained by the flotation-settling method and crystal protein obtained from a batch culture of *B. thuringiensis* subspecies *kurstaki* HD-1 ATCC 33679. The crystal protein from the three samples was dissolved with 0.02 N NaOH and the pH was decreased to 9.0 by adding 3 mL of carbonate buffer per mL of sample. Before the samples were applied to the gel, they were treated with one of two types of buffers: a non denaturing and a denaturing buffer, the latter containing mercaptoethanol as denaturing agent (Bateman, 1995).

4.1.4.4 High performance liquid chromatography

High Performance Liquid Chromatography (HPLC) may be used to identify and measure the concentration of crystal protein in solution. The procedure used is based on Witter et al., (1990). The protein sample must be prepared such that it is stable for some time (two-three days minimum) and does not interfere with the HPLC run (e.g. precipitation inside the chromatographic column). The delta-endotoxin must be solubilized in a denaturing agent or alkaline solutions. The samples were dissolved (10 mg of crystal protein powder), obtained by the flotation-settling method, equivalent to 8.5 mg of crystal protein, in 2 mL 0.02 N NaOH for 5 hours. The suspension was centrifuged at 7000 rpm (111 g) for 15 min. to remove the pellet. The supernatant (2 mL) was added to 2 mL of a solution composed of 2% SDS, 10% glycerol and 2.5% mercaptoethanol and the mixture was heated immediately to 100 °C for 10 min. This solution was used directly in the HPLC runs.

To test the presence of crystal protein in the samples from *B. thuringiensis* cultures, 20 mL of fermentation broth were taken from the reactor and centrifuged at 7000 rpm (111 g) for 15 min. to eliminate the fermentation broth. The supernatant was discarded, and the pellet was washed at least three times with 10 mL of a 0.14 M NaCl - 0.01% Triton X-100 solution, and dissolved in 0.02 N NaOH (pH 12.0) for five hours with stirring. The suspension was centrifuged at 7000 rpm (111 g) for 15 min, and the supernatant was used for the HPLC test. A two mL aliquot was added to two mL of a sample solution (2% SDS, 10% glycerol and 2.5% mercaptoethanol) and heated at 100 °C for 10 min. After cooling, this mixture was tested in the HPLC.

Acetonitrile, 0.1% trifluoroacetic acid (TFA) -solvent A- and water, 0.1 % TFA - solvent B- were used as carriers. The HPLC was run with a linear gradient in an Alltech Macrosphere 300 C4 column (pore size 5 μm, length 250 mm, I.D. 4.6 mm) for a total run time of 40 min. The detector was set at a wavelength of 220 nm.

The gradient used was as follows:

0-2 min.	40% solvent A
2-22 min.	linear gradient 40% to 80% solvent A
22-27 min.	80% solvent A
27-32 min.	Linear gradient 80% to 40% solvent A
32-40 min	40% solvent A

4.1.4.5 Scanning electron microscopy

The purified crystal protein obtained by a flotation-settling method was observed with an electron microscope. For the preparation of the sample for the electron micrograph, the crystal protein was dried under vacuum for 120 hours. The resulting white powder was used directly in the scanning electron microscope.

4.1.5 Cell morphology

The morphology of bacterial cells was observed and recorded in pictures during the different growth stages of *B. thuringiensis* in batch and continuous cultures. An optical phase contrast microscope and transmission electron microscope were used for this purpose.

4.1.5.1 Optical microscopy

An optical phase contrast microscope One-Ten Microstar American Optical was used for the observation and photography of the *B. thuringiensis* cells during batch and continuous cultures. The samples were taken directly from the reactor and diluted when necessary with

distilled water. An Olympus OM-1 camera was used to take the pictures with ASA 400 film using the maximum illumination.

4.1.5.2 Transmission electron microscopy

The bacterial cells from batch and continuous growth were examined in a transmission electron microscope. A two mL sample was taken from the reactor and chilled immediately in an ice bath. The sample was then centrifuged at 5000 RPM for 10 min. at 4 °C and the supernatant was discarded. The pellet was resuspended in 2 mL of 4% glutaraldehyde and kept in an ice bath until further processing. The samples were prepared for observation at the transmission electron microscope following standard procedures.

4.2 *Bacillus thuringiensis* growth

4.2.1 Microorganism

Bacillus thuringiensis subspecies *kurstaki* HD-1 ATCC 33679 was used in all the experiments. It was kept on nutrient agar slants at 4 °C. The slants were heated at 80 °C for 15 min. to activate the spores before use.

4.2.2 Medium composition

The medium used in all the cultures was that suggested by Anderson (1990). The medium composition is shown in Table 4.1

Table 4.1 Medium composition for the growth of *Bacillus thuringiensis* HD-1 subspecies *kurstaki* ATCC 33679

Component	g/L	Salts Solution Composition.	g/ L
Glucose	9.77	$MgSO_4$. $7H_2O$	3.0
Yeast extract	4.62	$CaCl_2$. $2H_2O$	1.06
Bacto peptone	4.62	Fe-Citrate	0.75
$(NH_4)_2SO_4$	1.00	$MnSO_4$. $7H_2O$	0.50
K_2HPO_4	4.15	$ZnSO_4$. $7H_2O$	0.075
KH_2PO_4	3.40	$CuSO_4$	0.045
Salts Solution	100 mL		

4.2.3 Bioreactor systems

A two-litre bioreactor was used for batch, continuous and fed-batch experiments. The bioreactor had a four-helix stirrer (Fischer Sc.) for mixing; air was added continuously to the bioreactor using a sparger located 10 cm above the bottom of the reactor. The pH was monitored with a pH electrode (Ingold type 465) coupled with a pH analyzer (Cole Parmer). The dissolved oxygen was measured with a D.O. galvanic probe (Cole Parmer), and recorded in a dissolved oxygen analyzer model DO-40 (New Brunswik Scientific Co.) and a chart recorder (Cole Parmer). The temperature in all the experiments was maintained constant at 30 °C with a water circulation bath. The foam was controlled manually by adding some drops of antifoam-water suspension as necessary.

The bioreactor had ports for the addition of antifoam, sample extraction, fresh medium, and withdrawal of reaction mixture (during the continuous runs), and gas exhaust. The air supplied to the reactor passed through a rotameter and glass fiber filter.

The bioreactor was attached to a computer which adjusted the impeller speed or the air flow rate to control the dissolved oxygen inside the reactor. The computer program can be used in a manual or an automatic control mode. During the batch, continuous and fed-

batch experiments it was found that manual control of the impeller speed was more appropriate, with the air flow rate kept constant at 1 L/min. In order to avoid the excessive foam formation, the impeller speed was maintained at the minimum necessary to keep at least 20% of the oxygen saturation in the reactor

During the continuous growth experiments, the bio-reactor was fed with fresh medium through a pump which could supply a constant volumetric flow rate. The reaction mixture was withdrawn using a Masterflex pump. The working volume was 1 L for batch cultures and 0.85 L for continuous cultures.

Figs. 4.1, 4.2 and 4.3 are schematic diagrams of the batch, continuous and fed-batch bioreactors. Plate 4.1 shows a picture of the two-liter bioreactor used for batch, fed-batch and single stage continuous growth experiments.

4.3 Experimental procedures

4.3.1 Batch reactor system operation

The medium was prepared in a 2-L flask with 800 mL distilled water. Glucose, yeast extract, bacto peptone, ammonium phosphate, potassium phosphate dibasic, and potassium phosphate monobasic were added to the water. The bioreactor was filled with this solution, and autoclaved for 20 min. at 121 °C before the inoculation.. The salt solution (90 mL) was autoclaved in a 250-mL flask at 121 °C and fed aseptically into the reactor when it was cold.

The inoculum was prepared in a 250-mL flask containing 90 mL of medium and 10 mL of salts solution. This medium was autoclaved for 15 min. at 121 °C. after cooling, it was inoculated with three to four loops of *B. thuringiensis* spores from a previously heat shocked slant, and incubated on a shaker at 30 °C for 12 hours.

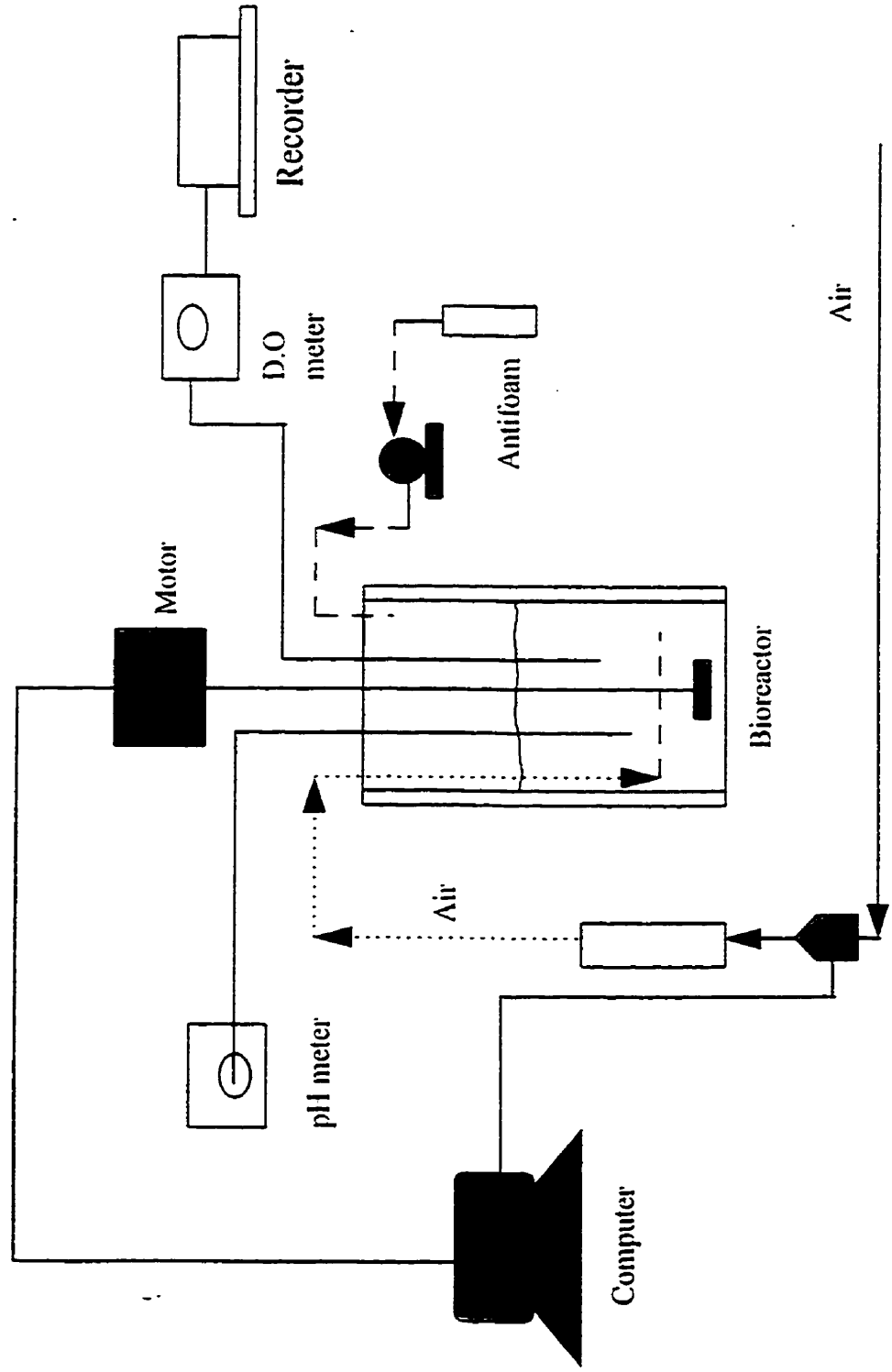

Fig. 4.1 Diagram of equiment used for Batch growth of *Bacillus thuringiensis* HD-1 subspecies *kurstaki* ATCC 33679

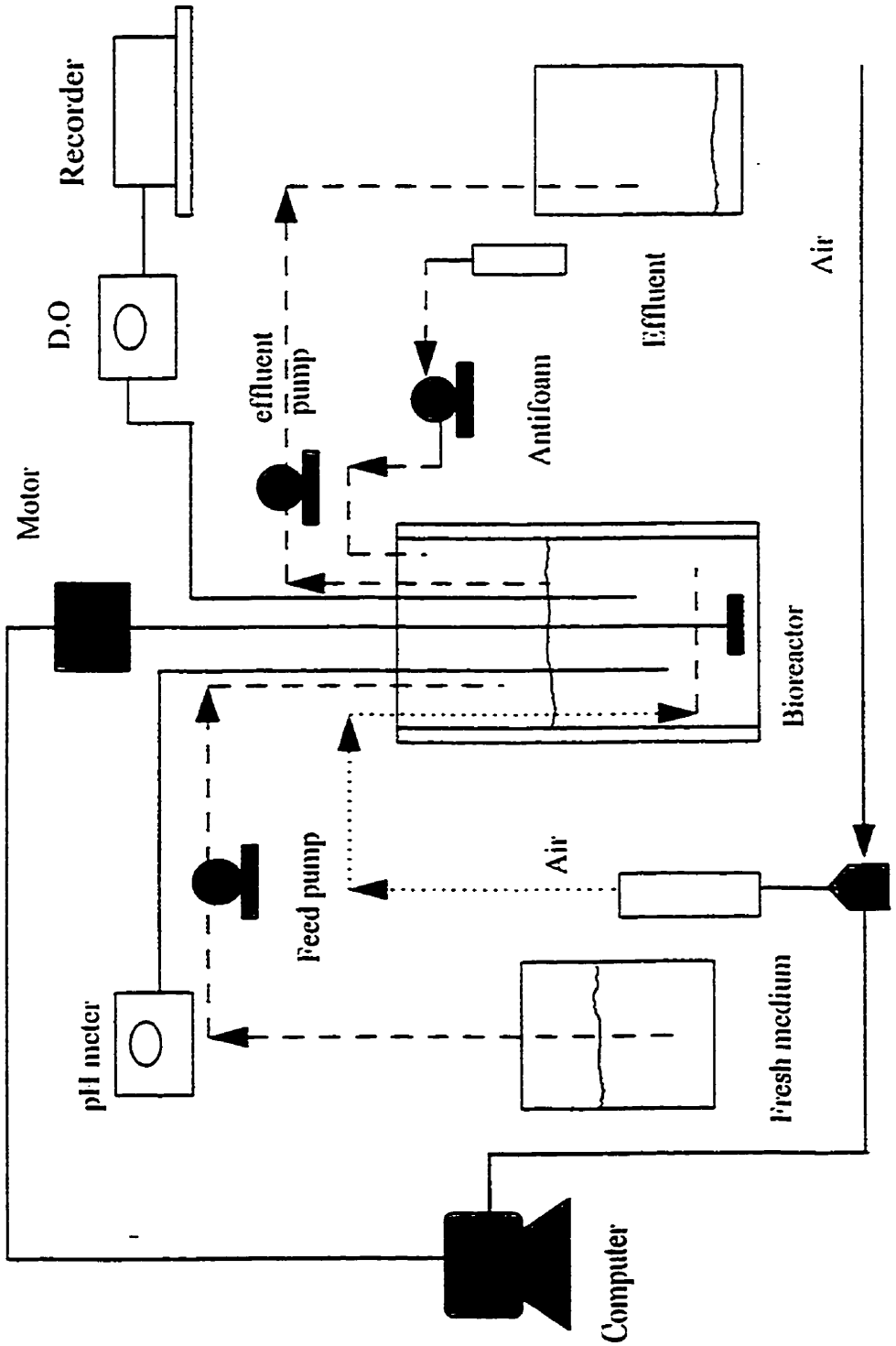

Fig. 4.2 Equipment for continuous growth of *Bacillus thuringiensis* IID-1 subspecies *kurstaki* ATCC 33679

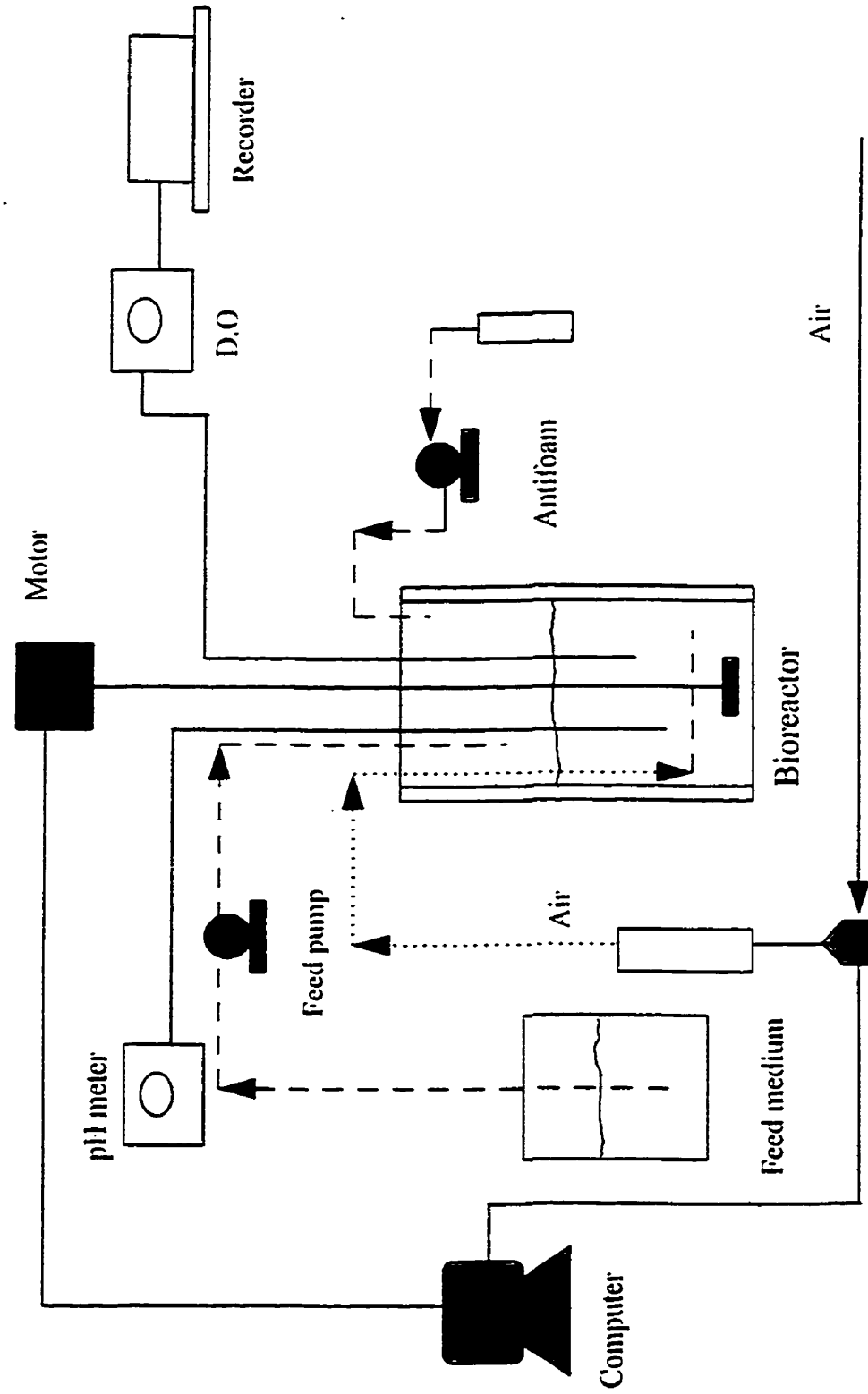

Fig. 4.3 Diagram of Equipment for Fed batch growth of *Bacillus thuringiensis* HD-1 subspecies *kurstaki ATCC 33679*

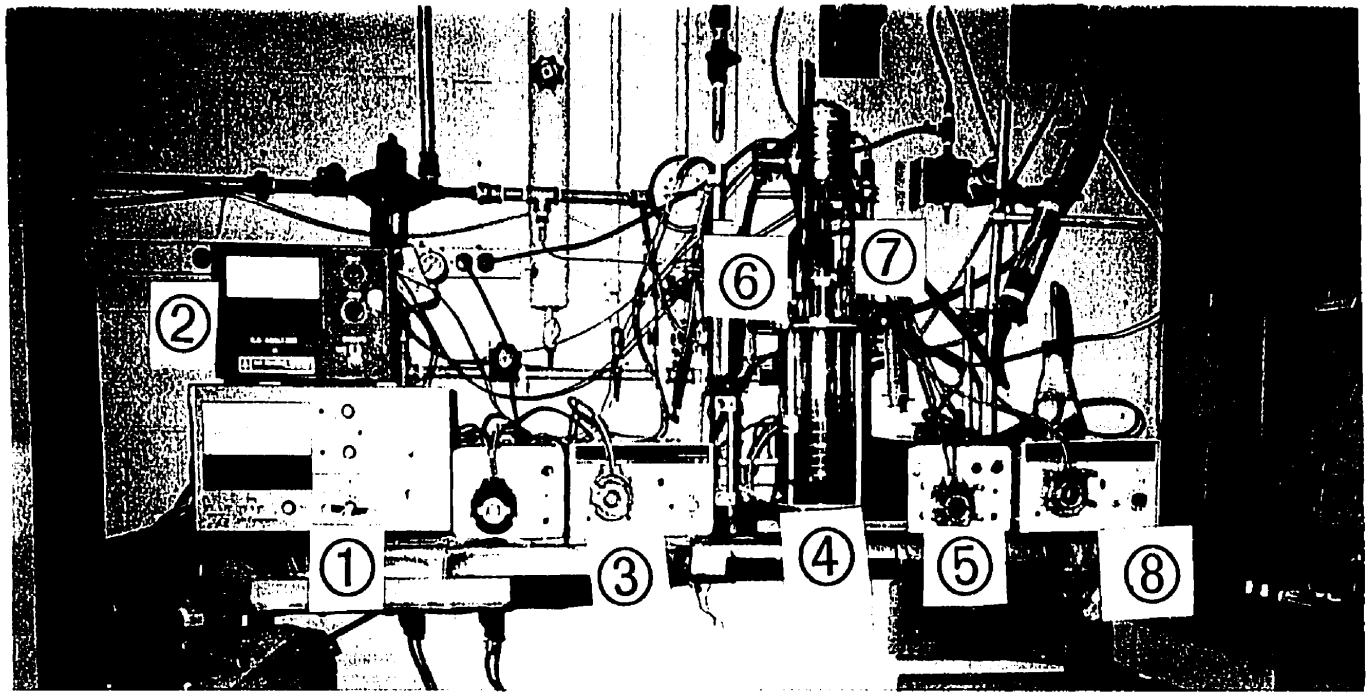

Plate 4.1 Two-litre bioreactor used for batch, fed-batch and single stage continuous growth of *B. thuringiensis* subspecies *kurstaki* HD-1 ATCC 33679.
(1) pH controller, (2) Dissolved oxygen analyzer, (3) Feed pump, (4) Bioreactor, (5) Effluent pump, (6) Dissolved oxygen electrode, (7) pH electrode, (8) Antifoam pump

The tubing connecting the antifoam and/or inoculum was also autoclaved at 121 °C for 20 min. The transfer of salts solution, inoculum and antifoam suspension from flasks into the reactor was performed aseptically using a peristaltic pump.

The reactor was cooled with a circulation bath. The temperature was verified with a thermometer inserted in the indicated port. When the medium reached 30 °C, the dissolved oxygen probe was calibrated according to the instructions in the operating manual for dissolved oxygen analyzer model DO-40 (New Brunswick Scientific Co.). Once the dissolved oxygen probe was calibrated and the temperature remained constant at 30 °C, the bioreactor was inoculated with 100 mL of 12 h old inoculum and the first sample was taken.

Samples were taken every hour or half hour, as necessary, depending on the growth stage, and used to determine the dry weight, the cell and spores count, and glucose concentration. Pictures of the cells were taken. The batch experiments lasted approximately 12 hours for the completion of the sporulation stage and 24 hours for the lysis stage.

4.3.2 Fed-batch reactor system operation

Fed-batch cultures were grown in the same equipment used for batch and continuous experiments. Fresh medium was fed into the reactor with a Cole-Parmer pump with a speed control. The volumetric flow rate was kept constant throughout the fed-batch culture. The fed-batch culture began with a batch operation until the cells reached the exponential stage, approximately after four hours of batch operation. During the fed-batch cultures, the reaction volume was recorded every half hour to calculate the dilution rate and to verify that the volumetric flow rate was constant. Samples from the reactor were taken every half hour to determine the biomass and glucose concentration.

4.3.3 Continuous stirred tank reactor system operation

For the continuous cultures, the same equipment as in the batch cultures was used, with some modifications. The continuous culture required the addition of fresh medium at a constant volumetric flow rate, the withdrawn of culture mixture, and a constant reaction volume.

The medium prepared beforehand was kept in a 20 L bottle connected to the feed medium port of the reactor with a tube (1/8 in. ID, 1/16 in. wall thickness). The fresh medium was fed at a constant volumetric flow rate with a Cole-Parmer pump with speed control. The removal of the culture mixture was carried out with a Masterflex pump with speed control.

The reaction volume was kept constant using a level control. The end of the effluent tube was located on the surface of the required level (Fig. 4.4). When the reaction mixture was removed excessively, the level of the liquid decreased and the effluent stream was stopped. The effluent pump was set at a higher volumetric flow rate than that used in the feeding stream, such that small variations in the feed stream did not increase the level of the liquid significantly. The level of the liquid medium in the reactor varied by no more than 10%

.

The continuous cultures began in a batch mode until the cells reached the exponential stage, that is, approximately 4 h after the inoculation of the reactor. The feed pump was set to the appropriate speed to give the desired volumetric flow rate and it was turned on at the beginning of the continuous operation. The effluent pump was turned on when the first drop of feed medium was supplied to the reactor. A sample was taken at the beginning of the continuous operation to determine biomass concentration and glucose concentration. Samples were taken every hour to verify the achievement of the steady state.

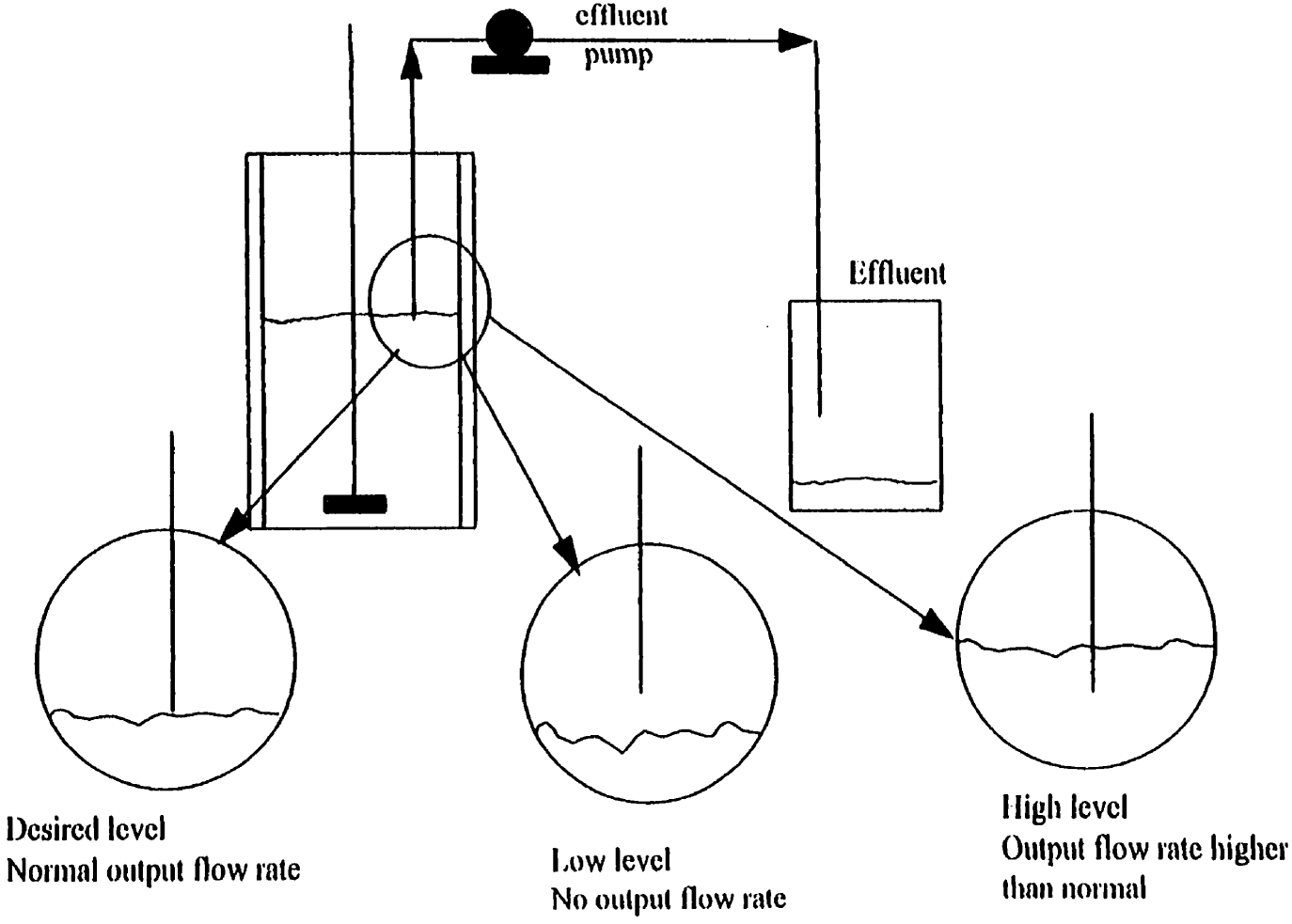

Fig. 4.4 Diagram of the Level Control in a Continuous Stirred Tank Reactor for growth of *B. thuringiensis* HD-1 subspecies *kurstaki* ATCC 36679

4.3.4 Continuous stirred tank reactor two-stage system operation

A series of continuous cultures of *B. thuringiensis* in a two-stage system were performed in order to test the viability of the production of the insecticidal crystal protein using continuous operation.

The two-stage continuous system consisted in a two-litre bioreactor and a 14 L New Brunswik bioreactor connected in series. The two-litre bioreactor, working at high dilution rate, was used in the first stage in order to obtain a massive production of biomass. The 14 L bioreactor, working at low dilution rate, was used in the second stage in order to enhance the production of the crystal protein or even to cause the lysis of the cells and therefore the release of the spores and the crystal protein into the liquid medium. Fig. 4.5 shows a diagram of the two-stage continuous system and Plate 4.2 shows a picture of the two-stage continuous growth system used to culture *B. thuringiensis*.

The 14 L bioreactor had a pH probe and a dissolved oxygen probe to monitor the pH and oxygen concentration, respectively. The air was sterilized with a glass wool filter and supplied to the bioreactor using a sparger in the bottom of the vessel. The air flow rate was measured with a rotameter. The formation of foam was controlled by adding small amounts of antifoam with a peristaltic pump when necessary.

The continuous culture in two-stages was performed in three steps:

a) The 2 L bioreactor was operated as a batch reactor until the exponential stage was reached by the cells (4 hours of batch operation).

b) The continuous operation in the first reactor (2 L bioreactor) began when the feed pump and the output pump was turned on at the appropriate velocities. The output stream was sent to the second reactor which was previously sterilized.

c) The second reactor, working as a fed-batch reactor, was filled with the output stream from the first reactor. When the desired working volume for the second reactor was

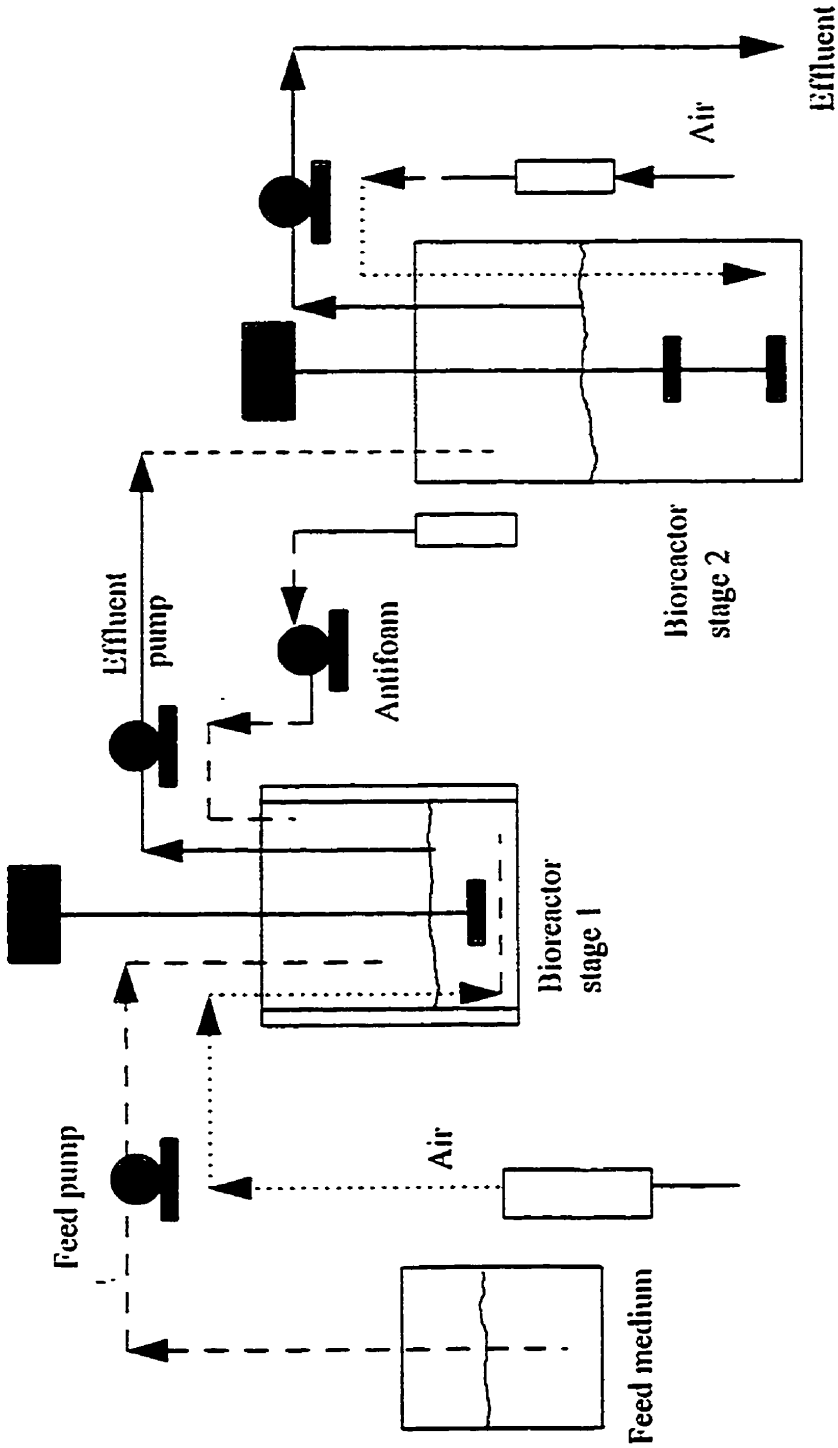

Fig. 4.5 Diagram of Two Stages Continuous Stirred Tank Reactor System for growth of *B. thuringiensis* HD-1 subspecies *kurstaki* ATCC 33679

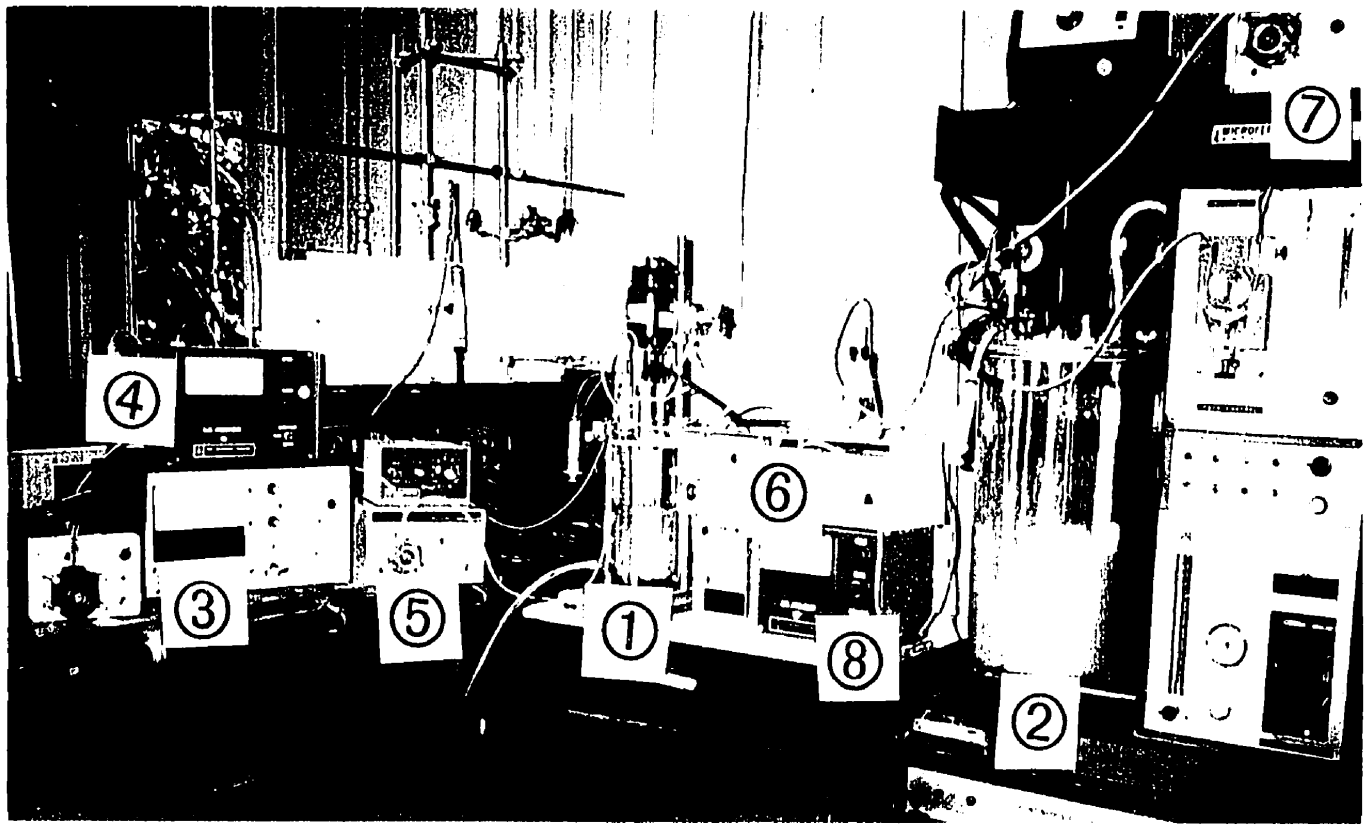

Plate 4.2 Two Stages Bioreactor System used for the culture of *B. thuringiensis* subspecies *kurstaki* HD-1 ATCC 33679. (1) 2 L. Bioreactor (stage 1), (2) 14 L. Bioreactor (stage 2), (3) pH controller, (4) Stage 1-Dissolved Oxygen Analyzer, (5) stage 1- Feed pump, (6) Stage 2 - Feed pump, (7) Stage 2 - Effluent pump, (8) Stage 2 - Dissolved Oxygen Analyzer

reached, the exit pump for the second reactor was turned on, beginning the continuous two-stage operation.

The sequence of a small reactor connected with a big reactor in series allowed to operate at different dilution rates using the same constant volumetric flow rate. While the small bioreactor can operate at high dilution rates, the second provides low dilution rates. The relationship of the dilution rates is given by:

$$D_1 V_1 = D_2 V_2$$

or $$D_1/D_2 = V_2/V_1$$

where: D_1 is the dilution rate (1/h) for the first reactor in series
D_2 is the dilution rate (1/h) for the second reactor in series
V_1 is the working volume (L) for the first reactor
V_2 is the working volume (L) for the second reactor

The ratio D_1/D_2 can be varied, changing the working volume for the second reactor.

The levels of the working volume for both reactors were maintained constant using the level control technique described in the previous section (Fig. 4.4).

4.3.5 Oxygen uptake rate and respiration rate coefficient

For batch and continuous cultures, the oxygen uptake rate was calculated using the dynamic air off-on method (Bandyopadhyay and Humprey, 1967). The dissolved oxygen electrode was connected to a New Brunswick Analyzer and to a chart recorder. At a given time, the air supply was interrupted and the stirrer speed was reduced to 340 rpm while the chart recorder was set at 30 mm /min. A plot of dissolved oxygen, expressed as % of

saturation, versus time was obtained using this procedure. The oxygen uptake rate was obtained from the slope of this graph.

The respiration rate coefficient was calculated by dividing the oxygen uptake rate by the biomass concentration, expressed as g D.W./L .

4.4 Conclusions.

While the experimental methods discussed in this chapter are consistent with well established biochemical engineering procedures, the new flotation-settling technique for isolation of the delta-endotoxin can be considered a significant new contribution. This new technique allows to obtain a relatively high pure crystal protein (up to 95% purity). Purification of the crystal protein, with this proposed method is relatively simple, requiring only standard laboratory equipment and not needing the use of reagents.

It is believed that a better and improved purification of the crystal protein can advance its characterization as well as it can allow better definition of the intrinsic toxicity of the crystal with minimum influence of spores or cell debris.

CHAPTER 5

RESULTS AND DISCUSSION

5.1 Batch growth

5.1.1 Growth phases, morphology, biomass, spore and delta endotoxin production

Biomass concentration, expressed as dry weight (g/L), glucose concentration, pH, oxygen uptake rate, qO_2*X, and respiration rate coefficient, qO_2, for batch growth experiments were measured and are shown in Table A.1 to Table A.3 (appendix A). The batch results of experiment NB6 are shown in this section in Figures 5.1 to 5.3 inclusive as a typical example of batch growth of *B. thuringiensis*, where we see the typical kinetics of bacterial growth phases: lag phase, exponential growth phase, transition growth phase, stationary phase, and declining or death. The growth phases were defined in section 3.1 and can be determined by observation of the graphs of biomass and glucose concentration versus time.

The number of cells and spores were measured as described in section 4.1.2. This method provides the number of colonies formed by the cells after being inoculated on a nutrient agar plate. Some experimental errors, such as colonies formed by more than one single cell, inadequate mixing during the preparation of the dilutions, and overlapped colonies (Postgate, 1969) may be sources of error in measuring the number of cells and spores present in the culture medium. These data were used to know the kinetics of spore formation and to verify if all the cells produced a spore at the end of the batch growth.

Concerning the definition of cell growth it can be argued that this parameter should be defined on the basis of the change in the number of cells with time. Moreover, cells could

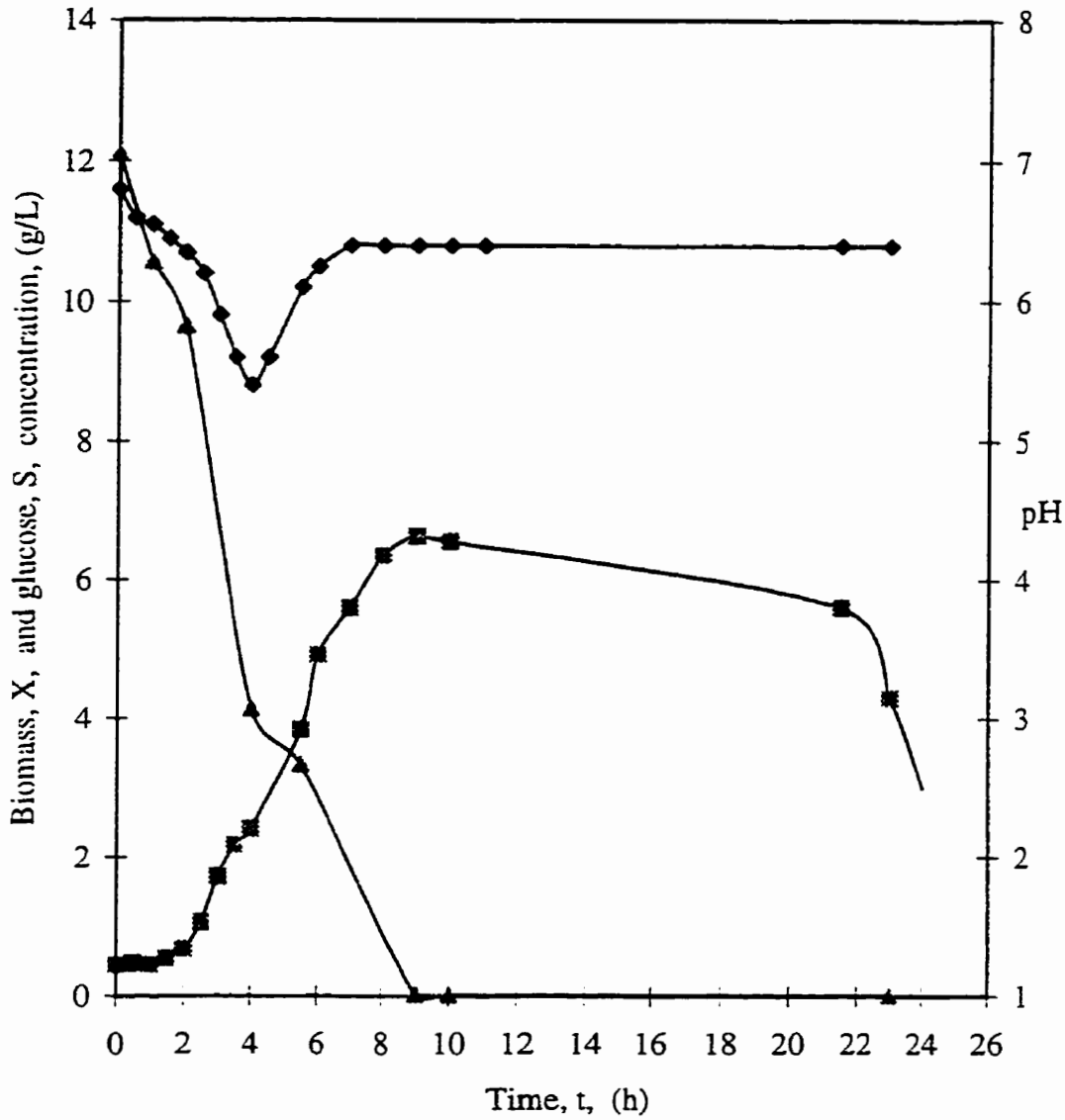

Fig. 5.1 Batch culture of *B. thuringiensis* subspecies *kurstaki* HD-1 ATCC 33679. pH and Biomass and glucose conc. Experiment NB6.

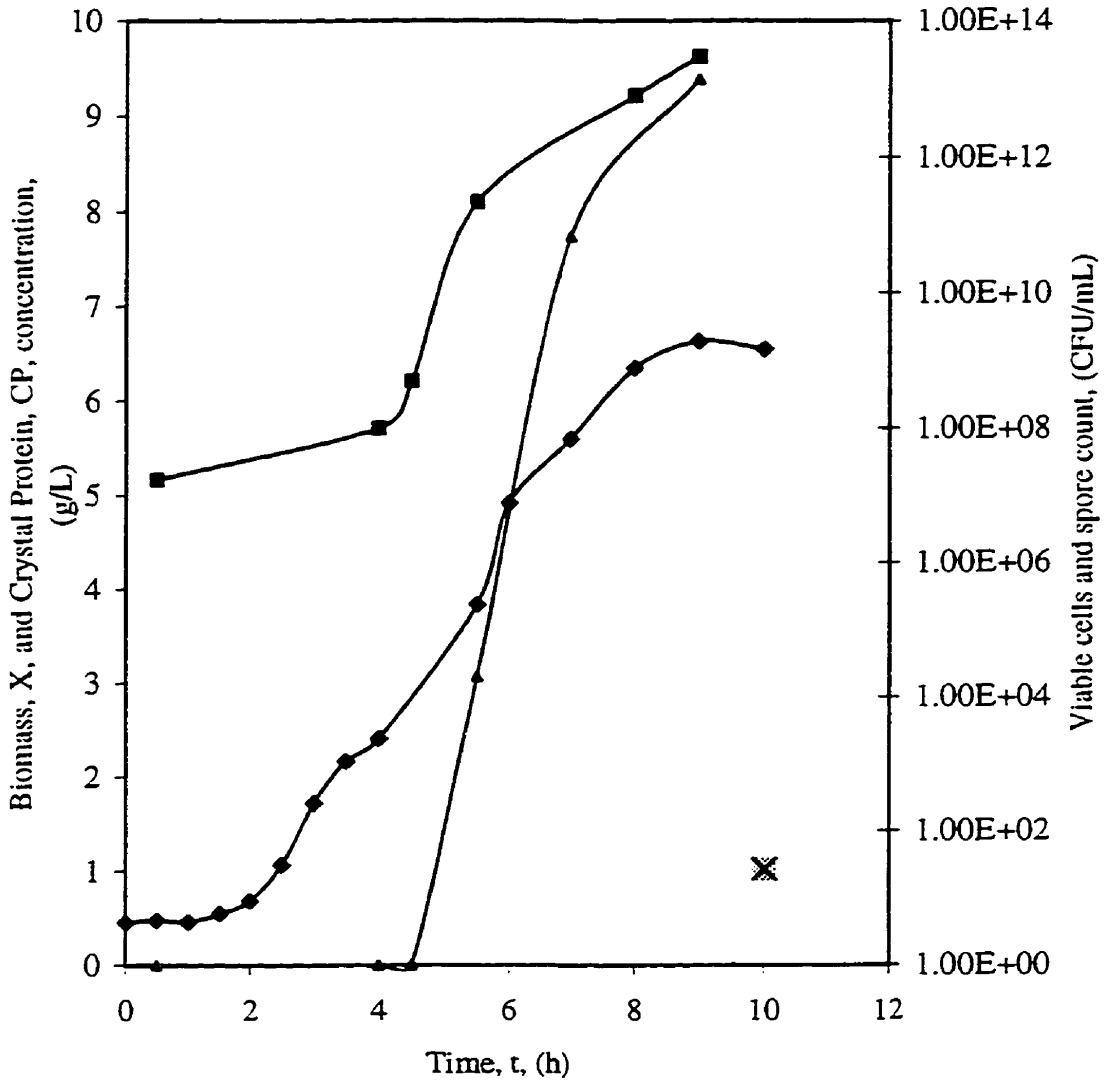

Fig. 5.2 Batch culture of *B. thuringiensis* subspecies *kurstaki* HD-1 ATCC 33679. Biomass and Crystal Protein conc. and Viable Cell and Spore Count. Experiment NB6.

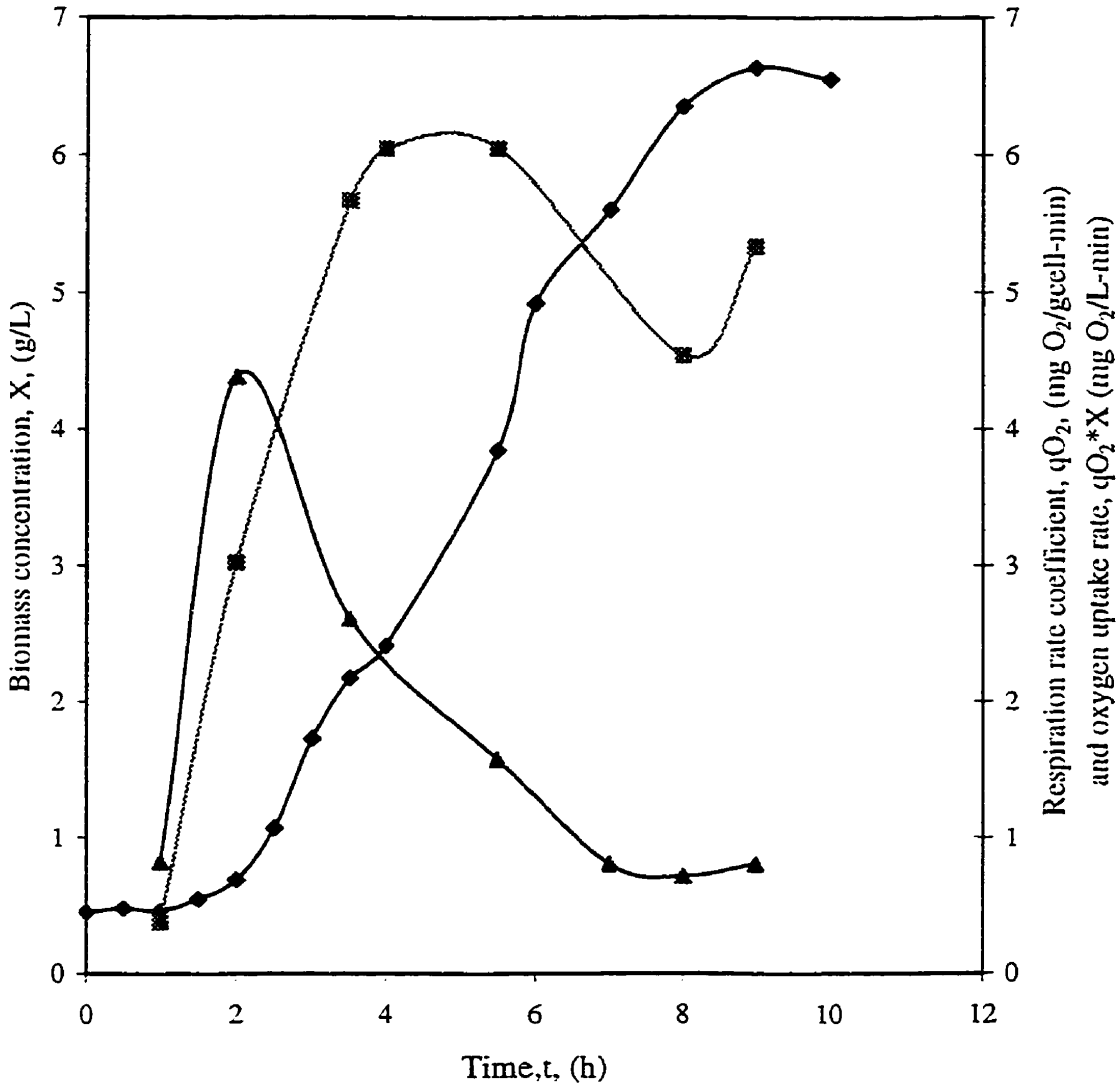

Fig. 5.3 Batch culture of *B. thuringiensis* subspecies *kurstaki* HD-1 ATCC 33679. Oxygen uptake rate and respiration rate coefficient. Experiment NB6.

increase their size before division and thus, changes in number of cells and changes in mass may not necessarily be related by a constant. However, it can be hypothesized that for a large number of cells in random phases of their individual growth, the average mass per cell is approximately constant, and thus the cell mass can be considered as proportional to the number of cells (Dean and Hinshelwood, 1966). Moreover, during the exponential stage, it is postulated that measurements that are proportional to the cell number are also proportional to the cell mass (Bu'Lock, 1988).

Considering the previous discussion and since the biomass concentration, expressed as grams dry weight/mL, is used extensively in the literature to study the bacterial cell growth, this parameter was used in this work to determine the specific growth rate and to estimate the different growth phases during the batch growth.

Regarding the lag phase of the batch culture it is characterized by a negligible increase in the biomass concentration. This is illustrated in Figs. 5.1 and 5.4 which show that during the first 1.5 hours, the biomass concentration grew very slowly, and increased from 0.45 g/L to 0.55 g/L only.

The exponential growth phase is characterized by a sharp exponential increase in the biomass concentration. Thus, a plot of the natural logarithm of biomass concentration versus time should produce a straight line. (Figs. 5.4 and 5.5). While this representation was considered in the present study, it was observed that the exponential growth phase ranged between 2.0 and 4.0 hours approximately following inoculation.

During the deceleration growth phase, the cells continued growing but at a lower pace due to the depletion of substrate and also due to the beginning of the sporulation process by *B. thuringiensis* cells. At the stationary phase, the cell growth essentially halted and finally during the death phase the cell growth, measured as biomass concentration, had a negative growth (there was cell depletion), due to cells lysis. These various growth phases are identified in Fig. 5.1. The deceleration growth phase lasted between 4 and 8 hours, the

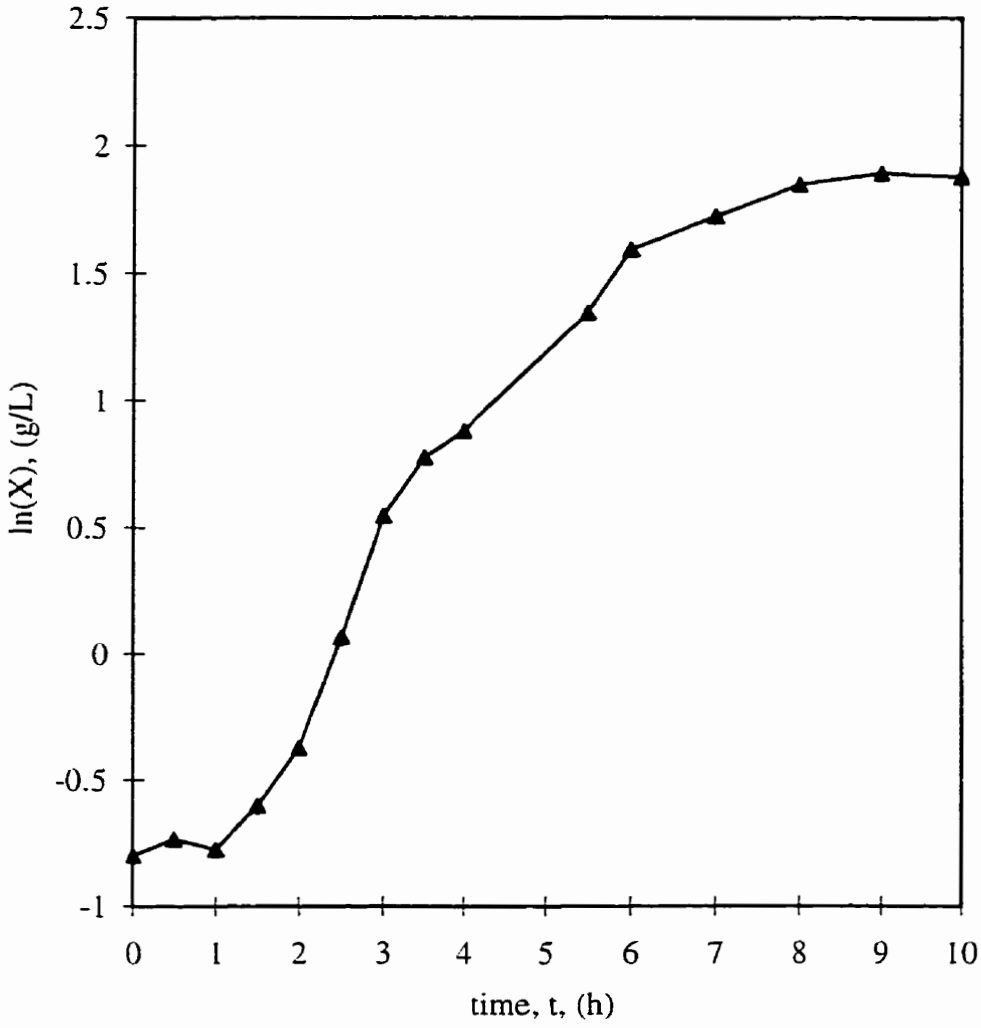

Fig. 5.4 Batch culture of *B. thuringiensis* subspecies *kurstaki* HD-1 ATCC 33679. Natural logarithm of biomass concentration , ln(X). Experiment NB6

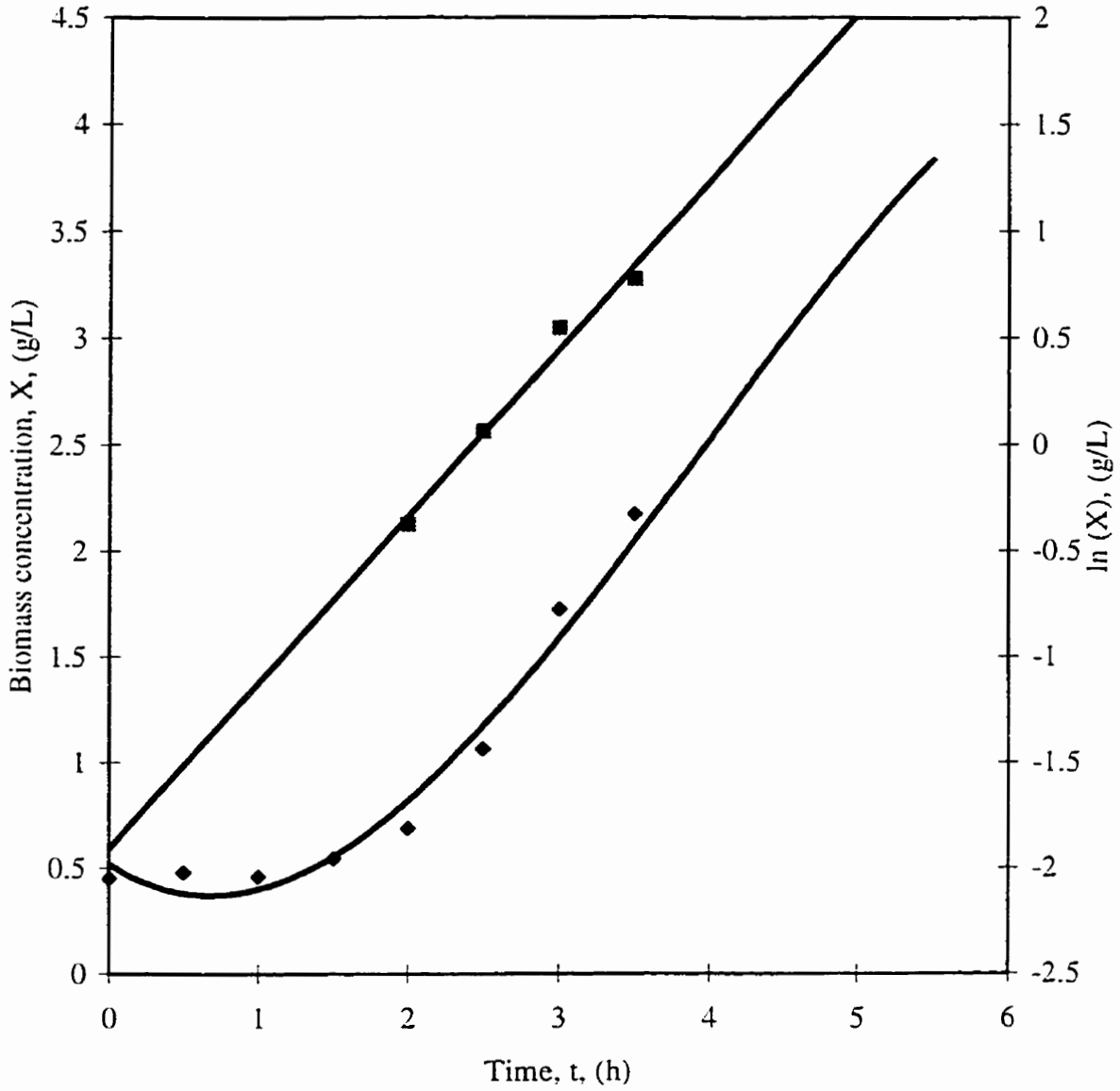

Fig. 5.5 Batch culture of *B. thuringiensis* subspecies *kurstaki* HD-1 ATCC 33679. Biomass and logarithm of biomass. Estimation of maximum specific growth rate.Experiment NB6

◆ X (g/L) ■ ln(X) (g/L)

$$\ln X = 0.7855\ t - 1.9067$$

$$R^2 = 0.981$$

stationary phase between 8 and 10 hours and the death phase between 10 and 23 hours after the beginning of the batch culture.

Considering the metabolism of *B. thuringiensis*, the growth process is divided into two main stages: vegetative stage and sporulation stage. A *B. thuringiensis* cell is in its vegetative stage if it is capable of dividing. On the other hand, a cell is in sporulation stage if the cell stops its division and uses the available energy to form a spore.

Unlike the growth phases, the metabolic stages cannot be identified by a change in the biomass concentration with time. The metabolic stages might, however, be identified by the cell morphology, the cell oxygen consumption and the change in the pH of the medium. Regarding the morphology of a vegetative *B. thuringiensis* cell it can be characterized on the basis of the simple internal cell structure, and the absence of a spore. In this respect, during the vegetative stage, the cells consume the substrates and require high amounts of oxygen and several acids are produced. As a result, the pH decreases in the liquid medium. (Nickerson et al., 1974; Bulla et al., 1969; Luthy et al., 1982).

Concerning sporulation, the shift from vegetative to sporulation stage occurs when the nutrients are depleted. In this case, the acids produced during the vegetative stage are already oxidized (Bulla et al., 1971) and the cells oxygen demand is very low. Therefore, the pH remains constant and the respiration rate coefficient will be at minimum level.

Based on the previous observations, the two main stages during the growth of *B. thuringiensis*, vegetative and sporulating phase, can be tracked with the experimental data following oxygen demand and the pH.

Regarding the oxygen uptake rate, as systematically observed in the present study, it reached a maximum after the beginning of the deceleration growth phase (4.5 hours) and decreased steadily as *B. thuringiensis* cells began forming their spores. On the other hand, the respiration rate coefficient reached a maximum at the beginning of the exponential growth

phase (two hours), decreased later with time, as the substrate was depleted, and reached its minimum level at the beginning of the stationary growth phase (8 hours, Fig. 5.3).

An interesting fact as well, is the change in pH with time. There was first a pH decrease, from 6.8, during the exponential growth phase with the pH reaching a minimum of 5.4 at the end of this phase (four hours). The decrease in pH is related with the production of acetic and pyruvic acids from glucose during the exponential growth. These acids were subsequently oxidized via the modified tricarboxylic acid cycle and this resulted in a pH increase (Yousten and Rogoff, 1969; Mignone and Avignone-Rossa, 1996). The pH stopped increasing at approximately eight hours, reaching a value of 6.4, and at this time, the stationary growth phase began. It was at this point when the accelerated formation of spores was initiated with the pH remaining constant for the rest of the sporulation process.

Another important factor to assess the changes related to vegetative and sporulation phases is to observe the changes in cell morphology during the batch growth. This is a very important feature of *B. thuringiensis* cells, given morphology indicates indirectly the metabolic state.

A series of optical and transmission electron microscopy pictures were taken at different growth phases to show the changes in the cells morphology as they evolve in their metabolic state. At the vegetative phase, the cells are motile and have a homogeneous cytoplasm (without spore) as evidenced from observation of cells under phase contrast microscope (see plate 5.1). In the stationary phase, however, the cells became thick and it was possible to observe the endospore as a refractile body inside the cell (plate 5.2).

In addition, transmission electron micrographs (TEMs) show the change in the cells morphology with more details. Plate 5.3 shows a *B. thuringiensis* vegetative cell present in the bioreactor at the beginning of the batch growth, immediately after inoculation (run NB6). Plate 5.4 shows that after three hours of batch growth, the cells are still in their vegetative growth phase. Plate 5.5 is a TEM of a cell after nine hours of batch growth, and shows the

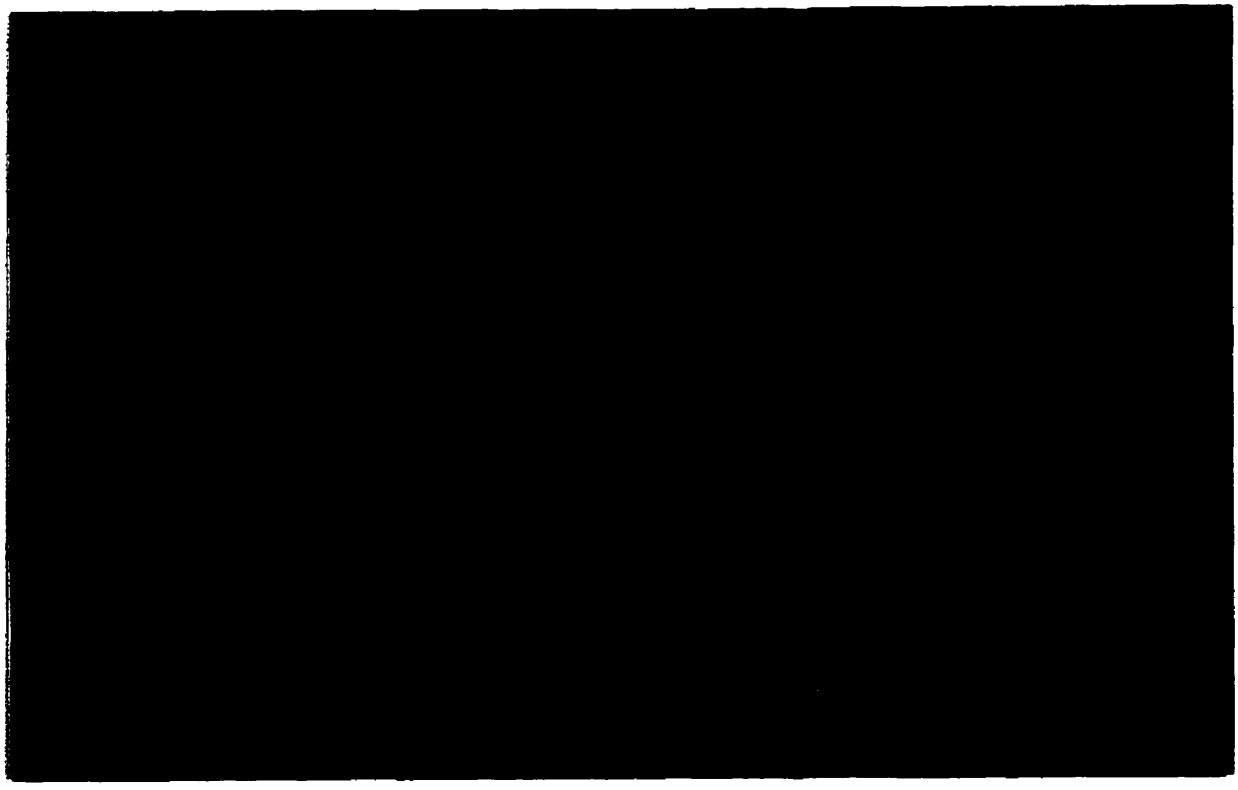

Plate 5.1 Vegetative cells of *B. thuringiensis* subspecies *kurstaki* HD-1 ATCC 33679, after 2 hours in a batch growth. Picture taken in a phase contrast microscope at 1500 X.

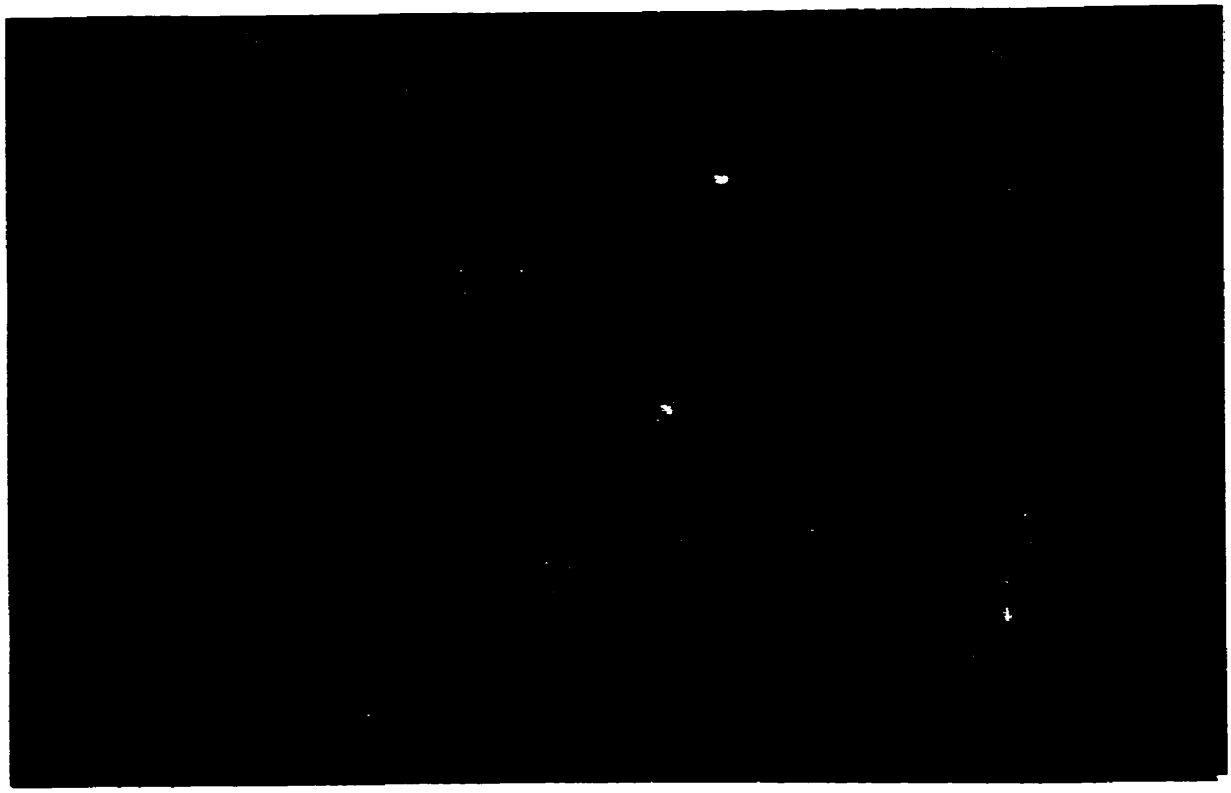

Plate 5.2 Mature cells of *B. thuringiensis* subspecies *kurstaki* HD-1 ATCC 33679. After nine hours of batch growth. Picture taken in a phase contrast microscope at 1500 X.

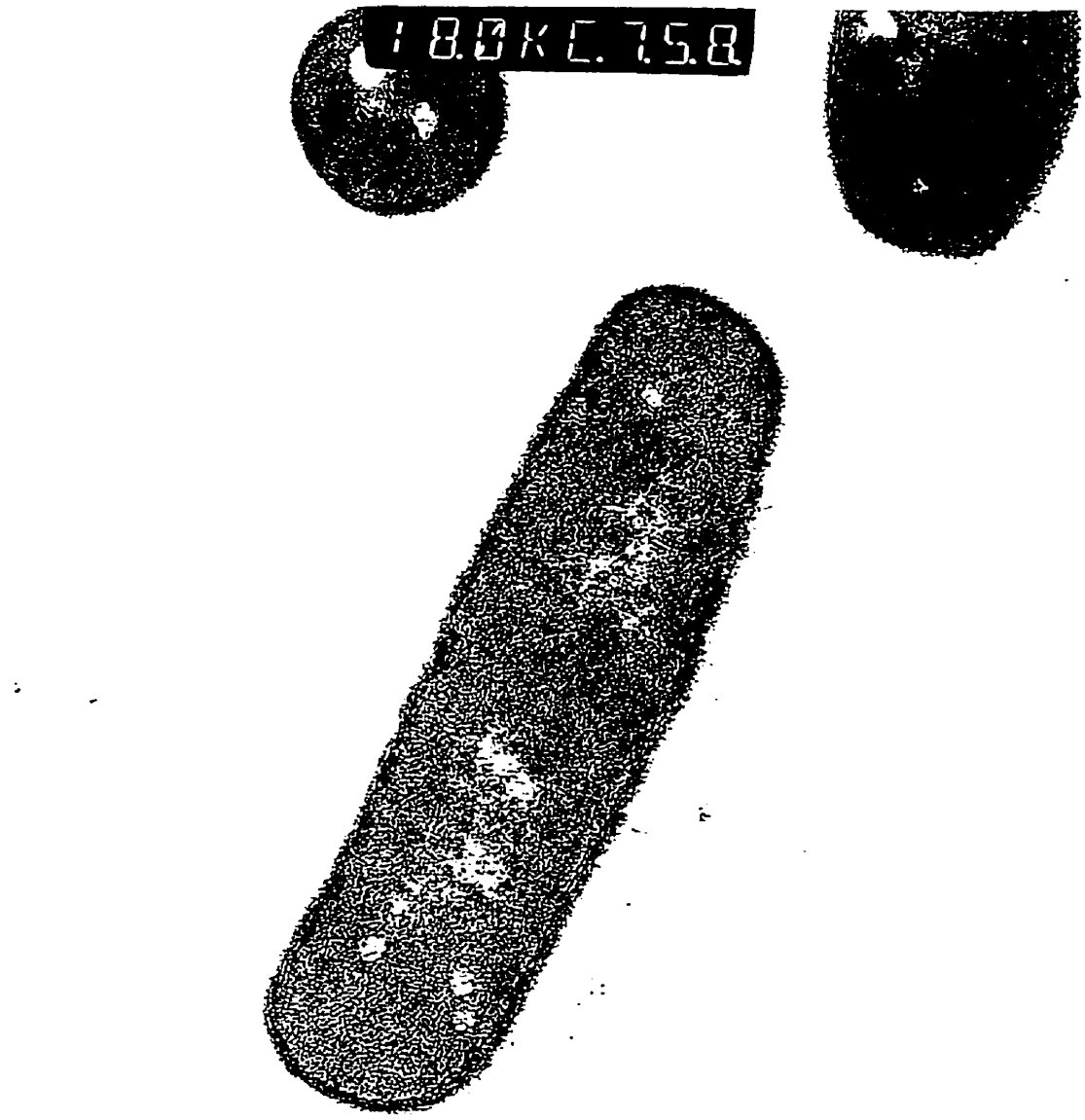

Plate 5.3 Transmission Electron Micrograph of *B. thuringiensis* vegetative cell present in the bioreactor in the beginning of the batch growth. Magnification 36,000X.

Plate 5.4 Transmission Electron Micrograph of *B. thuringiensis* vegetative cell present in the bioreactor after three hours of batch growth. Magnification 36,000X.

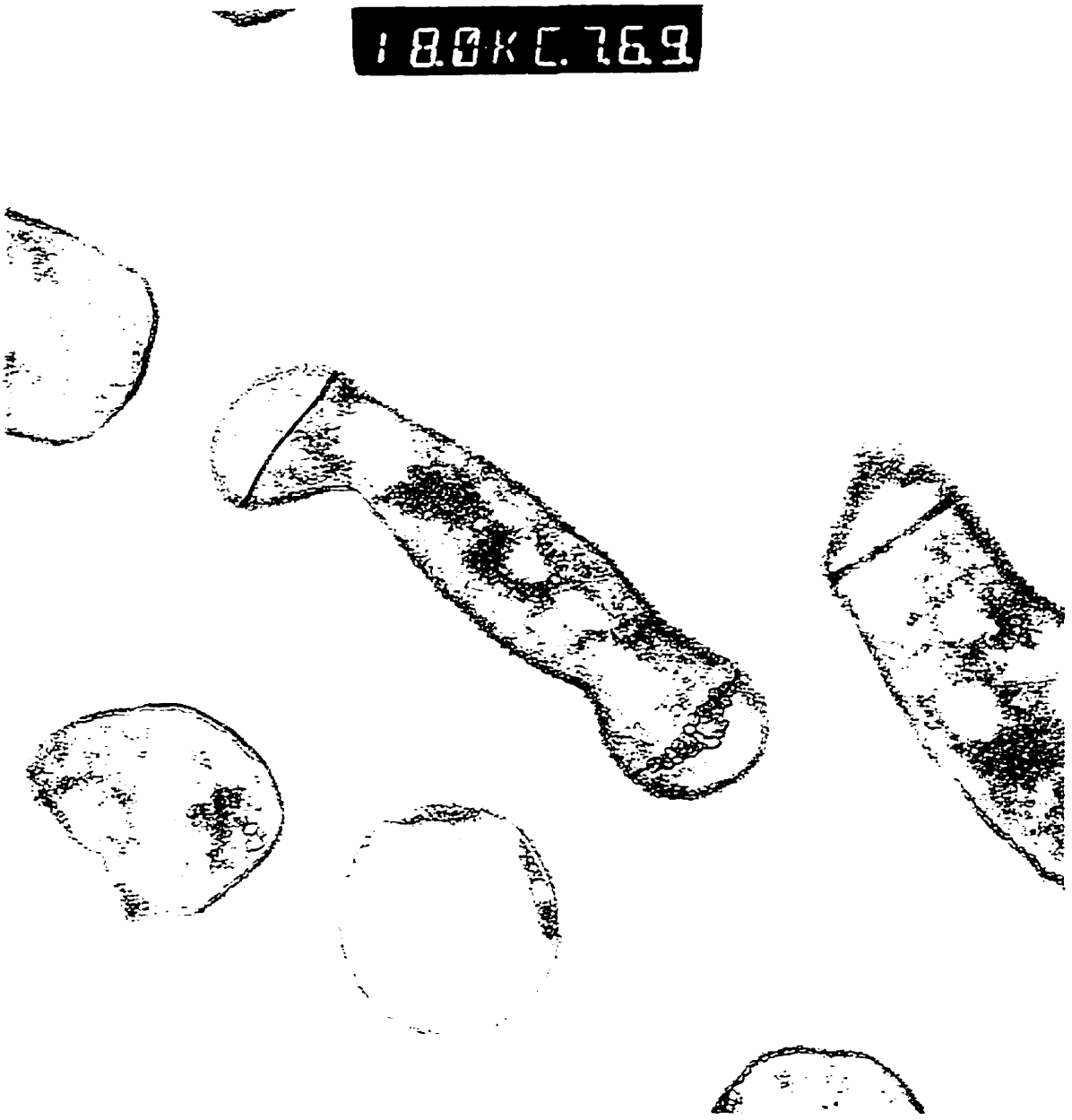

Plate 5.5 Transmission Electron Micrograph of *B. thuringiensis* vegetative cell present in the bioreactor after nine hours of batch growth. Magnification 36,000X.

presence of mesosomes in one end of the cells, forming the forespore septum, characteristic of the beginning of spore formation process (Bechtel and Bulla, 1976).

After approximately 24 hours, the cells undergo lysis, releasing the spores and the insecticidal crystal protein, delta-endotoxin, into the medium. Plate 5.6 shows the cross section of few spores and the cross section of some crystal proteins with the characteristic bypiramidal shape.

Given the previous considerations and with the information provided by Figs. 5.1 and 5.3, it can be concluded that the vegetative stage began immediately after inoculation of the bioreactor and lasted for approximately seven hours.

Regarding the sporulation phase, it is important to identify this phase because delta-endotoxin is produced during that stage. The best way to do so is by detecting the presence of spores in the culture following the procedure described in the section 4.1.2. Fig. 5.2 reports the presence of the first spores after 5.5 hours of batch culture, and this is observed at the middle of the deceleration growth phase. Thus, the presence of spores before the beginning of the stationary growth phase indicates a non homogeneous population of cells.

The spore number increased dramatically after 5.5 hours of the growth process (Fig. 5.2). The sudden increase in the number of spores suggests that the cells changed rapidly to a sporulated cell phase in a short period of time (3.5 h), as the glucose concentration approached zero. Moreover, a more detailed analysis of spore formation data during batch growth shows close to exponential rate in the spore forming process. Fig. 5.6 illustrates in a semi-logarithmic plot the exponential increase in the number of spores with time.

It should be mentioned that the number of spores reached that of the viable cells indicating that all cells contained a spore after approximately 10 hours of batch growth. Together with the spore, the crystal protein was formed. The concentration of crystal protein

Plate 5.6 Transmission Electron Micrograph of free spore and crystal protein produced by *B. thuringiensis* after 24 hours of batch growth, cell lysis occurs.Magnification 28,000 X

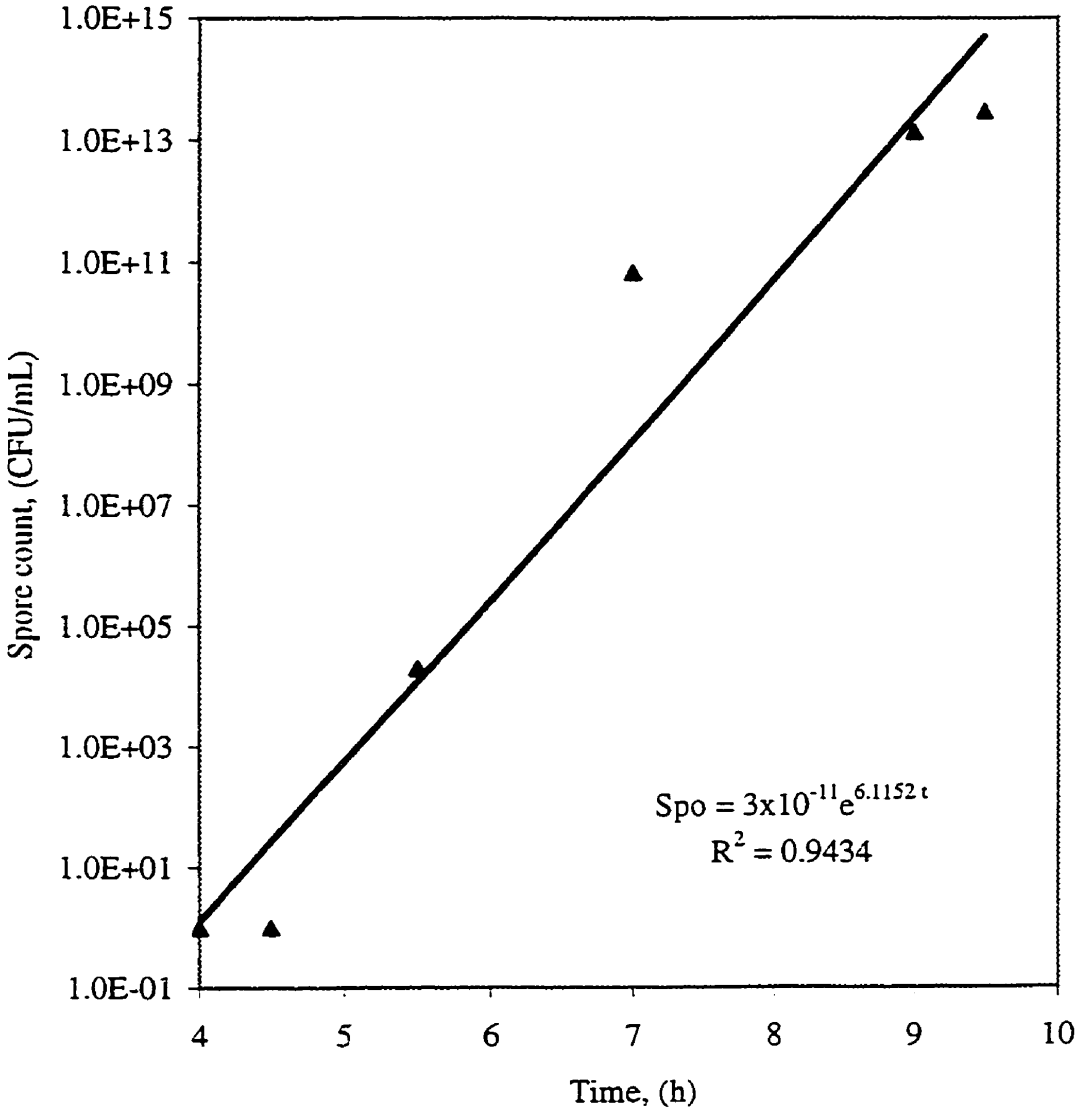

Fig. 5.6 Batch growth of *B. thuringiensis* . Spore formation kinetics. Exp. NB6

(CP) was determined with the biuret assay (section 4.1.4). The concentration of crystal protein at the end of the batch culture was 1.02 g/L.

5.1.2 Maximum specific growth rate, growth yield and biomass productivity

Fig. 5.4 presents a plot of the natural logarithm of biomass concentration versus time and Fig. 5.5 shows the linear segment of this plot which provide the maximum specific growth rate. The maximum specific growth rate was estimated to be 0.78 h^{-1}. The exponential growth phase began two hours after the inoculation and lasted for approximately two hours. The obtained maximum specific growth rate is close to the one reported under similar conditions in a batch growth (0.6 to 0.8 h^{-1}) by Anderson (1990). However, a number of other researchers reported maximum specific growth rate varying in a much wider range, (0.4 and 1.9 h^{-1}, Avignone-Rossa and Mignone, 1995; Rodriguez-Monroy and de la Torre, 1996).

In the case of batch growth, the cells are in a changing environment, and this encourages the formation of an heterogeneous cell population. Therefore, different growth rates can be expected. As a consequence, the maximum specific growth rate estimated in a batch culture can be only considered a pondered average value.

While strictly speaking an homogeneous population cannot be attained in a culture with environmental conditions changing with time, it is expected that under some constrained variation of conditions, as those of the present study, the estimated values of the parameters for the entire process are still a viable approximation. In this respect, the restricted variation of the maximum specific growth rate support this argument and the kinetic parameters resulting of these experiments can have sound physicochemical meaning.

The growth yield, $Y_{X/S}$, expressing the relationship between the biomass formed and the substrate consumed, it was calculated for the batch growth as the ratio of the net biomass produced to the glucose consumed. The global growth yield was 0.51 g cells/g substrate for

run NB6. While the definition of a global growth yield, $Y_{X/S}$, is suitable for cultures that do not change in substrate uptake rate during their growth, the growth yield for *B. thuringiensis* varies with the specific growth rate when cultured in a continuous process (Rodriguez-Monroy and de la Torre, 1996). Thus, *B. thuringiensis* culture changes its specific growth rate during the batch growth, and it can be expected that the growth yield may also change with time. As shown in Fig. 5.7, the relationship between biomass and glucose concentration was in the case of this study close to a straight line with a 0.57 g cells/g glucose slope. Consequently, this result shows that the growth yield does not change significantly during the batch growth. In addition, the growth yield obtained by this method is similar (± 26 %) to growth yield values reported in the literature (Anderson, 1990).

The volumetric biomass productivity was 0.74 g/L-h after 6 hours of batch culture (Fig. 5.8), at which time the spores and crystal protein were not yet formed. It was more interesting to find biomass productivity when the sporulation was completed. After approximately nine hours of batch culture, the productivity was 0.69 g/L-h. Although spores and the crystal protein are the desired products, the biomass volumetric productivity is an indicator of how efficient a batch process is. In addition, this indicator can be used for comparison of different culture methods.

Table 5.1. Maximum specific growth rate, yield growth, biomass productivity and crystal protein concentration for batch cultures of *B. thuringiensis* subspecies *kurstaki* HD-1 ATCC 33679. For experiment NB6

Exp. No.	Maximum Specific Growth Rate (1/h)	Global yield growth $Y_{X/S}$, (g/g)	Biomass Productivity (g/L-h)	Crystal protein concentration (g/L)
NB6	0.78	0.51 - 0.57	0.69-0.74	1.02

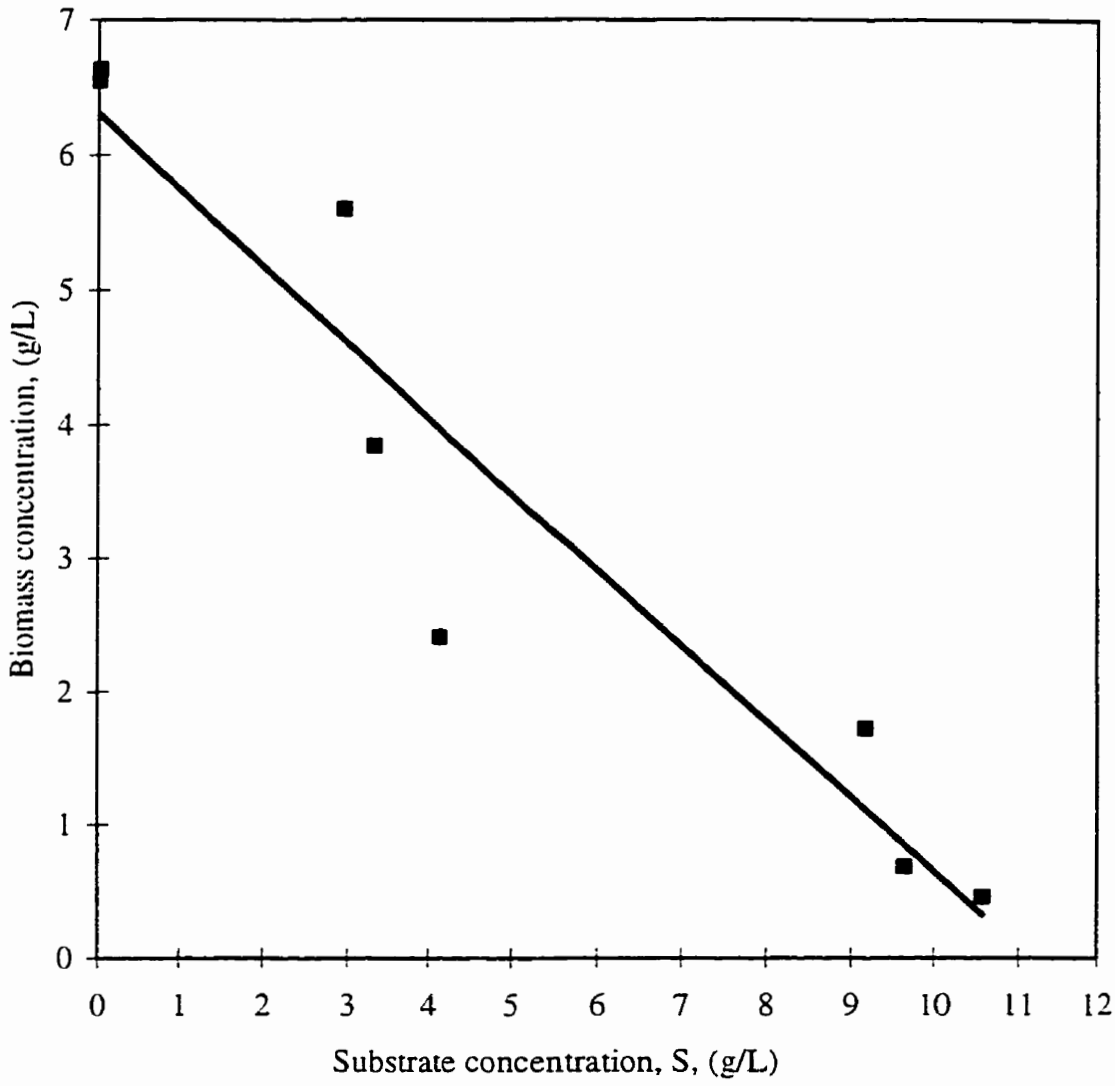

Fig. 5.7 Batch culture of *B. thuringiensis* . Exp. NB6. Relationship between biomas and glucose concentration. Estimation of growth yield.

$X = -0.5661S + 6.3104$

$R^2 = 0.9052$

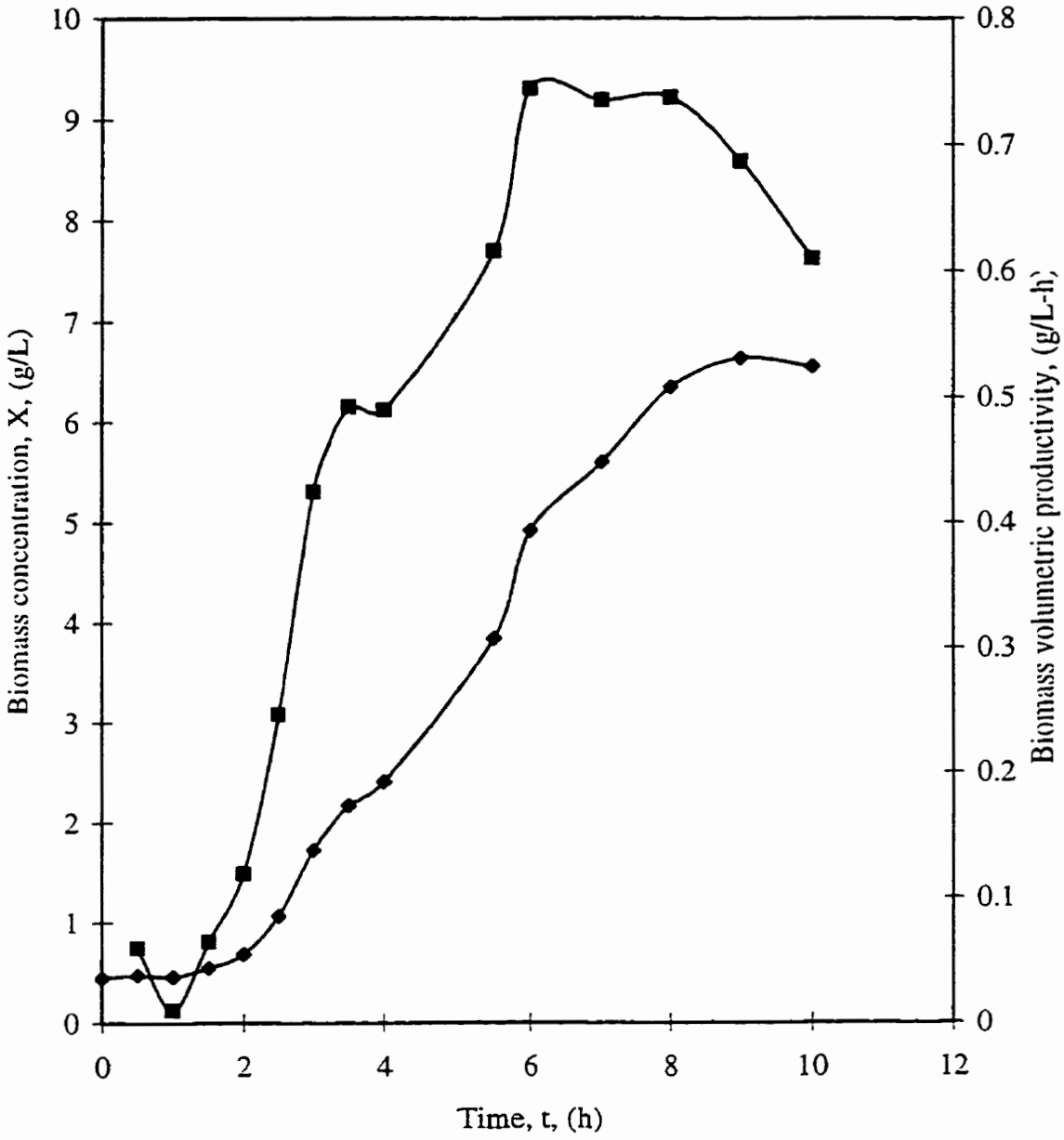

Fig. 5.8 Batch growth of *B. thuringiensis* .Exp. NB6. Biomass volumetric productivity

5.2 Fed-batch Growth

Two fed-batch experiments were performed to investigate the biomass formation and the degree of sporulation using this mode of operation. A first fed-batch culture was run with a high glucose concentration and high volumetric flow rate to encourage formation of biomass. A second fed batch culture was run with a low glucose concentration and low volumetric flow rate in order to promote spore formation. The different operational conditions for the fed-batch cultures of *B. thuringiensis* are listed in Table 5.2. The experimental results for the fed-batch culture NFB1 are presented in Table A.4 (appendix A) and in Fig. 5.9.

Table 5.2 Operational conditions for the fed-batch culture of *B. thuringiensis* HD-1 ATCC 33679. Experiments NFB1 and NFB2

Operational condition	Exp. NFB1	Exp. NFB2
Temperature	30 °C	30 °C
Initial pH	6.8	6.8
Air supply	1 L/min	1 L/min
Impeller speed	variable	variable
Initial reaction volume	0.85 L	0.75 L
Volumetric flow rate	0.117 L/h	0.08 L/h
Glucose concentration in the feed stream	39 g/L	10 g/L

Note: All the components of the culture medium, except glucose, were added at the same proportion as that in the basal medium.

As shown in Fig. 5.9, both the biomass concentration increased continuously during the fed-batch growth, as did the glucose concentration. This indicates that the limiting substrate input rate was higher than the substrate uptake rate for cell growth.

The substrate concentration of glucose in the feed stream was 39 g/L and according to the experimental data, the minimum value for the glucose concentration inside the reactor

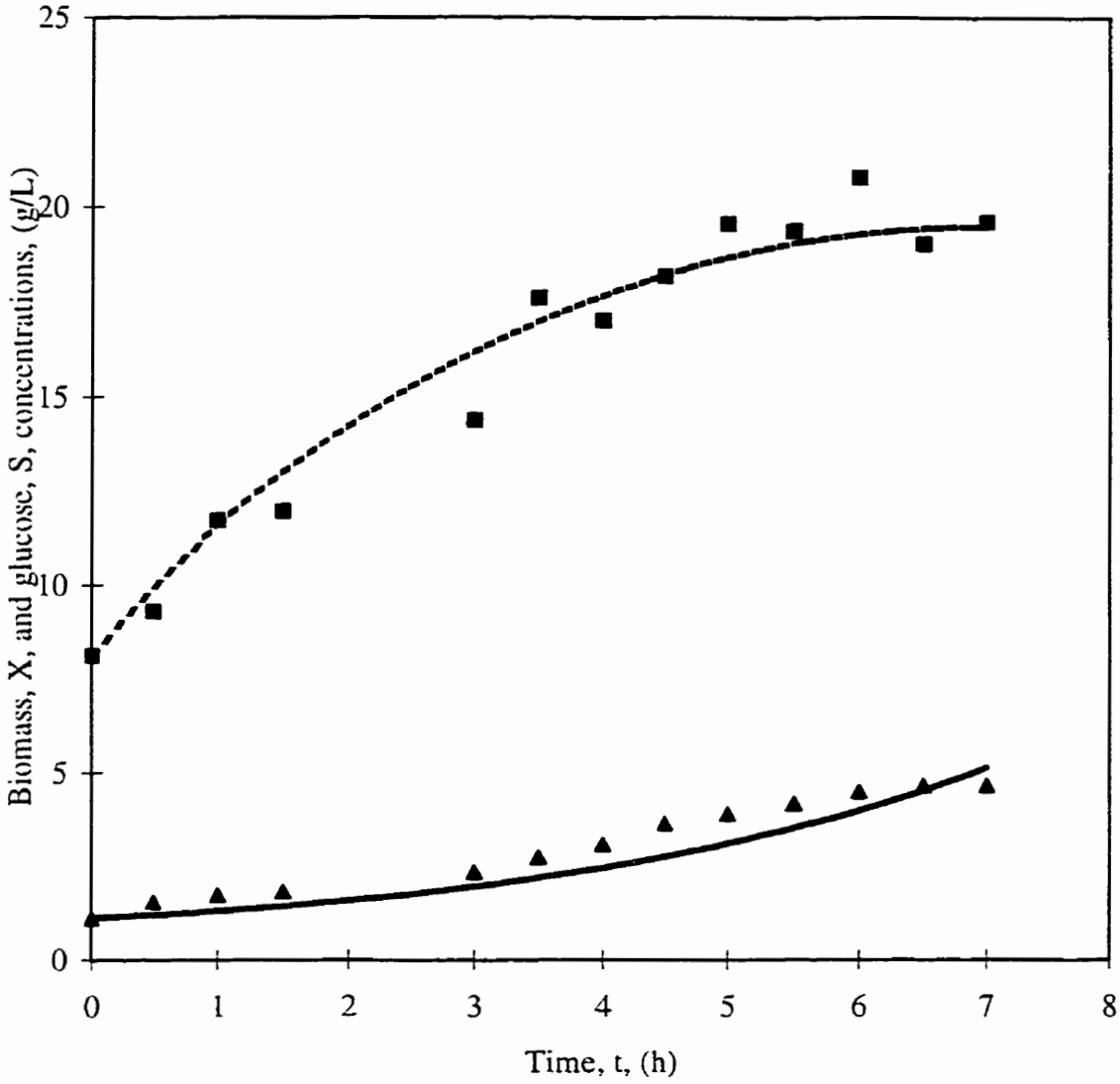

Fig. 5.9 Fed-batch growth of *B. thuringiensis* subspecies *kurstaki* . Exp. NFB1. Constant volumetric flow rate F = 0.117 L/h, substrate concentration in the feed stream S_0 = 39 g/L, μ_{max} = 0.38 h^{-1}, Ks = 3.1 g/L, $Y_{X/S}$ = 1.2 g/g

was 8.13 g/L. At this high substrate concentration the specific growth rate, μ, should be equal to the maximum specific growth rate, μ_{max}. The equation for a fed-batch culture at a constant specific growth rate (equation 3.32) was used to estimate the maximum specific growth rate from the experimental fed-batch growth data. According to this equation, plotting $\ln(X/X_0) + \ln(V/V_0)$ versus time should produce a straight line with the maximum specific growth rate being the slope. A graph (Fig. 5.10) with a close to straight line was observed. The maximum specific growth rate, μ_{max} obtained using this method was 0.34 h^{-1}. In spite of the high concentration of the limiting substrate, the specific growth rate was low, compared with the specific growth rate obtained in batch and continuous cultures performed at the same substrate concentration.

The maximum specific growth rate was also calculated by solving numerically the differential equations describing a fed batch culture. In this way, the maximum specific growth rate, μ_{max} and the saturation constant, K_s, were found to be 0.38 h^{-1} and 3.1 g/L respectively. With these parameters, the fed batch model agreed with the experimental data (Fig. 5.9).

In order to discuss these results in fed batch culture, it is important to consider the metabolic state of the cells. One way to estimate the metabolic state is to analyze the morphology of *B. thuringiensis* cells. At the beginning of the fed-batch growth, the cells were in its vegetative phase. After two hours of fed-batch growth, the cells were present in pairs or individual cells and were thin and motile. At the end of the culture, some cells formed clumps and contained shiny white bodies probably made up of β-hydroxybutyric acid (Macrae and Wilkinson 1958). This polymer is formed during the growth stage and reaches a maximum at the time the cells enter the stationary stage (Slepecky and Law, 1961). Spores were not detected in the cells at the end of the fed-batch growth. These observations indicate that the cells did not reach the vegetative stage. There is at least a fraction of them at the beginning of the stationary stage. This is contrary to what was expected for the high substrate concentration. This observation is also in agreement with the low maximum specific growth rate. This relatively low specific growth rate and the cells in stationary phase indicates that in the fed batch operation at high glucose concentration, the cells are not able to sustain

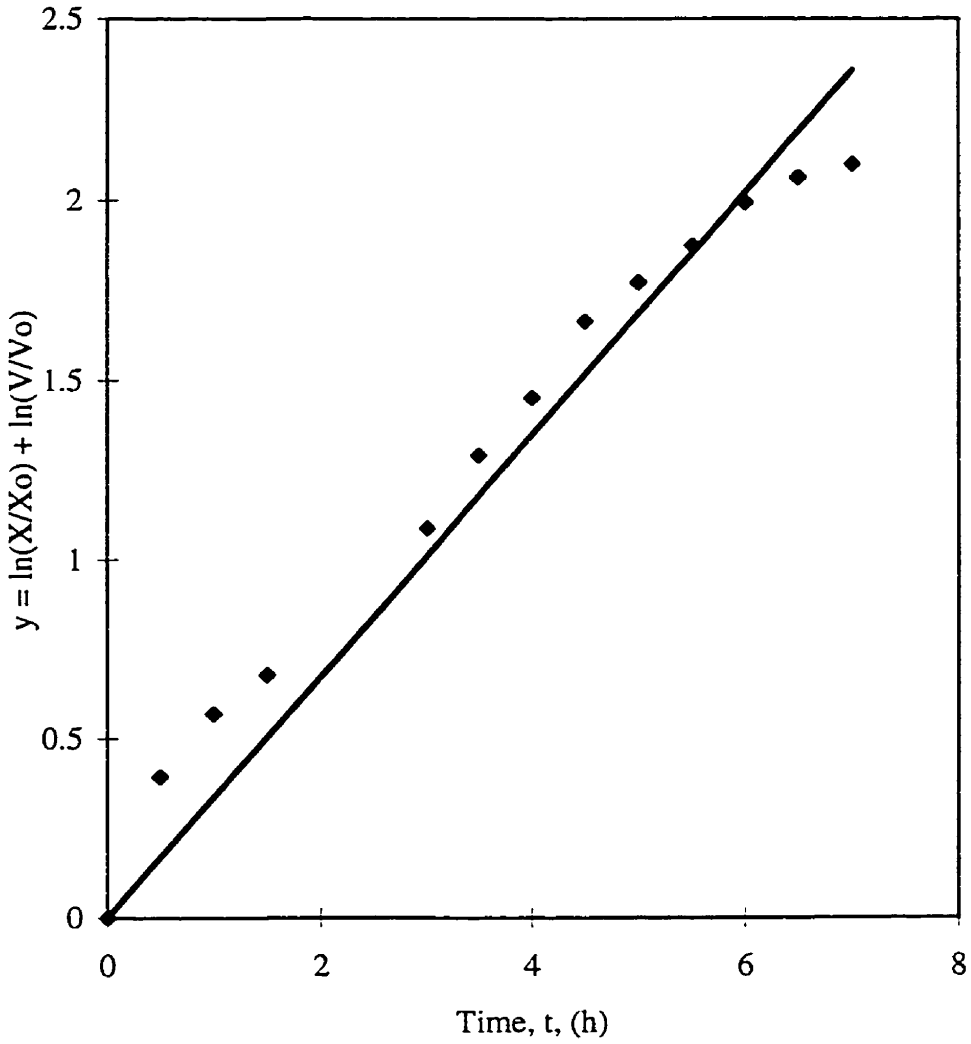

Fig. 5.10 Fed-batch culture of *B. thuringiensis*. Constant volumetric flow rate, F= 0.117 L/h, constant substrate concentration in the feed stream So = 39 g/L. Estimation of maximum specific growth rate.

Linear equation: $y = 0.337t$, $r^2 = 0.95$, μ_{max}

growth rates observed in batch cultures possibly due to an inhibitory effect of glucose. This conclusion may be sustained by the fact that the specific growth rate resulted to be lower at high load of glucose compared with the one obtained at low glucose concentration. A test to verify the inhibition effect of glucose on the cell growth is the estimation of the inhibition constant K_I. This can be done by using the Line-Weaver inverse plot ($1/\mu$ versus $1/S$). However, in the batch experiments performed during this study there was not change in the initial glucose concentration in the liquid medium, which is required to find K_I.

These results are in agreement with those obtained by other researchers with intermittent fed batch operation (Stradi 1992; Liu et al, 1994). Following addition of substrate at a constant feed rate, it was claimed that it was convenient to interrupt the feed for a period of time in order for the cells to adapt to the changing environment.

The experimental results for the fed-batch culture NFB2 with a low glucose concentration and a low volumetric flow rate are shown in table A.5 (appendix A) and Fig. 5.11. The glucose concentration in the feed stream was 10 g/L and the volumetric flow rate of the input stream was 0.08 L/h. The maximum glucose concentration in the bioreactor was 4.85 g/L and decreased continuously during the experiment.

The operation of the fed-batch bioreactor at low flow rate and relatively low glucose concentration produced an increase in the biomass concentration during the first five hours and the consequent reduction of the glucose concentration. During the last five hours of the fed-batch operation, the glucose concentration was reduced practically to zero because the demand of glucose for cell growth was higher than the glucose supply from the feed stream. The cells were present in clumps or in pairs. The cells contained white circular bodies (probably poly β-hydroxy butyric acid), suggesting that they were in the beginning of the stationary growth phase. At the end of the fed-batch growth, the concentration of viable cells was 6.5×10^{11} viable cells per mL, with no spores present.

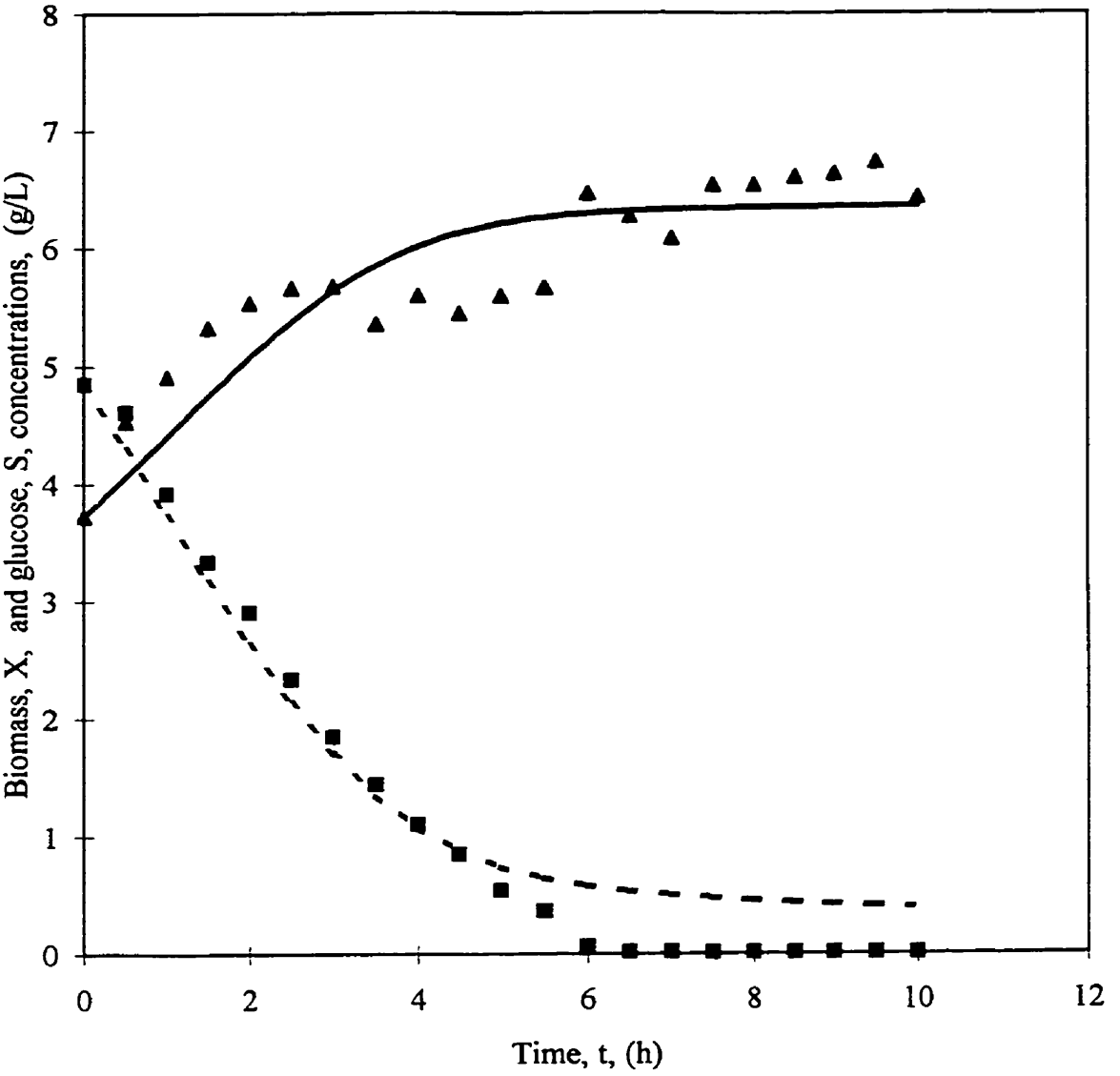

Fig. 5.11Fed-batch culture of *B. thuringiensis* subspecies *kurstaki*. Exp. NFB2. Constant volumetric flow rate F = 0.08 L/h, substrate concentration feed stream S_0 = 10 g/L, μ_{max} = 0.46 h^{-1}, K_s = 3.1 g/L, $Y_{X/S}$ = 0.64 g/g

During the batch growth of *B. thuringiensis*, the cells form spore in less than four hours after the depletion of glucose (section 5.1.1). In contrast, during the last five hours in the fed-batch process, even though the glucose was practically depleted, the cells did not show signs of complete maturation or formation of spores. This result suggests that low or zero concentration of substrate in a fed-batch bioreactor is not a sufficient condition to promote sporulation of *B. thuringiensis* cells.

In addition, the maximum specific growth rate was estimated by solving the differential equations for a fed batch culture. The best fitting with the experimental data was achieved with μ_{max} and K_s values of 0.46 h^{-1} and 3.1 g/L, respectively. Since the maximum specific growth rate is close to that obtained in batch cultures (μ_{max} = 0.53 h^{-1}) it can be concluded that unlike the experiment NFB1 (high load of glucose), a fed batch culture at low glucose load does not inhibit the cell grow. The volumetric productivity was for experiments NFB1 and NFB2, 0.58 and 0.47 g/L-h, respectively. These results show that operational conditions (volumetric flow rate and substrate concentration) may play a very important role on the metabolic processes. Fed-batch culture experiments also demonstrated the significance of the reactor operations for both cell growth and spore and crystal protein formation.

5.3 Continuous growth in a single stage CSTR bioreactor .

A series of continuous growth steady-state experiments were performed in a 2-L bioreactor, as described in the experimental procedures section. The main objectives of these experiments were to determine the growth kinetic constants μ_{max} and K_s and to test possible crystal protein production in a continuous process.

The estimation of the kinetic constants using the continuous experimental data is based on the assumption of a steady state operation of the bioreactor. Several experiments were performed at different volumetric flow rates, and constant biomass concentration was used as a criterion to determine whether the steady state was reached or not. Figures B.1 to

B.4 (Appendix B) show a typical continuous unsteady-state operation, starting at the end of batch growth until it reached a steady-state. The steady state was also confirmed using the non-steady state mathematical model (section 6.4, and Table D.5, appendix D). After steady-state was achieved, at a given dilution rate, D, a sample was taken from the bioreactor vessel to perform various required analysis.

5.3.1 Biomass and glucose concentrations and spore and crystal production at steady state in continuous growth

The results of a total of ten different dilution rates presented in Tables 5.3 and 5.4 are shown in Figures 5.12 and 5.13, respectively. At dilution rates greater than 0.2 h^{-1} no spores or crystal protein were detected. This was further corroborated by optical and transmission electron microscopy. Plates 5.7, 5.8, 5.9, and 5.10 show photomicrographs of samples taken at dilution rates of 1.05 h^{-1}, 0.47 h^{-1}, 0.2 h^{-1} and 0.14 h^{-1}, respectively. It has to be mentioned that there was an extensive degree of cell lysis and the presence of spores and crystal protein at the low dilution rate of 0.14 h^{-1}. Plates 5.11, 5.12 and 5.13 report the transmission electron microscope results of samples taken at dilution rates 0.47 h^{-1}, 0.2 h^{-1} and 0.14 h^{-1} respectively.

Table 5.3 Summary of results for steady-state continuous growth of *B. thuringiensis*, subspecies kurstaki HD-1 (ATCC 33679)

Dil Rate, D (h^{-1})	Glucose conc. S (g/L)	Biomass conc. X, (g/L)	Spore conc. (CFU/ml)	Crystal protein conc., CP, (g/L)
0.14	0.03	5.09	8.9×10^{12}	1.03
0.20	0.81	5.38	ND	ND
0.28	1.01	5.36	ND	ND
0.37	1.05	5.54	ND	ND
0.47	3.11	5.22	ND	ND
0.54	3.29	5.36	ND	ND
0.62	5.69	3.92	ND	ND
0.71	3.71	4.35	ND	ND
0.85	6.87	2.56	ND	ND
1.05	7.9	1.83	ND	ND

ND = Not detectable

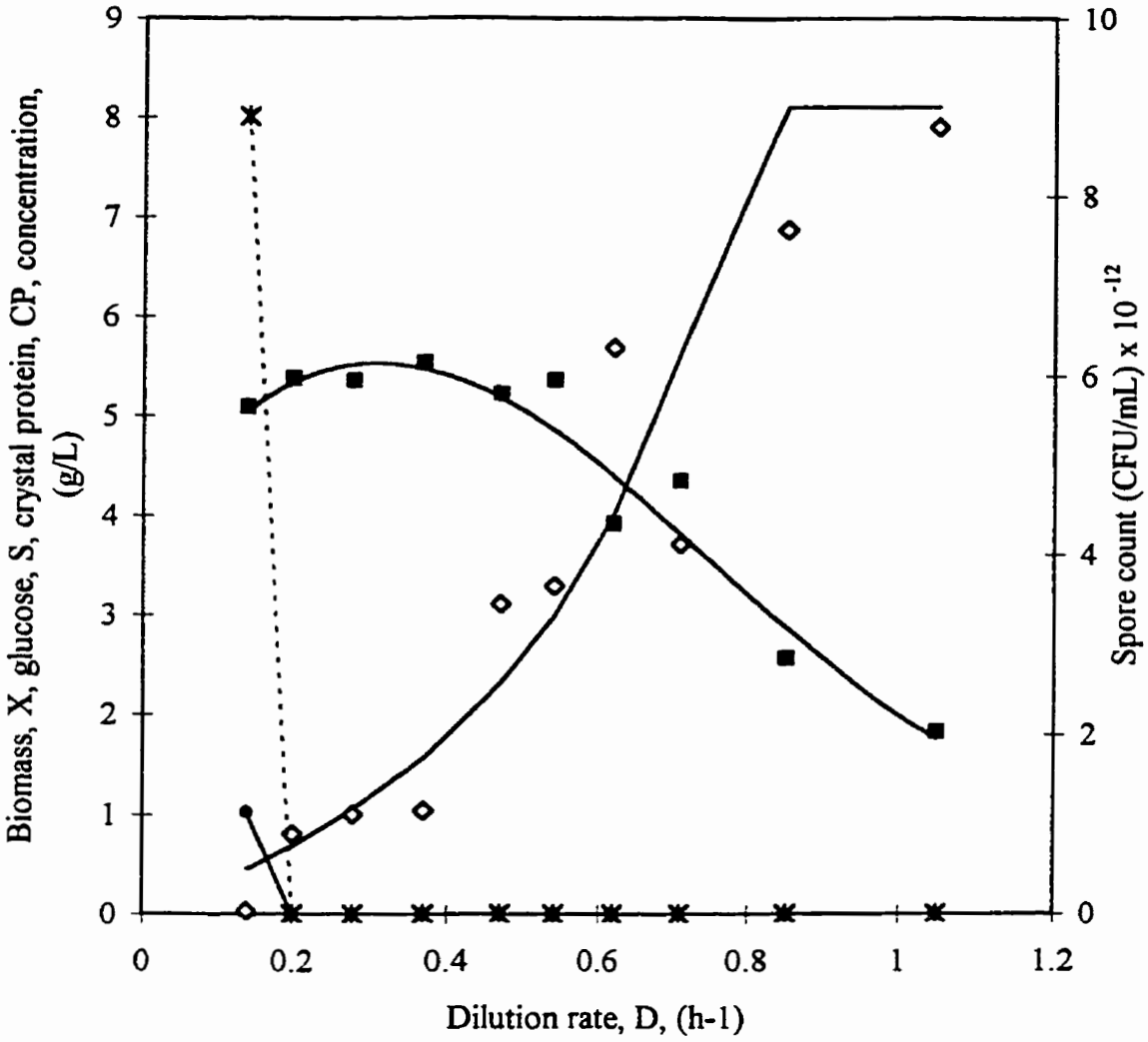

Fig. 5.12 Continuous steady-state growth of *B. thuringiensis*. Biomas, glucose, crystal protein and spore concentration as a function of dilution rate, D, in a single stage bioreactor system.

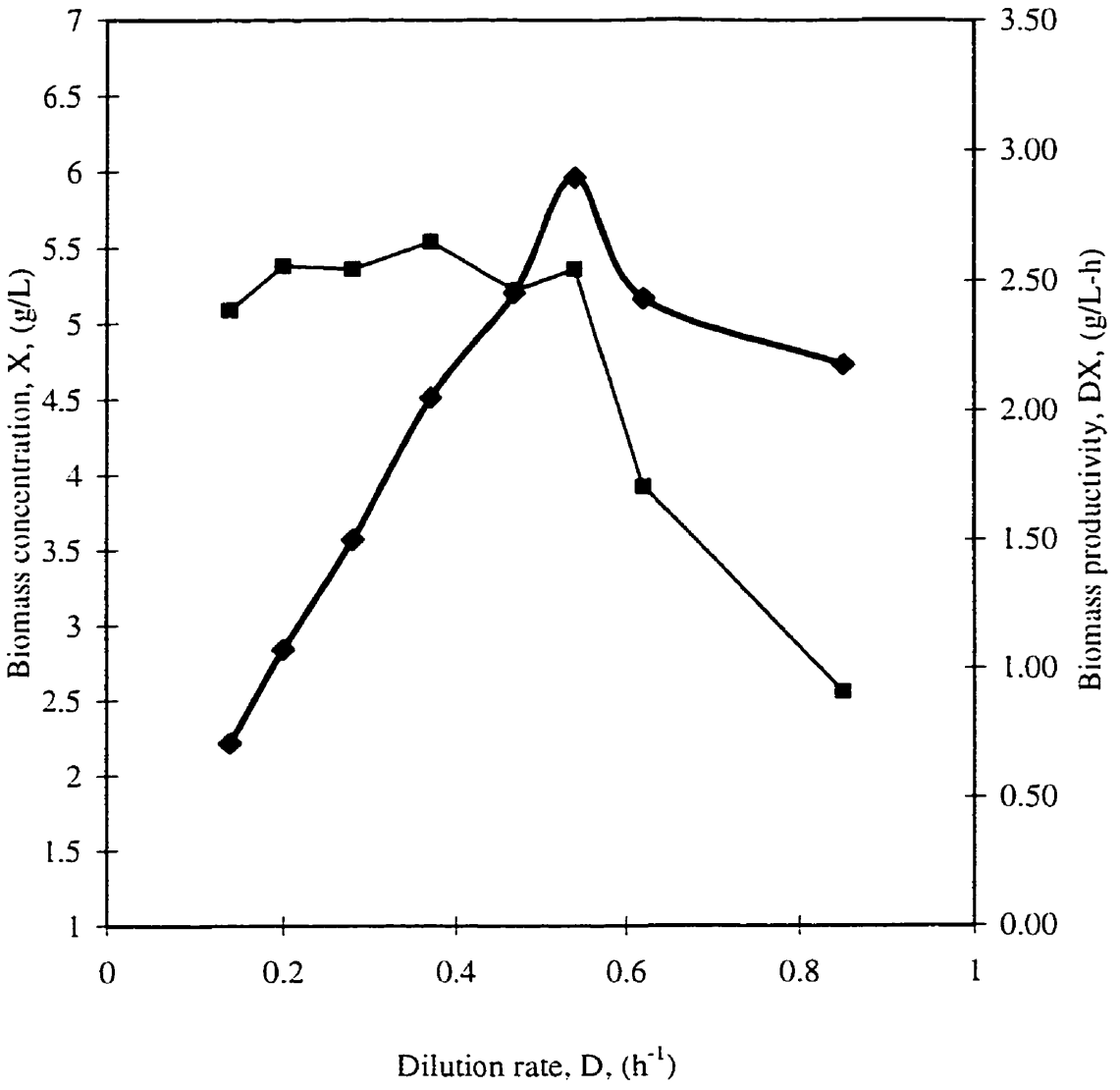

Fig. 5.13 Continuous steady-state growth of *B. thuringiensis* . Biomass concentration and corresponding bioreactor volumetric productivity as a function of dilution rate, D, in a single stage bioreactor system

Plate 5.7 Cells of *B. thuringiensis* HD-1 subspecies *kurstaki* from a continuous growth at a dilution rate of 1.05 h^{-1}. Picture taken in a phase contrast microscope at 1500 X

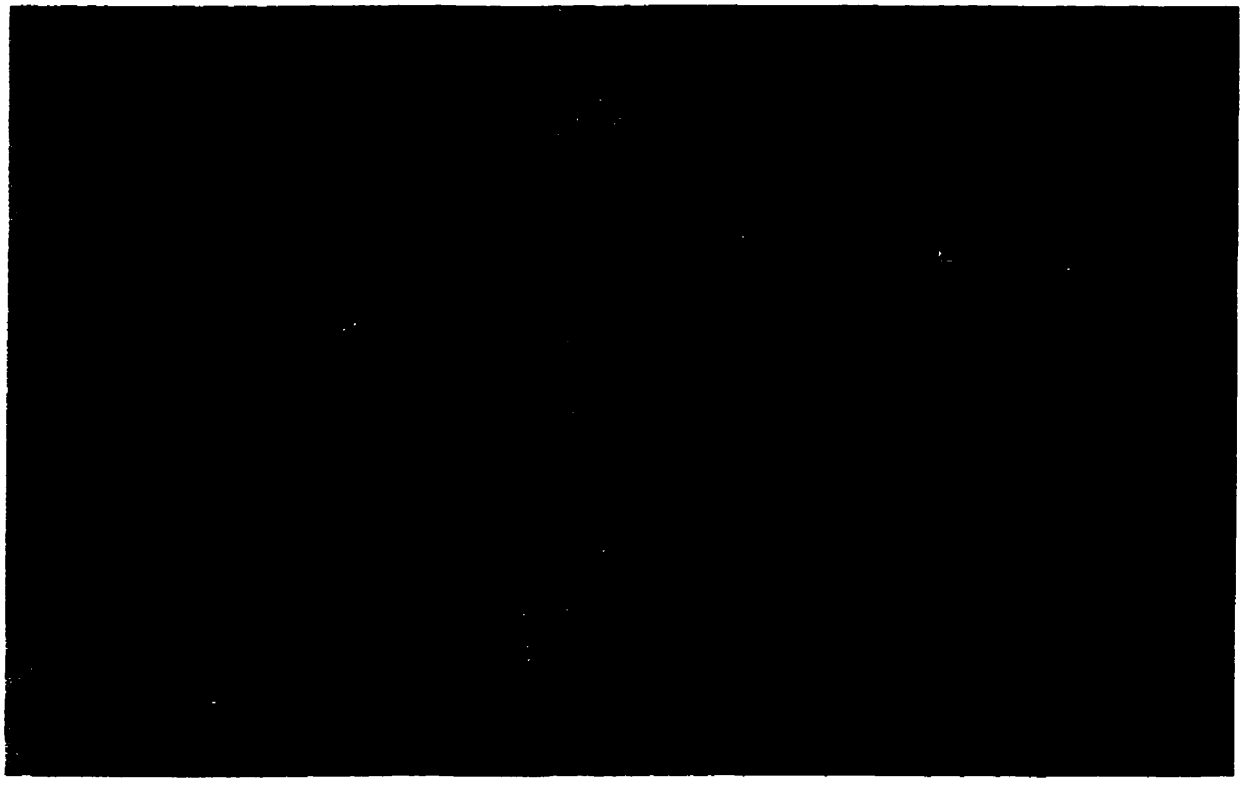

Plate 5.8 Cells of *B. thuringiensis* HD-1 subspecies *kurstaki* from a continuous growth at a dilution rate of 0.47 h^{-1}. Picture taken in a phase contrast microscope at 1500 X

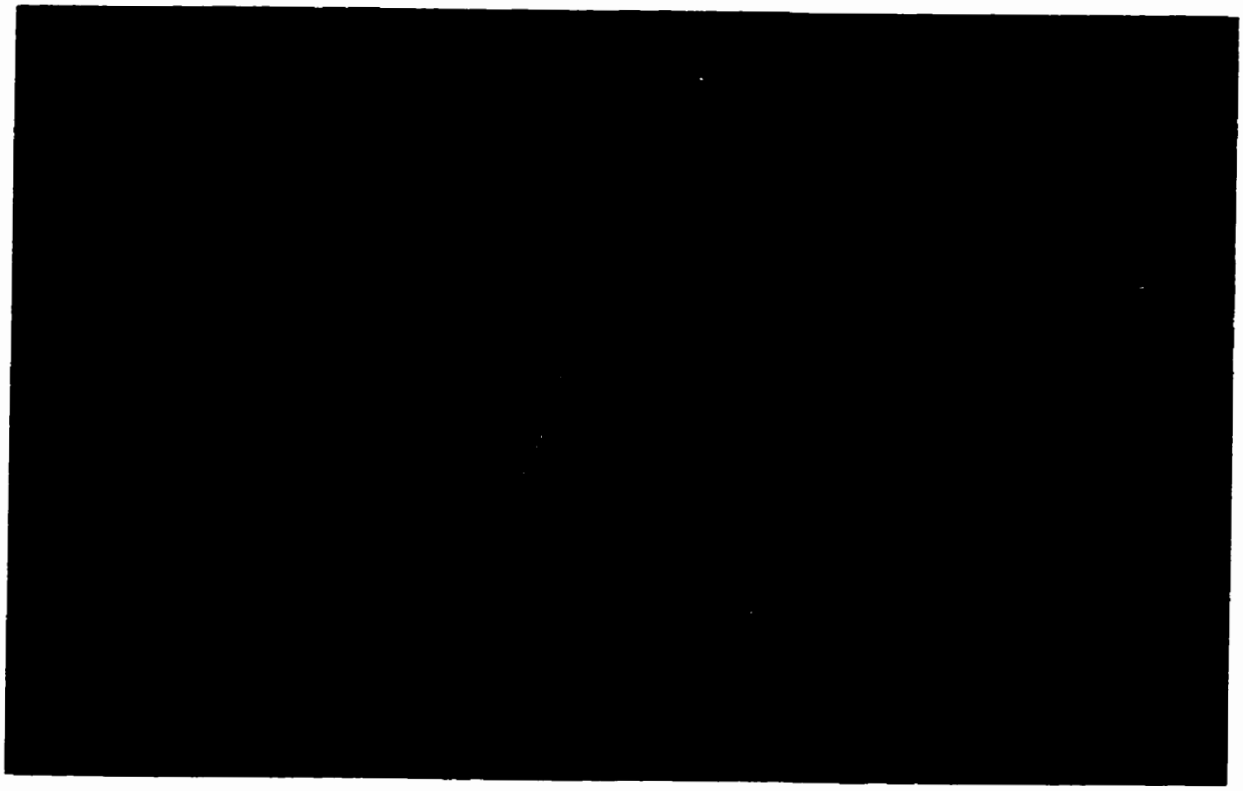

Plate 5.9 Cells of *B. thuringiensis* HD-1 subspecies *kurstaki* from a continuous growth at a dilution rate of 0.20 h^{-1}. Picture taken in a phase contrast microscope at 1500 X

Plate 5.10 Cells of *B. thuringiensis* HD-1 subspecies *kurstaki* from a continuous growth at a dilution rate of 0.14 h^{-1}. Picture taken in a phase contrast microscope at 1500 X

Plate 5.11 Transmission Electron Micrograph of *B. thuringiensis* cell cultured in continuous bioreactor at a dilution rate of 0.47 h^{-1}. Magnification 36,000 X

Plate 5.12 Transmission Electron Micrograph of *B. thuringiensis* cell cultured in continuous bioreactor at a dilution rate of 0.2 h^{-1}. Magnification 55,000 X

Plate 5.13 Transmission Electron Micrograph of *B. thuringiensis* cell cultured in continuous bioreactor at a dilution rate of 0.14 h^{-1}. Magnification 36,000 X

Table 5.4 Bioreactor volumetric productivity of biomass and crystal protein at steady-state continuous growth of *Bacillus thuringiensis* subspecies *kurstaki* HD-1 (ATCC 33679) in a single stage bioreactor system.

Dil Rate, D (h^{-1})	Biomass conc., X, (g/L)	Crystal protein conc., CP (g/L)	Bioreactor Vol. productivity Biomass, D*X (g/L-h)	Crystal protein,D*CP (g/L-h)
0.14	5.09	1.03	0.71	0.144
0.20	5.38	ND	1.08	ND
0.28	5.36	ND	1.50	ND
0.37	5.54	ND	2.05	ND
0.47	5.22	ND	2.45	ND
0.54	5.36	ND	2.89	ND
0.62	3.92	ND	2.43	ND
0.85	2.56	ND	2.18	ND

ND = Not detectable

These TEM photographs show the finer structure of individual *Bacillus thuringiensis* cells, and Plate 5.13 at the low dilution rate 0.14 h^{-1} shows a cross section of two protein crystals of delta-endotoxin, and a cross section of a single spore that shows the different layers of the spore structure of *B. thuringiensis.*

At dilution rates higher than 0.47 h^{-1}, the cells are in the vegetative growth stage only. At 0.2 h^{-1}, the cells are in the transition stage, and at 0.14 h^{-1} the cells have formed spores and suffered lysis. These changes in morphology provide evidence that growth rate of a culture alters in some degree the physiological state of that culture (Boudreaux, and Srinivasan, 1981). In this respect, it was observed that there were changes in morphology in *B. thuringiensis* cell depending on the conditions of its environment (dilution rate) during the continuous culture. These changes were evident at low dilution rates with the formation of spores.

At the low dilution rate of 0.14 h^{-1} the crystal protein concentration was 1.03 g/L and the spore count 8.9 x 10^{12} CFU/mL. It is apparent that at this low dilution rate of 0.14 h^{-1}

the rate of glucose supply to the bioreactor was low enough to keep a low glucose concentration (S_0 = 0.03 g/L) which promoted sporulation and cell lysis with the release of spores and bipyramidal shaped crystals of delta-endotoxin protein in the liquid medium. In contrast, for all dilution rates greater than 0.2 h^{-1}, there was enough glucose in the bioreactor to promote active vegetative cell growth without formation of spores and delta-endotoxin.

The biomass productivity with the change in dilution rate was calculated with those experimental data presented in Table 5.4. Experimental data corresponding to dilution rates higher than the critical dilution rate were disregarded due to the possibility that the steady state was not reached. The maximum biomass productivity was obtained at a dilution rate of 0.54 h^{-1}.

5.3.2 Growth kinetic constants

The continuous culture is an excellent tool to measure the Monod relationship between the specific growth rate, μ, and the glucose (substrate) concentration, S, under conditions where a bacterium is exposed to a constant environment which is not a function of time. In addition, the continuous steady-state experimental data can be used to calculate the Monod constants, K_S and the maximum specific growth rate, μ_{max}.

While knowledge of the growth kinetic constants is of significant importance in modeling, scale up, and optimization of bioreactors, for *B. thuringiensis* cultures, there is a lack of consistency in the growth kinetic constants reported in the literature. (Avignone-Rossa and Mignone, 1995; Rodriguez-Monroy and de la Torre, 1996). This section deals with the estimation of the growth kinetic constants (μ_{max} and K_s) using the continuous experimental data. Unlike other research works on this subject, in which these constants were estimated using a single experiment and/or a single method, in this dissertation a set of experimental data and two different methods were used to estimate the kinetic constants and the results were verified with three independent continuous experiments.

The data used in the estimation of the growth kinetic constants are reported in Table A.13 (appendix A) and a plot of glucose concentration versus dilution rate is shown in Fig. 5.14. Two methods were adopted in the parameters estimation. A first method is based on the plotting of the inverse of substrate concentration versus the inverse of dilution rate. This provides the maximum specific growth rate and the saturation constant (Fig. 5.15). The maximum specific growth rate (μ_{max}), using this method was 1.1 h^{-1}, and the saturation constant (K_s) was 3.1 g/L.

The second method for the kinetic constants estimation was a non-linear regression with Mathcad 6.0 software, to fit the equation 3.40 to the experimental data. The results were a maximum specific growth rate of 1.05 h^{-1} and a saturation constant of 2.8 g/L. As a result, close kinetic constants were obtained and it was demonstrated that the specific technique for parameter estimation did not affect the actual value of the μ_{max} and K_s parameters.

In order to further confirm the value obtained for μ_{max} with continuous experimental data (Table A.13 and Figures 5.14 and 5.15), a separate experiment was performed. In this run, so called "washout" run, the dilution rate selected was much greater than D = 1.1 h^{-1}. Table A.14 of appendix A gives experimental data for biomass concentration under washout conditions in a continuous culture at a dilution rate of 1.49 h^{-1} (Fig. 5.16). Under these conditions, and given the rate of cell removal was greater than the rate of cell generation, cells were completely removed after a given time period.

The μ_{max} value from the washout results (Fig. 5.16) was 1.16 h^{-1}, which agrees very well with the value of 1.1 h^{-1} found from the steady-state continuous growth experiments (Figures 5.14 and 5.15). Thus the above described experimental methods provided excellent means of independently checking the value of μ_{max}.

In order to verify the predictive ability of the Monod model with the estimated kinetic constants (μ_{max} = 1.1 h^{-1}, and Ks = 3.1 g/L) a separate series of three continuous growth experiments were run at different dilution rates (Table 5.5).

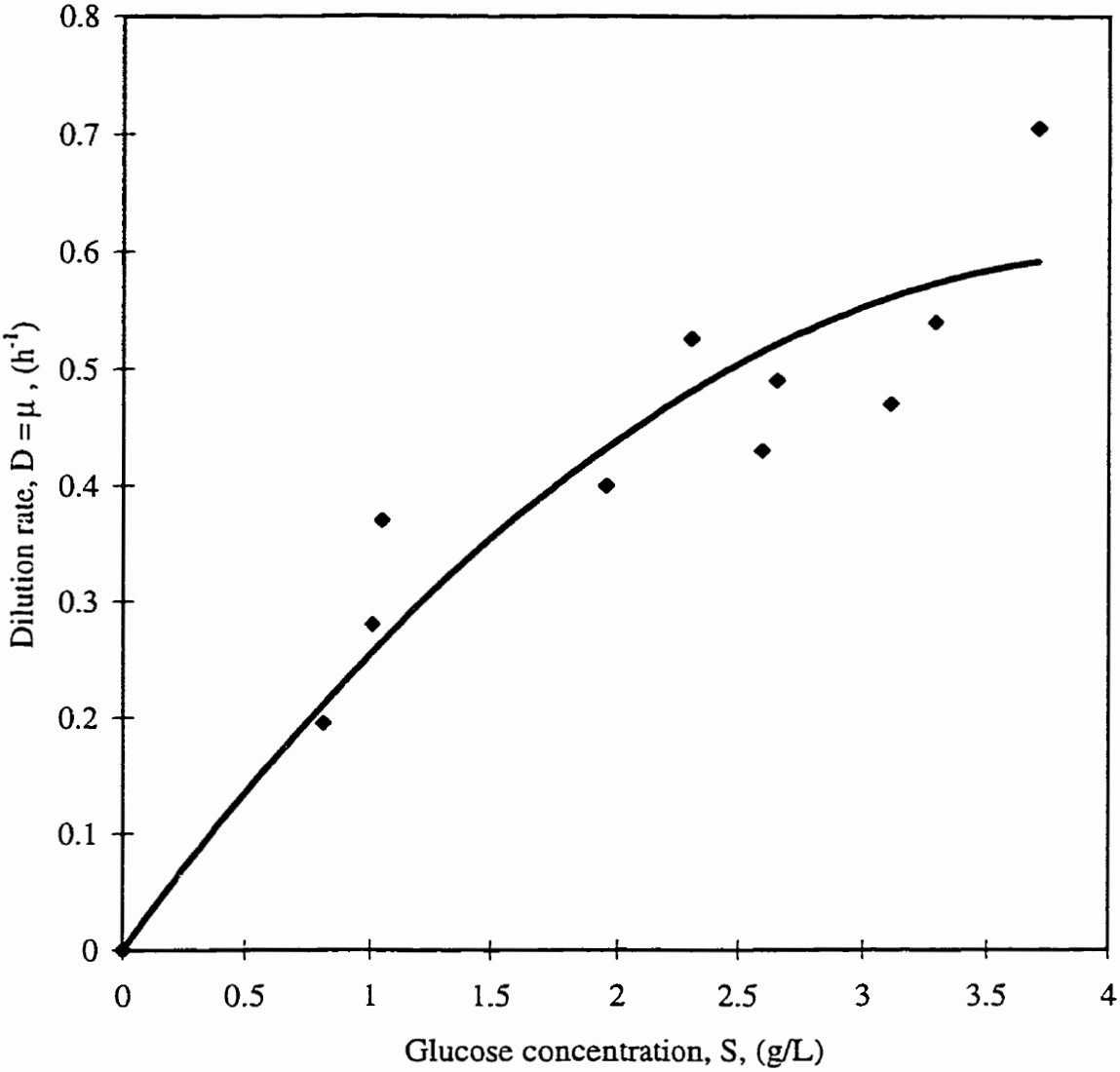

Fig. 5.14 Dilution rate (specific growth rate) steady-state data as a function of glucose concentration for continuous culture of *B. thuringiensis*

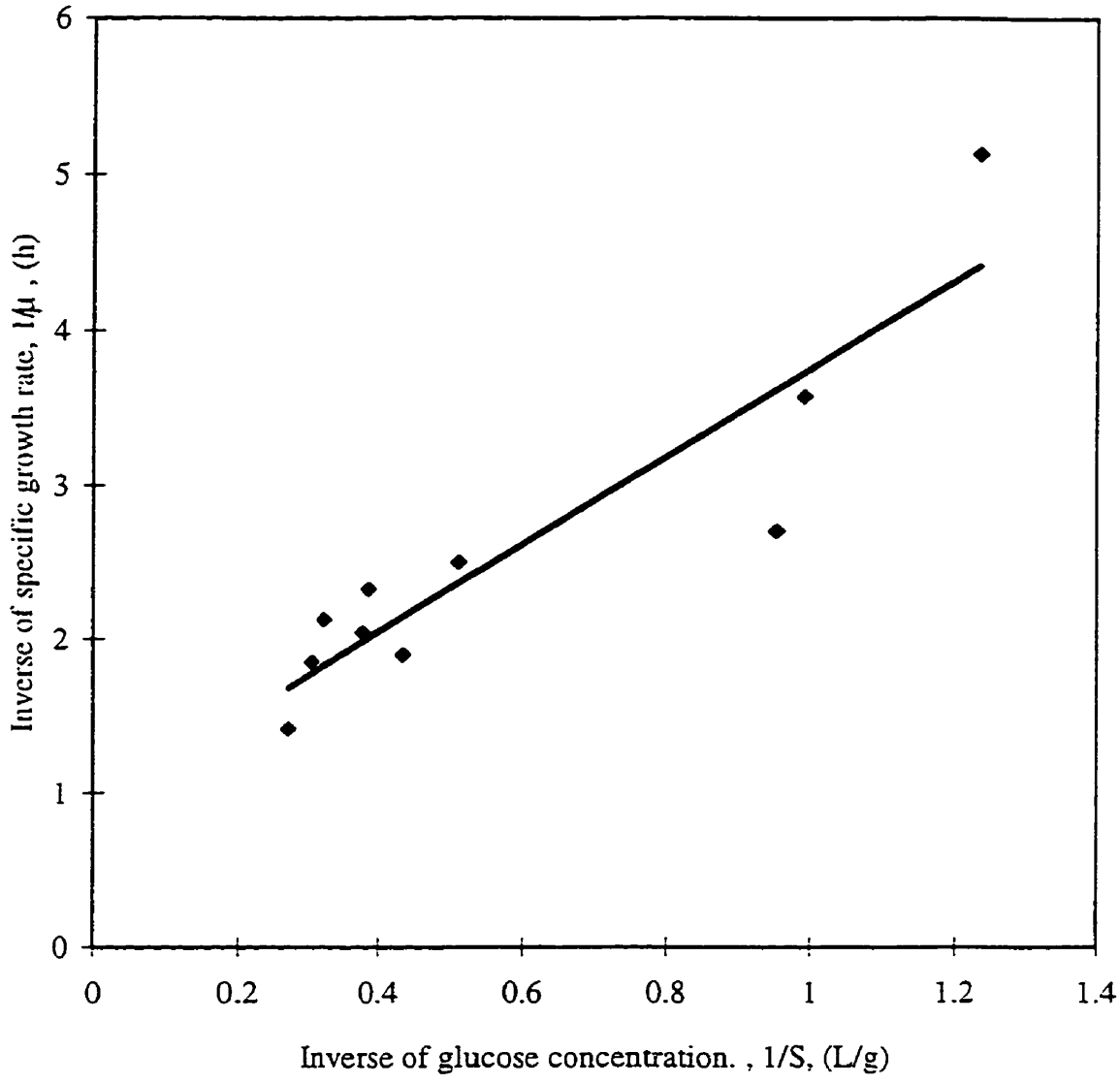

Fig. 5.15 Inverse plot of specific growth rate and glucose conc. for steady-state continuous growth of *B. thuringiensis*

$$1/\mu = 2.8314(1/S) + 0.9196$$

$$R^2 = 0.8348$$

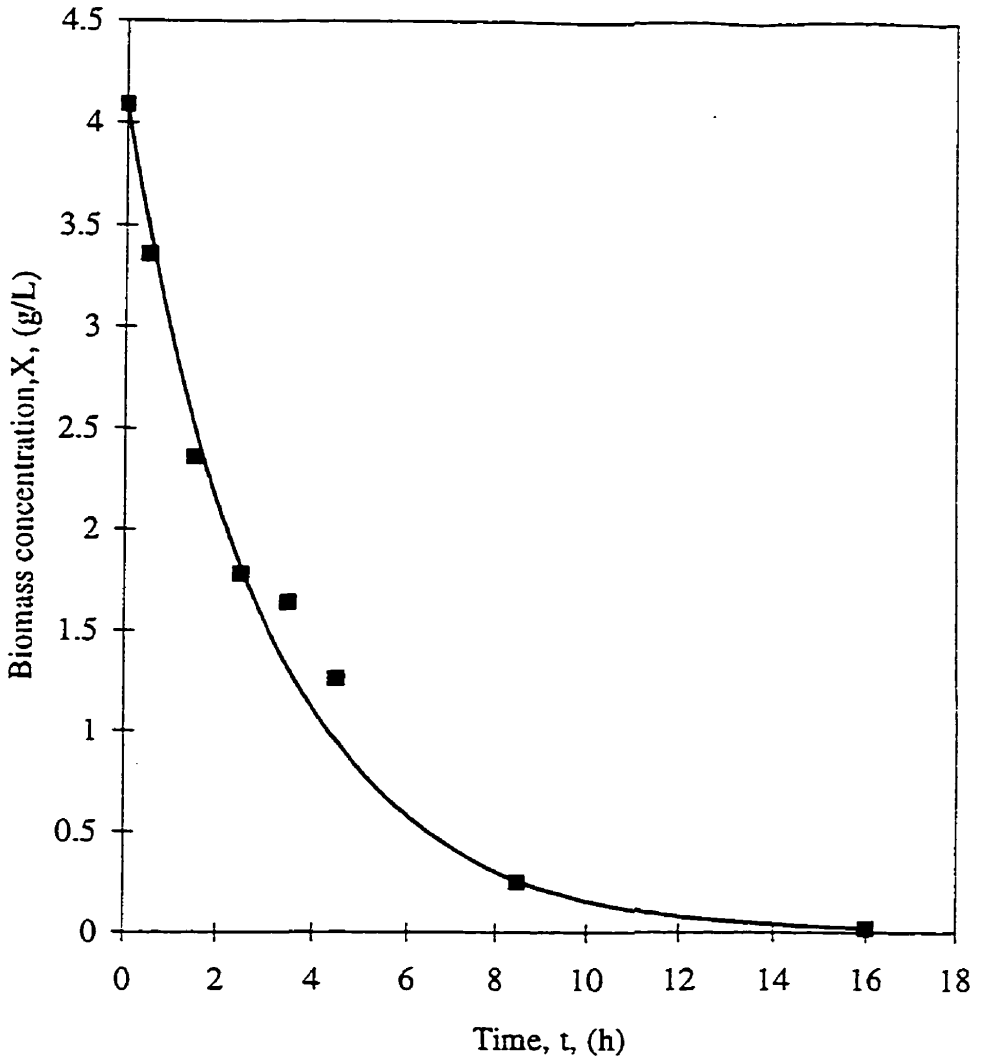

Fig. 5.16 Washout experiment to determine μ_{max} at D = 1.49 h^{-1} for *B. thuringiensis* subspecies *kurstaki* HD-1 ATCC 33679.

$X = 4.09 \exp(-0.3258)\, t$, $\mu_{max} = 1.16\ h^{-1}$

Table 5.5 Summary of results for three independent different experiments of continuous growth of *B. thuringiensis*

Exp. No	Dil rate, D, (h-1)	Biomass conc., X, (g/L)	Glucose conc., S, (g/L)
1	0.54	4.88	3.3
2	0.51	5.54	2.22
3	0.27	5.9	1.80

Fig. 5.17 reports the comparison of the Monod model prediction with the results of the three independent experiments. This figure confirms a fair agreement of the Monod model with the experimental results to predict the changes in substrate concentration. Moreover, in order to verify the kinetic constants obtained, the classical kinetic model for a continuous culture together with the Monod model was used to predict both the biomass and glucose concentration (Table A.15, Fig. 5.18 and also section 6.2).

The model predicts, as expected, an increasing glucose concentration for higher D values while the biomass concentration decreases with the same parameter. However, it was observed that the model displays lack of accurate predictions at both high dilution rates ($D > 0.7\ h^{-1}$) and low dilution rates ($D < 0.28\ h^{-1}$). A peculiar phenomenon, in the continuous growth of the *B. thuringiensis*, was the progressive decline of biomass at low dilution rates. This result was attributed to the formation of spores causing a slow down or even arrest of the cell growth at those conditions (refer to chapter 6). Moreover, deviations between model and experiments at high dilution rates could be assigned to a number of factors, such as presence of limiting nutrients beside glucose (Rodriguez-Monroy and de la Torre, 1996), and unstable operation while approaching the critical dilution rate, D*. D* was estimated, given that the feed glucose concentration was 8.1 g/L, assuming a maximum specific growth rate of 1.1 h^{-1}, and a saturation constant of 3.1 g/L, to be 0.8 h^{-1}. Therefore, a continuous bioreactor working at a dilution rate of 0.8 h^{-1} or higher should yield zero biomass concentration and a glucose concentration equal to the glucose concentration in the feed

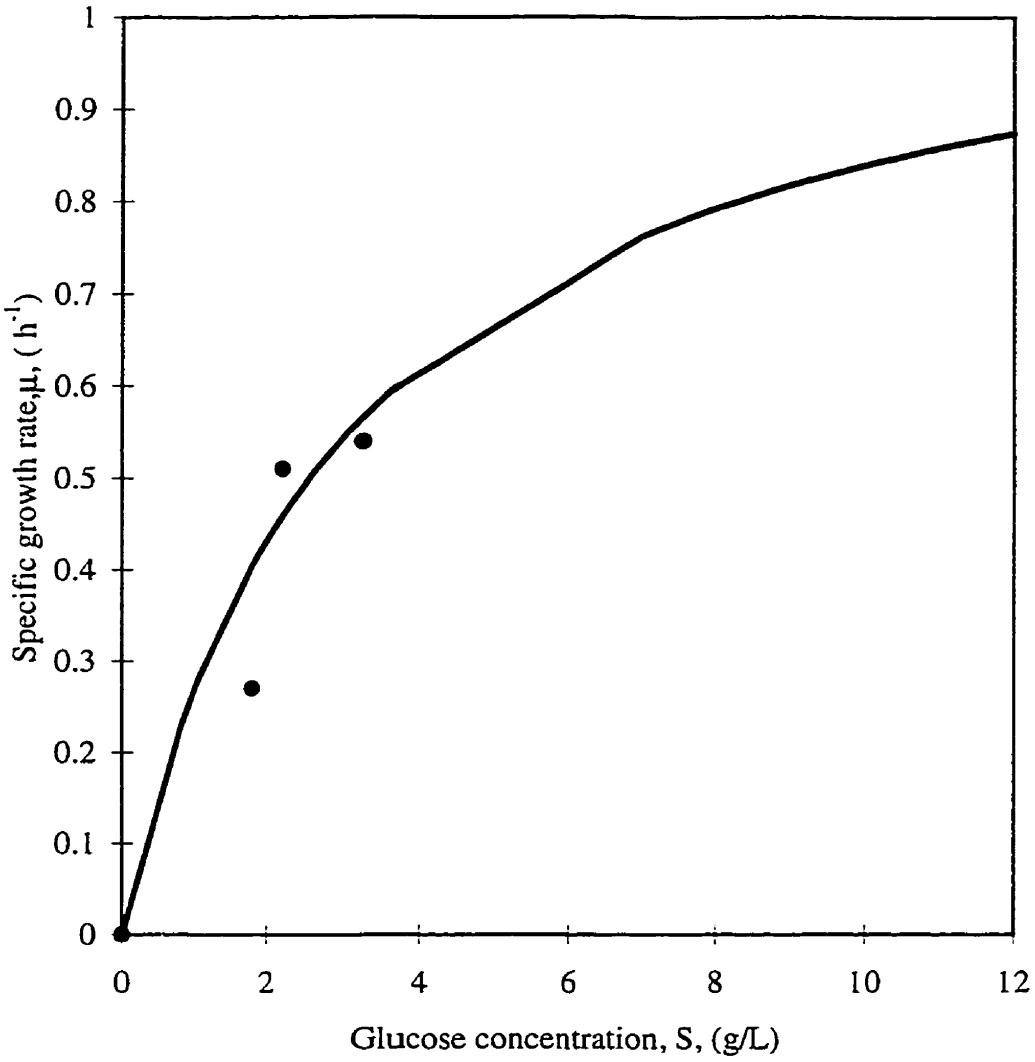

Fig. 5.17 Comparison of Monod model prediction with independent experimental data of specific growth rate versus dilution rate for continuous growth of *B. thuringiensis*.

Solid line is the Monod model prediction with μ_{max} = 1.1 h^{-1} and K_s = 3.1 g/L

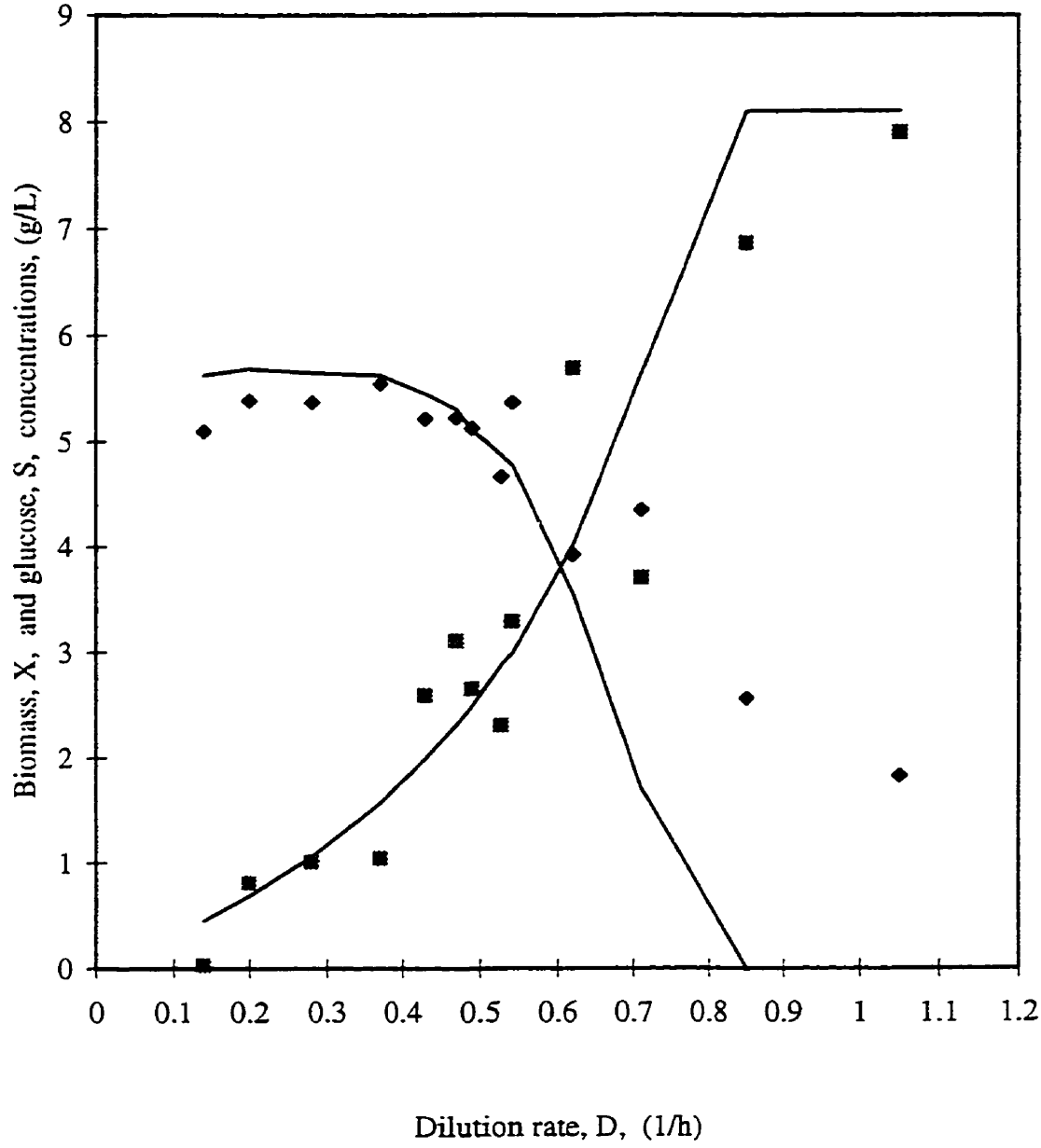

Fig. 5.18 Continuous growth of *B. thuringiensis*. Comparison of experimental data with traditional model

■ S ◆ X —— X mod —— S mod.

stream. Note that these values are model predicted values (Fig. 5.18) and were not used further in the calculation of the kinetic constants (Table A.13).

In the specific case of *B. thuringiensis* culture, it was reported that cells use as a carbon source, not only glucose, but also aminoacids (Anderson, 1990; Avignone-Rossa and Mignone, 1995). Moreover, it was determined that at high dilution rates ($D > 0.8\ h^{-1}$) the glucose is used exclusively as the energy source while the yeast extract is employed as the carbon source (Mignone and Avignone-Rossa, 1996). Consistent with these reports, it was observed that changes in glucose concentration did not increase dramatically the cell mass. Consequently, a $K_s = 3.1$ g/L, as obtained in this dissertation, even if somewhat higher than the only reported value in the literature ($K_s = 0.56$ g/L, Rodriguez-Monroy and de la Torre, 1996) is judged as a sound estimation of the affinity of the *B. thuringiensis* cells for glucose.

In summary, unlike what was done in other previous studies on growth kinetics, the parameters (μ_{max} and K_s) obtained in this dissertation were confirmed with additional runs. In addition, these constants incorporated in the Monod model were used together with the model of a continuous CSTR bioreactor to predict the biomass concentration and glucose concentration at steady state in a continuous CSTR bioreactor. In all these cases, the biomass and glucose concentration were adequately predicted by the model. Thus, it can be concluded that the growth kinetic constants were determined with a high reliability.

5.3.3 Oxygen uptake rate and growth yield

The oxygen uptake rate qO_2X is an important parameter given that it quantifies the demand of oxygen by the culture. The oxygen uptake rate depends on the number of cells and their metabolic state. In the case of the present study, the high concentration of cells and the active metabolism of the microorganism produced a high demand of oxygen by the culture. On the other hand, the respiration rate coefficient is another key indicator function of the metabolic state of the microorganisms. A high biological activity requires a high respiration

rate coefficient. Since for a continuous reactor operating at steady state, the dilution rate equals the specific growth rate, the relationship between qO_2 and the dilution rate provides the relationship between the demand of oxygen with respect to the metabolic state. The respiration rate coefficient increases as the dilution rate increases; that is, the demand of oxygen per cell increases when the cells are actively growing.

In the present dissertation, the oxygen uptake rate and the respiration rate coefficient were obtained using a dynamic method based on the oxygen consumption rate by the cells after a sudden interruption in the air supply (Bandyopadhyay and Humprey, 1967). Table A.16 and Fig. 5.19 show the relationship between the oxygen uptake rate and the respiration rate coefficient with the dilution rate. The respiration rate coefficient, qO_2 increased at dilution rates higher than 0.47 h^{-1} . This demonstrates not only that the metabolic activity was higher at high dilution rates but also that there was a shift in the metabolic activity at a dilution rate of approximately 0.47 h^{-1}. This change in the metabolic state was also evidenced by the morphology of the cells at a dilution rate of 0.47 h^{-1} compared to that at lower dilution rates. See Plates 5.8 to 5.10

The biomass yield coefficient was calculated for each dilution rate as the ratio of the biomass concentration to the difference between feed glucose concentration and glucose bioreactor steady-state concentration. Biomass yield coefficients for various dilution rates are shown in Table 5.6. Growth yield values estimated at high dilution rates ($D > 0.47\ h^{-1}$) varied in a wide range. For example, at dilution rates of 0.47 and 0.49 h^{-1} the growth yield was 1.11 and 0.85 (g cells/g glucose) respectively. This suggests experimental errors in the estimation of growth yields at high dilution rates. A similar situation was observed for dilution rates of 0.53 and 0.54 h^{-1}. These experimental errors avoid the use of all the experimental data for the calculation of the growth yield, and only those data considered more reliable were used in the estimation of the growth yield. In spite of the variability of the results, it is demonstrated that the growth yield increases with dilution rate in the continuous growth of *B. thuringiensis* (Fig. 5.20). The overall increase with dilution rate is also in general agreement with that reported by other researchers (Rodriguez-Monroy and de la Torre, 1996). The specific magnitude of

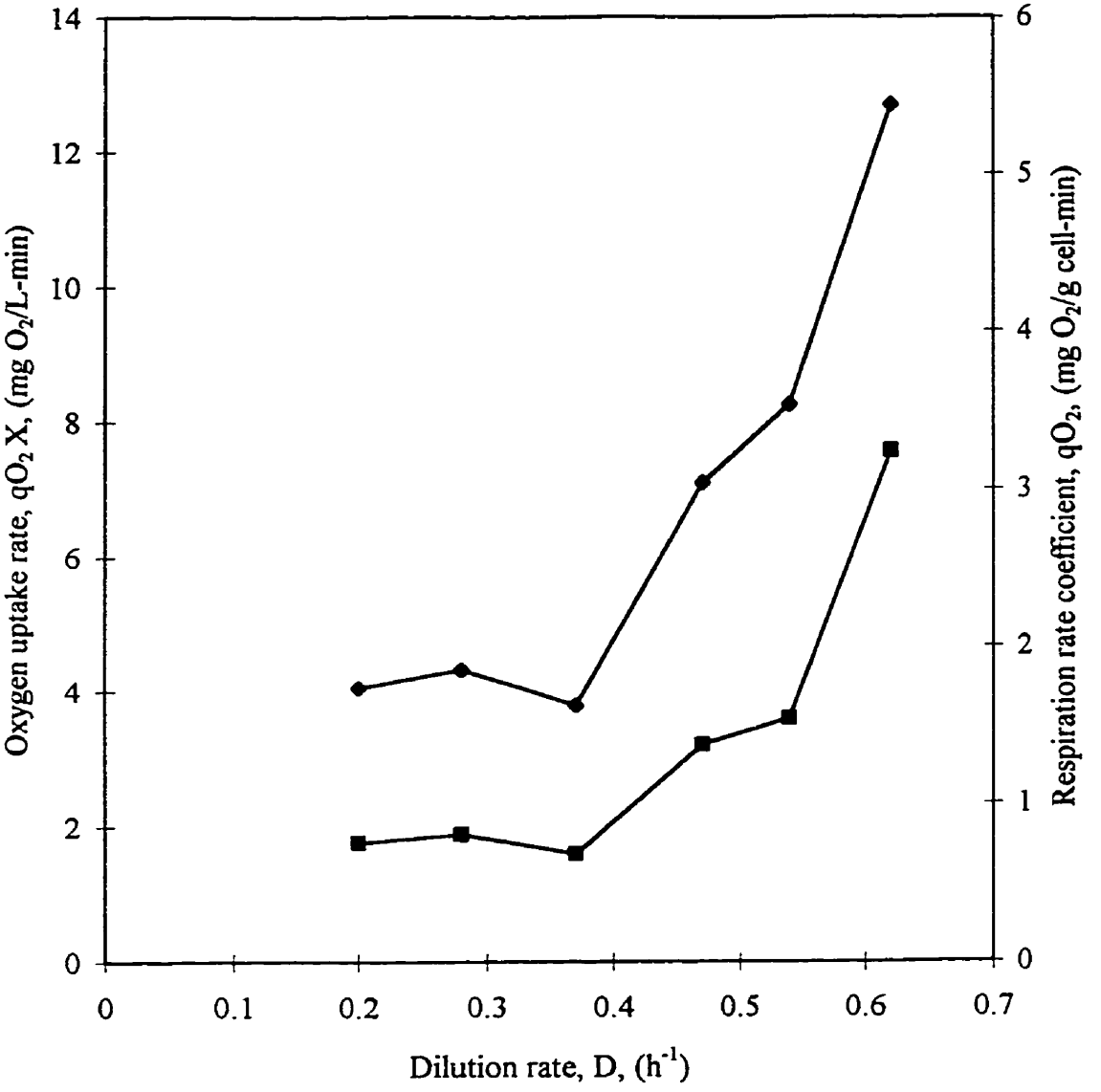

Fig. 5.19 Oxygen uptake rate and respiration rate coefficient of *B. thuringiensis* as a function of dilution rate.

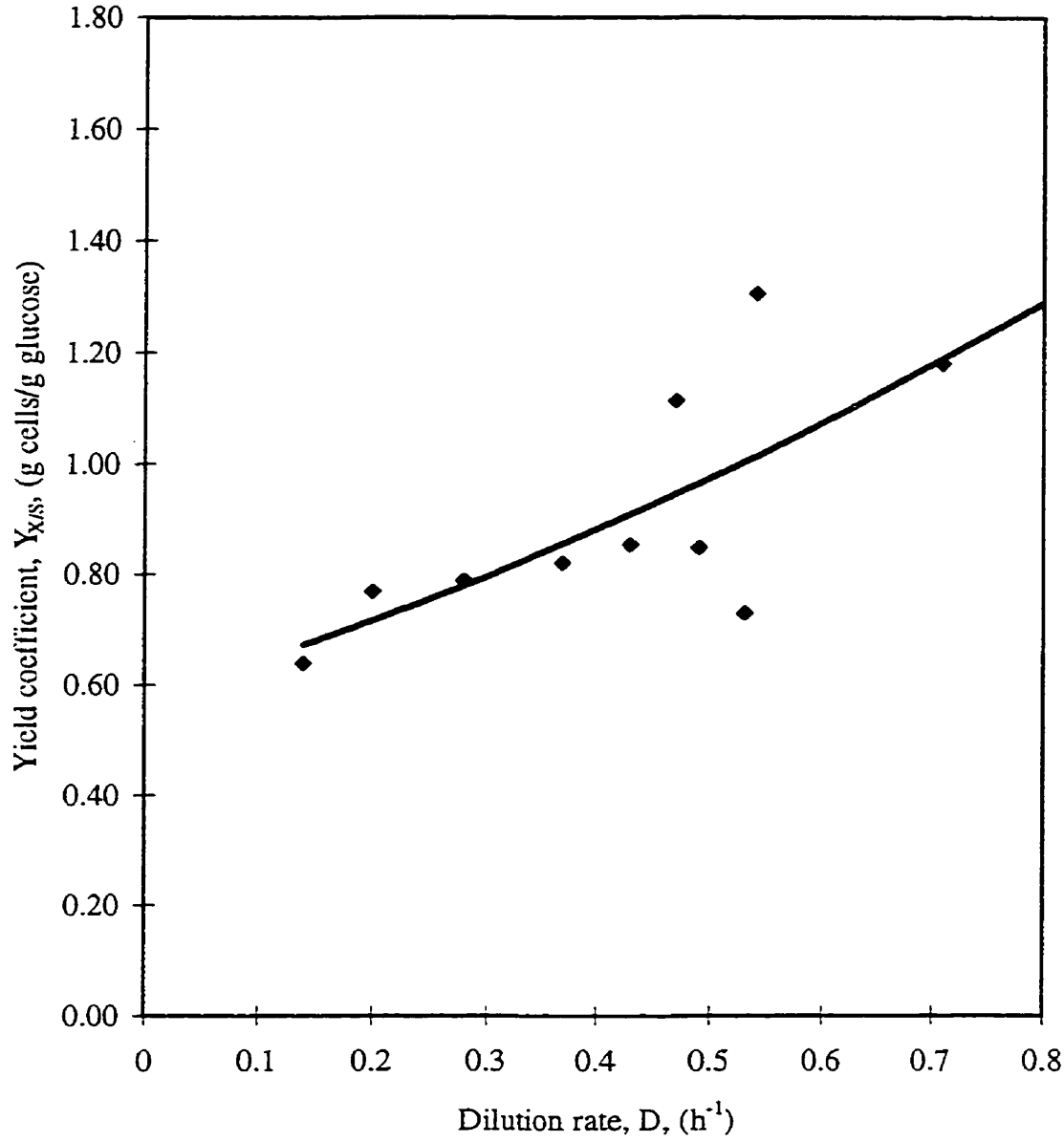

Fig. 5.20 Continuous growth of *B. thuringiensis* . Yield coefficient as a function of dilution rate.

the growth yield values based on glucose, as limiting substrate, are consistent with literature data (Anderson 1990; Liu et al, 1994).

Table 5.6 Biomass Yield Coefficient at various dilution rates for continuous culture of *B. thuringiensis* subspecies *kurstaki* HD-1 ATCC 33679.

Dilution rate, (h^{-1})	Biomass conc., X, (g/L)	Glucose conc., S, (g/L)	Glucose conc. in feed stream, S_0, (g/L)	Growth yield, $Y_{X/S}$, (g cell/g glucose)
0.14	5.09	0.03	8.0	0.63
0.20	5.38	0.81	7.8	0.77
0.28	5.36	1.01	7.8	0.79
0.37	5.54	1.05	7.8	0.82
0.43	5.21	2.60	8.7	0.85
0.47	5.22	3.11	7.8	1.11
0.49	5.13	2.65	8.7	0.85
0.53	4.66	2.31	8.7	0.73
0.54	5.36	3.29	7.4	1.3
0.71	4.35	3.71	7.4	1.17

The low yield growth at low dilution rates indicates that glucose is the main carbon source at low dilution rates only ($D < 0.47\ h^{-1}$) while at higher dilution rates cells use other carbon sources, as suggested by Mignone and Avignone-Rossa, (1996).

In summary, the progressive increase of oxygen uptake rate with the dilution rate is an indicator of high cell growth activity at high D values. Furthermore, the increase in the growth yield with D points to the glucose as the main carbon provider under some conditions only ($D < 0.47\ h^{-1}$).

5.4 Continuous stirred tank reactor (CSTR) two-stage system growth.

The objective of the two-stage continuous culture was to test more thoroughly the possibility of producing the crystal protein using a continuous culture. A sequence of two bioreactors was used with the first reactor operated at a high dilution rate to encourage high production of cells and the second reactor operated at low dilution rates to produce spores and crystal protein.

Fig. 5.13 reports the volumetric bioreactor productivities as a function of steady-state dilution rates for biomass and crystal protein productivities. It was found, as already described, that the maximum biomass volumetric productivity was obtained at D=0.54 h^{-1}. Thus, on that basis it can be concluded that the best strategy to operate a two-stage bioreactor system should be to have the first stage operated at D = 0.54 h^{-1} to maximize vegetative cell production. For the second stage, given the absence of crystal protein production at dilution rates higher than 0.2 h^{-1}, a dilution rate lower than 0.1 h^{-1} was selected. In summary, the operation of a two-stage process was proposed on the basis of the dilution rate conditions described in Table 5.7.

Table 5.7 Experimental Protocol for the Two-stage Continuous System.

Experiment		Reactor 1 First stage	Reactor 2 Second stage
NCS1	dilution rate	0.54 h^{-1}	0.078 h^{-1}
	working volume	0.8 L	5.5 L
	flow rate	0.43 L/h	0.43 L/h
	air flow rate	1 L/min	0 L/min
NCS4	dilution rate	0.5 h^{-1}	0.08 h^{-1}
	working volume	0.85 L	5.35 L
	flow rate	0.43 L/h	0.43 L/h
	air flow rate	1 L/min	2.97 L/min

To confirm the expected advantage of operating in a two-stages system, a first experiment was performed at a high dilution rate, 0.54 h^{-1} in the first reactor and at a low dilution rate, 0.078 h^{-1}, in the second reactor. The second rector was operated without aeration. As expected, the cells in the first reactor presented the typical morphology for a vegetative cells. The cell concentration at steady state was 4.88 g/L, the cell count was $4x10^8$ CFU/mL, and the spore count was zero. Therefore, in the first stage, the cells were in their vegetative stage. The lack of oxygen in the second reactor, however, stopped cell growth and the cells lysed without maturation. The pictures in Plates 5.14 and 5.15 show a vegetative cell and some cells disrupted before normal maturation.

Given these results, another experiment (NCS4) was performed in which air was supplied also to the second reactor and mixed with a stirrer at 250 rpm.

The steady state in the first reactor of the two-stage continuous system was achieved after 24 hours. The biomass concentration was 3.92 g/L, and the glucose concentration was 5.1 g/L. The cells presented the typical morphology of vegetative cells: thin and motile, forming long chains, and with no spores present in the cells (Plate 5.16). The second reactor now contained sporulated cells, free spores, and crystal protein (Plate 5.17). However, this reactor also contained vegetative cells. The number of cells and spores in the second reactor after 40 h of continuous growth was estimated to be 7.9×10^{12} CFU/mL and 4×10^{10} CFU/mL, respectively. It was concluded that the presence of vegetative cells in the second reactor, even though it was operated at a very low dilution rate, was due to the intrinsic characteristic of a mixing pattern in a CSTR where vegetative cells and unused nutrients are intermixed with fluid fractions that had already been in the system for an extended period. Thus it was concluded that the use of two CSTR's in series to produce crystal protein is not advisable and that the second reactor should be either a continuous plug flow unit or a discontinuous batch unit.

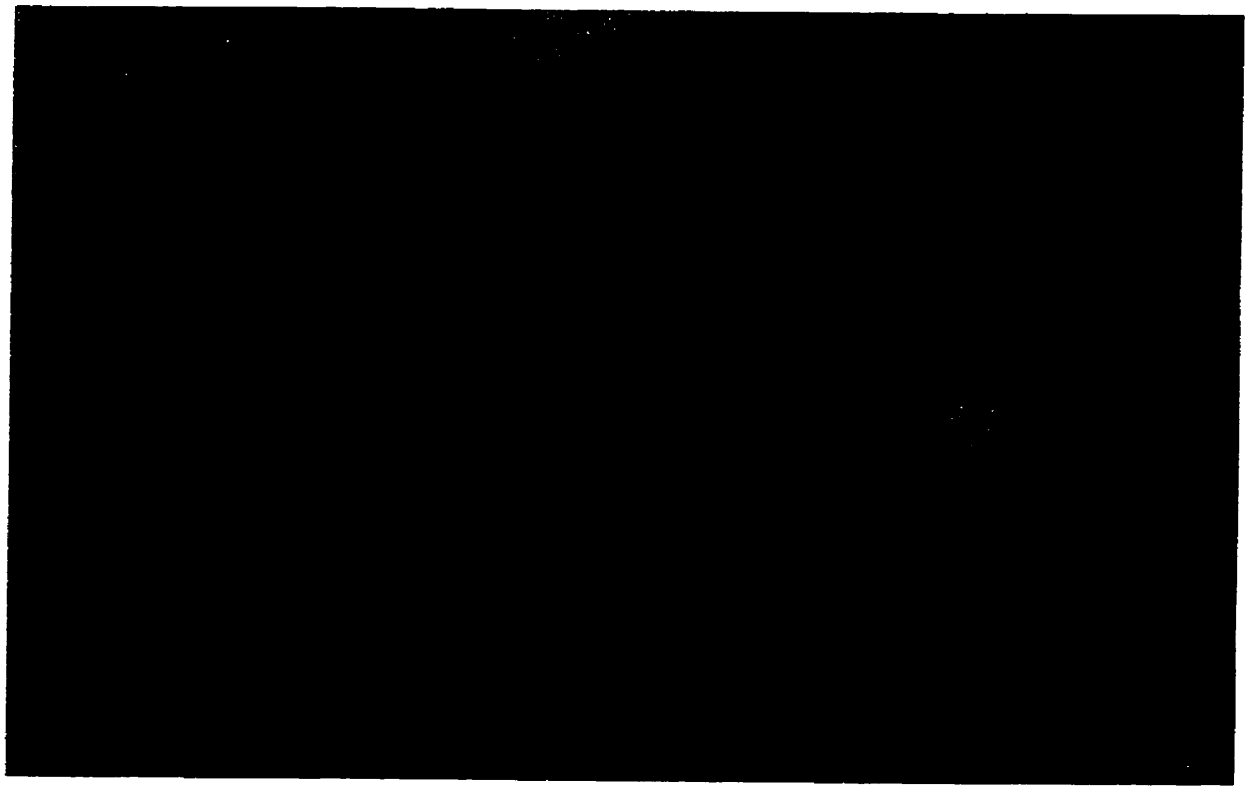

Plate 5.14 Cells of *B. thuringiensis* HD-1 subspecies *kurstaki* from the second reactor in the two-stages continuous growth system, cultured without oxygen, (experiment NCS1). Picture taken in a phase contrast microscope at 1500 X. The cells are disrupted before maturation. Some cells debris can be seen and the cell wall appears to be damaged.

Plate 5.15 Cells of *B. thuringiensis* HD-1 subspecies *kurstaki* from the second reactor in the two-stages continuous growth system, cultured without oxygen, (experiment NCS1). Picture taken in a phase contrast microscope at 1500 X. A long chain of vegetative cells and disrupted cells can be appreciated.

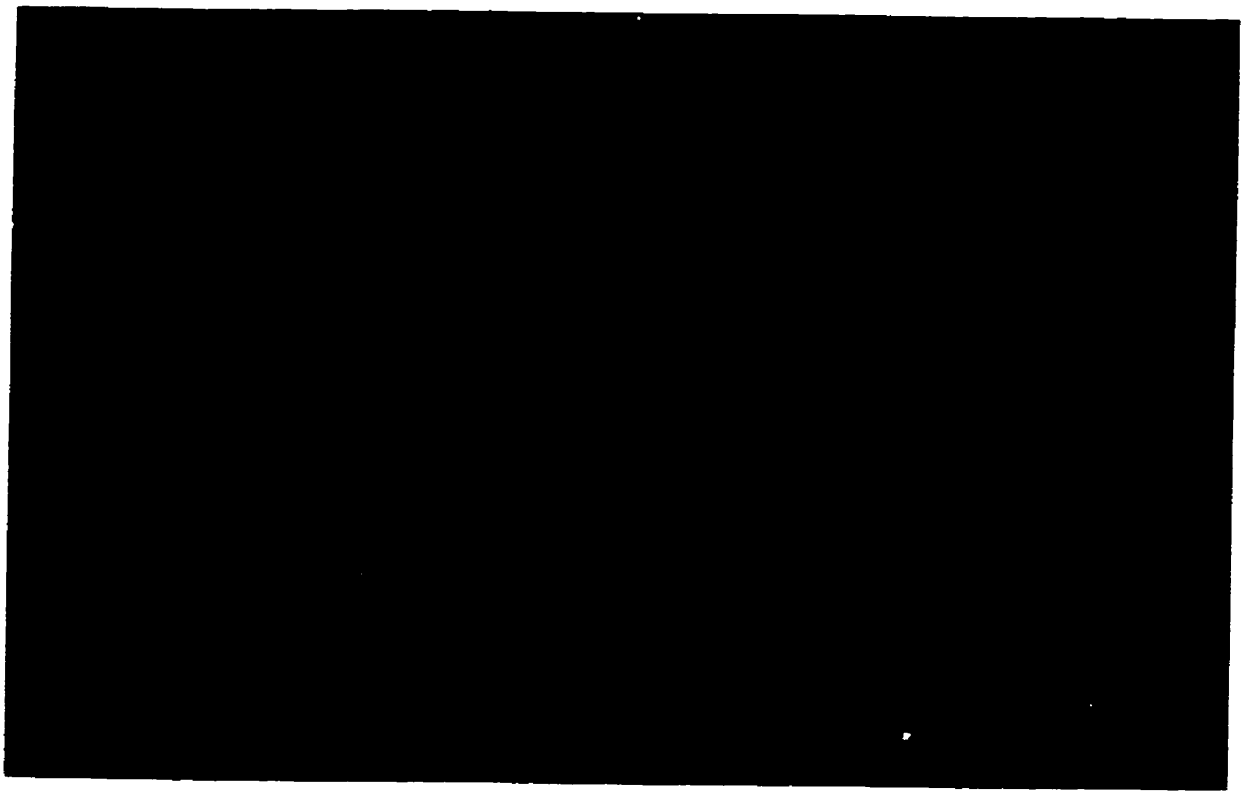

Plate 5.16 Cells of *B. thuringiensis* HD-1 subspecies *kurstaki* from the first reactor in the two-stages continuous growth system, (experiment NCS4) at a dilution rate of 0.5 h^{-1}. Picture taken in a phase contrast microscope at 1500 X. Vegetative cells in chains.

Plate 5.17 Cells of *B. thuringiensis* HD-1 subspecies *kurstaki* from the second reactor in the two-stages continuous growth system, (experiment NCS4) at a dilution rate of 0.08 h^{-1}. Picture taken in a phase contrast microscope at 1500 X. A mixture of vegetative cells and mature cells containing spores and crystal protein.

5.5 Comparison of batch, fed-batch and continuous cultures

One of the objectives of studying *B. thuringiensis* growth in several bioreactors modes is the comparison of their volumetric productivities. In this study, the biomass volumetric productivity was obtained for batch, fed-batch and continuous cultures. The crystal protein was obtained in batch growth after nine hours of operation, and in continuous (CSTR) cultures at a dilution rate of 0.14 h^{-1}. Table 5.8 reports these results.

Table 5.8 Biomass and crystal protein productivities for batch, fed-batch and continuous cultures.

Bioreactor	Biomass productivity (g cells/L-h)	Crystal protein productivity, (g/L-h)
Batch	0.74	0.11
Continuous	2.89	0.14
Fed-batch	0.58	0.00

Continuous cultures in a CSTR reactor had a biomass productivity almost four times higher than that of batch culture and five times higher than that of fed-batch growth. Unfortunately, the maximum productivity in the continuous bioreactor was found at a dilution rate of 0.54 h^{-1}, when the cells are still in their vegetative stage, and therefore unable to form spores and crystal protein. In contrast, crystal protein productivities of batch and continuous cultures were found to be similar. In addition, it was found that two continuous (CSTR) bioreactors operating at two different dilution rates (reactor 1 at D = 0.54 h^{-1} and reactor 2 at D = 0.08 h^{-1}) were not advisable. Replacing the second reactor for a batch or a plug flow unit might be a viable alternative.

On the basis of all the experimental data obtained, a best designed configuration could be the combination of a continuous (CSTR) unit and a batch or continuous plug flow reactor. The cells exiting the continuous CSTR should be in their vegetative phase and the formation of the crystal protein should take place in the batch reactor or in the continuous plug flow reactor.

5.6 Crystal protein assessment

The assessment of the crystal protein concentration obtained as a product of *B. thuringiensis* growth was based on the total protein determination after a purification procedure (sections 4.1.4 and 4.1.4.1). In order to verify that the crystal protein was the only chemical species measured by the spectrophotometric methods, pure crystal protein was compared with a sample taken directly from the fermentation broth by gel electrophoresis and HPLC. In this section, the results of the new method for the isolation of crystal protein, as well as the results of gel electrophoresis and HPLC are presented.

5.6.1 Purification of crystal protein by a flotation-settling method.

The new developed method for the isolation of crystal protein was described in section 4.1.4.2. The purity of the crystal protein obtained by this method was estimated to be 95 % ± 5%. Plate 5.18 shows a picture of crystal protein stained with basic fuchsin taken in a phase contrast microscope at 1500X and Plate 5.19 shows a picture of the purified crystal observed with the scanning electron microscope at 20,000 X. This pictures show that there were no spores and cell debris in the sample.

5.6.2 Gel electrophoresis.

Plate 5.20 shows a picture of the SDS gel electrophoresis of three samples of crystal protein: a) HD-1 S 16,000 IU/mg, b) crystal protein isolated by the flotation-settling method, and c) crystal protein extracted from the fermentation broth of a batch culture.

Plate 5.20, column A1, shows a faint band corresponding to the crystal protein HD-1 S 16,000 IU/mg. This sample was 100 % pure crystal protein, but its concentration was very

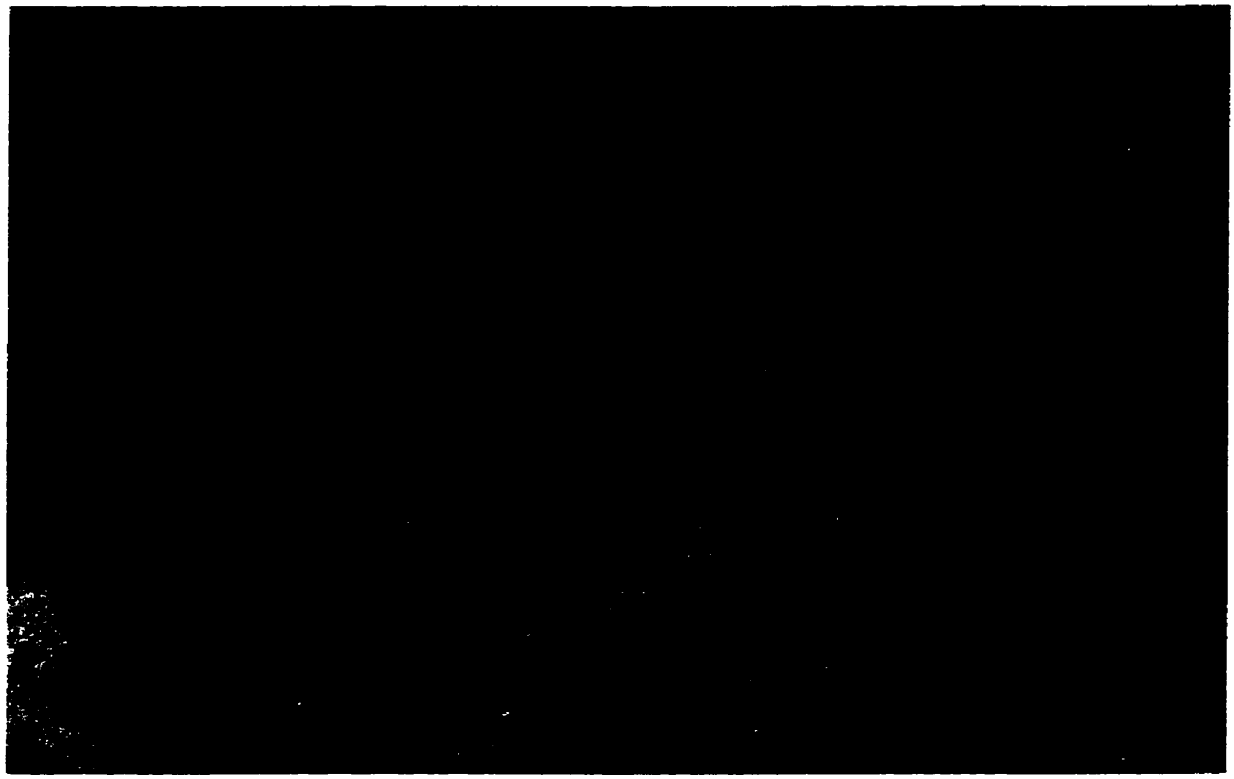

Plate 5.18 Picture of Crystal protein purified by the Flotation-settling method, taken in optical phase contrast microscope at 1,500X and stained with basic fuchsin.

Plate 5.19. Scanning electron micrograph of crystal protein purified by the Flotation-settling method. 20,000X

S A1 A2 B1 C1 C2 A1 B1 C1

Plate 5.20 SDS Gel electrophoresis of crystal protein. **S**: Standard protein broad range 72807 A Bio-Rad, **A1**: Crystal protein HD-1 S 16,000 IU/mg dissolved in 0.02 N NaOH, pH 12; **A2**: Crystal protein HD-1 S 16,000 IU/mg dissolved in 0.02 N NaOH, pH 12 and treated with denaturant buffer (SDS-mercaptoethanol); **B1**: Crystal protein 100% purity obtained by flotation-settling method, from batch culture of *B. thuringiensis* HD-1 subspecies *kurstaki* ATCC 33679, dissolved in 0.02 N NaOH, pH 12; **C1**: Crystal protein extracted by dissolution in 0.02 N NaOH, pH 12, from a mixture of spores and crystal protein obtained from a batch culture of *B. thuringiensis* HD-1 subspecies *kurstaki* ATCC 33679; **C2**: Crystal protein extracted by dissolution in 0.02 N NaOH, pH 12, from a mixture of spores and crystal protein obtained from a batch culture of *B. thuringiensis* HD-1 subspecies *kurstaki* ATCC 33679 and treated with denaturant buffer (SDS-mercaptoethanol)

low. A Lowry assay performed later showed that only the 15% of the powder original sample was crystal protein. Columns B1 and C1 show the bands corresponding to crystal protein isolated as discussed previously and crystal protein from the fermentation broth respectively. These bands are at the same position in the gel and also at the same position as that of the band in column A1. This confirms that the protein extracted from the batch bioreactor and processed as described in section 4.1.4 was crystal protein.

5.6.3 High performance liquid chromatography

High Performance Liquid Chromatography (HPLC) was used for the identification of the crystal protein. Two samples were used: a crystal protein purified with the flotation-settling method (see section 4.1.4.2) and crystal protein obtained from a batch growth of *B. thuringiensis* HD-1 subspecies *kurstaki* ATCC 33679. The chromatograms show mainly two peaks, at 900 and 1400 sec, which appeared to be related with the delta endotoxin. The peak area of one of these peaks was directly proportional to the concentration of the protein content in the samples. A calibration curve of the HPLC with crystal protein is shown in Fig. C.1 appendix C.

Figs. 5.21. 5.22 and 5.23 show the HPLC chromatogram of a blank sample, a crystal protein sample (85% purity) purified by the flotation-settling method, and a crystal protein sample obtained from a batch growth of *B. thuringiensis* HD-1 subspecies *kurstaki* ATCC 33679, respectively. Fig. 5.21 shows only a small peak at 400 sec., whereas Figs. 5.22 and 5.23 show peaks at 900 sec. and 1400 sec. The peak at 900 sec was related with the crystal protein (see appendix C) which makes the identification of the crystal protein in samples from the growth medium possible. The HPLC chromatograms also showed that the bioreactor contained the toxic protein delta-endotoxin. HPLC is an excellent method to identify and assess the concentration of crystal protein, but more research is needed in this area to define a standard method.

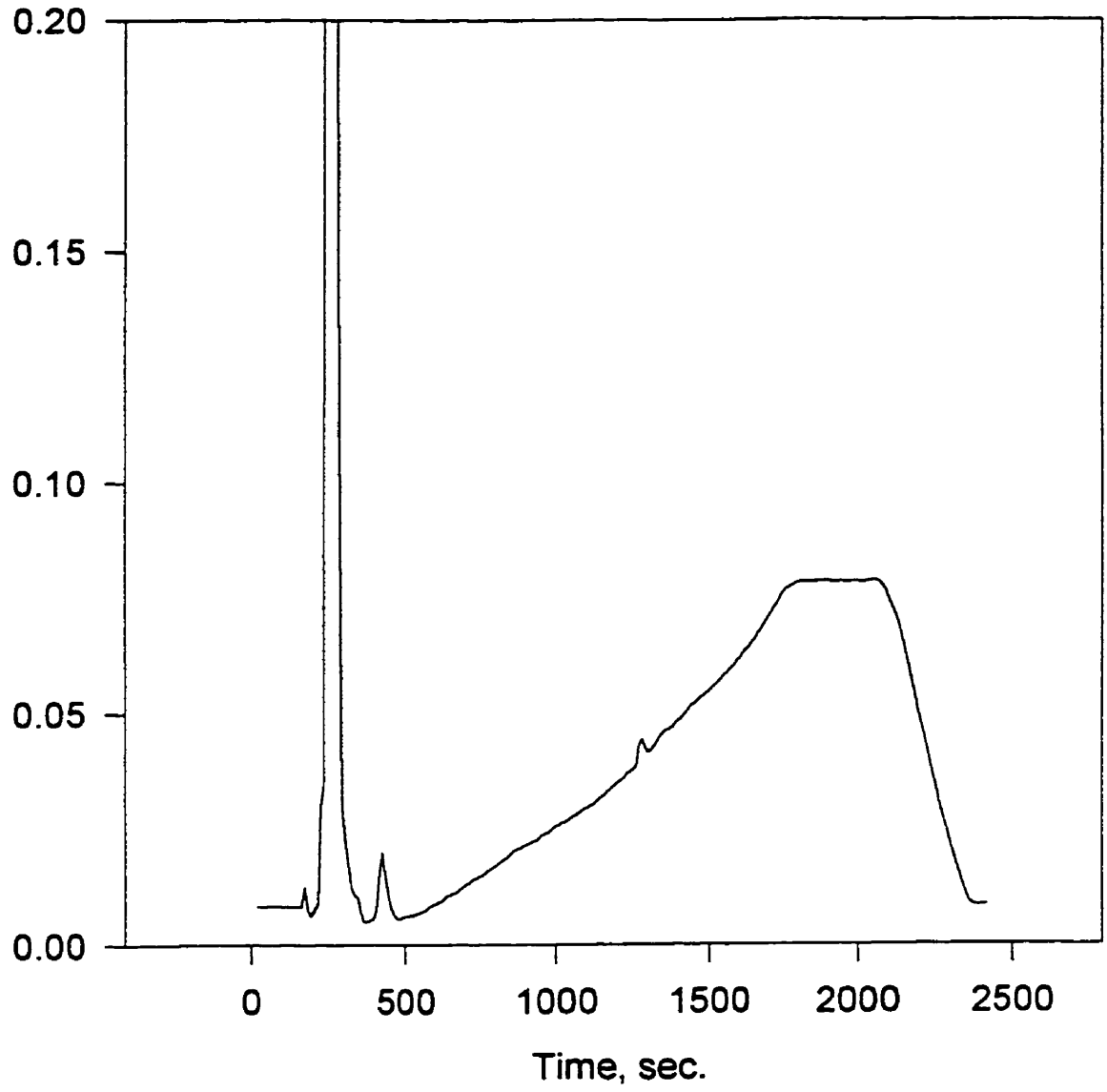

Fig. 5.21 HPLC Chromatogram for the Blank.

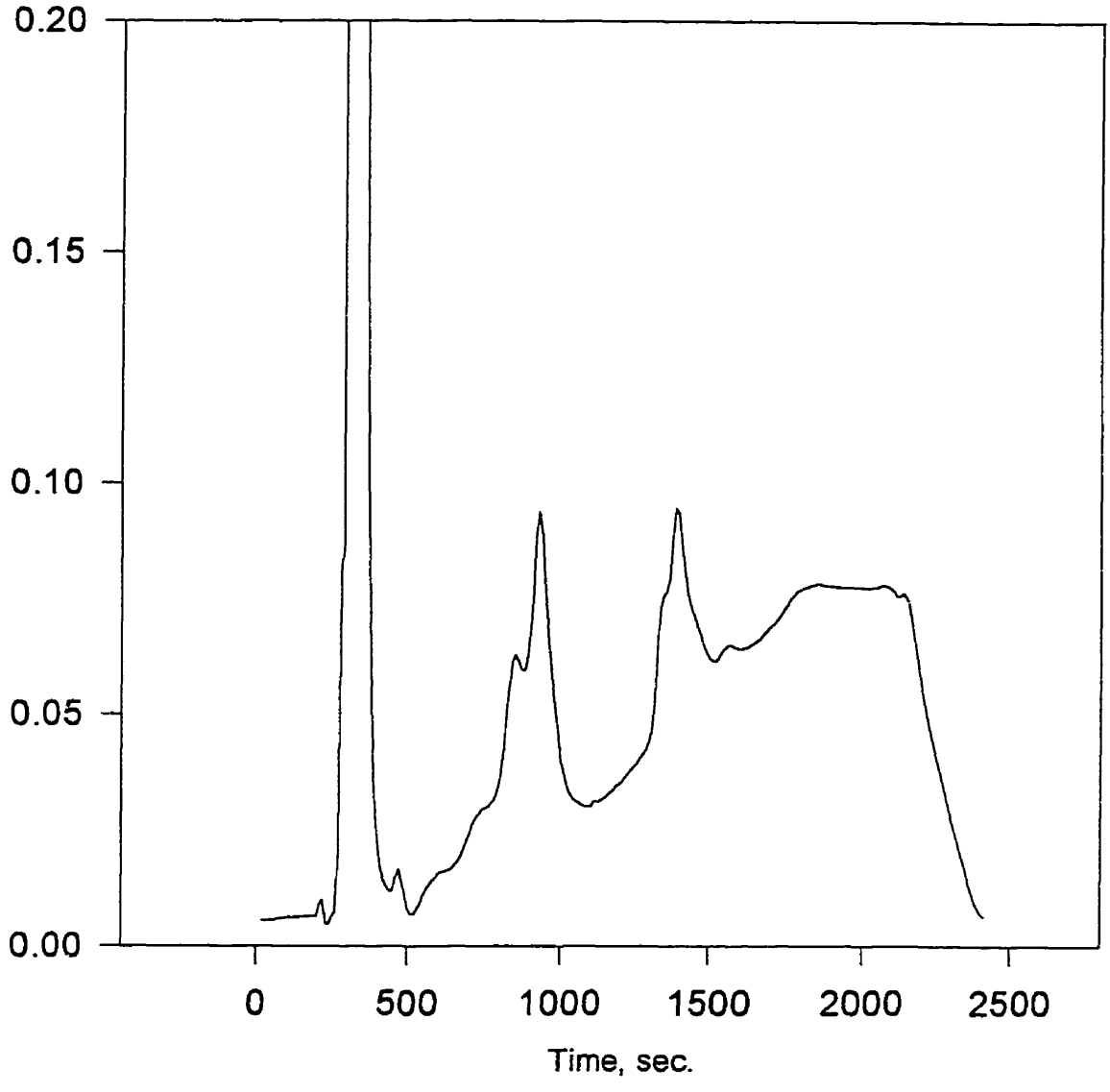

Fig. 5.22 HPLC Chromatogram of δ-endotoxin purified by Flotation-Settling method

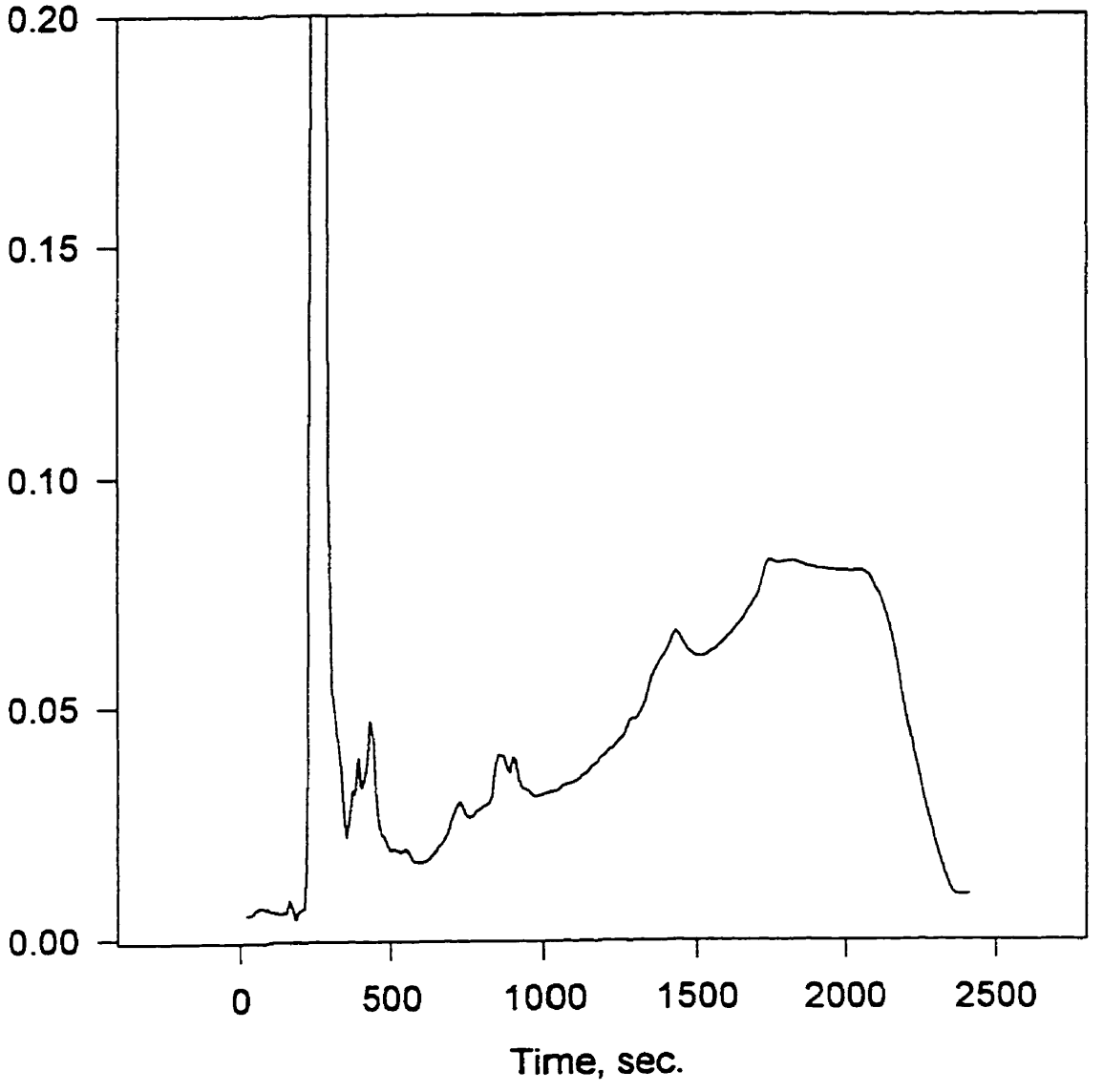

Fig. 5.23 HPLC Chromatogram of Crystal Protein from Batch Growth of *Bacillus thuringiensis* subspecies *kurstaki*

5.6.4 Conclusions

The two analytical techniques (gel electrophoresis and HPLC) were adequate to identify the crystal protein from various experiments. These techniques also demonstrated that the proposed method of crystal separation was adequate, yielding crystal protein up to 95% purity.

CHAPTER 6

B. thuringiensis GROWTH KINETIC MODELING

6.1 Application of the new growth with sporulation kinetic model in batch cultures.

This section deals with the application of the proposed new model in batch cultures of *B. thuringiensis*. The following equations, derived in chapter 3, describe the new growth with sporulation kinetic model.

1. Substrate consumption.

$$dS/dt = - [\mu_{max} S/(K_s + S)] (X-X_s)/Y_{X/S} \quad (3.16)$$

2. Total cells

$$dX/dt = ([\mu_{max} S/(K_s + S)] - k_s) (X - X_s) \quad (3.22)$$

3. Sporulating cells

$$dX_s/dt = k_s (X - X_s) \quad (3.23)$$

The experimental data (Table D.1, appendix D) for five replicas of batch cultures of *B. thuringiensis* were used to test the proposed model. The first step was the comparison of the experimental data with the classical model to verify whether it can describe the cell growth in a batch process.

In order to test the classical model, three constants (μ_{max}, K_s, and $Y_{X/S}$), as well as two initial conditions (S_0, and X_0) are needed. The average values of biomass concentration and

glucose concentration at the beginning of the batch culture for the five experimental replicas were 0.55 and 11.9 g/L, respectively.

The maximum specific growth rate, μ_{max} for a batch culture is approximated to the exponential specific growth rate, μ_{exp}. The exponential specific growth rate was estimated as the slope of the linear segment of the plot of logarithm of the average biomass concentration during the batch cultures versus time (see Fig. D.2 in appendix D). The exponential specific growth rate was found to be 053 h^{-1}. The saturation constant was obtained from the results of continuous growth of *B. thuringiensis* cultured under the same conditions than those used in batch cultures, and was estimated to be 3.1 g /L (Section 5.3.2).

The growth yield was estimated using a plot of biomass concentration versus glucose concentration for all the experimental data. This plot showed a linear trend whit the slope representing the growth yield. Fig. D.3 shows this plot with a slope of 0.55 g/g.

The classical model (equations 3.1, 3.3 and 3.7) was numerically solved with the following initial conditions, growth yield and kinetic constants:

$X_0 = 0.55$ g/L

$S_0 = 11.9$ g/L

$Y_{x/s} = 0.55$ g cells/g glucose

$\mu_{max} = \mu_{exp} = 0.53\ h^{-1}$

$K_s = 3.1$ g/L

As shown in Fig. 6.1 the classical model cannot predict the experimental cell growth results during all the time span of the batch culture. The deficiency is more noticeable at the end of the batch culture, when *B. thuringiensis* cells form spores and the crystal proteins.

One could argue that this finding is the result of an inadequate estimation of the kinetic constants (μ_{max} and K_s). In order clarify this matter, the classical model was tested with

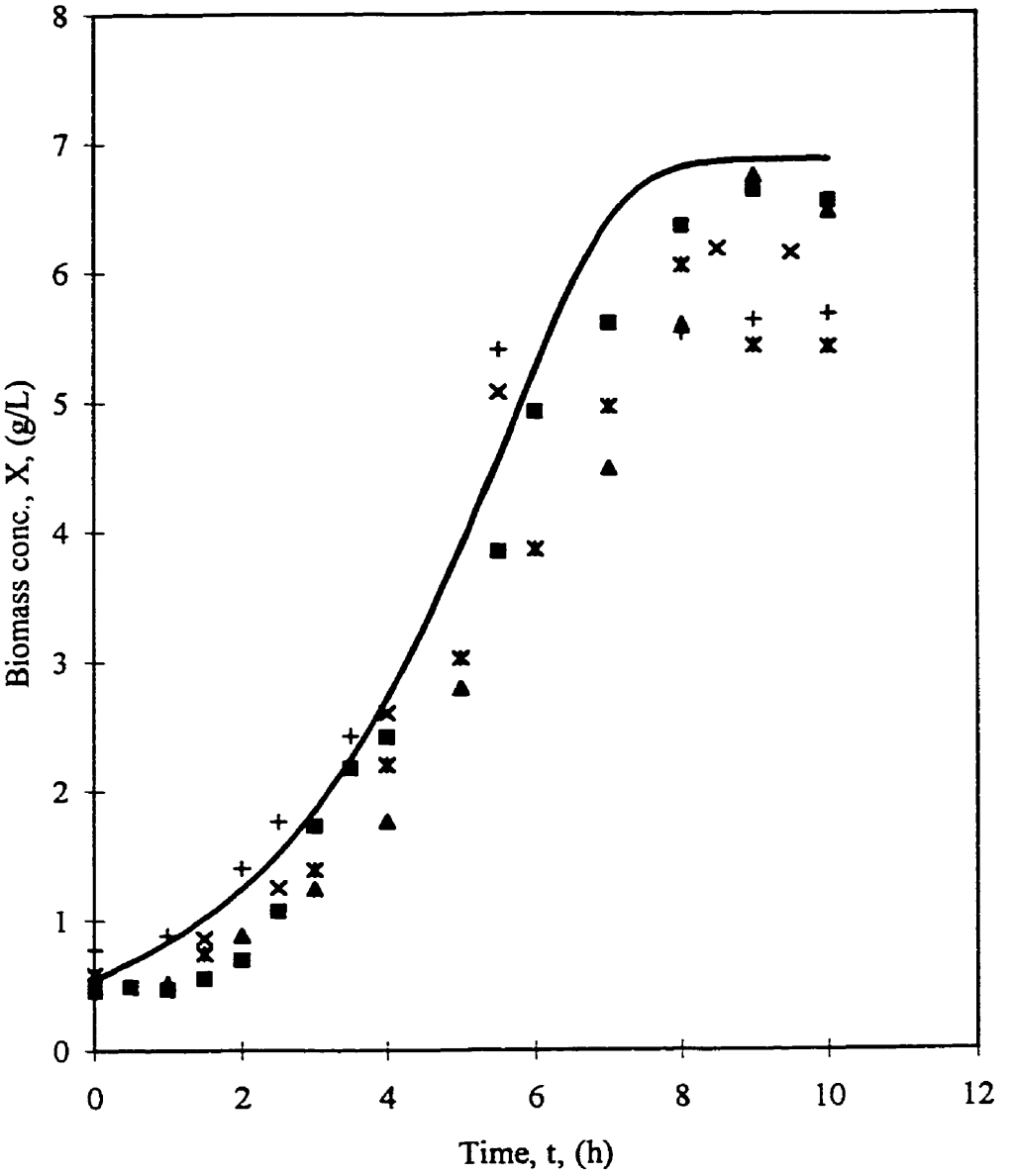

Fig. 6.1 Batch growth of *B. thuringiensis*. Comparison of experimental and classical growth model

several combinations of μ_{max} and K_s, and the agreement between the classical model and the experimental data was assessed by the sum squares of residuals (defined as the square of the difference between the experimental and predicted biomass concentrations). The results are presented in Table D.2 (appendix D). This test showed that the best fitting of the experimental data using the classical model, corresponding to a sum of square residuals of 3.36, was obtained with a μ_{max} and K_s equal to 0.53 h^{-1} and 5 g/L respectively. The μ_{max} was the same as the one calculated with the experimental data. This confirmed that this kinetic constant was correctly estimated. However, the evaluated saturation constant of 5 g/L was too high to be considered a reasonable parameter estimate. Even with the optimum combination of μ_{max} and K_s (with a minimum square of residuals) the classical model was unable to predict accurately the experimental data. Therefore, it was concluded that the lack of agreement between the classical model and experimental data cannot was not due to an inadequate selection of kinetic constants.

The second step in the data analysis was the comparison of the new kinetic model developed in this dissertation, which includes growth with sporulation, with the experimental data. The differential equations (3.16, 3.22, and 3.23) representing the proposed model were solved numerically using the same initial conditions, growth yield, and kinetic constants as those used in the classical model. The sum of squares of residuals was used also as the criterion for testing the adequacy of the model.

The new model was solved with different values of the constant k_s, kinetic constant associated to the spore formation in order to find the adequate k_s value. The new model can correctly describe cell growth for the complete experimental period. Table 6.1 shows the sum of residuals obtained when the new model was compared with experimental data for several values of the constant k_s.

Table 6.1 Sum of squares of residuals obtained from the comparison of the new gowth with sporulation kinetic model and experimental data from batch culture of *B. thuringiensis*.

k_s	Sum of squares of residuals
0.000 (classical model)	7.45
0.005	5.32
0.010	3.73
0.026	1.63
0.04	2.91

It was observed that the lowest sum of squares of residuals was obtained with a 0.026 value for k_s. This is remarkably low sum of residuals with normal residual distribution, indicates a good agreement between the experimental data and the new model.

In summary, Figs. 6.1 and 6.2 demonstrate that a new model for all growth with sporulation is required. The new model proposed here accurately describes the cell growth of *B. thuringiensis* during all the growth phases in a batch culture.

6.2 Application of the growth with sporulation kinetic model to continuous cultures

Although the new kinetic model was developed under batch culture considerations, it was expected that this model could be applied to any type of continuous culture. First, the experimental data were compared with the classical model in order to verify if the classical model can predict the biomass and glucose concentrations in a continuous CSTR culture of *B. thuringiensis* at different dilution rates.

The equations for a continuous CSTR culture are obtained through a cell and substrate mass balance in the bioreactor. The classical model uses the typical cell growth rate $r_x = \mu X$ and the substrate rate consumption $r_s = \mu X/Y_{X/S}$ to obtain the following equations that describe the continuous bioreactor operation at non-steady state:

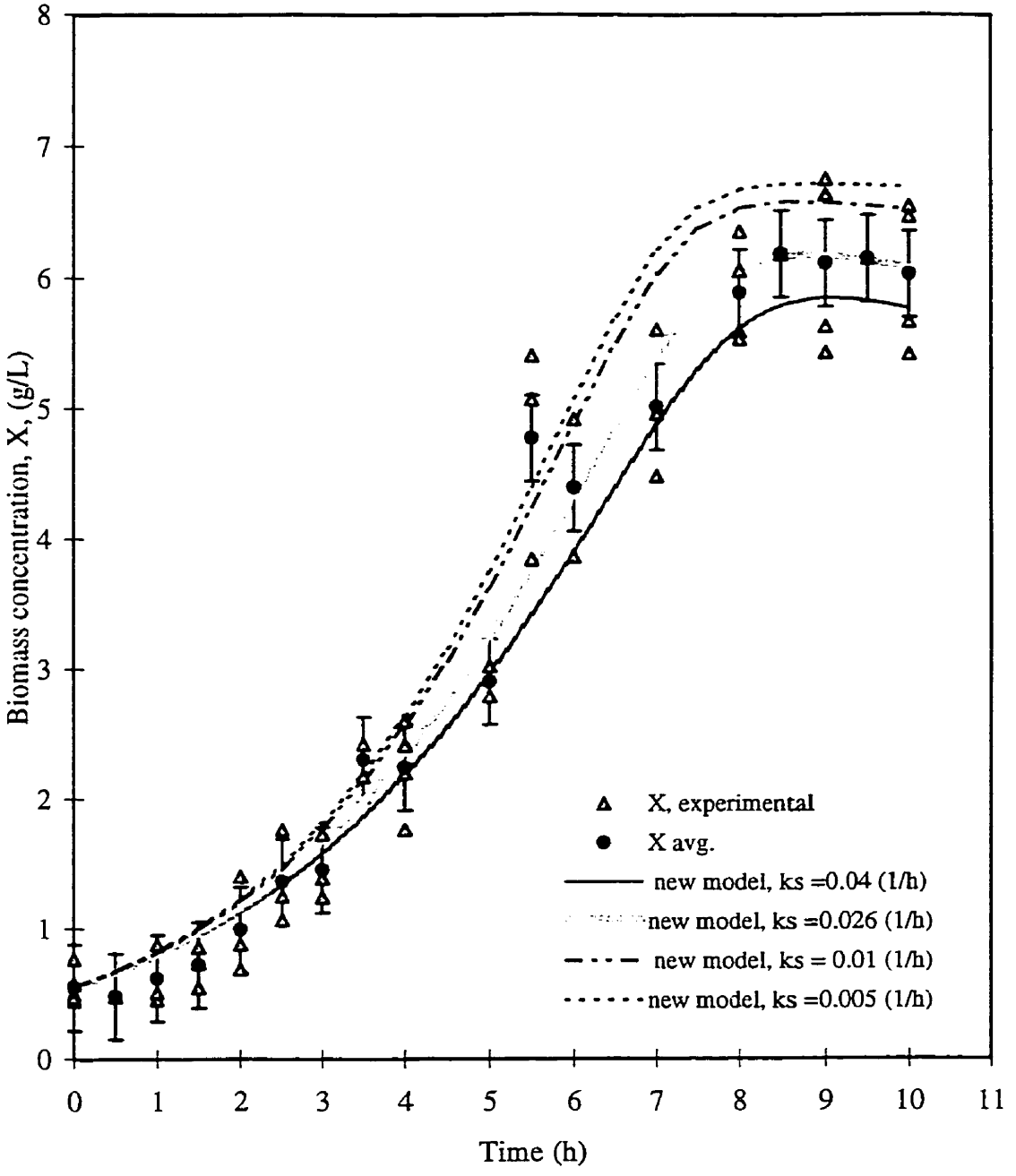

Fig. 6.2 Batch growth of *B. thuringiensis* . Comparison of experimental data with new growth kinetic model at different values of sporulation rate constant, k_s

Error bars represent the standard deviation of the average biomass concentration.

$$dX/dt = (\mu - D)\, X \qquad (3.35)$$

$$dS/dt = D(S_0 - S) - \mu\ X/Y_{X/S} \qquad (3.36)$$

and

$$\mu = \mu_{max}\, S/(K_s + S) \qquad (3.3)$$

The most common approach to determine the biomass and glucose concentrations in a continuous CSTR bioreactor is to assume a steady state where the dilution rate is equal to the specific growth rate. Moreover, although the growth yield may change with dilution rate, the typical plots of biomass and glucose concentrations versus dilution rate are obtained assuming an identical growth yield for all the dilution rates. Under these conditions, for a given dilution rate, the glucose concentration is obtained by the equation 3.3, where μ is equal to D when the bioreactor works at steady state. The biomass concentration is then obtained solving for X in the equation 3.36.

A different approach was used in this study to obtain the biomass and glucose concentrations predicted by the continuous bioreactor model. The non steady state equations were solved numerically, using the initial conditions of biomass and glucose concentrations at the beginning of the transient state and the glucose concentration in the feed stream for each one of the dilution rates (appendix A). The kinetic constants μ_{max} and K_s used in the model were those obtained with steady-state experimental data (section 5.3.2 and 5.3.3). Since the estimated growth yield obtained with the experimental data varies from 0.63 to 1.1 g cell/g glucose, depending on the dilution rate, the expression for the growth yield was incorporated in the equation 3.36.

The expression for growth yield is given as $Y = X/(S_0 - S)$, where X is the biomass concentration in the reactor, S_0 is the glucose concentration in the feed stream, and S is the glucose concentration in the bioreactor. Incorporating this expression in equation 3.36 yields equation 6.1.

$$dS/dt = (D - \mu)\ (S_0 - S) \qquad (6.1)$$

The solution of differential equations 3.35 and 6.1 gives the biomass and glucose concentrations with time for a transient operation of the continuous bioreactor. A numerical method was used to solve these equations and to obtain the results until the steady state was reached, that is, when the dilution rate was equal to the specific growth rate (appendix D). The final biomass and glucose concentrations were used then to be compared with the experimental data.

To solve numerically equations 3.3, 3.35 and 6.1 two kinetic constants (μ_{max} and K_s), the initial conditions for biomass and glucose concentrations, and the glucose concentration in the feed stream are needed. The following constants were used in the solution of equations 3.3, 3.35 and 6.1, and Table 6.2 shows the initial conditions used to solve the classical model applied to a non steady state continuous reactor.

$\mu_{max} = 1.1\ h^{-1}$

$K_s = 3.1\ g/L$

Table 6.2 Experimental data of transient culture of *B. thuringiensis* in a continuous bioreactor. D: dilution rate, S_i: initial glucose concentration, X_i: initial biomass concentration, S_0: glucose concentration in the feed stream.

D, (h^{-1})	S_i, (g/L)	X_i, (g/L)	S_0, (g/L)
0.14	2.5	4.10	8.0
0.20	1.2	5.30	7.8
0.28	1.2	5.52	7.8
0.37	2.0	5.23	7.8
0.43	7.1	1.30	8.7
0.47	7.4	0.39	7.8
0.49	2.4	5.19	8.7
0.53	2.4	5.03	8.7
0.54	3.0	4.75	7.4
0.62	6.2	1.65	8.10
0.71	2.0	5.33	7.4
0.85	5.7	3.89	8.1
1.05	6.8	3.37	8.1

The solution of these equations gave the biomass and glucose concentrations with time during transient state operation of a continuous bioreactor. The solution converged as the dilution rate approached the specific growth rate, and hence, the biomass and glucose concentration remained unchanged with time. Table D.4 shows an example of the tabulated data obtained in the solution of equations 3.3, 3.35 and 6.1.

As shown in Fig. 6.3, the classical model cannot accurately predict the experimental data for high and low dilution rates. According to the classical model, the cellular mass should increase with decreasing the dilution rate, but the experimental data showed the opposite trend at low dilution rates. A possible explanation for the growth rate to be slower than that predicted by the classical model, is due to the fact of spores formation.

Since the new growth kinetic model considers the decrease in cell growth rate due to the beginning of sporulation process, the new model was tested at low (0.14, 0.2 and 0.28 h^{-1}) and at medium dilution rates (0.37, 0.47, 0.62 h^{-1}) in order to verify if the new model could fit the experimental data.

With the new model the cell growth rate and the substrate consumption rate are given by the equations 3.22 and 3.16 respectively, and the total cell mass balance in the continuous reactor gives equation 3.46.

$$dX/dt = (\mu - k_s)(X - X_s) - DX \qquad (3.46)$$

The substrate mass balance in the continuous reactor produces the equation (3.47)

$$dS/dt = D(S_0 - S) - \mu (X - X_s)/Y_{X/S} \qquad (3.47)$$

The mass balance of cells forming spore in the continuous reactor is given by equation 3.48.

$$dX_s/dt = k_s (X - X_s) - D X_s \qquad (3.48)$$

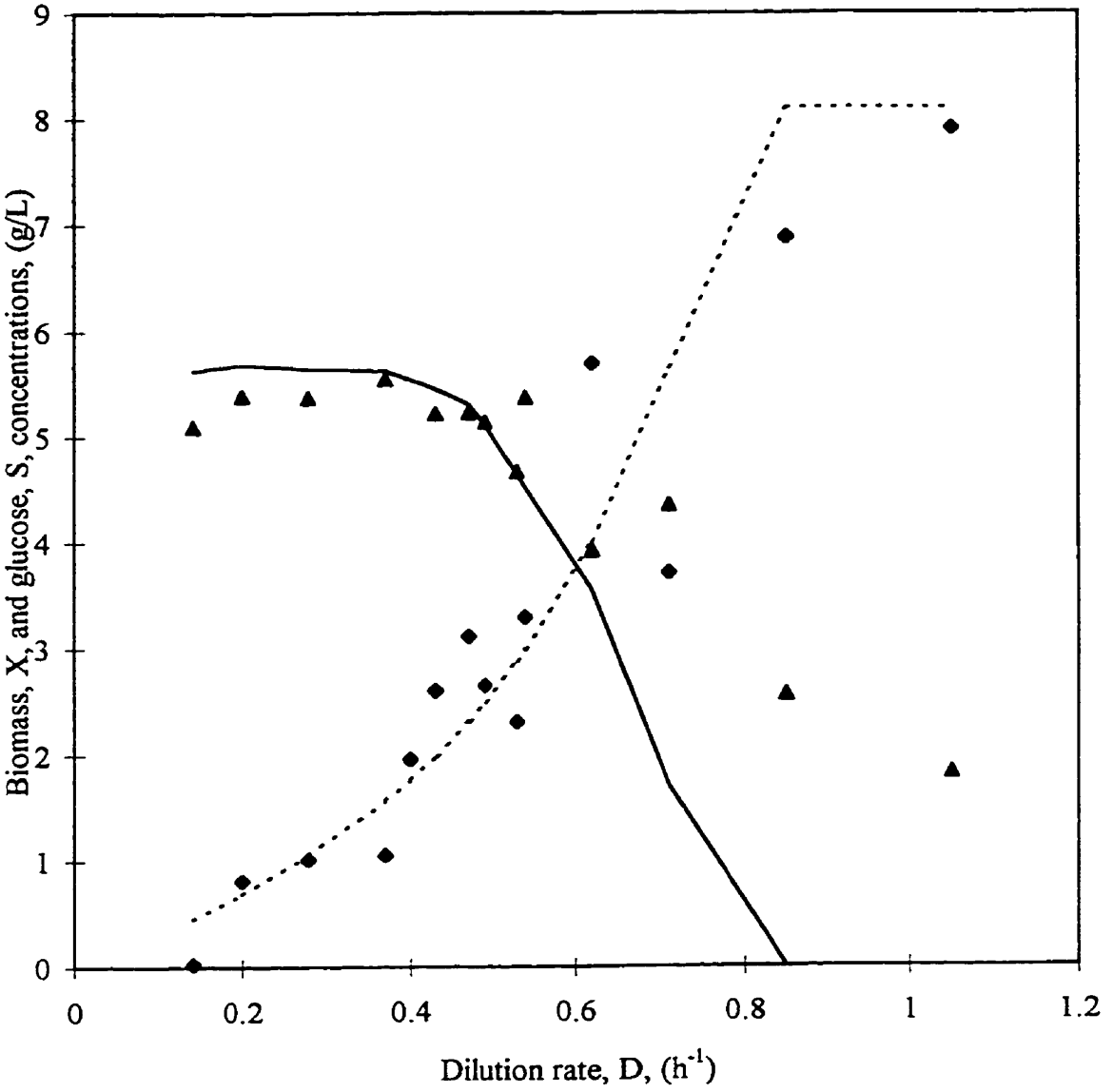

Fig. 6.3 Continuous growth of *B. thuringiensis* .Comparison ofclassical model with experimental data.

◆ S, experimental data ▲ X, experimental data

- - - - - - S, classical model ——— X, classical model

The application of the new kinetic model to a continuous bioreactor at non-steady state produces then the equations 3.3, 3.46, 3.47, and 3.48.

Simultaneous numerical solution of the set of three differential equations provides the changes in substrate concentration (S), cell concentration (X) and forming-spore cell concentration (X_s) in a non-steady operation of a continuous reactor.

The kinetic constants (μ_{max} and K_s) used to test the new growth with sporulation kinetic model were obtained from the continuous growth experimental data (See sections 5.3.2 and 5.3.3). Since as stated above, the growth yield varies depending on the dilution rate, the new model was tested using the growth yield obtained when solving the equations for the classical model (appendix D). The initial conditions for biomass and substrate concentrations in the bioreactor and the glucose concentration in the feed stream used to test the models were those determined for each experiment (Table 6.2).

Results obtained using the new kinetic model showed that when the spore formation process is taken into consideration, steady-state in a continuous bioreactor cannot be reached (Table D.6, appendix D). Thus, the biomass and glucose concentrations obtained at a time equal to that used in the corresponding transient continuous experiment were used to compare the new kinetic model with the experimental data.

Fig. 6.4 illustrates the comparison of the experimental data with the new growth with sporulation kinetic model. This plot shows that at low dilution rates, the new kinetic model predicts accurately the biomass concentration at steady state in a continuous bioreactor.

The use of the new growth with sporulation kinetic model in a continuous CSTR culture of *B. thuringiensis* demonstrated the influence of the change in metabolic state on the continuous bioreactor operation.

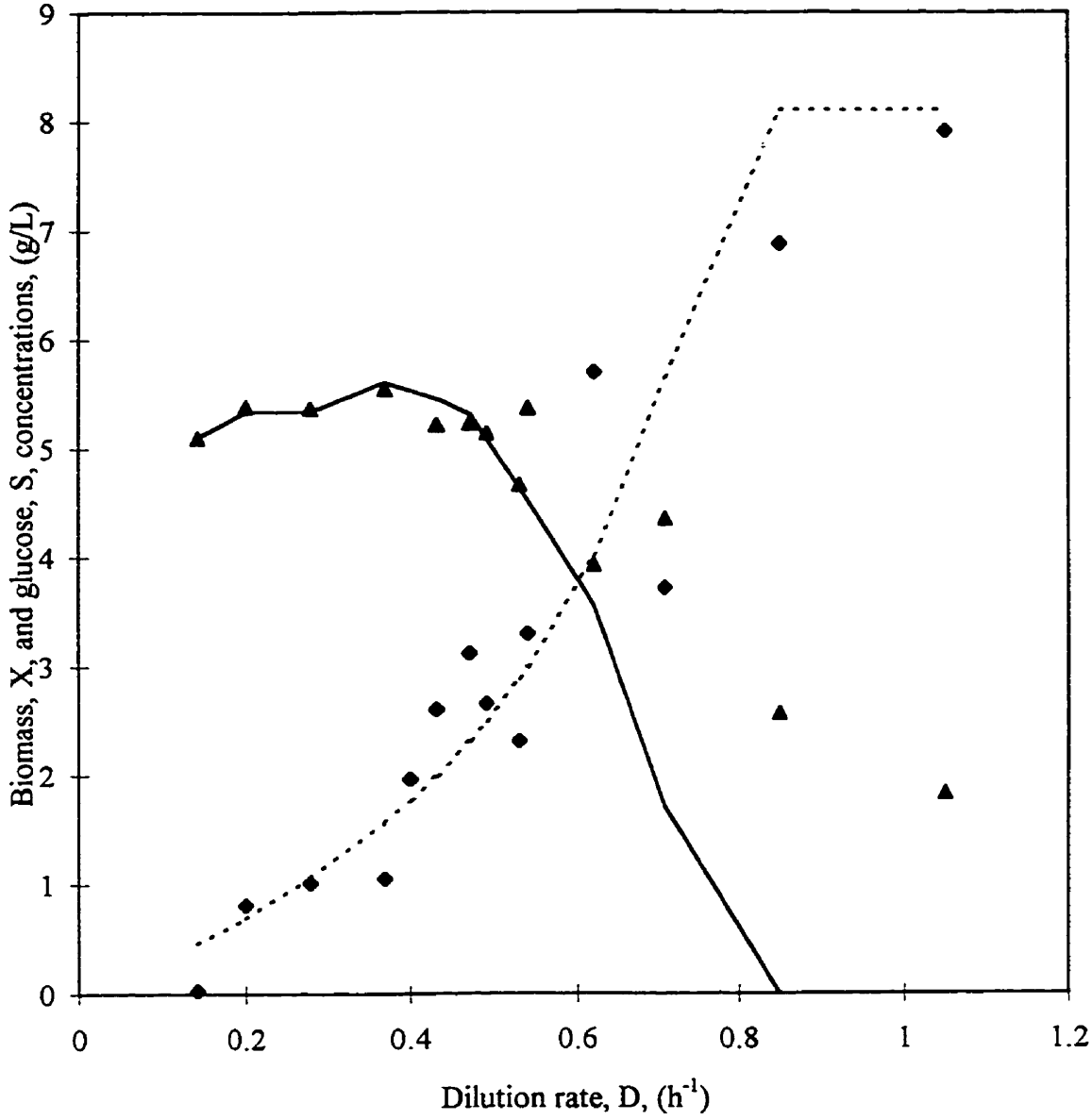

Fig. 6.4 Continuous growth of *B. thuringiensis*.Comparison of new growth with sporulation kinetic model with experimental data.

6.3 Discussion of *B. thuringiensis* new cells growth with sporulation kinetic model.

As noted in Fig 6.2, the traditional growth model deviates from the experimental data, and this is particularly true since the middle of the batch culture. This deviation increases at the end of the batch culture, this deviation is assigned the inability of the classical model to describe the cell growth when the cells are producing the spore.

In contrast, the proposed new model with sporulation is able to better represent experimental data for the entire time span for a batch culture. The proposed modified model improves predictions accounting for the cell growth slow down due to sporulation.

The transformation rate of vegetative cells (with complete ability to divide) to sporulating cells (with loss in the ability to divide) depends on the concentration of vegetative cells and the constant k_s. This constant represents the specific transformation rate of the vegetative cells and it was estimated to be 0.026 h^{-1}.

The different models proposed in the literature are modified versions of the Monod model (Arbige et al., 1993) and some of them are basically empirical. In contrast, in the proposed model the cell kinetic growth equation is modified based on the evidence in the metabolic and functional change of the cells during the batch growth.

Unlike the traditional cell growth kinetic models, the cell growth in the new proposed model does not depend on the total concentration of cells in the culture, but on the concentration of cells with ability to divide only. The substrate consumption is also corrected because not all the cells use it for the purpose of growth. In this respect, the new model assumes that the majority of the substrate is consumed in the cells division process.

The formation of the spore and the crystal protein are carried out during the stationary phase, but the harvest of the product is at the end of the batch growth, thus, it is important

to predict accurately the maximum concentration of biomass and spores at the end of the culture. The proposed model can also be used for the estimation of biomass concentration in all the growth phases during the batch culture and this requires the estimation of one constant only. Unlike the classical model, the new model predicts very well the final concentration of biomass and the time when the cell growth is halted (i.e. the time for harvest) and therefore it can be used with confidence for simulation or for scale up purposes.

In spite of many studies showing that the cells begin the formation of spore in a batch culture only after the exponential growth stage is over, the new model assumes that the cells may initiate, in principle, their sporulation at the very beginning of the batch process. While this assumption is difficult to establish, this assumption does not have a great implication for modeling given the low value assigned to the constant k_s and the low cell concentration at the initiation of the culture.

Another important assumption of the new growth with sporulation kinetic model is that those cells that begin the spore formation cannot contribute to cell growth. While the validity of this postulate is difficult to establish, it appears that the cells stop their division close to or immediately after the initiation of the spore formation.

In summary, the new model is an improvement of the classical kinetic growth model, given it can predict with more accuracy the biomass concentration during a batch culture. This model considers the decreasing in cell growth rate not only as a result of the depletion of substrate but also as a function to the special characteristic of *B. thuringiensis* forming spores and crystal proteins. The proposed model can be used to predict with reliability the experimental results in both a continuous and in a batch growth. This model is particularly suitable to predict the maximum biomass concentration at the end of a batch culture.

CHAPTER 7

CONCLUSIONS AND RECOMMENDATIONS

7.1 Conclusions

Bacillus thuringiensis cells change their metabolism and morphology from vegetative to sporulated cells during their growth depending on the environmental conditions. These changes affect the specific growth rate, and thus the cell growth. Therefore, a comprehensive study that includes the evolution of *B. thuringiensis* cells is necessary to predict the performance of bioreactors used to culture *B. thuringiensis*.

This study has shown that the morphology and metabolism of *B. thuringiensis* cells change with time in batch and with dilution rate in continuous CSTR growth. These changes were followed by observation of the cell morphology under optical and transmission electron microscope, by the change in the pH of the medium, and by the change in the respiration rate coefficient.

One significant achievement of the present study was the development of the crystal protein separation method. The new technique allowed up to a purity estimated very close to 100% (95% ● 5%). The ability to obtain a high purity crystal protein, free of residual cell debris, may have significant impact on characterization of the protein and on the study of the intrinsic toxicity of the delta-endotoxin.

In batch growth of *B. thuringiensis*, vegetative cells were observed during the first seven hours, although spores were detected as early as 5 hours of batch culture. After 10 hours of batch growth, almost all the cells contained a spore. In continuous CSTR growth no spores were detected at dilution rates higher than 0.2 h^{-1}. Cells in transition stage were present at dilution rates between 0.2 and 0.4 h^{-1}, and only vegetative cells were detected at dilution

rates higher than 0.47 h^{-1}. The presence of vegetative cells in both batch and in continuous CSTR cultures were also confirmed by the high respiration rate coefficients. In the batch culture, respiration rate coefficients between 4.38 and 1.57 (mg O_2/g-min) were observed between 2 and 5.5 hours of culture time. Whereas in continuous culture respiration rate coefficients between 1.36 to 3.24 (mg O_2/g-min) were recorded for dilution rates of 0.47 and 0.62 h^{-1}. These findings demonstrate that there is a relationship between the specific growth rate and the metabolic state of *B. thuringiensis* cells.

The determination of reliable kinetic constants of *B. thuringiensis* cells growth is a difficult task due to limitations in the usual laboratory procedures to measure biomass and substrate concentrations and also due to the dynamic response of the cells under different environmental conditions. In this study, the growth kinetic constants were determined by three different methods: non linear regression of the Monod relation, linear regression of the inverse plot of specific growth rate versus substrate concentration, and washout technique. These three methods produced similar values of μ_{max} and K_S kinetic parameters. These kinetic constants were verified with the results from three independent continuous growth experiments, and with the results from the solution of the differential equations for the non steady-state operation of a continuous bioreactor. The outcome was the determination of reliable kinetic constants, μ_{max} and K_S, for *B. thuringiensis* growth.

The study of *B. thuringiensis* growth in different bioreactors showed some special features of the different reactor configurations. During the transition and stationary stages in the batch culture, and at low dilution rates in the continuous CSTR cultures, the experimentally measured biomass concentration was lower than the one predicted by the model. This phenomenon was attributed to a lower growth rate as a consequence of the spore formation in *B. thuringiensis* cells. In fed batch cultures, the μ_{max} and K_s parameters obtained were consistent with batch operation at the lower glucose concentration level. However, at high concentrations of glucose the μ_{max} obtained was lower. This was assigned to a glucose concentration inhibition effect.

Furthermore, the experimental research developed on *B. thuringiensis* growth demonstrated that the classical growth kinetic model has intrinsic limitations in predicting the biomass and glucose concentrations in batch and continuous cultures. This lack of agreement between the experimental results and the classical model was attributed to the cells metabolic changes during the spore formation process. Therefore, in order to have available a kinetic model that describe accurately *B. thuringiensis* cells growth it is necessary to account for these changes.

On this basis, a new *B. thuringiensis* cells growth with sporulation kinetic model was developed in this study. This model incorporates a number of sounds assumptions including a main consideration that the reduction in the cell growth rate is caused mainly by the spore formation process. This new growth kinetic model accurately predicted the experimental data obtained in both batch and in continuous growth of *B. thuringiensis*.

The biomass productivity was found to be four times larger in continuous cultures CSTR than in batch growth. Nevertheless, the crystal protein productivity was similar for both processes. Therefore, the use of a single CSTR continuous bioreactor to produce crystal protein is not advisable. Two CSTR continuous in series reactors system was also tested to produce a high concentration of cells in the first stage and cells with spores in the second one. However, a mixture of vegetative and sporulated cells was always present in the second stage. Therefore, it is suggested to further consider this system using a second reactor either a batch or a plug flow unit.

7.2 Recommendations

The simulation of the cell growth on any culture system requires an adequate kinetic model and accurate determination of the kinetic constants under the working conditions. As well, in this respect, classical growth models should be revised to include the sporulation process. The methods for the estimation of these constants must be used carefully and the

results must be verified by several methods. Therefore, it is important to develop new procedures for the accurate determination of both the maximum specific growth rate and the saturation constant and to account for the metabolic changes that can alter the performance of the culture under different growth conditions.

Fed-batch cultures of *B. thuringiensis* at high glucose concentrations showed differences in μ_{max} compared with other results of the present study. This discrepancy was assigned to the glucose inhibitory effect. This finding could help in designing appropriate process control systems in order to operate a *B. thuringiensis* culture at optimum conditions.

Finally, additional research involving reactors such as plug flow are advisable. The continuous stirred tank reactor two-stages system is not the most suitable alternative to increase the productivity of the delta-endotoxin production. This is the result of the diversity of fluid elements residence time in the unit. In this respect, the use of a plug flow system could be a good alternative given it has the advantages of a continuous unit, with the characteristics of a batch reactor. However, the use of a plug flow system for *B. thuringiensis* growth involves challenges that need to be addressed in future research..

Bibliography

Afkhami, P., Ozcengiz, G., Alaeddinoglu, N.G., 1993, Production of the Lepidoptera-specific Crystal Protein by a Local Isolate of *Bacillus thuringiensis*, Biotechnology Letters, 15 (12): 1253-1258

Agaisse, H., and Lereclus, D., 1995, How does *Bacillus thuringiensis* produce so Much Insecticidal protein ? Minireview., Journal of Bacteriology. 177, 21: 6027-6032

Anderson, T., 1990, Effects of Carbon:Nitrogen Ratio and Oxygen an the Growth Kinetics of *Bacillus thuringiensis* and Yield of Bioinsecticidal Crystal Protein, MESc Thesis, The University of Western Ontario, London, Canada.

Arbige, M.V., Bulthuis, B.A., Schultz, J., Crabb, D., 1993, Fermentation of Bacillus In *Bacillus subtilis* and other Gram-Positive Bacteria, Biochemistry, Physiology and Molecular Genetics, Sonenshein, A.L., Hoch, J.A., and Losick, R., (eds) American Society for Microbiology, Washington D.C.

Arcas, J., Yantorno, O., Arraras, E., Ertola, R., 1984, A New Medium for Growth and delta-ebdotoxin Production by *Bacillus thuringiensis* var. *kurstaki*, Biotechnology letters, 6 (8): 495-500

Arcas J., Yantorno O., Ertola R., 1987, Effect of High Concentration of Nutrients on *Bacillus thuringiensis* Cultures, Biotechnology Letters, 9 (2): 105-110

Aronson, J.N., Borris., D.P., Doerner, J.F., and Akers, E., 1975, γ-Aminobutyric Acid Pathway and Modified Tricarboxylic Acid Cycle Activity During Growth and Sporulation of *Bacillus thuringiensis*, Applied Microbiology, 30, 3: 489-492

Avignone-Rossa, C., Mignone, C.F., 1995, *Bacillus thuringiensis* Growth and Toxicity. Basic and Applied Considerations, Molecular Biotechnology, 4 (1): 55-71

Bandyopadhyay, B., Humprey, A.E., 1967, Dynamic Measurement of the Volumetric Oxygen Transfer Coefficient in Fermentation Systems, Biotechnology and Bioengineering, Vol IX, pp 533-544

Bateman, R., 1995, The Effect of a Medium Shift on the Sporulation and Production of δ-endotoxin in *Bacillus thuringiensis* subsp. *kurstaki* HD-1, MESc Thesis The University of Western Ontario, London, Canada.

Bazin, M., Gray, S., Rashit, E., 1990., Stability properties of microbial populations, In Microbial Growth Dynamics, Poole, R.K., Bazin, M.J., and Keevil, C.W., (eds.) IRL Press

Bechtel, D.B., Bulla, L.A. Jr., 1976, Electron Microscope Study of Sporulation and Parasporal Crystal Formation in *Bacillus thuringiensis*, Journal of Bacteriology, 127, (3):1472-1481.

Boudreaux, D.P., and Srinivasan, V.R., 1981, A Continuous Culture Study of Growth of *Bacillus cereus* T., Journal of General Microbiology, 122:129-136

Bryant, J.E., 1994, Commercial Production and Formulation of *Bacillus thuringiensis*, Agriculture, Ecosystems and Environment, 49 (1): 31-35

Bulla, L.E., Julian, G.S., and Rodhes, R.A., 1971, Physiology of Sporeforming Bacteria Associated with Insects: Radiorepirometry of Pyruvate, Acetate, Succinate, and Glutamate Oxidation, Canadian Journal of Microbiology, 17: 1073-1079

Bulla, L.A., Kramer, K.J., Cox, D.J., Jones, B.L., Davidson, L.I., and Lookhart, G.L., 1981, Purification and Characterization of the Entomocidal Protoxin of *Bacillus thuringiensis*, The Journal of Biological Chemistry, 256, (6):3000-3004

Bulla, L.A., Bechtel, D.B., Kramer, K.J., Shethna, Y.I., Aronson, A.I., Fitz-James, P.C., 1980, Ultrastructure, Physiology and Biochemistry of *Bacillus thuringiensis*, CRC Critical Reviews in Microbiology, 8: 174-204

Bulla, L.E., Julian, G.S., and Rodhes, R.A., and Hesseltine, C.W., 1969, Physiology of Sporeforming Bacteria Associated with Insects. I. Glucose Catabolism in Vegetative Cells, Canadian Journal of Microbiology, 16: 243-248

Bulla, L.E., Davidson, L.I., Kramer, K.J., and Jones, B.L., 1979, Purification of the Insecticidal toxin from the Parasporal Crystal of *Bacillus thuringiensis* subsp. *kurstaki*, Biochemical and Biophysical Research Communications, 91 (3):1123-1130

Bulla, L.A., Kramer, K.J., and Davidson, L.I., 1977, Characterization of the Entomocidal Parasporal Crystal of *Bacillus thuringiensis*, Journal of Bacteriology, 130 (1):375-383

Bu'Lock, J.D., 1988, What can the microbiologist learn from the biochemical engineer ?, in Horizons of Biochemical Engineering, Aiba, S. (ed.) Oxford University Press.

Cannon, R.J.C., 1993, Prospects and Progress for *Bacillus thuringiensis*-Based Pesticides, Pesticide Science, 37:331-335

Carlton, B.C., Gonzalez, J.M., (1984), Plasmid-associated delta-endotoxin Production in *Bacillus thuringiensis*, In Genetics and Biotechnology of Bacilli, Ganesan, A.T., and Hoch, J.A. (eds), Academic press Inc. p: 387-400

Carlton, B.C., and Gonzalez, J.M., (1985b), The Genetics and Molecular Biology of *Bacillus thuringiensis*, In The Molecular Biology of the Bacilli, vol. II Dubnau, D.A. (ed.), Academic press Inc. pp 211-249

Carlton, B.C., Gonzalez, J.M., (1980), Patterns of Plasmid DNA in Crystalliferous and Acrystalliferous Strains of *Bacillus thuringiensis*, Plamid, 3: 92-98

Carlton, B.C., Gonzalez, J.M., (1985a), Plasmids and delta-endotoxin Production in Different Subspecies of *Bacillus thuringiensis*, In: Molecular Biology of Microbial Differentiation., Hoch, J.A., and Setlow, O. (eds), American Society for Microbiology, Washington D.C. p:246-252

Damm, H.G., Besch, P.K., Couri D., Golwyn, A.J., (ed), (1966), Methods and References in Biochemistry and Biophysics, The World Publishing Co., Cleveland, New York,

Dean, A.C.R., and Hinshelwood, C., Growth, Function and Regulation in Bacterial Cells, Oxford at the Claredon Press.

Dean. D.H., 1984, Biochemical Genetics of the Bacterial Insect-Control Agent *Bacillus thuringiensis*: Basic Principles and Prospects for Genetic Engineering, In: Biotechnology and Genetic Engineering Reviews, Vol 2., Rusell, G.E. (ed), Intercept, New castle upon Tyne, England.

Debabov, V.G., Azizbekyan, R.R., Stepanov, V.M., Chestukhina, G.G., 1984, Genetic and Biochemical Study of *Bacillus thuringiensis*, In: Genetics and Biotechnology of Bacilli, Ganesan, A.T., and Hoch, J.A., (eds), Acadmeic Press Inc., pp:345-358

Dubois, N.R., and Dean, D.H., 1995, Synergism between Cry1A insecticidal crystal proteins and spores of *Bacillus thuringiensis*, other bacterial spores, and vegetative cells against *Lymantria dispar* (Lepidoptera: Lymantriidae) larvae. Environmental Entomology, 24: 1741-1747

Esener, A.A., Roels, J.A., and Kossen, N.W.F., 1981, Fed-batch culture: Modeling and Applications in the Study of Microbial Energetics, Biotechnology and Bioengineering, Vol XXIII, pp 1851-1871

Estruch, J.J., Carozzi, N.B., Duck, N.B., Warren, G.W., Koziel, M.G., 1997, Transgenic Plants: An Emerging Approach to Pest Control, Nature Biotechnology, 15: 137-141

Faust, P.G., 1972, The δ-endotoxin of *Bacillus thuringiensis* III. A rapid method for separating parasporal bodies from spores, Journal of Invertebrate Pathology, 20:130-149

Feitelson, J.J., Payne, J., and Kim, L., 1992, *Bacillus thuringiensis*: Insects and Beyond, Biotechnology, 10:271-276

Foda M.S., Salama H.S., Selim M (1985), Factors affecting growth physiology of *Bacillus thuringiensis*, Appl Microbiol Biotechnol, 22, 50-52

Freiman, V.B., and Chupin, A.A., 1973, Aspects of Continuous Cultivation of Spore-forming Microbes from the group *Bacillus thuringiensis*, Biotechnology Bioengineering Symposio, No. 4, 259-265

Golberg., I., Sneh, B., Battat, E., Klein, D., 1980, Optimization of a Medium for a High Yield Production of Spore-Crystal Preparation of *Bacillus thuringiensis* Effective Against the Egyptian Cotton Laf Worm *Spodoptera littoralis boisd*, Biotechnology Letters, 2 (10):419-426

Gonzalez, J.M., Dulmage, H.T., Carlton, B.C., (1981), Correlation Between Specific Plasmids and δ-endotoxin Production in *Bacillus thuringiensis*, Plasmid, 5: 351-365

Hofte, H. and Whiteley. H.R., 1989, Insecticidal Crystal proteins of *Bacillus thuringiensis*, Microbiological Reviews, 53:2, pp 242-255

Holmberg, A., and Sievanen, R., 1980, Exotoxin Production: Process Analysis Study, Biotechnology and Bioengineering, 23:1707-1724

Holmes, K.C., and Monro, R.E., 1965, Studies on the Structure of Parasporal Inclusions from *Bacillus thuringiensis*, Journal of Molecular Biology, 14:572-581

Holmes, B., 1997, Caterpillar's revenge. In the fight to protect crops, some pests may have the last laugh, New Scientist, December 6, 156 (2111):7

Ignatenko Yu N., Sakharova Z.V., Khovrychev M.P., and Shevstov V.V, 1983, Effect of temperature and aeration on growth and spore formation in *Bacillus thuringiensis*, Mikrobiologiya, Vol 52, No. 5, pp 716-718, September-October, 1983

Jong, J., Hsiun, D., Wu, W., 1995, Fed-batch Culture of *Bacillus thuringiensis* for Thuringiensin Production in a Tower Type Bioreactor, Biotechnology and Bioengineering, 48: 207-213

Johnson, D.E., and McGaughey, W.H., 1996, Contribution of Bacillus thuringiensis spores to toxicity of purified Cry proteins towards Indianmeal moth larvae, Current Microbiology, 33: 54-59

Kamdar H. and Jayaraman, K., 1983, Spontaneous Loss of a High Molecular Weight Plasmid and the Biocide of *Bacillus thuringiensis* var. *israeliensis*, Biochemical and Biophysical Research Communications, 110, (2): 477-482

Kang, B.C., Lee, S.Y., and Chang, H.N., 1993, Production of *Bacillus thuringiensis* Spores in Total Cell Retention Culture and Two-Stage Continuous Culture Using an Internal Ceramic Filter System, Biotechnology and Bioengineering, 42:1107-1112

Khovrychev, M.P., Sakharova, Z.V., Ignatenko, Yu.N., Blokhina, T.P., and Rabotnova, I.L., 1985, Spore Formation and Biosynthesis of Protein Crystals During Continuous Culturing of *Bacillus thuringiensis*, Mikrobiologiya, 5, 6: 983-988 (English trans)

Kumar, P.A., Sharma, R.P., and Malik, V.S.,1996, The Insecticidal Proteins of *Bacillus thuringiensis*, In: Advances in Applied Microbiology, Neideleman, S.L., and Laskin. A.I.(eds) Vol 42 pp 1-43, Academic Press Inc.

Lereclus D., Lecadet, M.M., Ribier, J., Dedoner, R., 1982, Molecular Relationships Among Plasmids of *Bacillus thuringiensis*: Conserved Sequences Through 11 Crystalliferous Strains, Molecular General Genetics, 186:391-398

Li., J., Carroll., J. and Ellar, D.J., 1991, Crystal Structure of Insecticidal δ-endotoxin from *Bacillus thuringiensis* at 2.5 Å Resolution, Nature, 353: 815-821

Liu, W., Bajpai, R., and Bihari, V., 1994, High-Density Cultivation of Sporeformers, Annals of the New York Academy of Sciences, 721: 310-325

Liu, W.M., Bajpai, R.K., 1995, A Modified Growth Medium for *Bacillus thuringiensis*, Biotechnology Progress, 11:589-591

Luthy, P., Cordier, J. L., Fischer, H.M., 1982, *Bacillus thuringiensis* as a Bacterial Insecticide: Basic Considerations and Application, In: Microbial and Viral Pesticides, Kurstak, E., (ed) Marcel Dekker Inc., New York.

Mahillon, J., and Delcour, J., 1984, A convenient procedure for the preparation of highly purified parasporal crystals of *Bacillus thuringiensis*, Journal of Microbiological Methods, 3:69

Macrae, R.M., and Wilkinson, J.F., 1958, Poly-β-hydroxybutyrate Metabolism in Washed Suspensions of *Bacillus cereus* and *Bacillus megaterium*, Journal of General Microbiology, 19:210-222

McGaughey, W. H., Gould, F., Gelernter, W., 1998, Bt Resistance Management, Nature Biotechnology, 16, 144-146.

Mignone C.F., and Avignone-Rossa, C., 1996, Analysis of Glucose Carbon Fluxes in Continuous Cultures of *Bacillus thuringiensis*, Appl. Microbiol. Biotechnol, 46:78-84

Monro, R.E., 1961, Protein Turnover and the Formation of Protein Inclusions During Sporulation of *Bacillus thuringiensis*, Biochem. J., 81:225-232

Moser, A., 1990, Tubular Bioreactors: case Study of Bioreactor Performance for Industrial production and Scientific Research, Biotechnology and Bioengineering, 37:1054-1065

Nickerson, K.W., Julian, G., and Bulla L.E., 1974, Physiology of Sporeforming Bacteria Associated with Insects: Radiorespirometric Survey of carbohydrate Metabolism in the 12 Serotypes of *Bacillus thuringiensis*, Applied microbiology, 28, 1:129-132

Nickerson K.W., Bulla A., 1974, Physiology of Spore Forming Bacteria Associated with Insect Minimal Nutritional Requirements for Growth, Sporulation and Parasporal Crystal Formation of *Bacillus thuringiensis*, Applied Microbiology, 28, 1:124-128

Nickerson, K.W., and Bulla L.A., 1975, Lipid Metabolism During Bacterial Growth, Sporulation and Germination: an Obligate Nutritional Requirement in *Bacillus thuringiensis* for Compounds that Stimulate Fatty Acid Synthesis, Journal of Bacteriology, 123, 2: 598-603

Pearson, D., and Ward, O.P., 1988, Effect of Culture Conditions on Growth and Sporulation of *Bacillus thuringiensis* subsp. *israelensis* and Development of Media for Production of the Protein Crystal Endotoxin, Biotechnology letters, 10 (7):451-456

Pirt, S.J., 1975, Principles of Microbe and Cell Cultivation, John Wiley and Sons, New York.

Pirt., S.J., 1990 The dynamics of microbial processes: a personal view. In Microbial Growth Dynamics, Poole, R.K., Bazin, M.J., and Keevil, C.W., (eds.) IRL Press

Postgate, J.R., Calcott, P.H., 1990, Ageing and Death of Microbes., In Comprrehensive Biotechnology. The Principles, Applications and Regulations of Biotechnology in Industry, Agriculture and Medicine, Moo-Young, M., Bull, A.T., and Dalton, H., (eds.), Pergamon Press.

Postgate, J.R., 1969, Viable Counts and Viability, in Methods in Microbiology, Norris, J.R., Ribbons, D.W., (eds) Academic Press, London.

Proom, H. and Knight, B.C.J.G., 1955, The Minimal Nutritional Requirements of Some Species in the Genus *Bacillus*, Journal of General Microbiology, 13: 474-480

Rodriguez-Monroy, M., de la Torre, M., 1996, Effect of the Dilution Rate on the Biomass Yield of *Bacillus thuringiensis* and Determination of its Rate Coefficients Under Steady-state Conditions, Appl. Microbiol. Biotechnol, 546-550

Rowe, G., 1990. Central Metabolism of *B. thuringiensis* During Growth and Sporulation Ph.D. thesis, The University of Western Ontario, London, ON. Canada.

Rowe, G. and Margaritis, A., 1987, Bioprocess Developments in the Production of Bioinsecticides by *Bacillus thuringiensis*, Critical reviews in Biotechnology, 6:87-127

Roy, B.P., Selinger, L.B., Khachatourians, G.G., (1987), Plasmid Stability of *Bacillus thuringiensis* var. *kurstaki* (HD-1) During Continuous Phased Cultivation, Biotechnology Letters, 9 (7): 483-488

Sachidanandham, R., Jenny, K., Fiechter, A., Jayaraman, K, 1997, Stabilization and Increased Production of Insecticidal Crystal Proteins of *Bacillus thuringiensis* subsp. *galleriae* in Steady-and Transient-state Continuous Cultures., Appl Microbiol Biotechnol, 47: 12-17

Sachidanandham, R., Jayaraman, K., 1993, Formation of Spontaneous Asporogenic Variants of *Bacillus thuringiensis* subsp. *galleriae* in Continuous Cultures., Appl Microbiol Biotechnol, 40: 504-507

Sakharova, Z.V., Ignatenko, YU.N., Shchul'ts, F., Khovrychev, M.P., and Rabotnova, I.L., 1985, Kinetics of the Growth and Development of *Bacillus thuringiensis* During Batch Culturing. Mikrobiologiya, (Engl. transl.) 54, 483-488

Salama H.S., Foda M.S., Dulmage H.T., El-Sharaby, 1983, Novel Fermentation Media for Production of δ-endotoxin from *Bacillus thuringiensis*, Journal of Invertebrate Pathology 41: 8-19

Sharpe, E.S., Nikerson, K.W., Bulla, L.A., and Aronson, J.N., 1975, Separation of spores and parasporal crystals of *B. thuringiensis* in gradients of certain X-ray contrasting agents, Applied Microbiology, 30:1052-1053

Scherrer, Luthy, P., Trumpi B., 1973, Production of δ-endotoxin by *Bacillus thuringiensis* as a Function of Glucose Concentrations, Applied Microbiology Vol 25, No. 4 , p 644-646

Schnepf, H.E., and Whiteley, H.R., 1985, Endotoxin Formation in Sporulating Organisms. Protein toxin of Bacillus spp., In Molecular Biology of Microbial Differentiation., Hoch, J.A., and Setlow, O. (eds), American Society for Microbiology, Whashington D.C. p: 209-216

Selinger, L.B., Dawson, P.S.S., Khachatourians, G.G., 1988, Behavior of *Bacillus thuringiensis* var. *kurstaki* Under Continuous Phased Cultivation in a Cyclone Fermentor, Appl Microbiol Biotechnol, 28:247-253

Sikdar, D.P., Majumdar, M.K., Majumdar, S.K., 1993, Optimization of Process for Production of delta-endotoxin by *Bacillus thuringiensis* var. *israelensis* in a 5-liter Fermentor., Biochemical Archives, 9: 119-123

Slater, J.H., 1990, Microbial Growth Dynamics, In Comprehensive Biotechnology. The Principles, Applications and Regulations of Biotechnology in Industry, Agriculture and Medicine, Moo-Young, M., Bull, A.T., and Dalton, H., (eds.), Pergamon Press.

Slepecky, R.A., and Law, J.H., 1961, Synthesis and Degradation of Poly-β-Hidroxybutyric Acid in Connection with Sporulation of *Bacillus megaterium*, Journal of Bacteriology, 82:37-42.

Sneath, P.H.A., 1986, Endospore-forming Gram-positive Rods and Cocci, In: Bergey's Manual of Systematic Bacteriology, Vol.2, Sneath, P.H.A., Mair N.S., Sharpe, M.E., Holt, J.G., (eds.) Williams and Wilkins, Baltimore, USA.

Stix, G., (1998), Resistance fighting. Will natural selection outwit the king of biopesticides?, Scientific American, 278 (5), 38

Stouthamer, A.H., Bulthuis, B.A., Van Verseveld, H.W., 1990, Energetics of growth at low growth rates and its relevance for the maintenance concept. In Microbial Growth Dynamics, Poole, R.K., Bazin, M.J., Keevil, C.W., (eds), Society for General Microbiology, IRL Press, Oxford University Press

Stradi B., 1992, Fed-batch Fermentation and δ-endotoxin Production by *Bacillus thuringiensis* subspecies, MESc Thesis, The University of Western Ontario, London, Canada.

Tyrell, D.J., Bulla, L.A., Andews, R.E., Kramer, K.J., Davidson, L.I., and Nordin, P., 1981, Comparative Biochemistry of Entomocidal Parasporal Crystals of Selected *Bacillus thuringiensis* Strains, J. Bacteriol, 145: 1502-1062

Webster, I.A., 1983, The Continuously Fed Batch Reactor for Measuring Microbial Growth Rates, Biotechnology and Bioengineering, Vol. 25, pp 2981-2990

Witter, L., Colburn, D., Hickle, L.A., Sambandan, T.G., 1990, Development of a High Performance Liquid Chromatography Assay for *Bacillus thuringiensis* var. *san diego* delta-endotoxin, In: Analytical Chemistry of *Bacillus thuringiensis*, Hickle, L.A., and Fitch, W.L. (eds.) American Chemical Society.

Wong, H.Ch., Schnepf, H.E., and Whiteley, H.R., 1983, Transcriptional and Translational Start Sites for the *Bacillus thuringiensis* Crystal Protein Gene, The Journal of Biological Chemistry, 258 (3):1960-1987

Yousten, A.A., and Rogoff, M.H., 1969, Metabolism of *Bacillus thuringiensis* in Relation to Spore and Crystal Formation, Journal of Bacteriology, 100, 3: 1229-1236

Yudina, T.G., Salamakha, O.V., Olekhnovich, E.V., Rogatykh, N.P., and Egorov, N.S., 1992, Effect of Carbon Source on the Biological Activity and Morphology Paraspore Crystals from *Bacillus thuringiensis*, Translated from Mikrobiologiya, Vol 61, No. 4, pp 577-584, July-August 1992.

APPENDIX A

Appendix A

Experimental data

1. Experimental data for batch growth

2. Experimental data for fed-batch growth

3. Experimental data for continuous growth

    3.1 Transient state continuous growth experiments

    3.2 Experimental data for estimation of kinetic parameters, oxygen uptake rate, respiration rate coefficient, growth yield, and traditional kinetic model

Appendix A

1. Experimental Data for Batch Growth.

Table A.1 Experimental data for batch growth of *B. thuringiensis* subspecies *kurstaki* HD-1 ATCC 33679. Experiments NB1, NB2 and NB5

Time (h)	Exp. NB1 Biomass conc. (g/L)	Exp. NB2 Biomass conc. (g/L)	Exp. NB5 Biomass conc. (g/L)
0	0.47	0.5	0.77
1	0.51	na	0.88
1.5	na	0.74	na
2	0.88	na	1.4
2.5	na	na	1.76
3	1.24	1.39	na
3.5	na	na	2.42
4.0	1.76	2.2	na
5.0	2.79	3.02	na
5.5	na	na	5.4
6.0	na	3.86	na
6.5	na	na	5.31
7.0	4.48	4.96	na
8.0	5.59	6.05	5.53
9.0	6.75	5.43	5.65
10	na	5.42	5.67
10.5	6.47	na	na

na: not available

Table A.2 Experimental results of batch culture of *B. thuringiensis* HD-1 ATCC 33679 Experiment NB4

Time (h)	pH	D.W. (g/L)	Glucose (g/L)	qO_2X (mg O_2/L-min)	qO_2 (mgO_2/g-min)	Cell count (CFU/mL)	Spore count (CFU/mL)
0	7.2	0.58	11.67	na	na	8.0E+07	0
1.5	6.8	0.86	---	2.88	3.35	na	na
2.5	6.7	1.25	10.07	na	na	4.00E+09	0
4.0	6.4	2.60	6.09	5.04	1.94	4.00E+10	0
5.5	6.4	5.07	3.96	4.12	0.81	na	na
6.5	6.6	6.44	1.22	4.12	0.64	1.83E+11	1.5E+04
7.5	6.9	6.37	0.10	3.49	0.55	1.8E+12	na
8.5	7.0	6.18	0.13	3.02	0.49	na	1.2E+12
9.5	7.0	6.15	0.63	na	na	na	na
Crystal protein concentration					0.91 g/L		

na: not available

Table A.3 Experimental results of batch culture of *B. thuringiensis* HD-1 ATCC 33679 Experiment NB6

Time (h)	pH	D.W. (g/L)	Glucose (g/L)	qO_2X (mg O_2/L-min)	qO_2 (mg O_2/g-min)	Cell count (CFU/mL)	Spore count (CFU/mL)
0	6.80	0.45	12.11	na	na	na	
0.5	6.60	0.48	na	na	na	1.70E+07	0
1.0	6.55	0.46	10.57	0.378	0.822	na	0
1.5	6.45	0.55	na	na	na	na	na
2.0	6.35	0.69	9.65	3.024	4.385	na	na
2.5	6.20	1.07	na	na	na	na	na
3.0	5.90	1.72	9.18	na	na	na	na
3.5	5.60	2.17	na	5.670	2.609	na	na
4.0	5.40	2.41	4.14	6.048	2.508	1.00E+08	0
4.5	5.60	na	na	na	na	5.00E+08	0
5.5	6.10	3.84	3.34	6.048	1.575	2.20E+11	2.00E+04
6.0	6.20	4.92	na	na	na	na	na
7.0	6.40	5.6	2.96	6.978	0.802	na	6.80E+10
8.0	6.40	6.35	na	4.536	0.714	8.00E+12	na
9.0	6.40	6.63	0.025	5.336	0.805	3.00E+13	1.40E+13
10.0	6.40	6.55	0.009	na	na	na	na
11	6.4	na	na	na	na	na	na
21.5	6.4	5.6	na	na	na	na	na
23	6.4	4.3	0.009	na	na	na	na
crystal protein concentration				1.02 g/L			

na: not available

2. Experimental data for fed-batch growth

Table A.4 Experimental data for the fed-batch culture of *B. thuringiensis* subspecies *kurstaki* HD-1 ATCC 33679. Substrate concentration in the feed stream (S_0) 39 g/L and volumetric flow rate (F_0) 0.117 L/h. Experiment NFB1.

Time (h)	Biomass conc. (g/L)	Glucose conc. (g/L)	Reaction volume (L)
0.0	1.12	8.133	0.85
0.5	1.55	9.312	0.91
1.0	1.74	11.733	0.97
1.5	1.83	11.960	1.02
3.0	2.35	14.382	1.20
3.5	2.75	17.589	1.26
4.0	3.08	17.012	1.32
4.5	3.65	18.719	1.38
5.0	3.90	19.572	1.43
5.5	4.15	19.365	1.49
6.0	4.5	20.770	1.50
6.5	4.65	19.042	1.61
7.0	4.65	19.620	1.67

Table A.5 Experimental data for the fed-batch culture of *B. thuringiensis* subspecies *kurstaki* HD-1 ATCC 33679. Substrate concentration in the feed stream (S_0) 10 g/L and volumetric flow rate (F_0) 0.08 L/h. Experiment NFB2.

Time (h)	Biomass conc. (g/L)	Glucose conc. (g/L)	Reaction volume (L)
0.0	3.727	4.848	0.75
0.5	4.525	4.604	0.79
1.0	4.906	3.916	0.83
1.5	5.32	3.334	0.87
2.0	5.529	2.900	0.91
2.5	5.655	2.339	0.95
3.0	5.671	1.842	0.99
3.5	5.351	1.439	1.03
4.0	5.588	1.101	1.07
4.5	5.436	0.847	1.11
5.0	5.587	0.54	1.15
5.5	5.653	0.364	1.19
6.0	6.462	0.064	1.23
6.5	6.266	0.013	1.27
7.0	6.076	0.015	1.31
7.5	6.533	0.012	1.35
8.0	6.533	0.012	1.39
8.5	6.600	0.011	1.43
9.0	6.626	0.011	1.47
9.5	6.727	0.011	1.51
10.0	6.430	0.012	1.55

Cell Count	6.5×10^{11}	CFU/mL
Spore Count	Zero	CFU/mL

3. Experimental Data for Continuous Experiments

3.1 Transient state in continuous growth experiments

Table A.6 Experiment NC1. Glucose concentration in the feed stream, S_0 = 8.0 g/L

Dilution rate = 0.14 h^{-1}

Time , h	Biomass conc. g/L
0	4.07
14	5.57
22	5.09
24	5.09
Glucose conc. at steady state, g/L	0.03
crystal protein concentration, g/L	1.03
spore count, CFU/mL	8.9×10^{12}

Table A.7 Experiment NC2. Glucose concentration in the feed stream, S_0 = 8.7 g/L

Dilution rate 0.40 h^{-1}		Dilution Rate 0.49 h^{-1}		Dilution rate = 0.53 h^{-1}	
Time , h	**Biomass Conc., g/L**	**Time, h**	**Biomass Conc., g/L**	**Time , h**	**Biomass conc. g/L**
0	2.56	16.5	5.19	21.5	5.03
0.5	3.37	17.5	4.80	22.5	5.08
1.5	3.94	18.5	4.09	23.5	5.11
3.5	4.74	19.5	4.44	24.5	4.47
5.5	5.91	20.5	4.65	25.5	5.12
7.5	6.49	21	5.22	26	4.63
8.5	6.27	21.5	5.13	26.5	4.66
9.0	6.27				
Glucose conc. at steady state, g/L	1.96	Glucose conc. at steady state, g/L	2.65	Glucose conc. at steady state, g/L	2.31

Table A.8 Experiment NC3 Glucose concentration in the feed stream, S_0 = 7.8 g/L

Dilution rate 0.47 h^{-1}		Dilution Rate 0.37 h^{-1}	
Time , h	**Biomass Conc., g/L**	**Time, h**	**Biomass Conc., g/L**
1	0.39	11.0	5.23
3.5	0.80	11.5	5.34
5	1.55	12	4.97
6.5	2.61	19.5	6.19
7.5	3.71	20	5.05
9.0	3.99	20.5	5.56
10.0	4.69	21	5.54
10.5	5.09		
11.0	5.22		
Glucose conc. at steady state, g/L	3.11	Glucose conc. at steady state, g/L	1.05

Table A.9 Experiment NC3 Glucose concentration in the feed stream, S_0 = 7.8 g/L

Dilution rate 0.28 h^{-1}		Dilution Rate 0.20 h^{-1}	
Time , h	**Biomass Conc., g/L**	**Time, h**	**Biomass Conc., g/L**
21	5.52	26	5.27
25	4.86	33	5.34
25.5	5.45	36	5.20
26	5.36	36.5	5.43
		37	5.34
		37.5	5.41
		38	5.39
		38.5	5.38
Glucose conc. at steady state, g/L	1.01	Glucose conc. at steady state, g/L	0.81

Table A.10 Experiment NC6 Glucose concentration in the feed stream, S_0 = 7.37 g/L

Dilution rate 0.54 h^{-1}		Dilution Rate 0.71 h^{-1}		Dilution rate = 1.49 h^{-1}	
Time , h	**Biomass Conc., g/L**	**Time, h**	**Biomass Conc., g/L**	**Time , h**	**Biomass conc. g/L**
0	4.75	19.0	5.33	26	4.09
3.0	4.8	22	4.62	26.5	3.36
6.0	5.48	24	4.41	27.5	2.36
17.0	5.48	25	4.35	28.5	1.78
18.0	5.42			29.5	1.64
18.5	5.39			30.5	1.26
19	5.36			34.5	0.25
				42	0.02
Glucose conc. at steady state, g/L	3.29	Glucose conc. at steady state, g/L	3.71		

Table A.11 Experiment NC7 Glucose concentration in the feed stream, S_0 = 8.7 g/L

Dilution rate = 0.43 h^{-1}

Time , h	Biomass conc. g/L
0	1.3
1.0	2.33
4.0	4.04
5.0	4.56
16.0	5.26
18.0	5.26
20.0	5.16
21.0	5.21
Glucose conc. at steady state, g/L	2.60

Table A.12 Experiment NC8 Glucose concentration in the feed stream, S_0 = 8.09 g/L

Dilution rate 0.62 h^{-1}		Dilution Rate 0.85 h^{-1}		Dilution rate = 1.05 h^{-1}	
Time , h	**Biomass Conc., g/L**	**Time, h**	**Biomass Conc., g/L**	**Time , h**	**Biomass conc. g/L**
0	1.65	0	3.89	0	3.37
1.5	2.6	1.5	3.31	9.5	2.00
2.5	3.02	3.5	2.97	10.5	2.11
14.0	3.76	5.5	2.76	11.5	2.05
14.5	3.88	9.5	2.54	12	1.88
15	3.96	11.0	2.56	12.5	1.71
15.5	3.92				
Glucose conc. at steady state, g/L	5.69	Glucose conc. at steady state, g/L	6.87	Glucose conc. at steady state, g/L	7.9

3.2 Experimental data for estimation of kinetic paramenters, oxygen uptake rate, respiration rate coefficient, gowth yield, and traditional kinetic model.

Table A.13 Experimental data from continuous growth experiments used to determine the growth kinetic constants.

Dilution rate (h^{-1})	Glucose conc. (g/L)	Dilution rate (h^{-1})	Glucose conc. (g/L)
0.2	0.81	0.47	3.11
0.28	1.01	0.49	2.65
0.37	1.05	0.53	2.31
0.40	1.96	0.54	3.29
0.43	2.60	0.71	3.71

Table A.14 Experimental data from the washout stage during continuous culture of *B. thuringiensis* HD-1 ATCC 33679. Experiment NC6. Dilution rate, D = 1.49 h^{-1}.

time (h)	biomass conc, X (g/L)	Ln (X/X0)
0	4.09	0
0.5	3.36	-0.196
1.5	2.36	-0.549
2.5	1.78	-0.813
3.5	1.64	-0.914
4.5	1.26	-1.177
8.5	0.25	-2.795
16	0.02	-5.321

Table A.15 Experimental data from continuous culture of *B. thuringiensis* and theoretical data from traditional model for a steady-state continuous bioreactor. The theoretical data were obtained by numerically solving the non steady state differential equations for a continuous bioreactor with the following kinetic constants: $\mu_{max} = 1.1\ h^{-1}$, and $K_S = 3.1$ g/L

D (1/h)	X, (g/L)	S, (g/L)	S0, (g/L)	S model, (g/L)	X model, (g/L)
0.14	5.09	0.03	8	0.45	5.62
0.2	5.38	0.81	7.8	0.69	5.68
0.28	5.36	1.01	7.8	1.06	5.64
0.37	5.54	1.05	7.8	1.57	5.62
0.43	5.21	2.60	8.7	1.99	5.45
0.47	5.22	3.11	7.8	2.31	5.30
0.49	5.13	2.65	8.7	2.49	5.11
0.53	4.66	2.31	8.7	2.88	4.64
0.54	5.36	3.29	7.4	2.99	4.77
0.62	3.92	5.69	8.1	4.02	3.55
0.71	4.35	3.71	7.4	5.64	1.71
0.85	2.56	6.87	8.1	8	0
1.05	1.83	7.9	8.1	8	0

Table A.16 Oxygen uptake rate, qO_2*X, and respiration rate coefficient, qO_2 at various dilution rates for continuous culture of *B. thuringiensis* subspecies *kurstaki* HD-1 ATCC 33679.

Dilution rate (h^{-1})	qO_2*X (mgO_2/L-min)	qO_2 (mgO_2/g cell-min)
0.20	4.05	0.75
0.28	4.32	0.81
0.37	3.78	0.68
0.47	7.09	1.36
0.54	8.25	1.54
0.62	12.7	3.24

Table A.17 Biomass yield coefficient at various dilution rates for continuous culture of *B. thuringiensis* subspecies *kurstaki* HD-1 ATCC 33679.

Dilution rate, (h^{-1})	Biomass conc., X, (g/L)	Glucose conc., S, (g/L)	Glucose conc. in feed stream, S_0, (g/L)	Growth yield, $Y_{X/S}$, (g cell/g glucose)
0.14	5.09	0.03	8.0	0.63
0.20	5.38	0.81	7.8	0.77
0.28	5.36	1.01	7.8	0.79
0.37	5.54	1.05	7.8	0.82
0.43	5.21	2.60	8.7	0.85
0.47	5.22	3.11	7.8	1.11
0.49	5.13	2.65	8.7	0.85
0.53	4.66	2.31	8.7	0.73
0.54	5.36	3.29	7.4	1.3
0.71	4.35	3.71	7.4	1.17

APPENDIX B

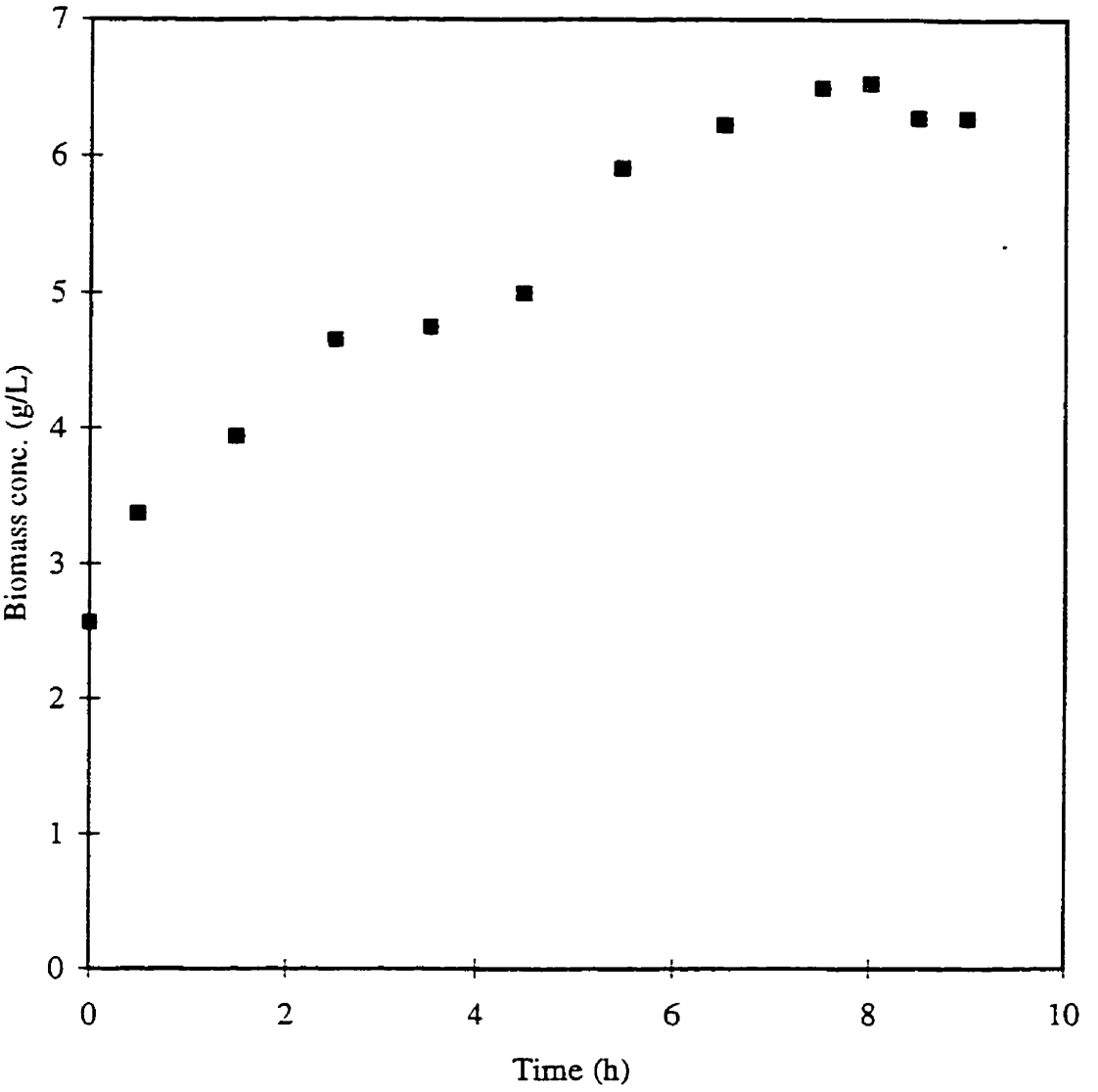

Fig. B.1 Transient state experimental data for continuous culture of *B. thuringiensis* . Exp. NC2. D = 0.4 1/h

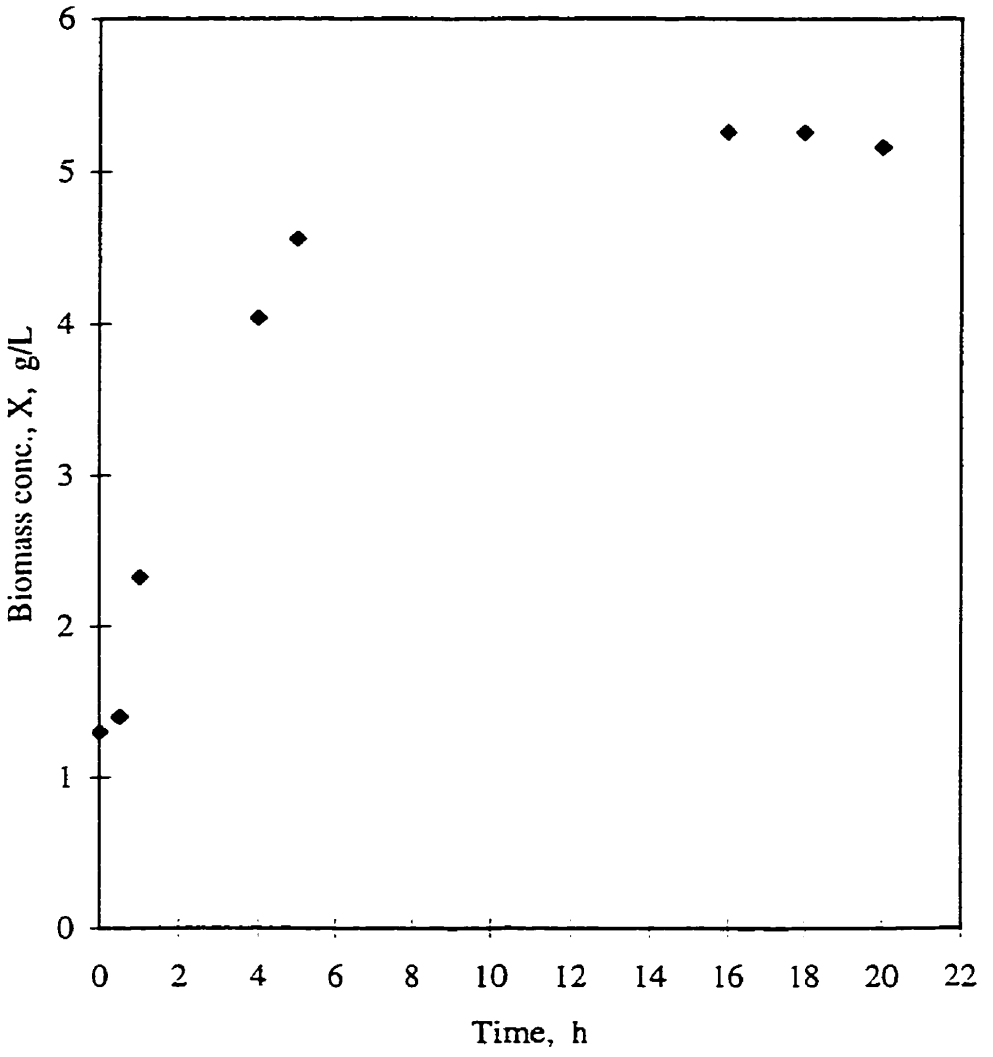

Fig. B.2 Transient state in continuous growth of *B. thuringiensis* subspecies *kurstaki*.
Exp. NC7. D = 0.43 h^{-1}

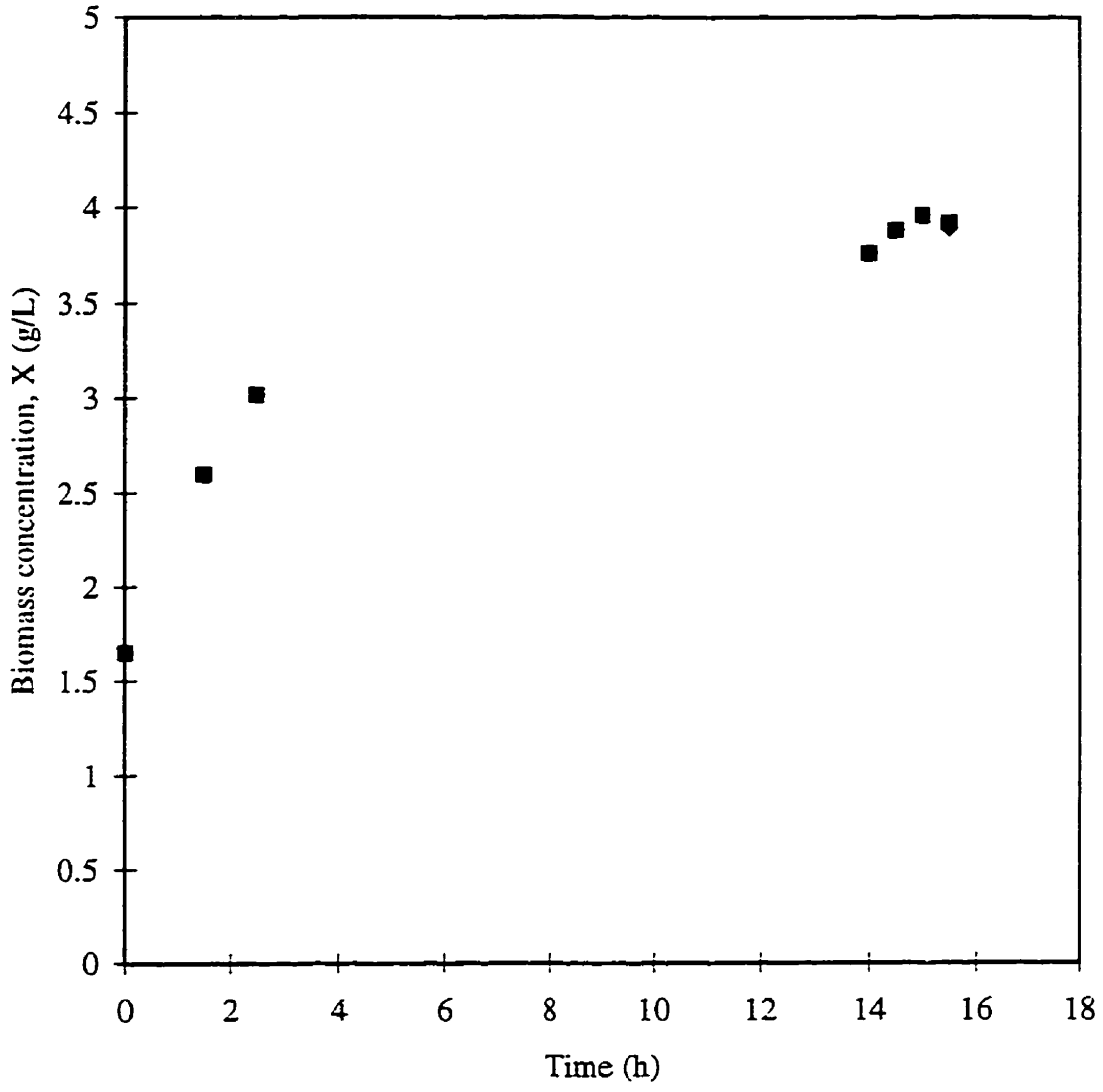

Fig. B.3 Continuous culture of *B. thuringiensis* subspecies *kurstaki*. Exp. NC8. D = 0.62 h^{-1}

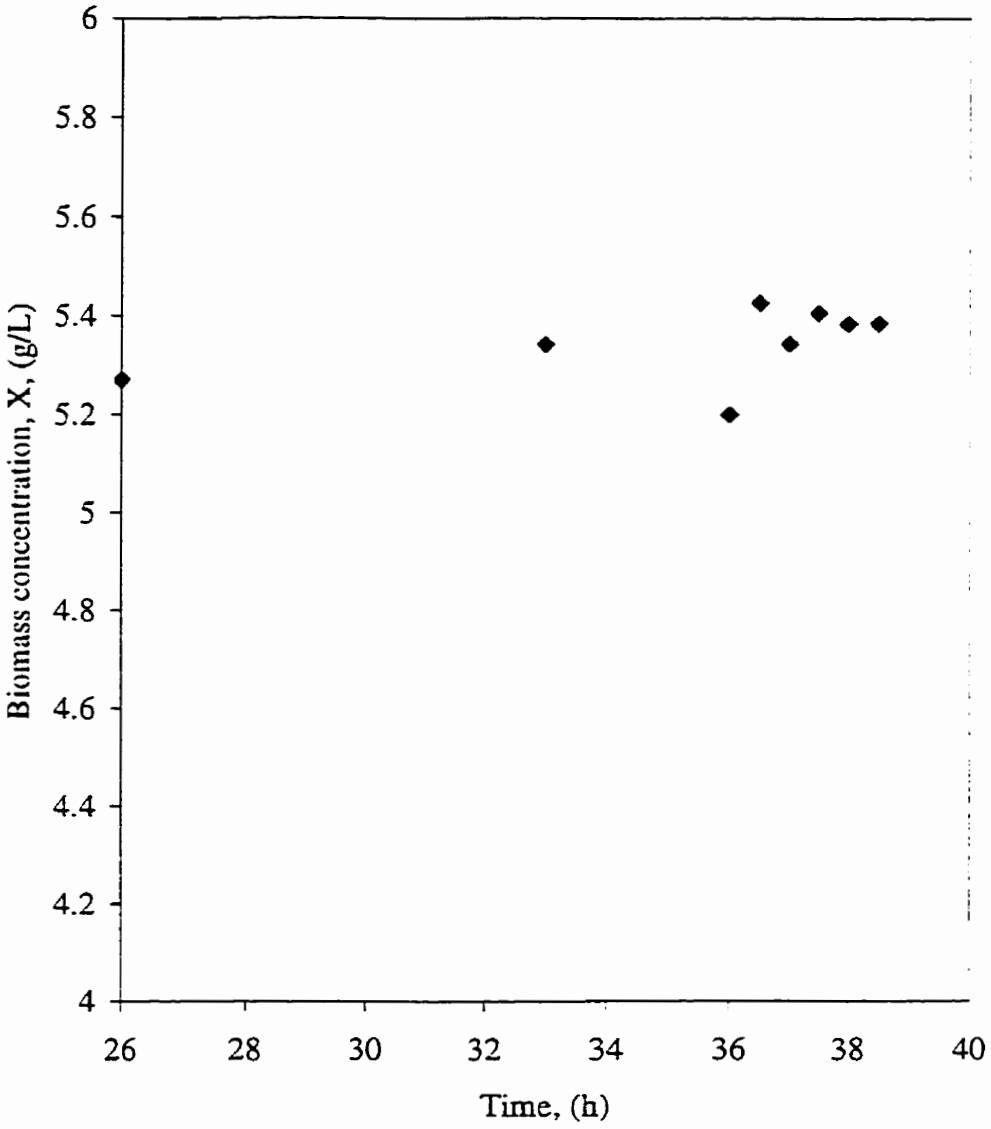

Fig. B.4 Transient state experimental data for continuous culture of *B. thuringiensis* subspecies *kurstaki*. Exp. NC3. D = 0.2 h^{-1}

APPENDIX C

Calibration curve for crystal protein concentration measurement in HPLC

Appendix C

1. Calibration Curve for Crystal Protein Concentration Measurement with HPLC

The HPLC tests were run with samples of delta endotoxin 85% purity. This crystal protein sample was obtained from a batch culture of *B. thuringiensis*. The mixture spores-cell debris-crystal protein was washed with 0.14 N NaCl-0.1% Triton X-100 solution three times. The pellet was re-suspended in the same salt solution and the spores were separated by flotation-settling in a separating funnel. After a centrifugation, the pellet was dried at room temperature under the vacuum.

The purity was verified taking 7.7 mg of the crystal protein powder and dissolved in 1.9 mL 0.021 N NaOH (7.7 mg/1.9 mL or 4.05 mg/mL of protein) for five hours at room temperature. The suspension was centrifuged and the supernatant, containing the crystal protein in solution, was used to determine the protein content by the Lowry test. The total protein determined by the Lowry assay was 3.46 mg/mL, that is, the crystal protein content in the powder was 85% (3.46 mg protein/4.05 mg powder)

The samples for the HPLC test were prepared dissolving 10 mg of crystal protein powder 85% purity (CP50), equivalent to 8.5 mg of crystal protein, with 2mL 0.02 N NaOH for five hours. The suspension was centrifuged at 7000 RPM for 15 min. to remove the pellet. The supernatant (2 mL) containing the delta-endotoxin in solution was added to 2 mL of a solution composed by 2% SDS, 10% glycerol and 2.5% Mercaptoethanol and the mixture was heated immediately at 100 C for 10 min. This solution was used directly in the HPLC runs.

In order to make a correlation between the concentration of crystal protein and the peak area obtained in the HPLC, three dilutions (1/2, 1/4 and 1/8) of the crystal protein solution were prepared, adding a solution of 0.1% TFA in water.

The samples used in the HPLC runs and their concentrations are shown in the following table:

Sample	Crystal Protein conc. in the sample (mg/mL)	Protein conc. detected by HPLC (mg/mL)
d1	2	2.0356
d2	1	0.7904
d3	0.5	0.6238
d4	0.25	0.2966
blank	0.0	0.0439

Fig. C.1 shows the Calibration curve for Crystal Protein Concentration Measurement with HPLC

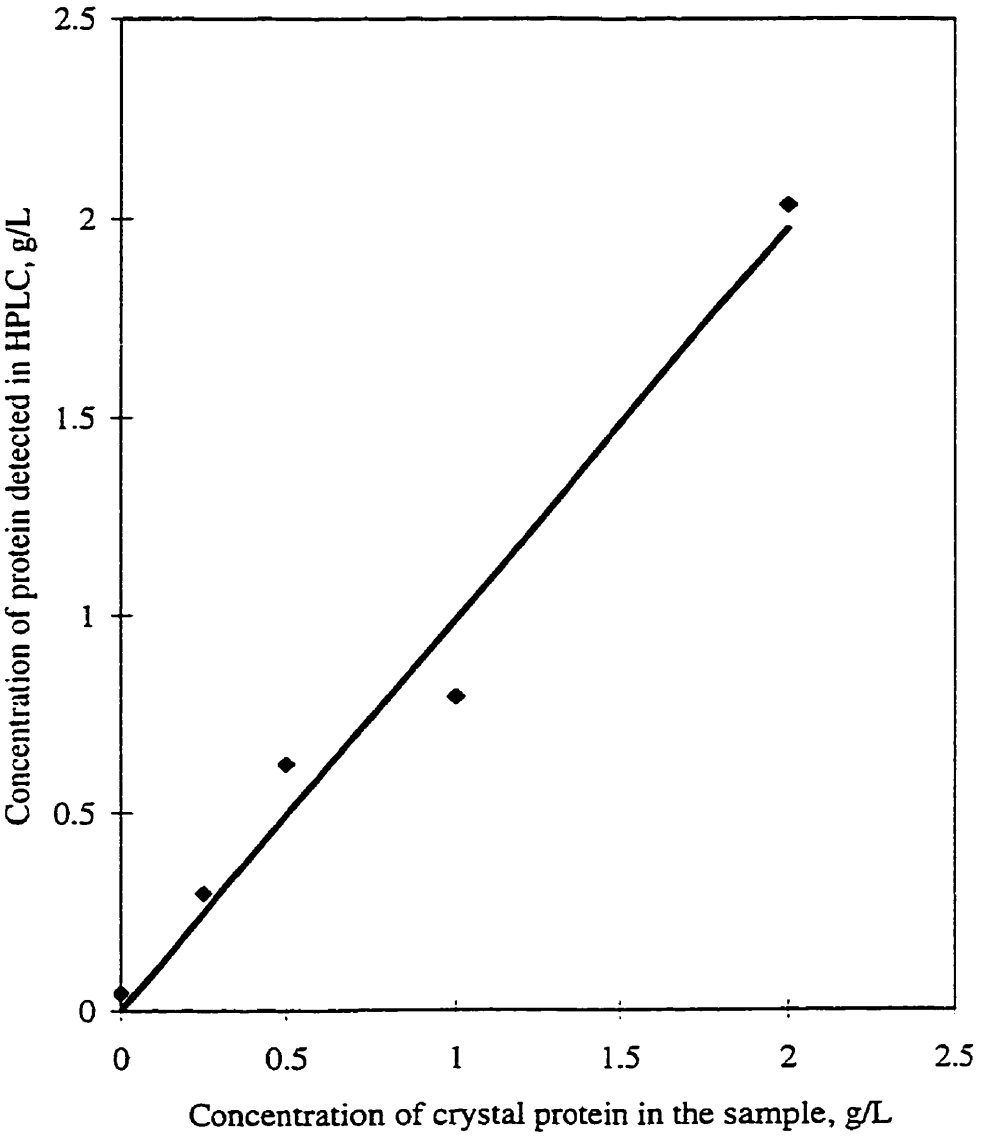

Fig. C.1 Calibration curve for crystal protein identification in HPLC

APPENDIX D

Appendix D

Development of a new growth kinetic model of *B. thuringiensis*

1. Batch growth

    1.1 Experimental data used to test the new model

    1.2 Estimation of initial conditions, growth yield, and maximum specific growth rate

    1.3 Test of classical model

2. Continuous culture

    2.1 Test of classical model

    2.2 Test of new growth kinetic model

3. Corrections results from the application of sporulation kinetic model

Appendix D

Development of a new kinetic growth model of *B. thuringiensis*

1. Batch growth.

1.1 Experimental data used to test the new model

Five experimental data sets for biomass concentration versus time were used to test the new model for a batch culture. Table D.1 shows the raw experimental data used.

Table D.1 Experimental data for five *B. thuringiensis* batch growth

Time (h)	X, NB1 (g/L)	X , NB2 (g/L)	X, NB4 (g/L)	X ,NB5 (g/L)	X, NB6 (g/L)	X, Avg. (g/L)
0.0	0.47	0.5	0.58	0.77	0.45	0.55
0.5					0.48	0.48
1.0	0.51			0.88	0.46	0.62
1.5		0.74	0.86		0.55	0.72
2.0	0.88			1.4	0.69	0.99
2.5			1.25	1.76	1.07	1.36
3.0	1.24	1.39			1.70	1.45
3.5				2.42	2.17	2.30
4.0	1.76	2.2	2.6		2.41	2.24
5.0	2.79	3.02				2.90
5.5			5.07	5.4	3.84	4.77
6.0		3.86			4.92	4.39
7.0	4.48	4.96			5.6	5.01
8.0	5.59	6.05		5.53	6.35	5.88
8.5			6.18			6.18
9.0	6.75	5.43		5.63	6.63	6.11
9.5			6.15			6.15
10.0	6.47	5.42		5.67	6.55	6.03
Initial glucose concentration, (g/L)			11.67		12.1	

Fig. D.1 reports a plot of biomass concentration, X, (g/L) versus time (h) for all the experimental data. This plot shows consistency in the relationship between biomass concentration and time for the batch growth.

1.2 Estimation of initial conditions, growth yield and exponential specific growth rate

The initial conditions, of biomass and glucose concentration, to be used to test the new kinetic growth model were obtained from the average values of these variables from five replicas of batch experimental data. The average values of biomass concentration and glucose concentration at the beginning of the batch culture for the five experimental replicas were 0.55 and 11.9 g/L, respectively.

The average values of biomass concentration were used to estimate the exponential specific growth rate. The slope of the linear section of the plot of the natural logarithm of biomass concentration versus time gave an exponential specific growth rate of 0.53 h^{-1} (See Fig. D.2). This value was used as an estimation of the maximum specific growth rate, μ_{max}, for these batch cultures.

The growth yield was estimated by a plot of biomass concentration versus glucose concentration for all the experimental data. This plot showed a linear trend with the slope representing the growth yield. Fig. D.3 shows this plot with a slope of 0.55 g/g. From the continuous experiments, the saturation constant was estimated to be 3.1 g/L. With these constants, the classical growth kinetic model and the proposed model were used to predict the biomass concentration with time for a batch growth of *B. thuringiensis*.

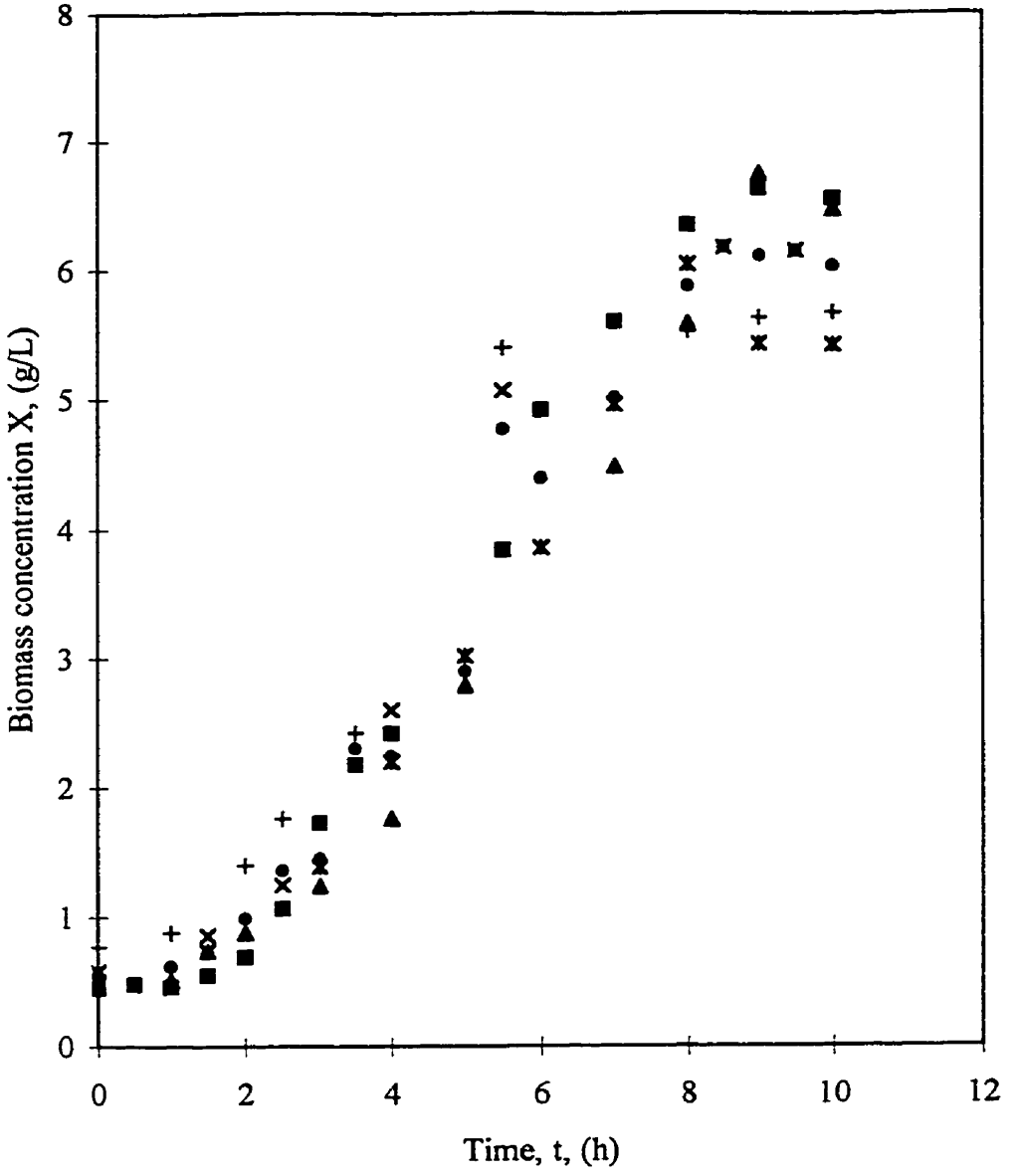

Fig. D.1 Batch growth of *B. thuringiensis*. Experimental results

■ NB6 (g/L) ✕ NB4 (g/L) ✱ NB2 (g/L)

▲ NB1 (g/L) + NB5 (g/L) ● AVG X

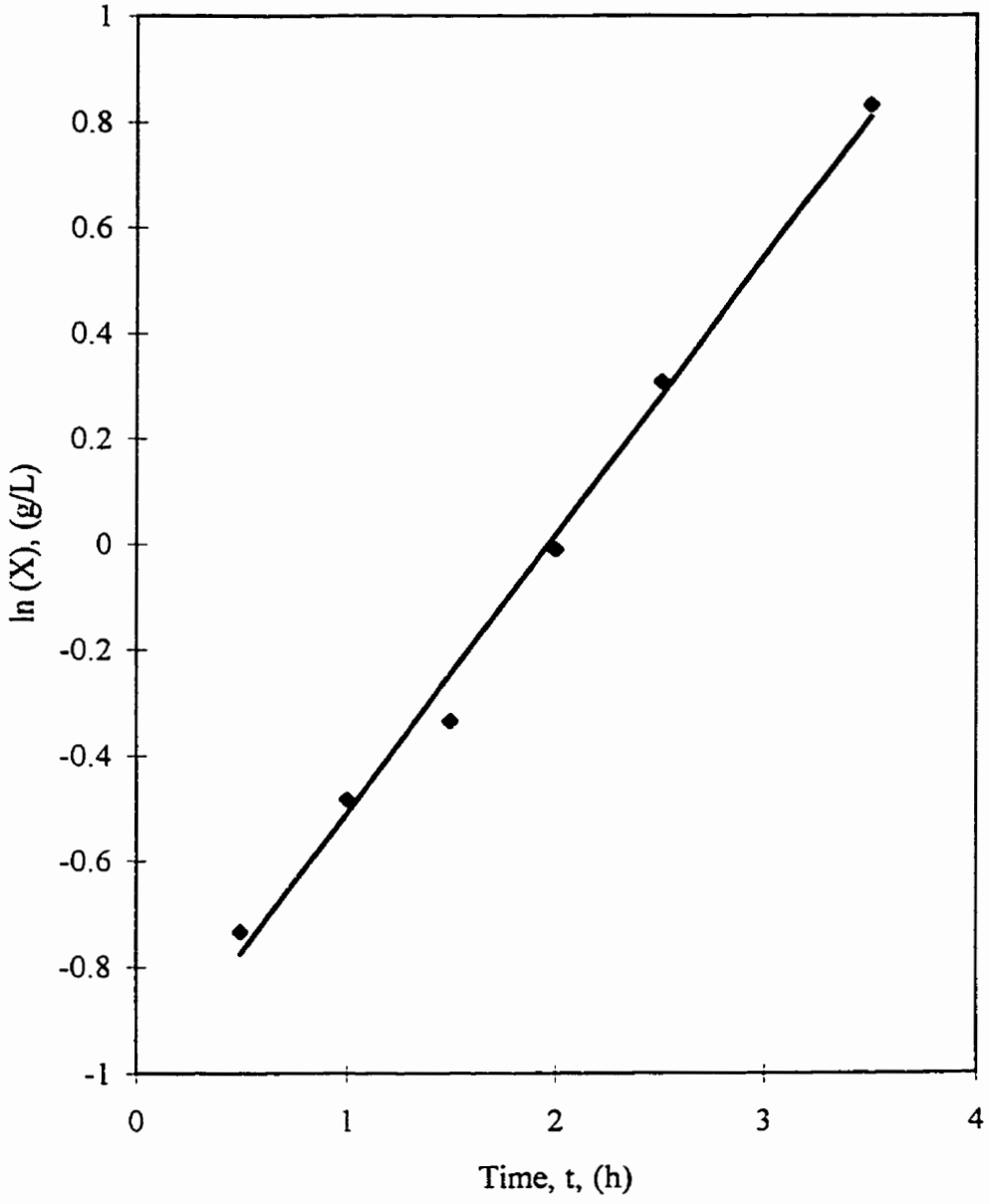

Fig. D.2 Batch growth of *B. thuringiensis*. Results of five batch growth experiments. Estimation of exponential specific growth rate. $\mu_{exp} = 0.528\ h^{-1}$

$\ln (X) = 0.5282\ t - 1.0391$

$R^2 = 0.9927$

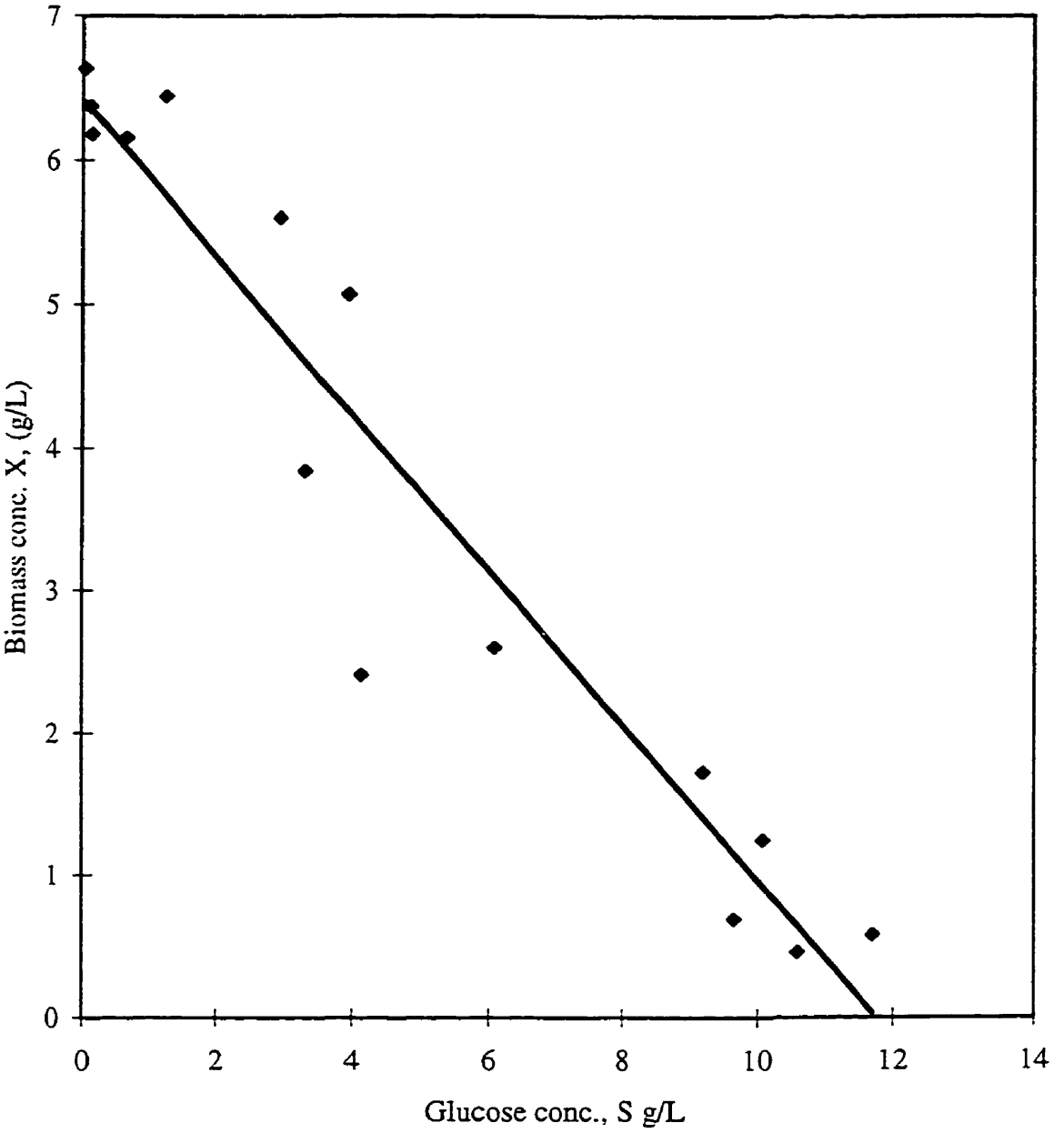

Fig. D.3 Batch growth of *B. thuringiensis* . Results of five batch culture experiments. Estimation of growth yield. Yx/s = 0.546 (g cell/g glucose)

$X = -0.5462\ S + 6.4198$

$R^2 = 0.9219$

1.3 Test of classical model

The equations that describe the classical model were solved numerically by Euler method, using the initial conditions and the kinetic constants obtained as discussed in the previous section.

The agreement between the classical model and the experimental data was assessed by the sum squares of residuals, defined as the square of the difference between the experimental and predicted biomass concentrations.

The classical model was tested with different values of K_s and μ_{max} in order to test this model. Table D.2 shows the sum of squares of residuals obtained.

Table D.2 Sum of squares of residuals obtained when comparing the classical model with experimental data varying the constants μ_{max} and K_s

μ_{max} Ks	0.1	0.2	0.3	0.4	0.5	0.53	0.6	0.8
0	162.16	68.69	39.64	1059.14	9888.41	18016	68972.8	2.65E+06
0.5	165.29	78.33	11.56	7.72	24.59	31.08	43.05	83.39
1	168.1	87.23	15.25	5.76	18.5	24.59	38.4	74.84
1.5	170.73	34.99	20.84	5.07	13.48	18.74	32.2	67.22
2	173	101.44	27.51	4.98	9.98	14.04	26.29	59.71
2.5	174.94	107.63	33.93	5.53	7.41	10.52	20.96	53.4
3	176.8	113.24	41.16	6.8	5.61	7.89	16.46	47.91
3.1	177.19	114.3	42.61	7.15	5.32	**7.45**	15.67	46.85
3.5	178.76	118.98	49.39	8.69	4.5	5.95	11.14	39.51
4	180.35	123	55.224	11.76	3.76	4.61	9.89	37.76
4.5	181.61	127.23	61.86	15.35	3.59	3.76	7.59	33.01
5	182.96	11.14	68.15	19.51	3.91	**3.36**	5.82	28.58
5.5	184.22	134.74	74.09	24.09	4.72	3.41	4.5	24.5
6	185.39	138.06	79.7	28.9	6.04	3.92	3.6	20.8

1.4 Test of the new model.

The following equations that describe the new kinetic model were solved simultaneously by Euler method.

$$dS/dt = \mu\,(X\text{-}X_s)/Y_{X/S} \qquad (D.1)$$

$$dX_s/dt = k_s\,(X - X_s) \qquad (D.2)$$

$$dX/dt = (\mu - k_s)\;(X - X_s) \qquad (D.3)$$

$$\mu = \mu_{max}\,S/(K_s + S) \qquad (D.4)$$

To solve the models the following initial conditions and constants were used.

μ_{exp}	0.53 h^{-1}
K_s	3.1 g/L
$Y_{X/S}$	0.55 g/g
X_0	0.55 g/L
S_0	11.9 g/L
t_0	0.0 h

The constant k_s was estimated by iteration and by solving the system of differential equations as given by equations D.1 to D.4. The value of the constant k_s which gave the minimum sum of squares of residuals was considered as the appropriate value for this constant. The iteration process showed that as k_s increased the sum of squares of residuals was decreased. This sum of residuals reached a minimum when the constant k_s had a value of 0.026 and increased again for higher values of k_s. This finding confirms that only this value of k_s gives the global minimum of sum of squares of residuals and therefore, the best fit with the experimental data. See table 6.1 and Fig. 6.2.

The new model was also tested assuming a lag time during the batch culture. The procedure used is the same as described previously. Fig. D.4 shows the comparison of the

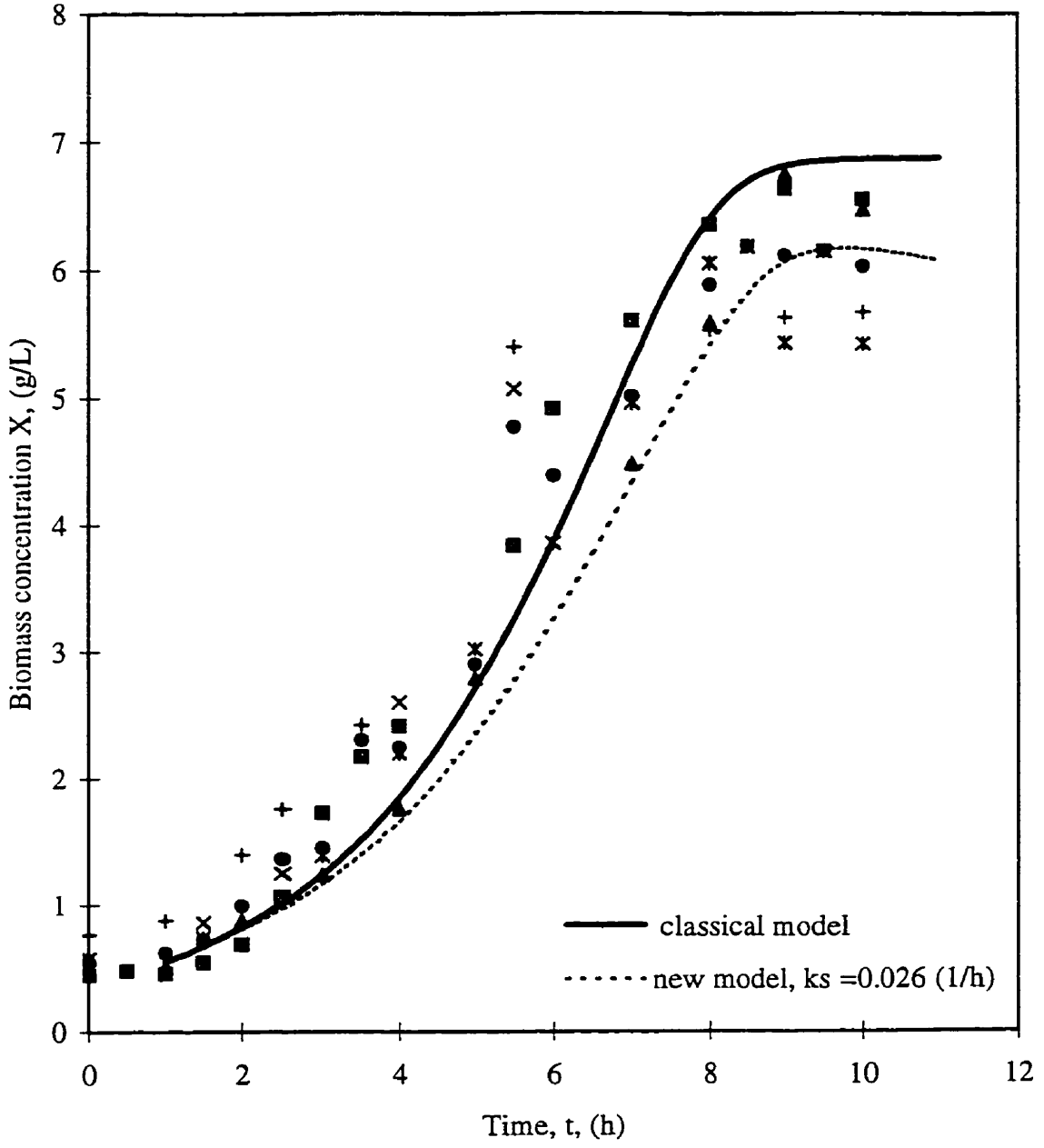

Fig. D.4 Batch growth of *B. thuringiensis* .Comparison of the classical model and the new model with experimental data. Lag time = 1 h

classical and the new model with the experimental data, assuming a lag time of 0.5 h. This figure shows that a lag time in the beginning of the batch culture is not responsible for the lack of agreement between the classical model and the experimental data.

2. Continuous culture

2.1 Test of classical model

The classical model was compared with the experimental data for continuous growth experimental results at steady state. In order to obtain the biomass and glucose concentrations at steady state as predicted by the classical model, a simulation was performed by solving numerically the set of differential equations describing the transient state operation of a continuous culture. Table D.3 reports the experimental data for different dilution rates, D, and initial biomass, X_i, and glucose, S_i, concentrations. S_0 represents the glucose concentration in the feed stream. These various parameters were used as initial conditions to solve the set of differential equations.

Table D.3 Experimental data of transient culture of *B. thuringiensis* in a continuous bioreactor. D: dilution rate, S_i: initial glucose concentration, X_i: initial biomass concentration, S_0: glucose concentration in the feed stream.

D, (h^{-1})	S_i, (g/L)	X_i, (g/L)	S_0, (g/L)
0.14	2.5	4.10	8.0
0.20	1.2	5.30	7.8
0.28	1.2	5.52	7.8
0.37	2.0	5.23	7.8
0.43	7.1	1.30	8.7
0.47	7.4	0.39	7.8
0.49	2.4	5.19	8.7
0.53	2.4	5.03	8.7
0.54	3.0	4.75	7.4
0.62	6.2	1.65	8.10
0.71	2.0	5.33	7.4
0.85	5.7	3.89	8.1
1.05	6.8	3.37	8.1

As described in chapter 3, a mass balance in a continuous reactor gives the following set of equations for a transient state operation:

$$dX/dt = (\mu - D)\, X \qquad (D.5)$$

$$dS/dt = D(S_0 - S) - \mu\ X/Y_{X/S} \qquad (D.6)$$

and

$$\mu = \mu_{max}\, S/(K_s + S) \qquad (D.7)$$

Since the growth yield changes with dilution rate, the expression for growth yield, $Y_{X/S} = X/(S_0 - S)$, was incorporated in equation D.6 to give equation D.8.

$$dS/dt = D(S_0 - S) - \mu\, X/(X/(S_0 - S)) \qquad (D.8)$$

This equation is simplified to:

$$dS/dt = D(S_0 - S) - \mu\, (S_0 - S) \qquad (D.9)$$

and

$$dS/dt = (D - \mu)\, (S_0 - S) \qquad (D.10)$$

The equations D.5, D.7, and D.10 were solved numerically for each dilution rate using the initial conditions shown in Table D.3, and the kinetic constants obtained in sections 5.3.2 and 5.3.3. The solution of these equations gives the biomass and glucose concentrations with time during transient state operation of a continuous bioreactor. It should be mentioned that the numerical solution converges as the dilution rate approaches the specific growth rate, and hence, the biomass and glucose concentration remains unchanged with time. Table D.4 shows an example of the tabulated data obtained in the solution of equations D.5, D.7, and D.10.

Table D.4 Tabulated data obtained in the numerical solution of the equations D.5, D.7, and D.10 . Dilution rate, D = 0.28 h^{-1}, S_0 = 7.8 g/L, X_i = 5.52 g/L, S_i = 1.2 g/L, μ_{max} = 1.1 h^{-1}, K_S = 3.1 g/L.

Time, (h)	μ, (h^{-1})	X, (g/L)	S, (g/L)
0	0.306977	5.52	1.2
0.2	0.300355	5.572375	1.137378
0.6	0.291377	5.602097	1.10184
0.8	0.288451	5.611566	1.090519
1	0.286258	5.618589	1.082121
1.2	0.284624	5.623786	1.075908
1.6	0.282513	5.630451	1.067939
1.8	0.28185	5.632534	1.065448
2	0.281361	5.634067	1.063616
2.2	0.281	5.635194	1.062268
2.6	0.28054	5.636631	1.060549
2.8	0.280397	5.637079	1.060015
3	0.280291	5.637407	1.059622
3.2	0.280214	5.637648	1.059334
3.6	0.280115	5.637956	1.058966
3.8	0.280085	5.638051	1.058852
4	0.280062	5.638121	1.058768
4.2	0.280046	5.638173	1.058707
4.6	0.280025	5.638238	1.058628
4.8	0.280018	5.638259	1.058604
5	0.280013	5.638274	1.058586
5.2	0.28001	5.638285	1.058573
5.6	0.280005	5.638299	1.058556
5.8	0.280004	5.638303	1.058551
6	0.280003	5.638306	1.058547
6.2	0.280002	5.638308	1.058544
6.6	0.280001	5.638311	1.058541
6.8	0.280001	5.638312	1.05854
7	0.280001	5.638313	1.058539
7.2	0.28	5.638313	1.058538
7.6	0.28	5.638314	1.058537
7.8	0.28	5.638314	1.058537
8	0.28	5.638314	1.058537

Table D.5 reports a comparison of experimental biomass and glucose concentrations (steady state) in the continuous culture of *B. thuringiensis* with the same concentrations as predicted by the classical model.

Table D.5 Comparison of continuous growth experimental data with classical model, D: dilution rate, X: biomass concentration, S: glucose concentration, S_0: glucose concentration in the feed stream, $Y_{X/S}$: growth yield.

D (h^{-1})	X, (g/L)	S, (g/L)	S, model, (g/L)	X model, (g/L)	Error (X_{exp}-X_{model})	$Y_{X/S}$, (g cells/g glucose)
0.14	5.09	0.03	0.45	5.62	-0.53	0.74
0.2	5.38	0.81	0.69	5.68	-0.30	0.80
0.28	5.36	1.01	1.06	5.64	-0.28	0.84
0.37	5.54	1.05	1.57	5.62	-0.08	0.90
0.43	5.21	2.60	1.99	5.45	-0.24	0.81
0.47	5.22	3.11	2.3	5.30	-0.08	0.97
0.49	5.13	2.65	2.49	5.11	0.02	0.82
0.53	4.66	2.31	2.88	4.64	0.02	0.80
0.54	5.36	3.29	2.99	4.77	0.59	1.09
0.62	3.92	5.69	4.02	3.55	0.37	0.87
0.71	4.35	3.71	5.64	1.71	2.64	0.99
0.85	2.56	6.87	8.10	0	2.56	----
1.05	1.83	7.9	8.10	0	1.83	----

2.2 Test new growth kinetic model

The new growth kinetic model was tested, for transient conditions, following the same procedure described above for the classical model. The equations for the new model are the following:

$$\mu = \mu_{max}\, S/(K_s + S) \qquad (D.7)$$

$$dX/dt = (\mu - k_s)\,(X - X_s) - DX \qquad (D.11)$$

$$dS/dt = D(S_0 - S) - \mu\,(X - X_s)/Y_{X/S} \qquad (D.12)$$

$$dX_s/dt = k_s\,(X - X_s) - D\,X_s \qquad (D.13)$$

The new kinetic model was tested with the same constants used in the classical model. The growth yield calculated with the classical model was assumed constant for each dilution rate and used to test the new model.

The initial biomass and glucose concentrations, X_i, and S_i, and the glucose concentration in the feed stream, S_0, were selected for each dilution rate from the corresponding experimental data. The set of differential equations (Eqs. D7, D.11, D.12 and D.13) for the new growth with sporulation kinetic model was solved numerically. Table D.6 reports an example of the tabulated data obtained while solving equations D.7, D.11, D.12, and D.13. Table D.7 reports a comparison of model results with experimental data at steady state for a continuous growth of *B. thuringiensis*.

Table D.6 Tabulated data obtained in the numerical solution of the equations D.7, D.11, D.12, and D.13. Dilution rate, $D = 0.28\ h^{-1}$, $S_0 = 7.8$ g/L, $X_i = 5.52$ g/L, $S_i = 1.2$ g/L, $\mu_{max} = 1.1\ h^{-1}$, $K_S = 3.1$ g/L, $Y_{X/S} = 0.84$ g/g, and $k_s = 0.012\ h^{-1}$.

Time, (h)	μ, (h^{-1})	X, new model, (g/L)	S, new model, (g/L)
0	0.306977	5.52	1.2
0.2	0.306977	5.536534	1.164391
0.4	0.300355	5.545022	1.139281
0.6	0.295618	5.547531	1.12217
0.8	0.292358	5.5457	1.11107
1	0.290229	5.540789	1.104439
1.2	0.288953	5.533747	1.101108
1.4	0.288309	5.525281	1.100196
1.6	0.288133	5.515906	1.101051
1.8	0.288298	5.505997	1.103188
2	0.288711	5.495823	1.106253
2.2	0.289302	5.485574	1.109982
2.4	0.29002	5.475383	1.114185
2.6	0.290828	5.465343	1.118721
2.8	0.291698	5.455515	1.123488
3	0.29261	5.445939	1.128409
3.2	0.29355	5.436638	1.13343
3.4	0.294507	5.427625	1.138512
3.6	0.295472	5.418904	1.143625
3.8	0.296442	5.410474	1.148749
4	0.297411	5.402329	1.153869
4.2	0.298377	5.394462	1.158974
4.4	0.299338	5.386863	1.164059
4.6	0.300292	5.37952	1.169117
4.8	0.30124	5.372423	1.174147
5	0.30218	5.365559	1.179147
5.2	0.303112	5.358916	1.184117
5.4	0.304037	5.352483	1.189056
5.6	0.304953	5.346247	1.193966
5.8	0.305862	5.340199	1.198847
6	0.306764	5.334327	1.203701

Table D.7 Comparison of continuous growth experimental data with the new growth with sporulation kinetic model, D: dilution rate, X: biomass concentration, S: glucose concentration, S_0: glucose concentration in the feed stream, ks: constant in the new kinetic model.

D (h^{-1})	X, (g/L)	S, (g/L)	S, new model, (g/L)	X, new model, (g/L)	Error (X_{exp}-X_{model})	k_s, (h^{-1})
0.14	5.09	0.03	0.66	5.08	0.01	0.012
0.2	5.38	0.81	0.84	5.33	0.05	0.010
0.28	5.36	1.01	1.18	5.36	0.00	0.012
0.37	5.54	1.05	1.58	5.60	-0.06	0.00
0.43	5.21	2.60	1.99	5.45	-0.24	0.00
0.47	5.22	3.11	2.32	5.31	-0.09	0.00
0.49	5.13	2.65	2.49	5.08	0.05	0.00
0.53	4.66	2.31	2.88	4.64	0.02	0.00
0.54	5.36	3.29	2.99	4.77	0.59	0.00
0.62	3.92	5.69	4.02	3.55	0.37	0.00
0.71	4.35	3.71	5.64	1.71	2.64	0.00
0.85	2.56	6.87	8.10	0	2.56	0.00
1.05	1.83	7.9	8.10	0	1.83	0.00

3. Corrections resulting from the application of the sporulation kinetic model

The sporulation kinetic model is used to predict the biomass concentration during batch and continuous growth of *B. thuringiensis*. The model accounts for the effect of the sporulation process on the cell growth, and as a result, the correction on the predictions from the classical kinetic model by the new model is relevant at the beginning of the stationary stage in batch cultures and at low dilution rates in continuous cultures.

The correction provided by the new model, when applied to batch cultures, is evident by the reduction in the sum of squares of residuals, as showed in Table 6.1. The reduction in

the sum of squares of residuals from 7.45 to 1.63 represents a 78 % improvement in the prediction in biomass concentration. The difference in the specific growth rate and the parameter k_s is also a measure of the correction factor of the new model. The specific growth rate at the beginning of the batch culture is much higher than the parameter k_s, indicating a negligible correction by the new model. Assuming a substrate concentration of 11.9 g/L, a maximum specific growth rate of 0.53 h^{-1}, and a saturation constant of 3.1 g/L, the specific growth rate resulted in 0.42 h^{-1}. This value compared to ks = 0.026 h^{-1} is 16 times higher, and therefore, the correction provided by the new model is negligible (approximately 6% correction).

In contrast, when the substrate is present at low concentrations in the medium (during the transition state), the correction by the new model is more noticeable. Assuming a substrate concentration of 0.5 g/L, the specific growth rate is estimated in 0.07 h-1. Under these conditions, the net specific growth rate (μ - k_s) is only 0.044, that is, a 37 % reduction in the specific growth rate.

The correction by the new model in the prediction in biomass concentration during a continuous culture can be perceived by comparing the difference between the experimental and the predicted biomass concentrations reported in Tables D.5 and D.7. For instance at a dilution rate of 0.14 h^{-1}, the error in the prediction by the classical model is 0.53, whereas that by the sporulation model is 0.1. That is, 81 % improvement in the prediction. However, at high dilution rates, the correction by the new model is negligible. This fact is explained given that the new model assumes a sporulation process, which is absent at high dilution rates (dilution rates higher than 0.2 h^{-1}) during the continuous culture.